

NanoBio Integration for Medical Innovation

-Targeting Therapy by Supramolecular Nanodevices-

Kazunori Kataoka

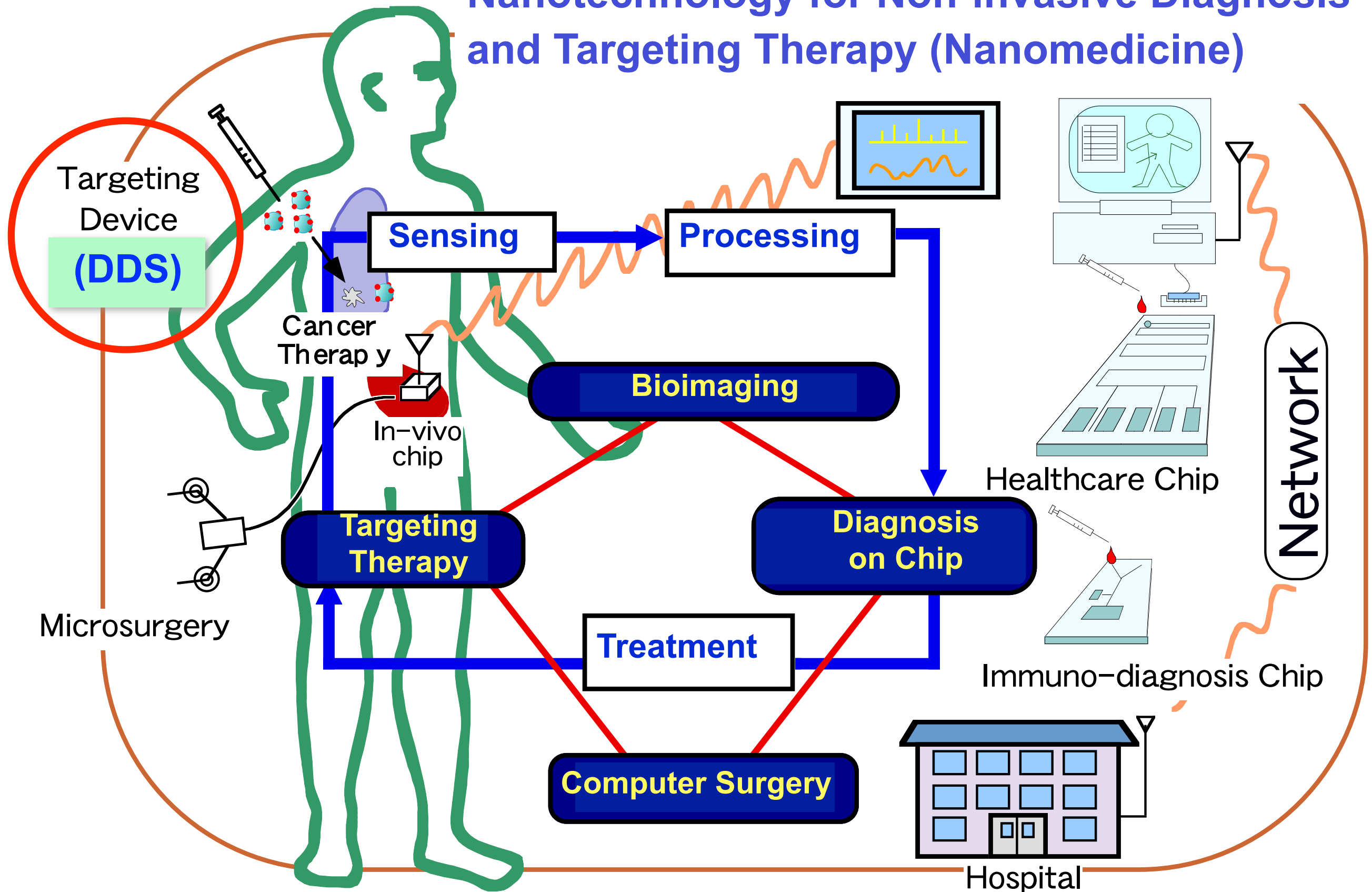
Center for NanoBio Integration

*Department of Materials Engineering, Graduate School of
Engineering, and Center for Disease Biology and Integrative
Medicine, Graduate School of Medicine, The University of Tokyo*

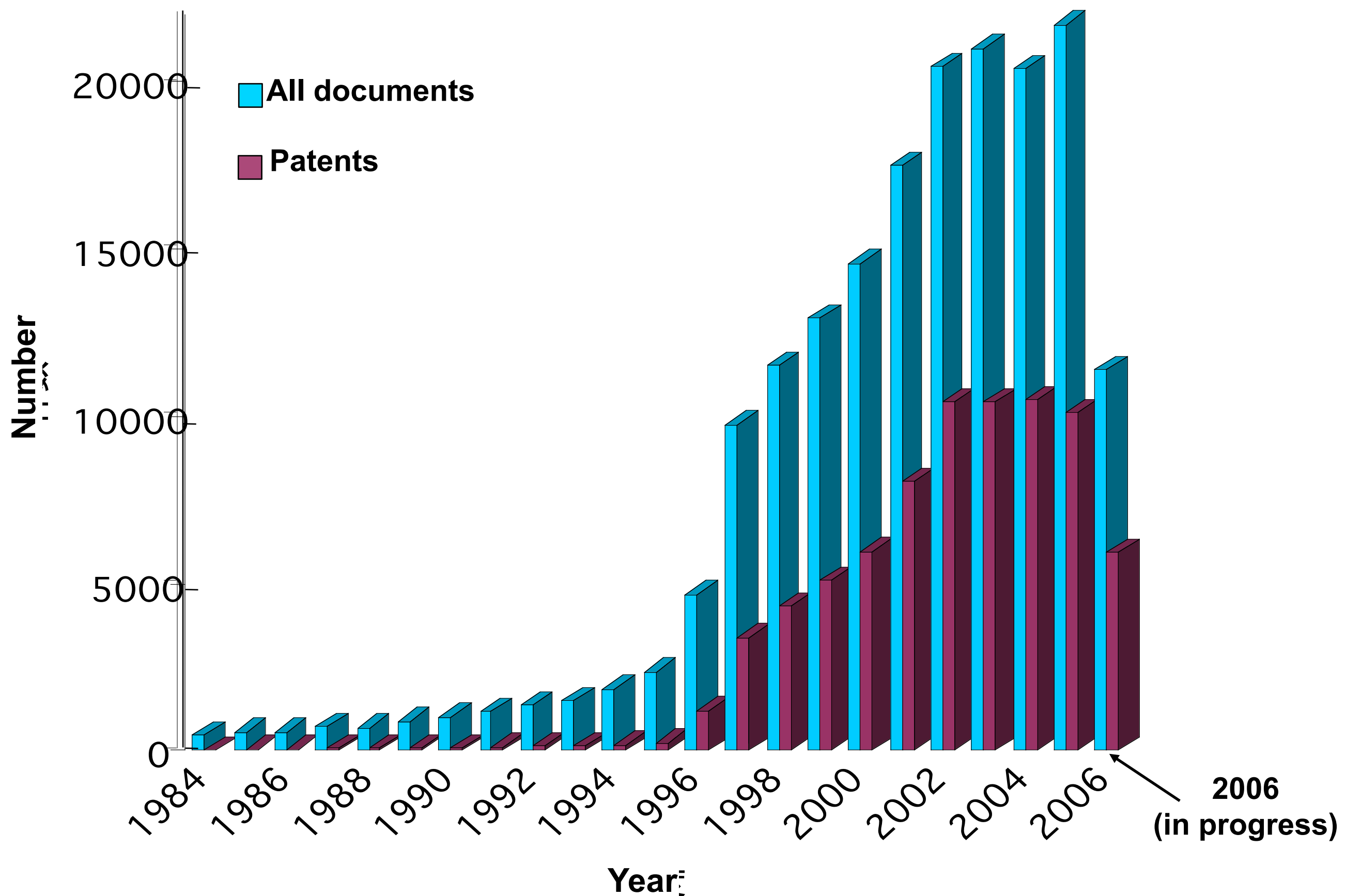
November 25, 2009
UT-SNU Exchange Lecture Course
Introduction to Bioengineering



Nanotechnology for Non-invasive Diagnosis and Targeting Therapy (Nanomedicine)

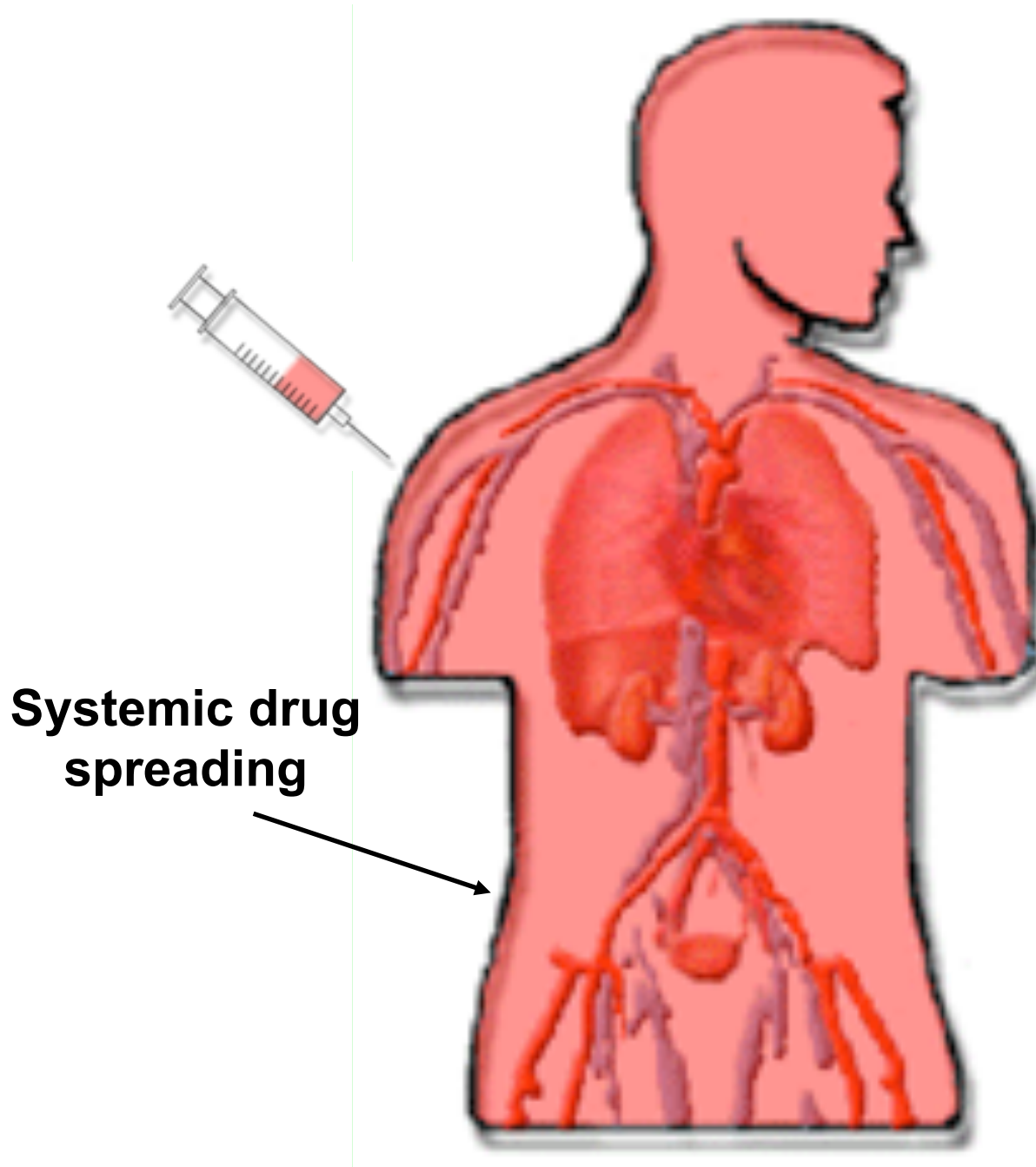


Number of scientific papers and patents related to DDS

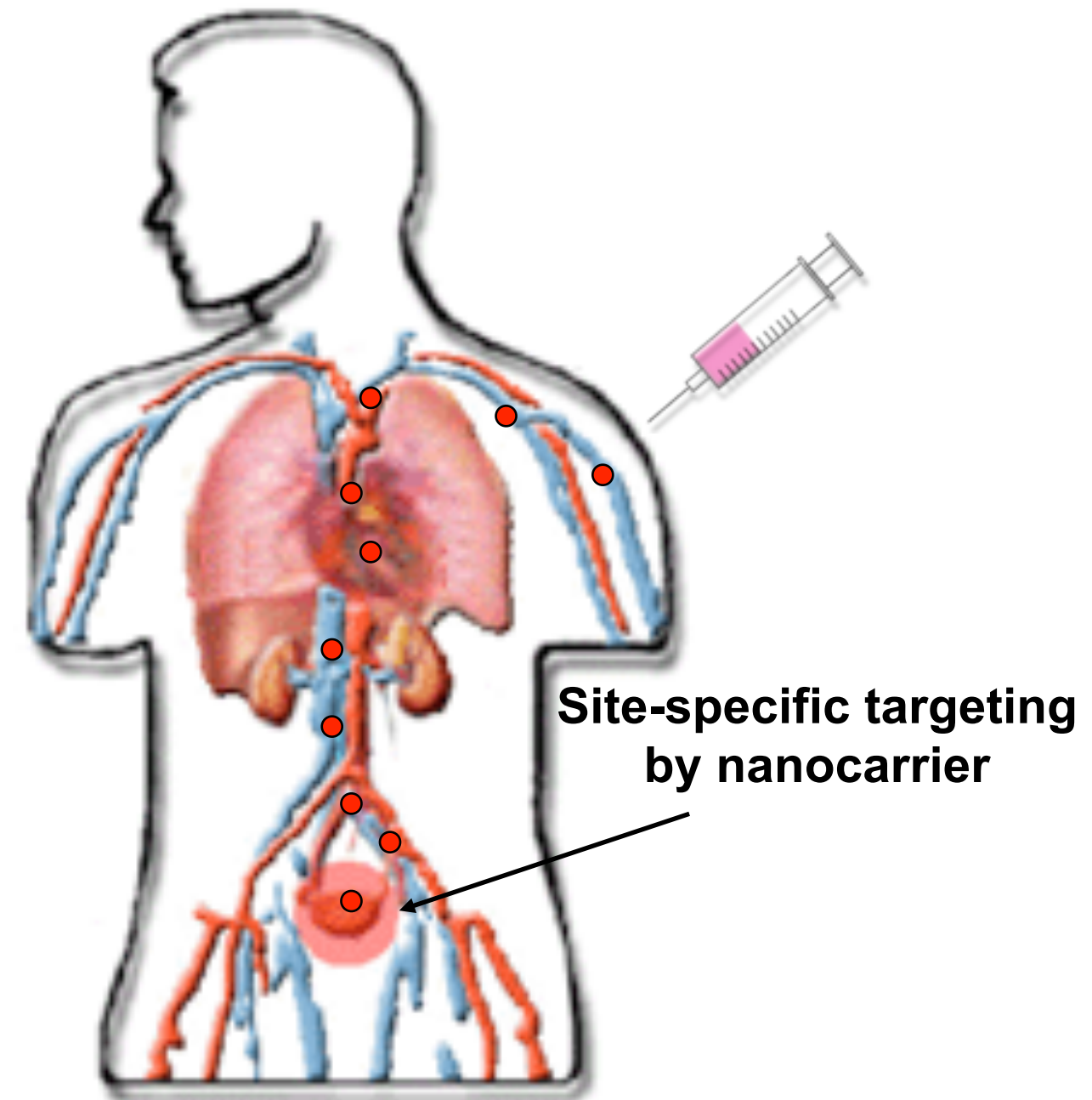


*Source: SciFinder

Targeting Therapy by Nanotechnology-based Medicine

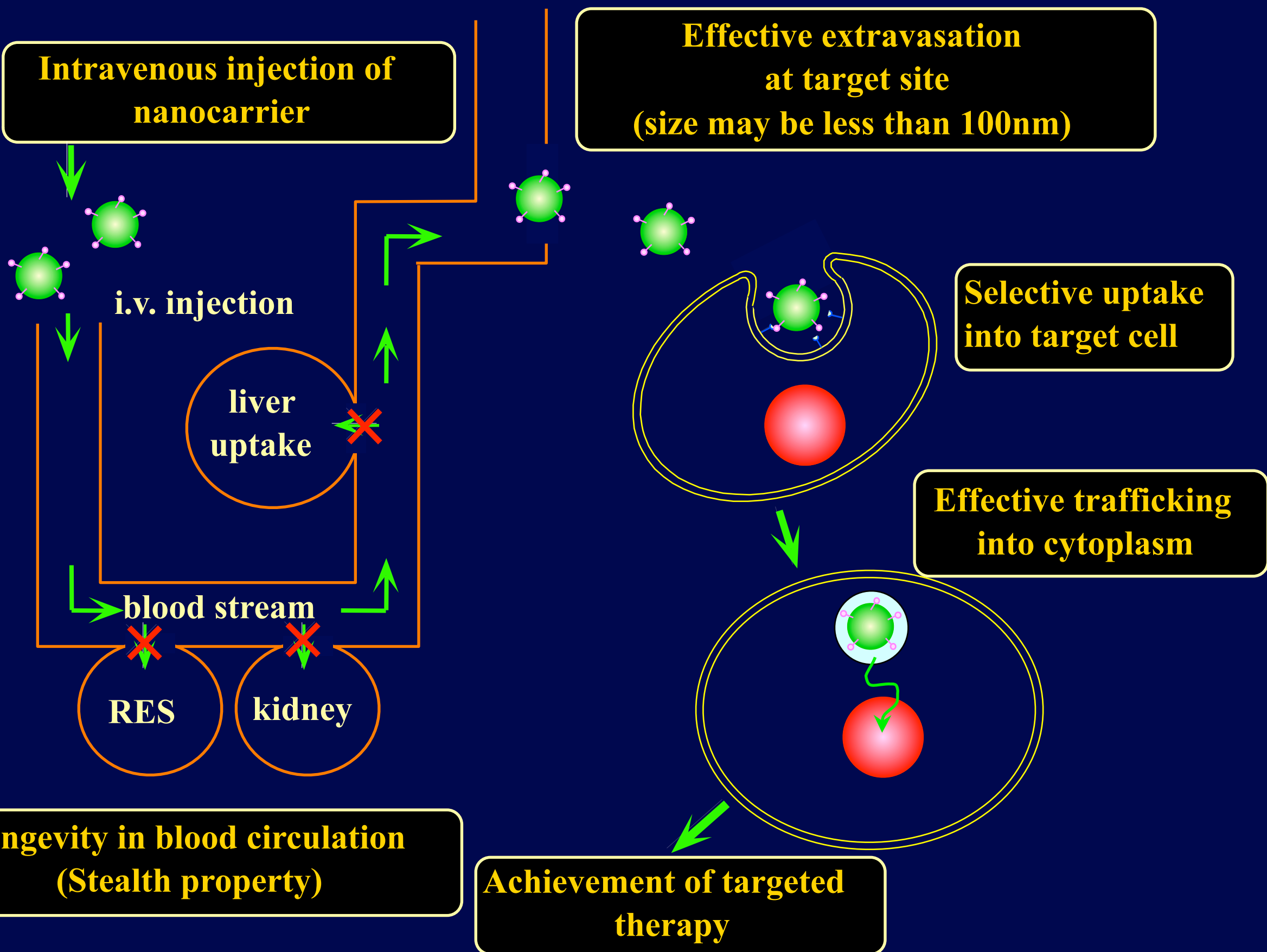


General Chemotherapy

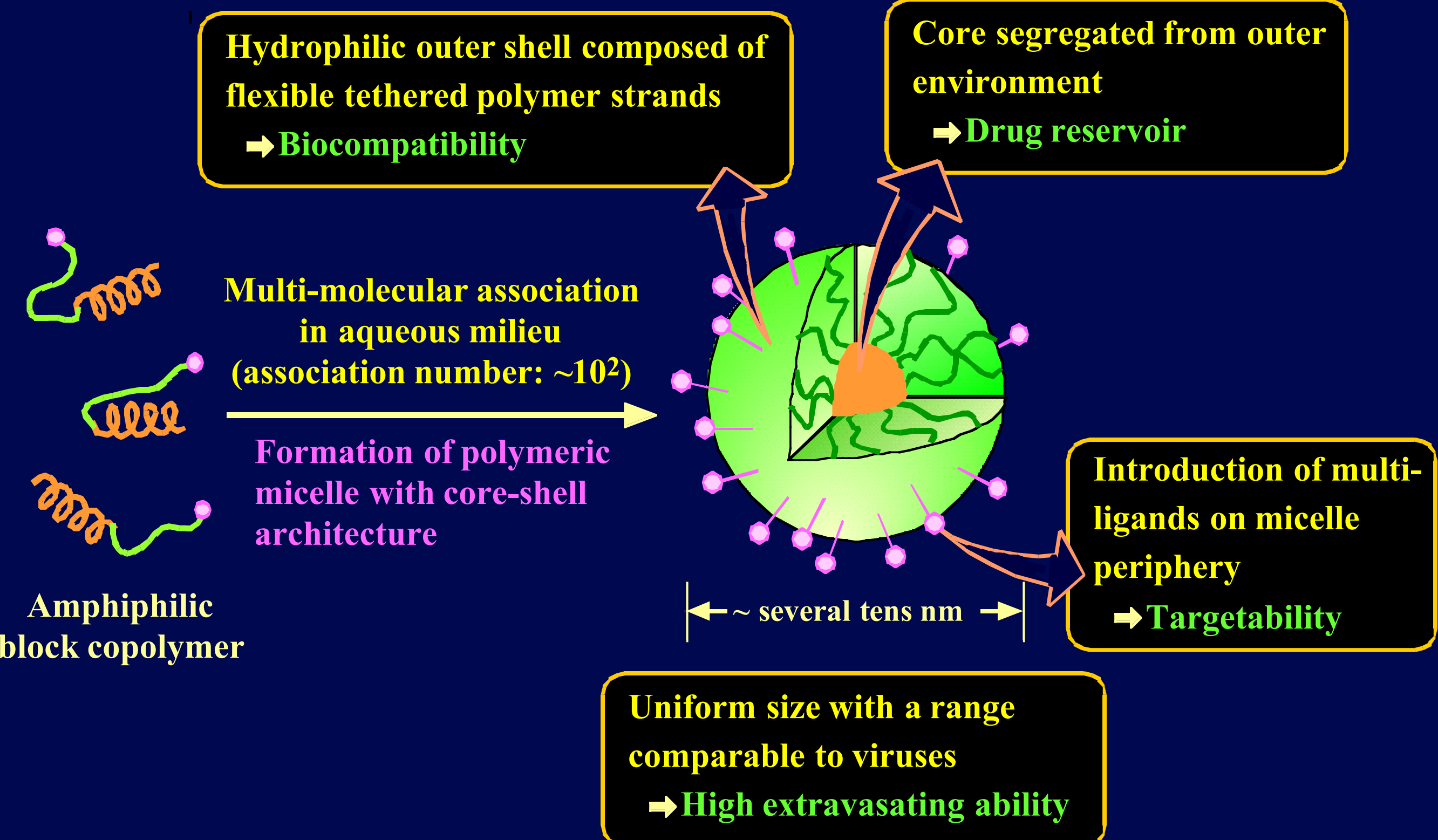


Targeting Therapy

Itinerary of intravenously-injected nanocarriers

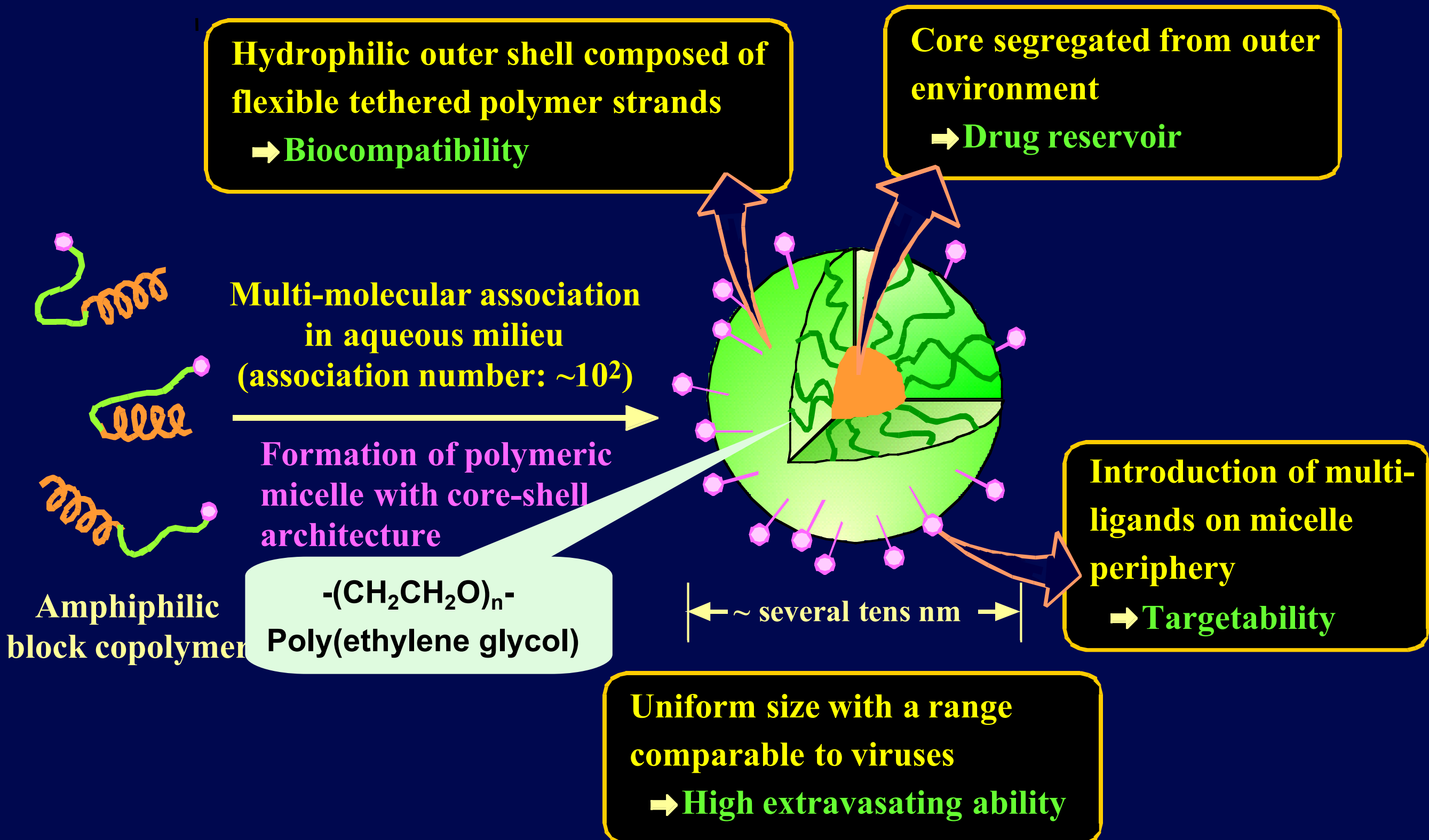


Structural Design of Polymeric Micelles for DDS



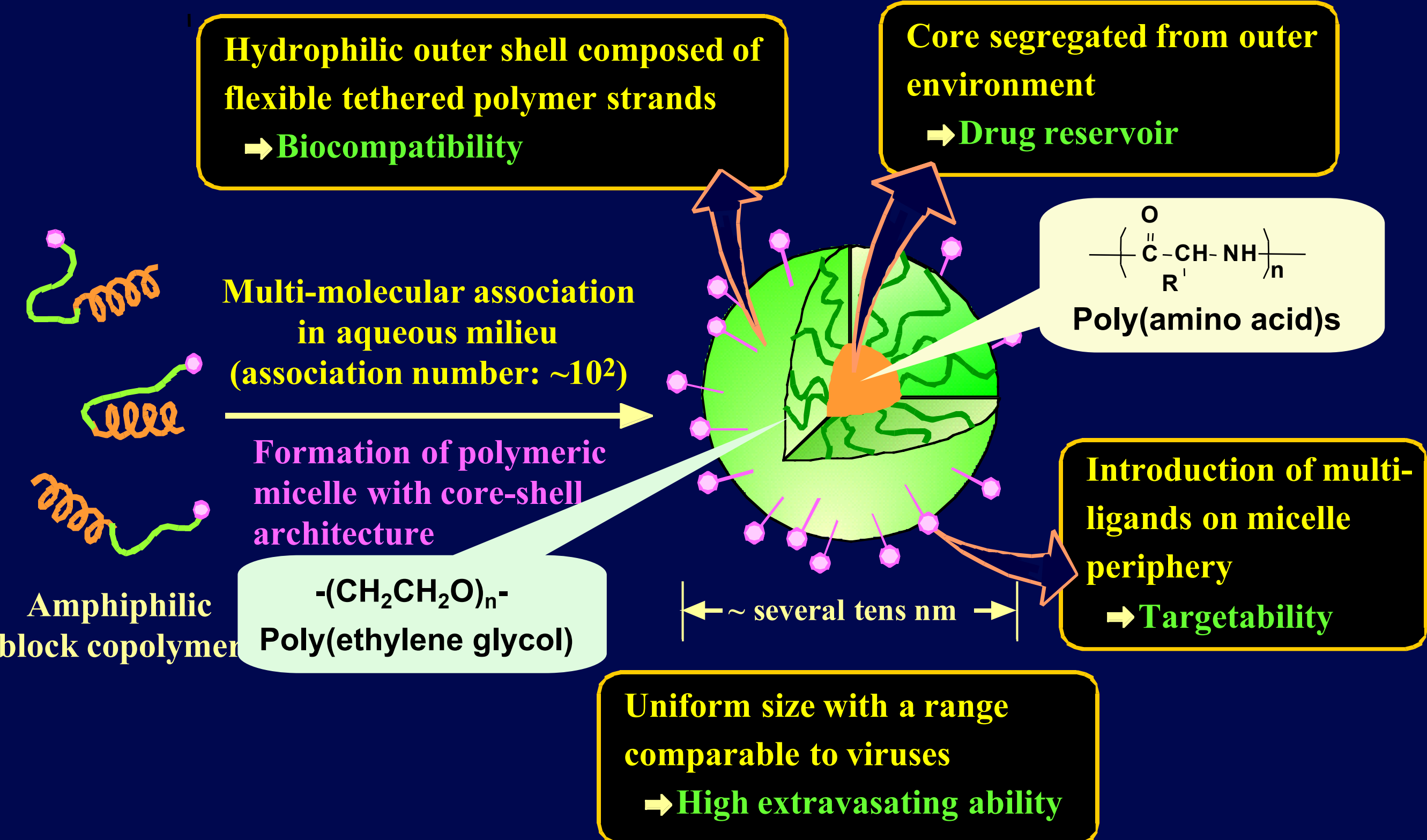
M. Yokoyama, K. Kataoka, et al, *J. Contrl. Rel.* 11, 269 (1990); K. Kataoka, G. S. Kwon et al, *J. Contrl. Rel.* 24, 119 (1993); G. S. Kwon, K. Kataoka, et al, *J. Contrl. Rel.* 29, 17 (1994); A. Harada, K. Kataoka, *Science* 283, 65 (1999)

Structural Design of Polymeric Micelles for DDS



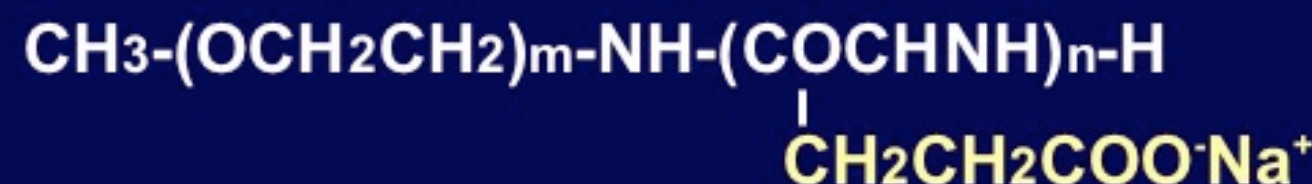
M. Yokoyama, K. Kataoka, et al, *J. Contrl. Rel.* 11, 269 (1990); K. Kataoka, G. S. Kwon et al, *J. Contrl. Rel.* 24, 119 (1993); G. S. Kwon, K. Kataoka, et al, *J. Contrl. Rel.* 29, 17 (1994); A. Harada, K. Kataoka, *Science* 283, 65 (1999)

Structural Design of Polymeric Micelles for DDS

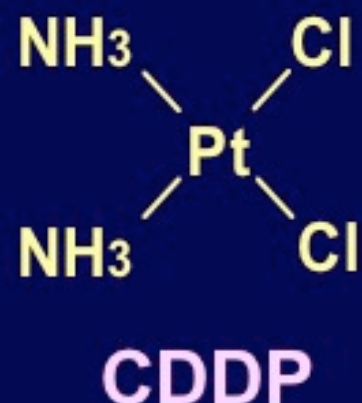


M. Yokoyama, K. Kataoka, et al, *J. Contrl. Rel.* 11, 269 (1990); K. Kataoka, G. S. Kwon et al, *J. Contrl. Rel.* 24, 119 (1993); G. S. Kwon, K. Kataoka, et al, *J. Contrl. Rel.* 29, 17 (1994); A. Harada, K. Kataoka, *Science* 283, 65 (1999)

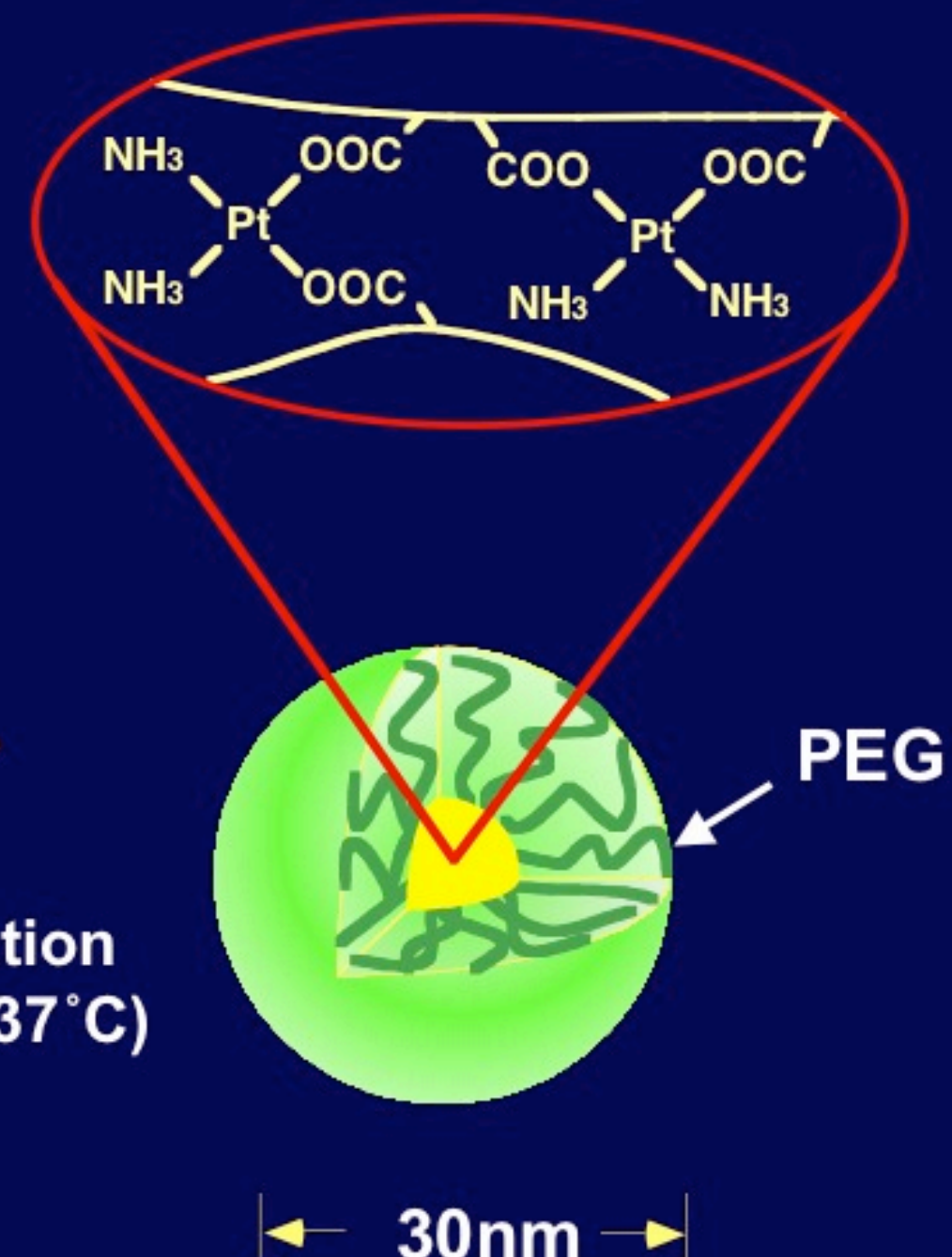
Preparation of cisplatin (CDDP)-incorporated polymeric micelles



PEG-P(Glu)

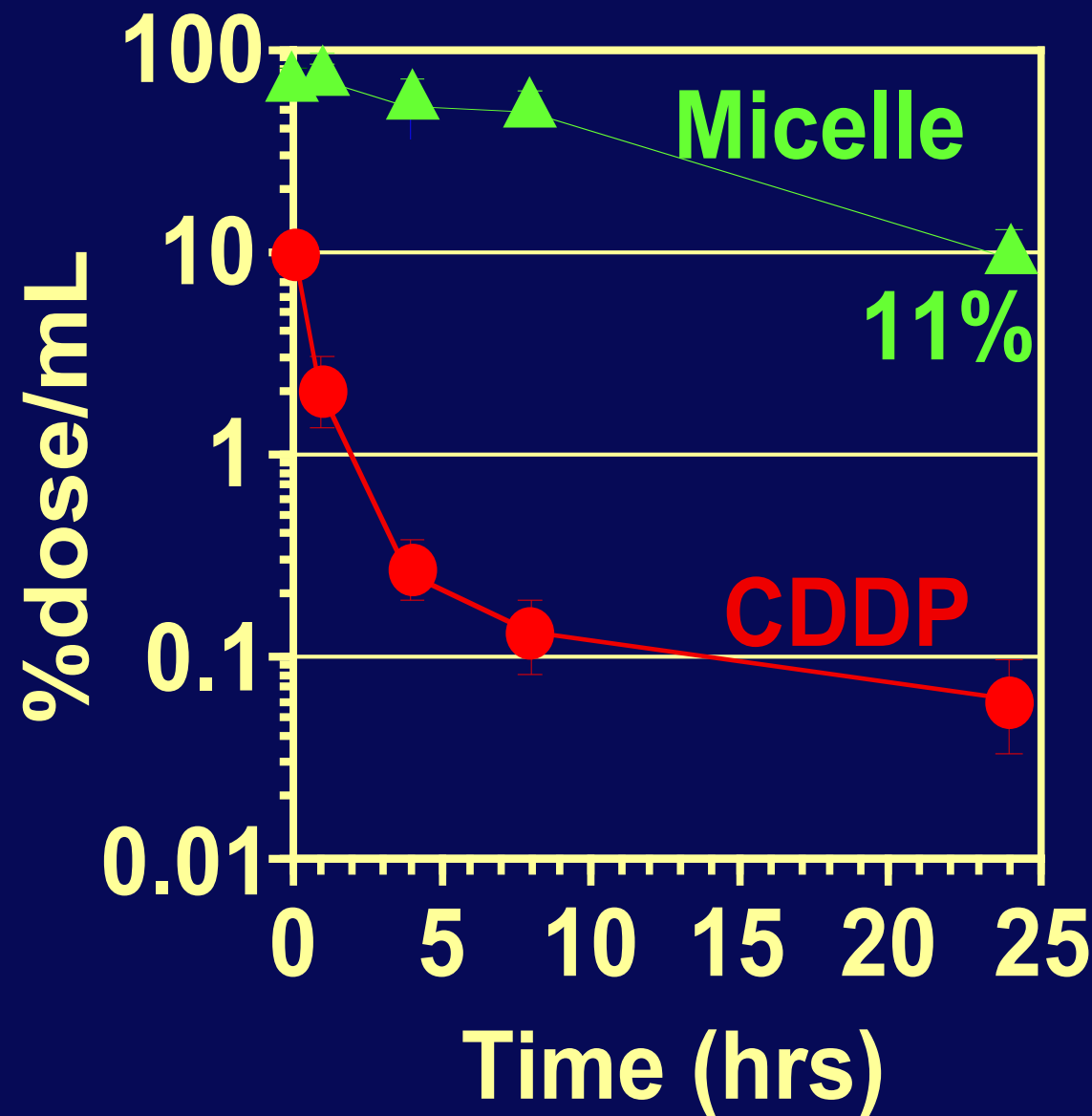


self-association
(in water at 37 °C)

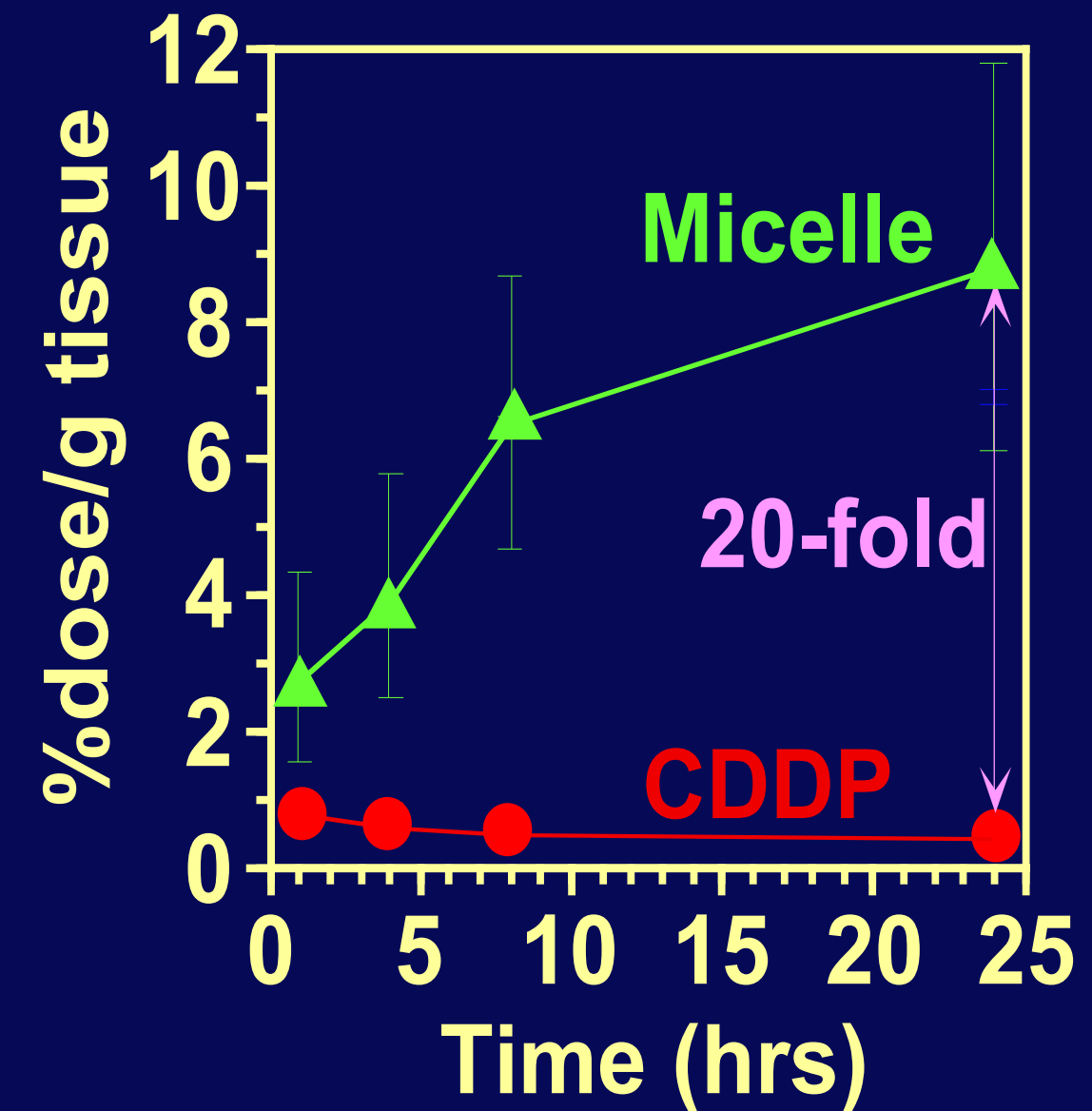


Biodistribution of CDDP-incorporated micelles

Plasma Pt concentration

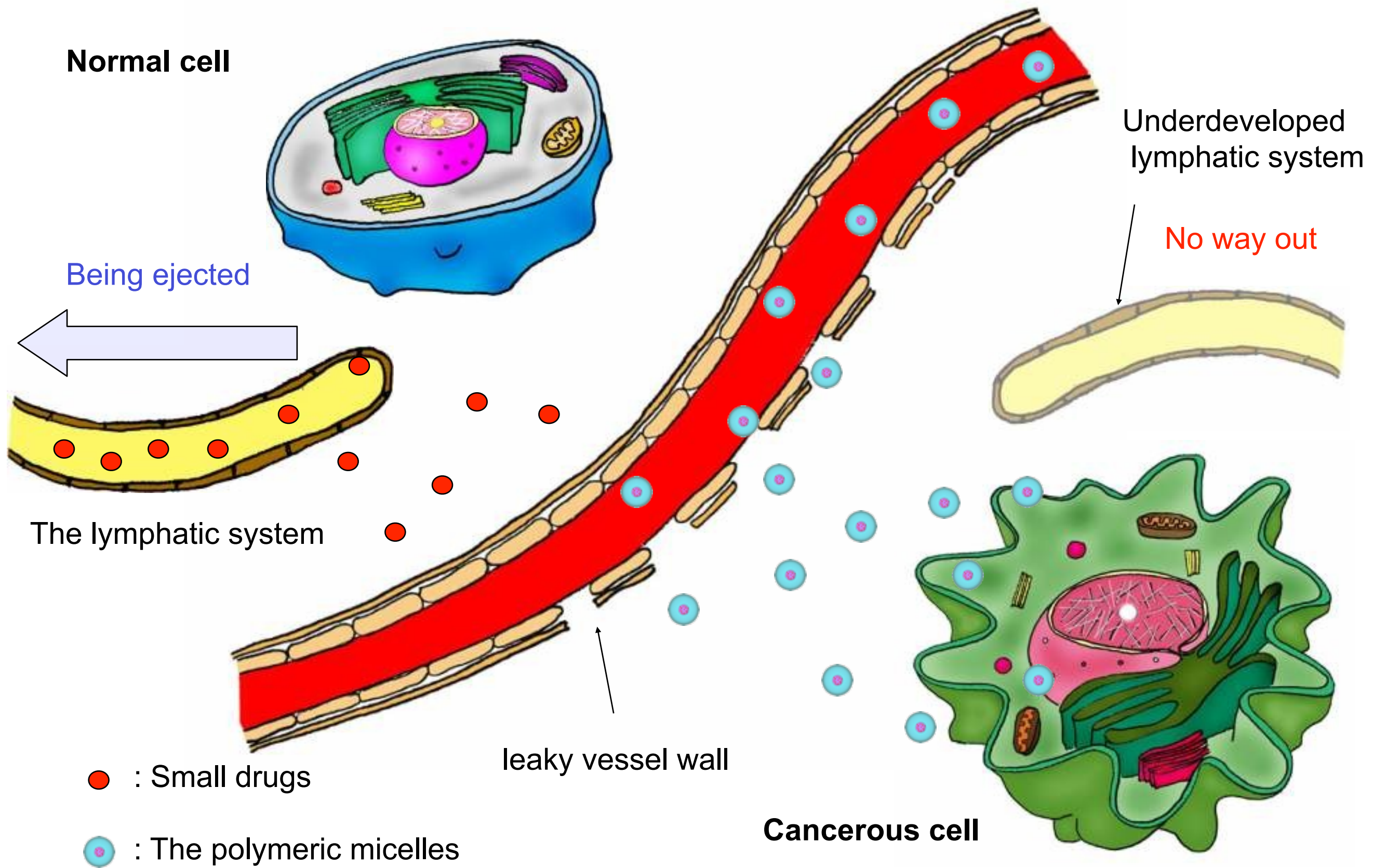


Tumor accumulation



CDDP and CDDP-incorporated micelles were administered i.v. to Lewis lung carcinoma (LLC)-bearing C57BL6N mice (male, 6 week old, n=4)

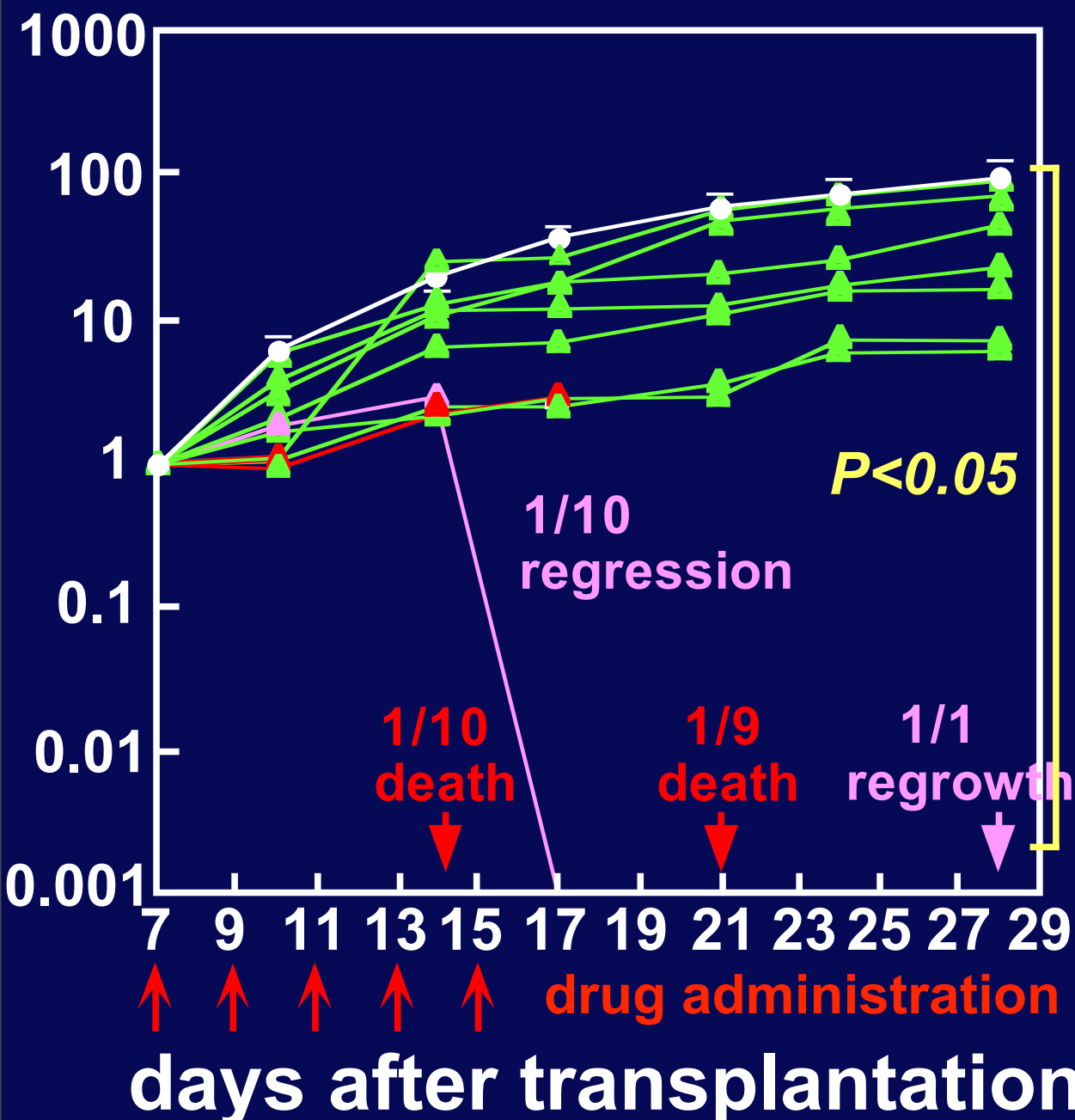
Enhanced Permeability and Retention(EPR) Effect



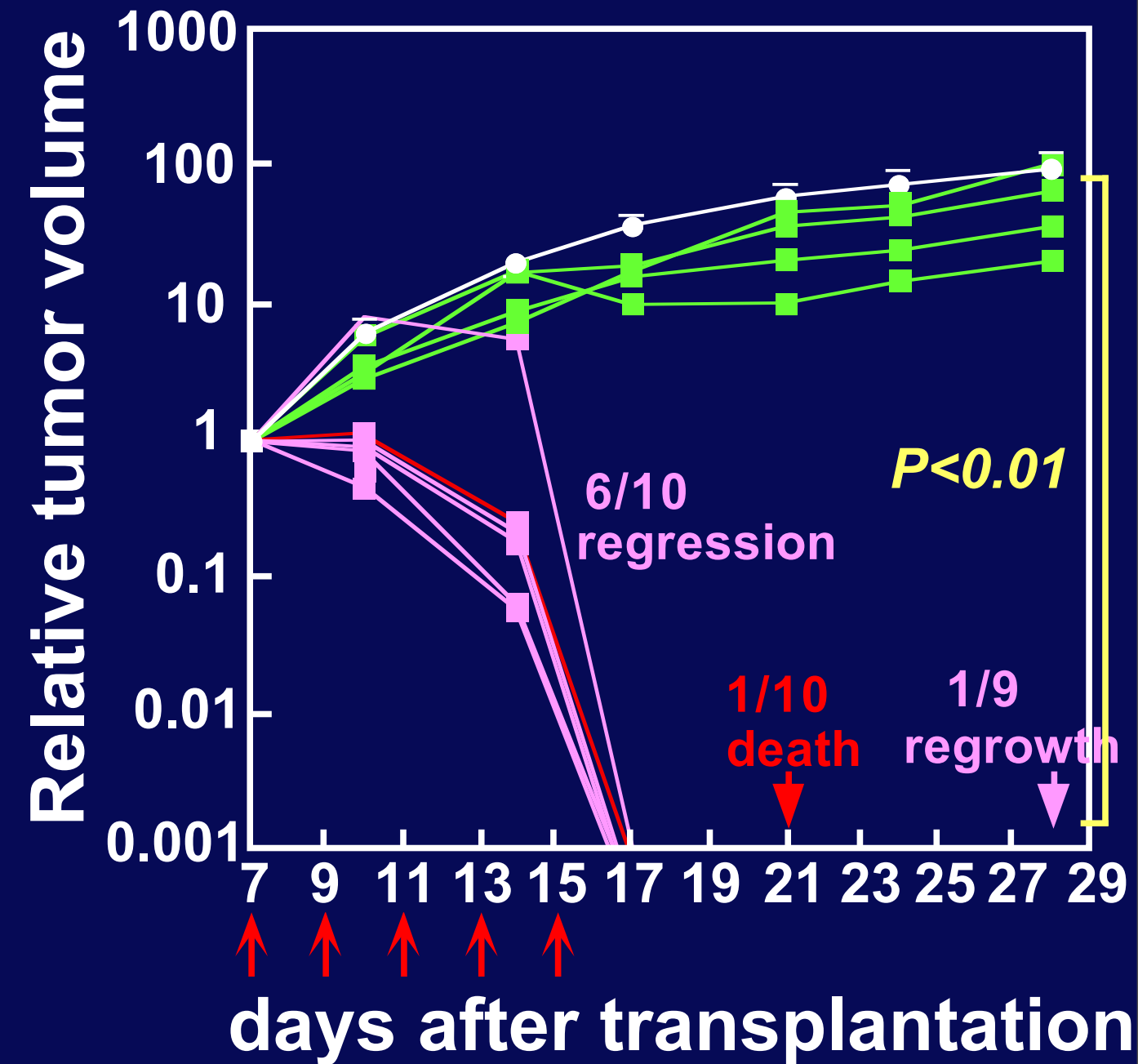
Anti-tumor activity of CDDP-incorporated micelles

Colon 26-bearing CDF₁ mice (female, 6 week old, n=10) were treated 5 times with CDDP and CDDP-incorporated micelle (4mg/kg/day).

CDDP 4mg/kg/day

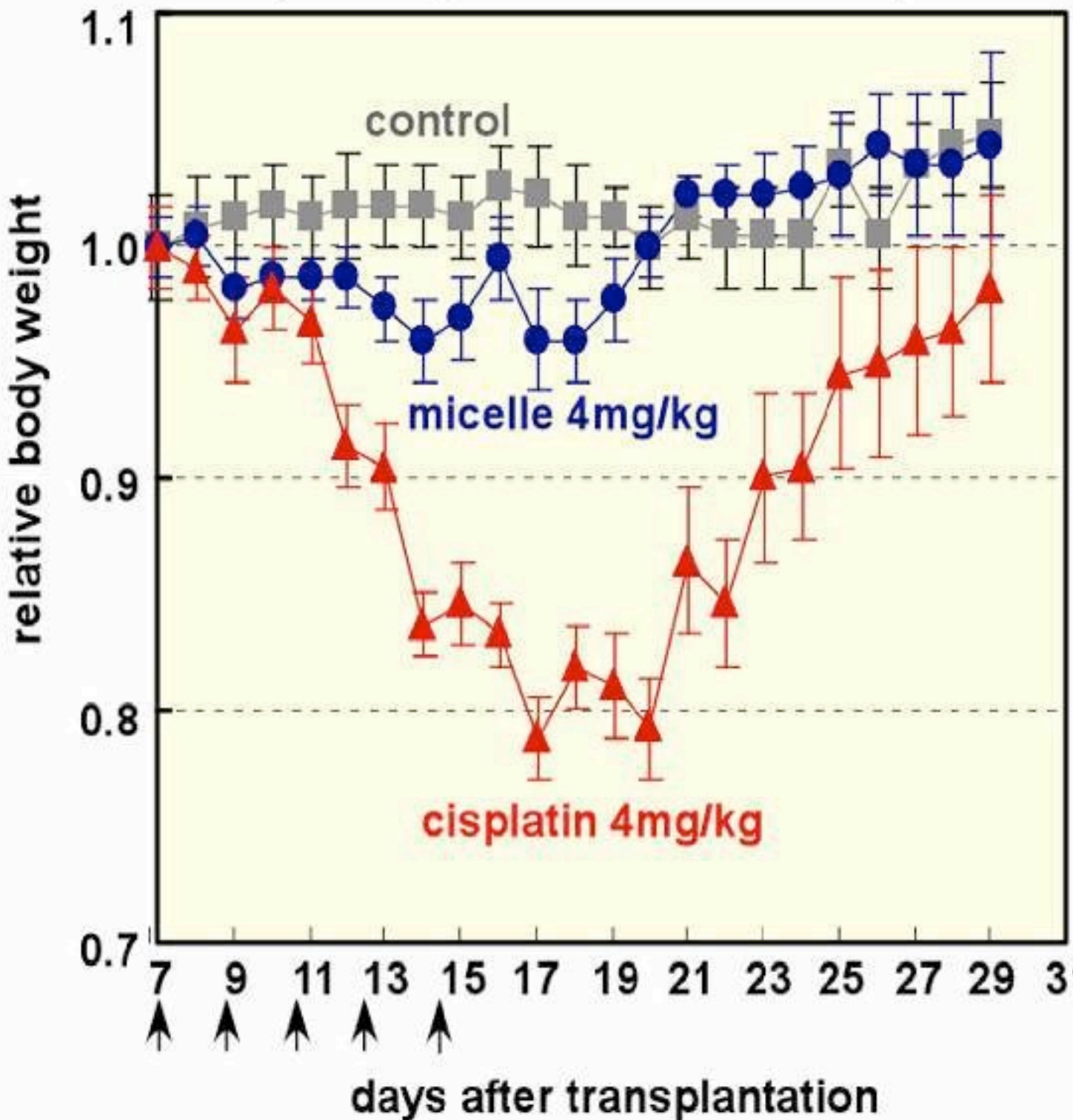


Micelles 4mg/kg/day



Change in body weight of mice treated with cisplatin and PEG-P(Glu(CDDP)) (12-60) micelles

(Data are presented as mean \pm SE.)



Decrease in body weight

cisplatin 20%

micelle 5%

Disappearance of primary tumor

control 0/10

cisplatin 0/8

micelle 4/9

PEG-P(Glu(CDDP)) (12-60)
micelles achieved lower toxicity and higher antitumor activity than same dose of cisplatin.

Polymeric Micelles from PEG-poly(amino acid) Block Copolymers in Clinical Development

Adriamycin (NK911:Nippon Kayaku Co.) :

Phase II Clinical Trial

Paclitaxel (NK105:NanoCarrier Co./Nippon Kayaku Co.) :

Phase II Clinical Trial

Cisplatin (NC6004:NanoCarrier Co.) :

Phase I/II Clinical Trial

Camptothecine derivative (SN-38) (NK012:Nippon Kayaku Co.) :

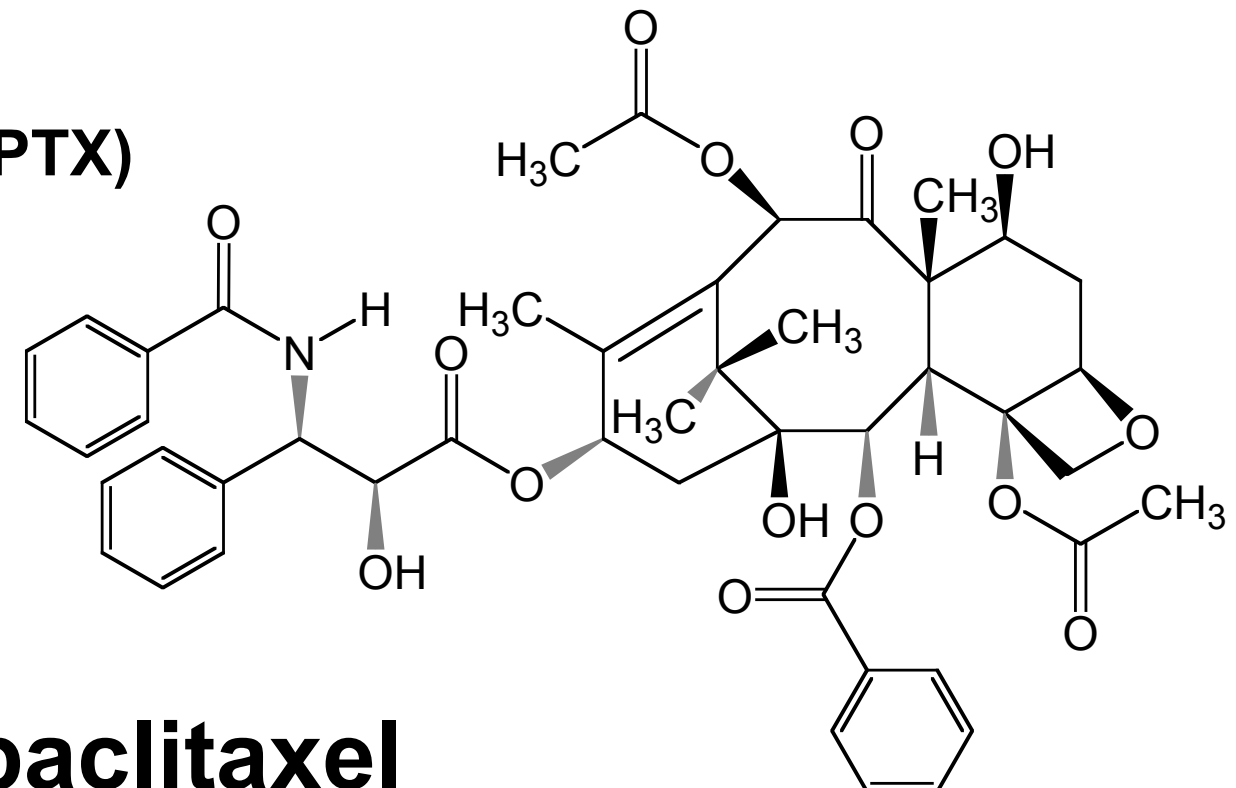
Phase I Clinical Trial

Dachplatin (NC4016/ND-1:NanoCarrier Co./Debio Pharm Co.) :

Phase I Clinical Trial

Preparation of Paclitaxel-loaded Polymeric Micelle (NK105)

Structure of paclitaxel (PTX)



Preparation of the micellar paclitaxel

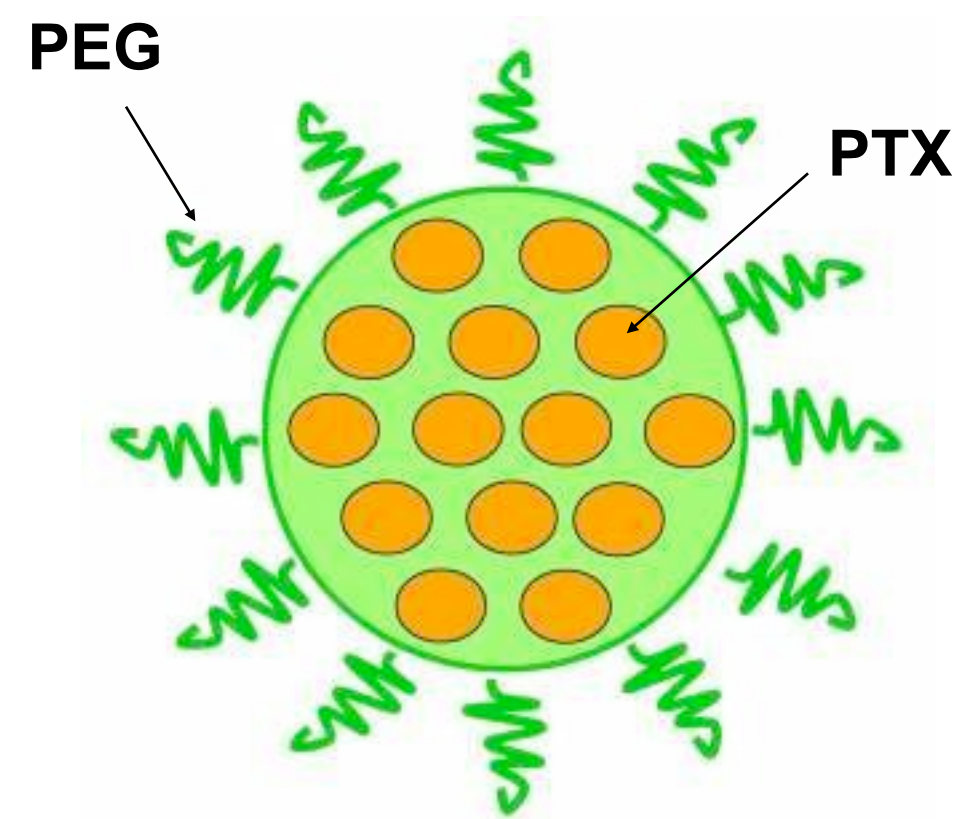
PEG-Hydrophobically modified poly(amino acid)
block copolymer

+ (Mixed in dichloromethane)

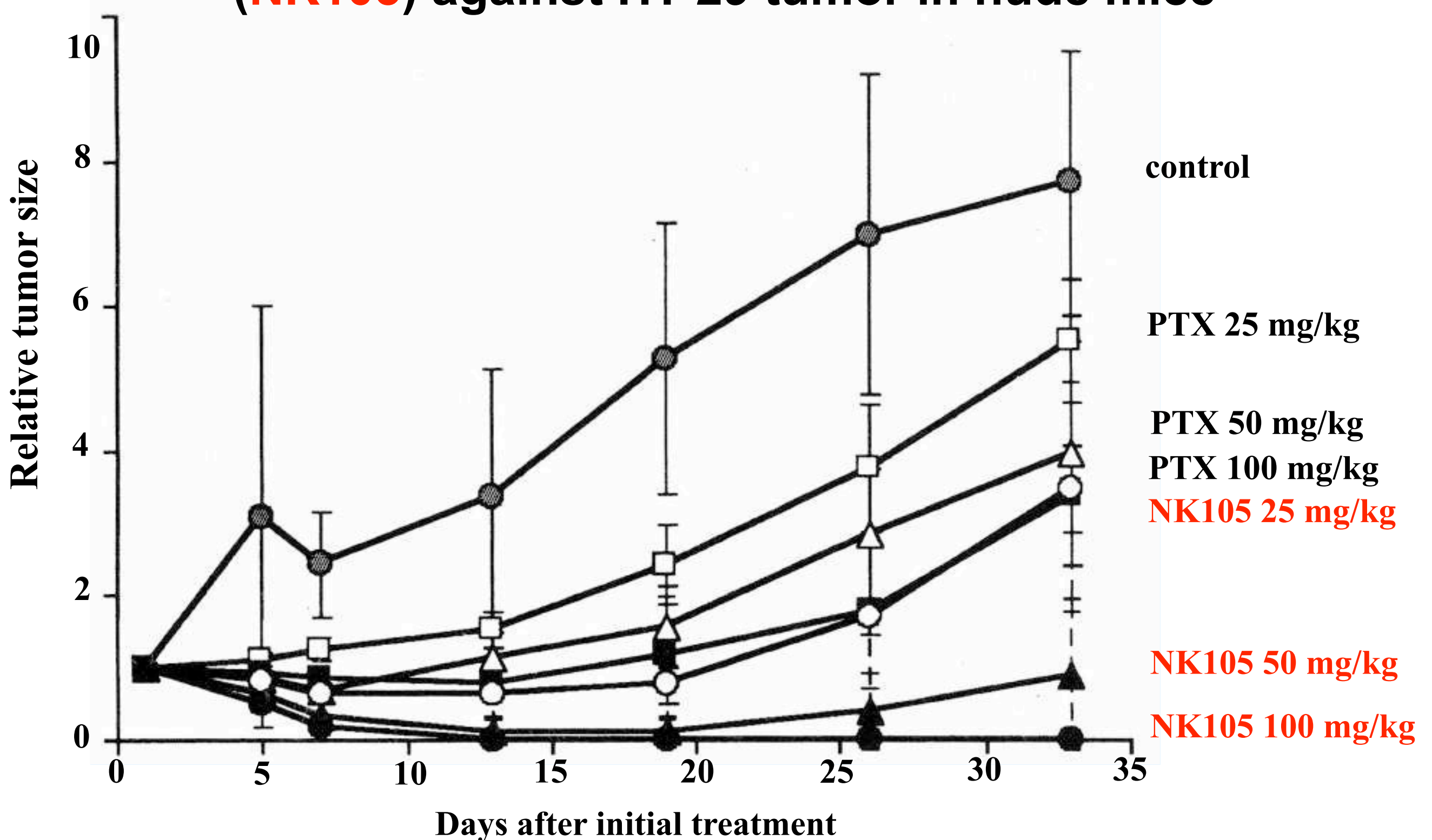
paclitaxel

↓
Emulsification
Evaporation

Micellar paclitaxel (NK105)

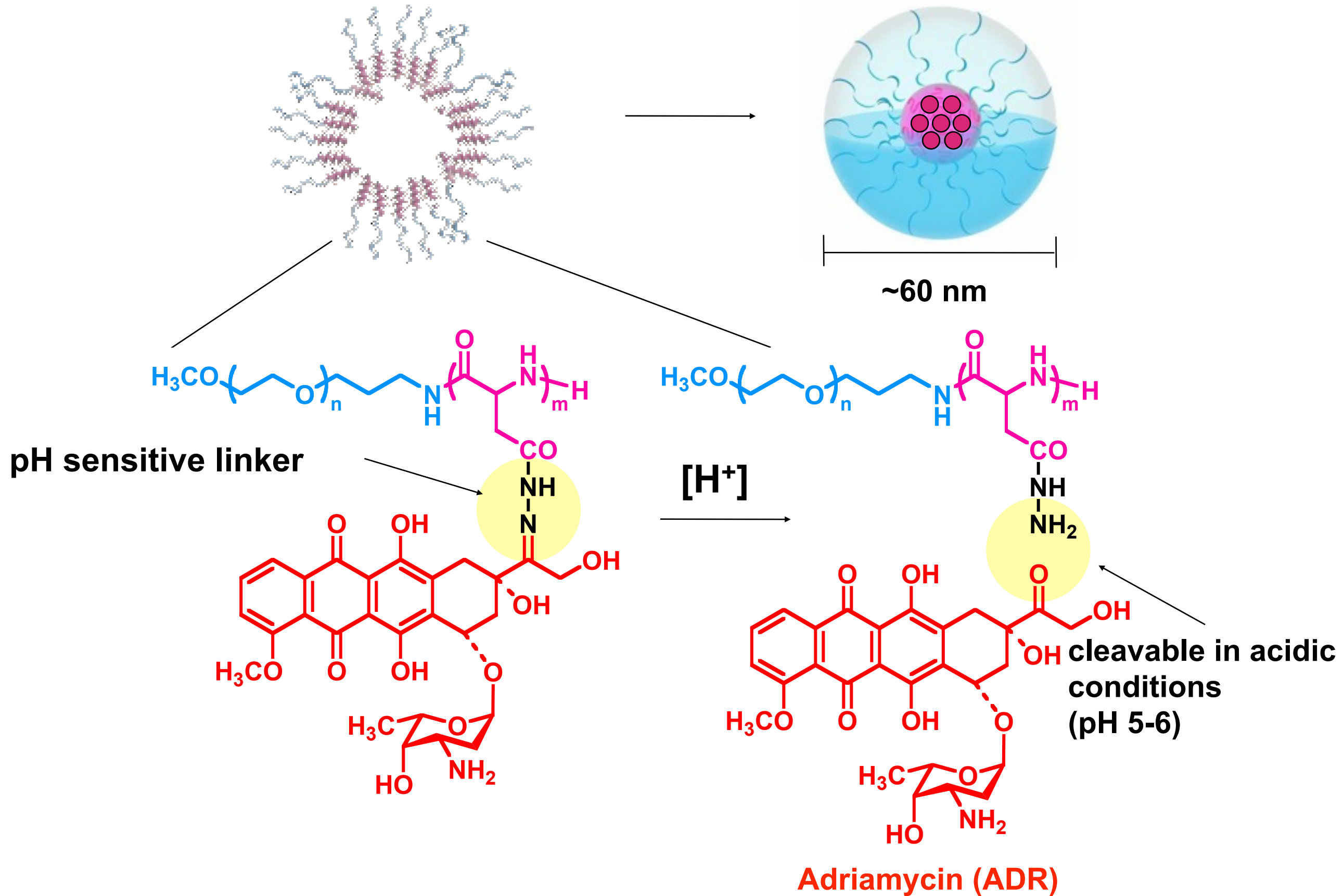


Anti-tumor activity of paclitaxel-loaded polymeric micelles (NK105) against HT-29 tumor in nude mice

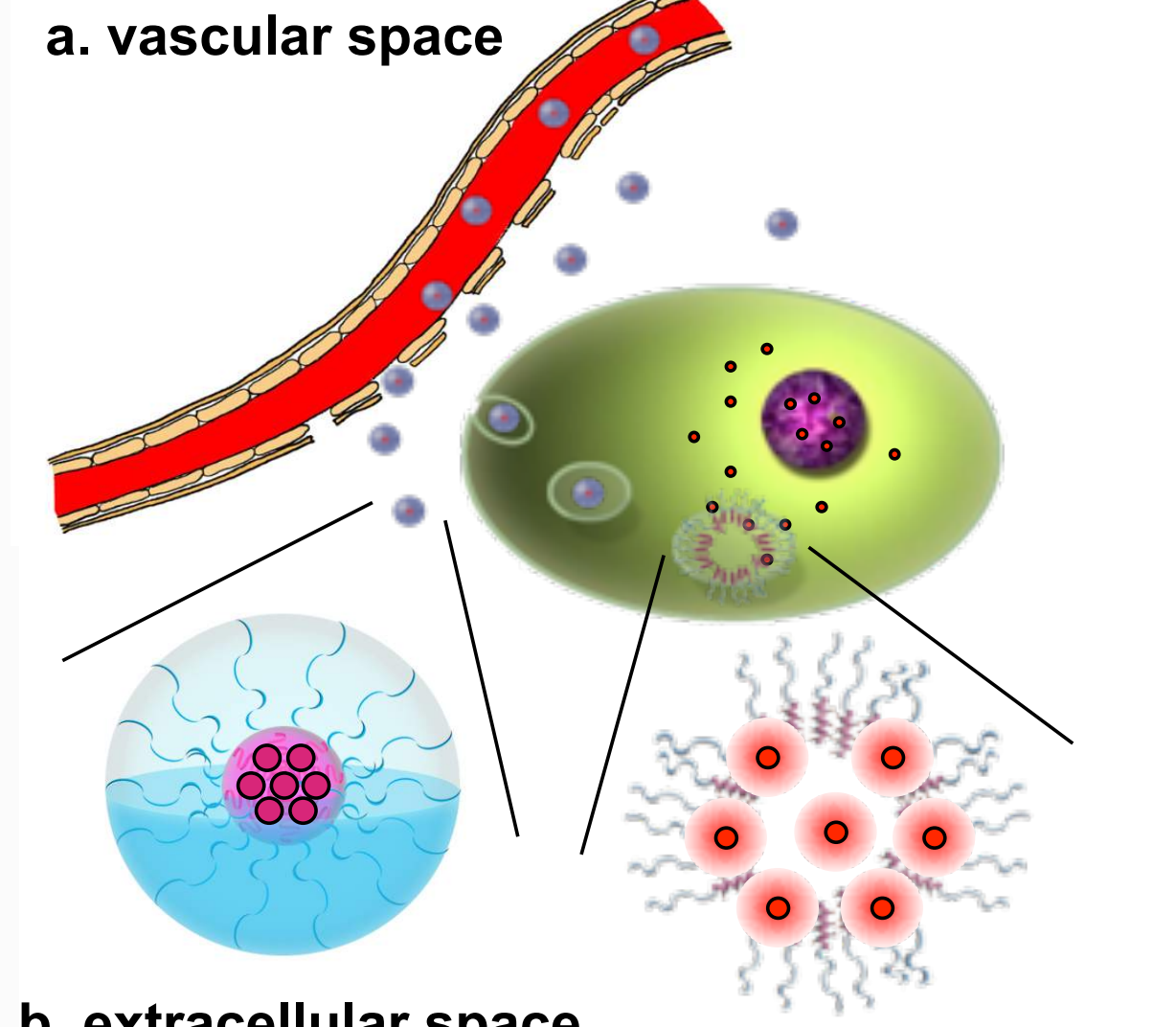
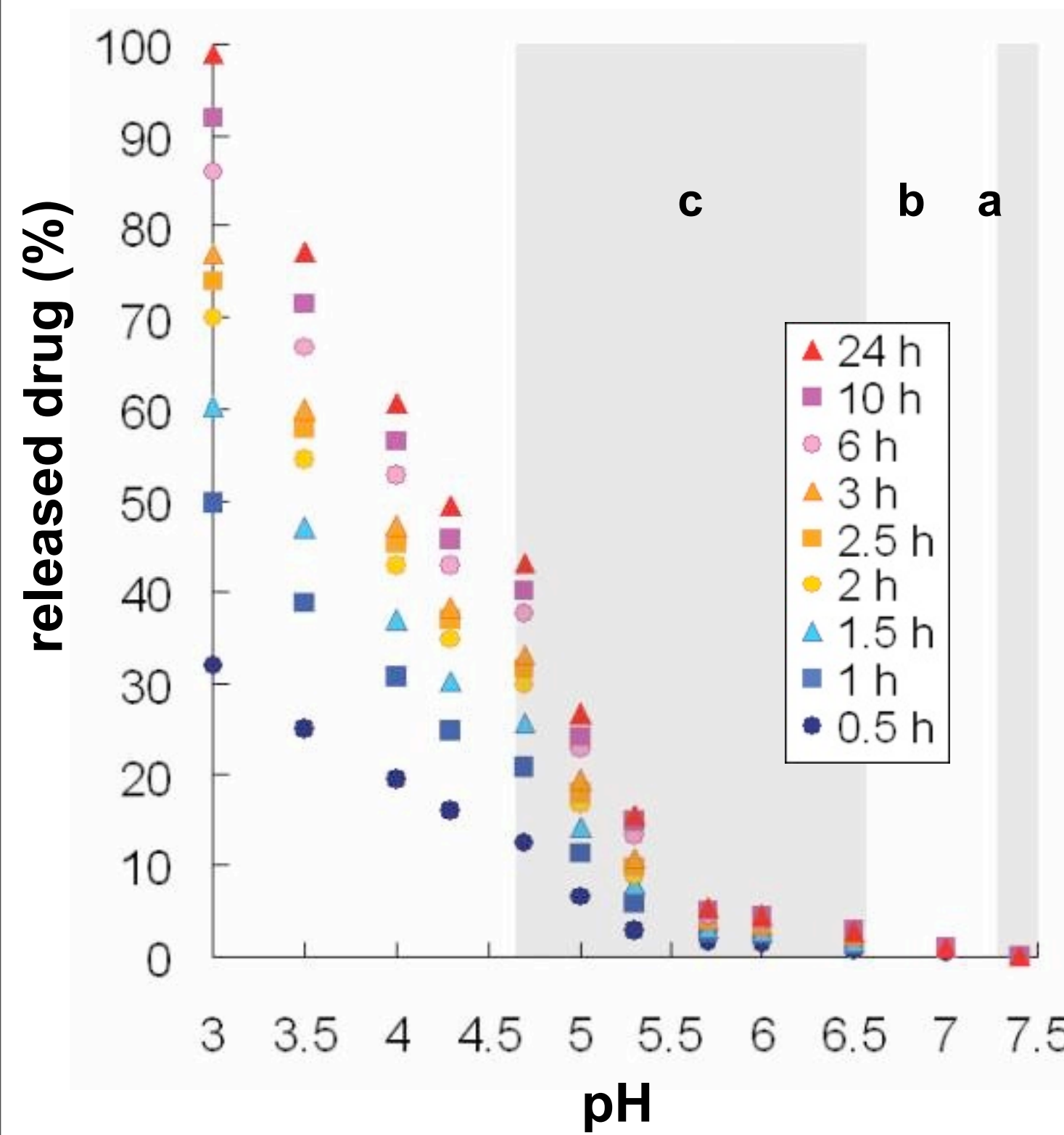


PTX (open) and NK105 (closed) were injected intravenously once weekly for 3 weeks at PTX-equivalent doses of 25, 50, and 100 mg/kg.

The pH-sensitive polymeric micelles

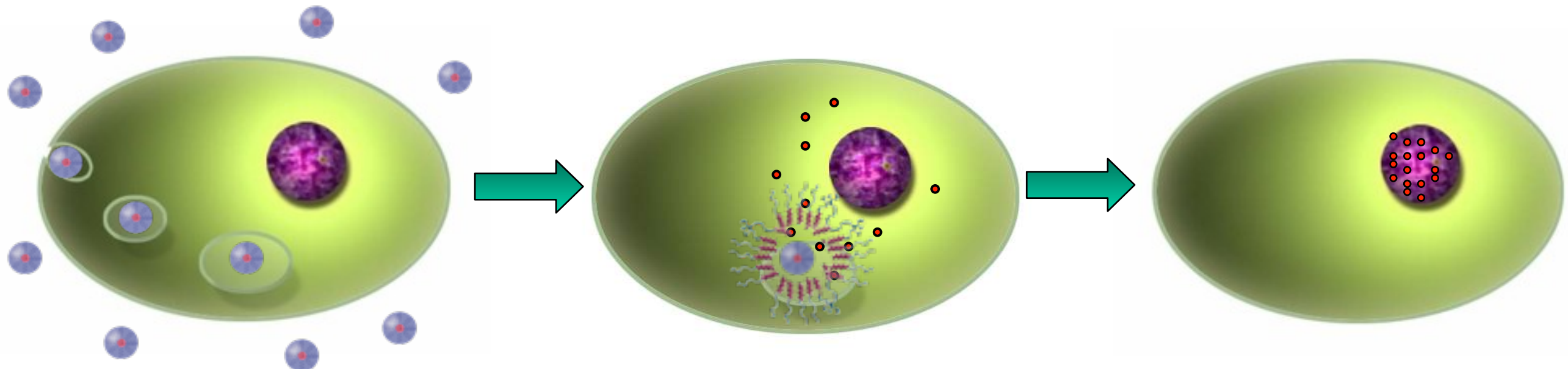


pH-sensitivity adjusted to intracellular endosomal space



c. intracellular space

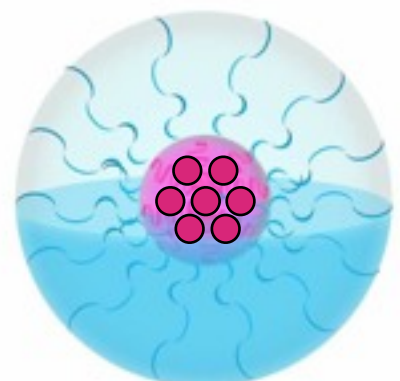
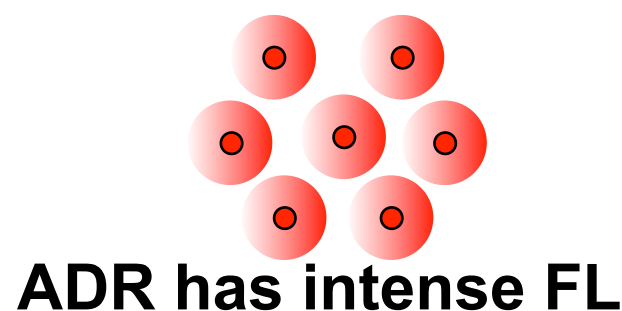
Observation of intracellular drug release by fluorescence



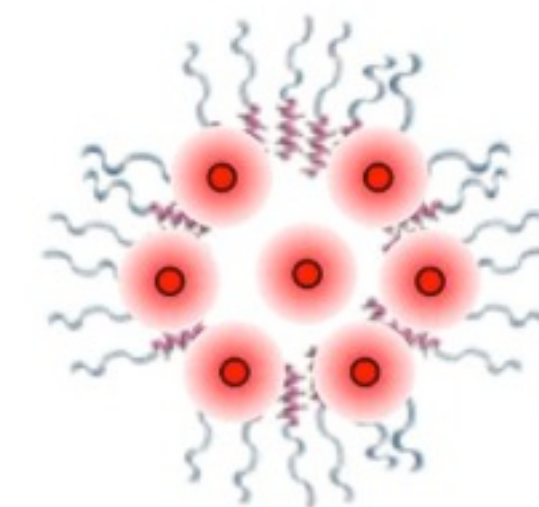
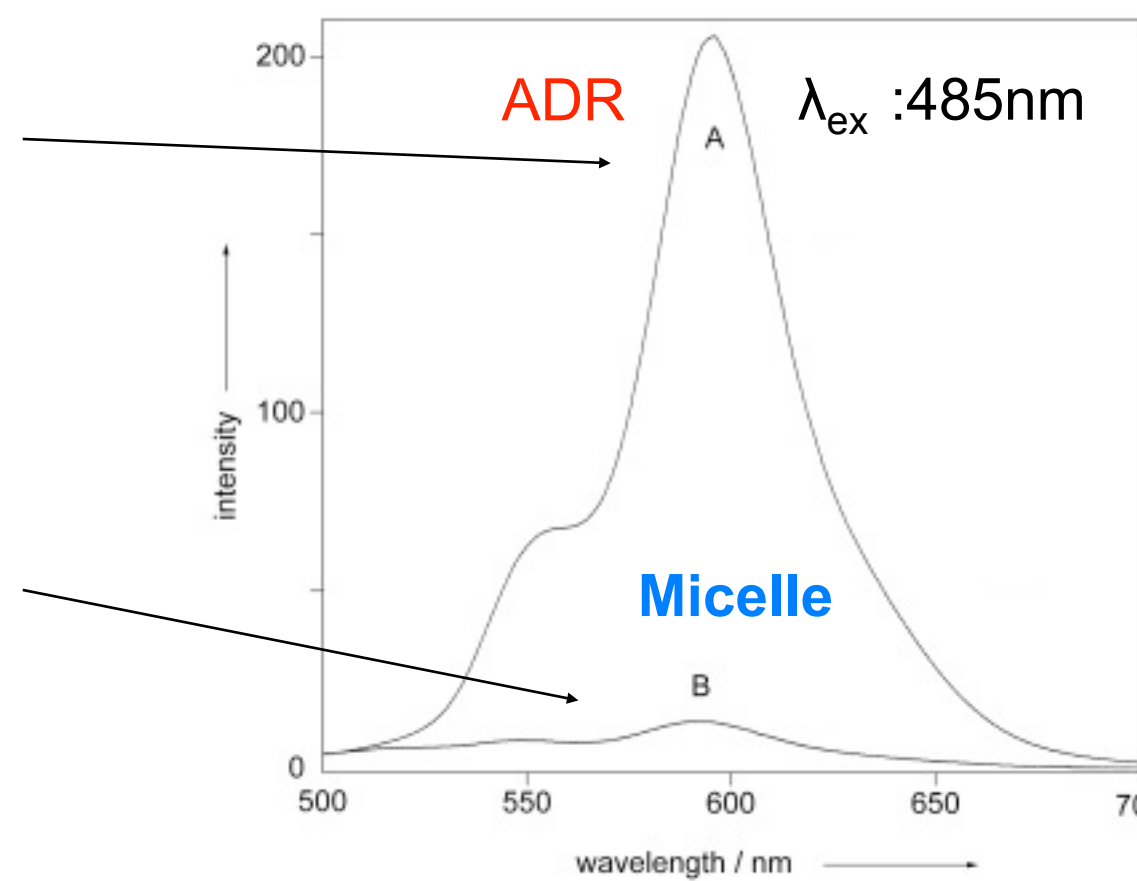
FL remains quenched as long as the micelles are stable

Intracellular localization and drug release of the micelles are detectable

We can expect fate of released drugs in the cell

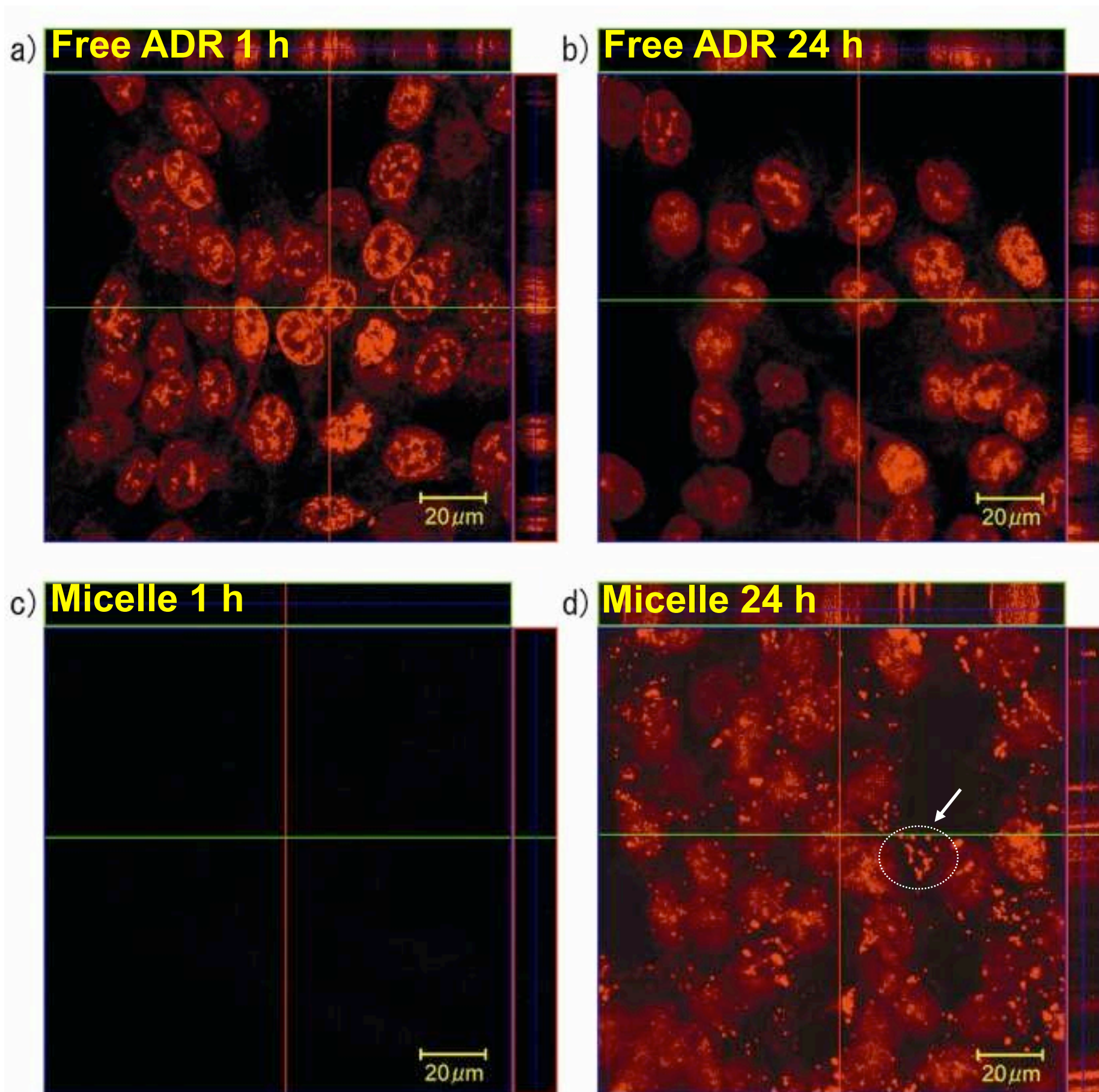


FL is quenched in the micelle core

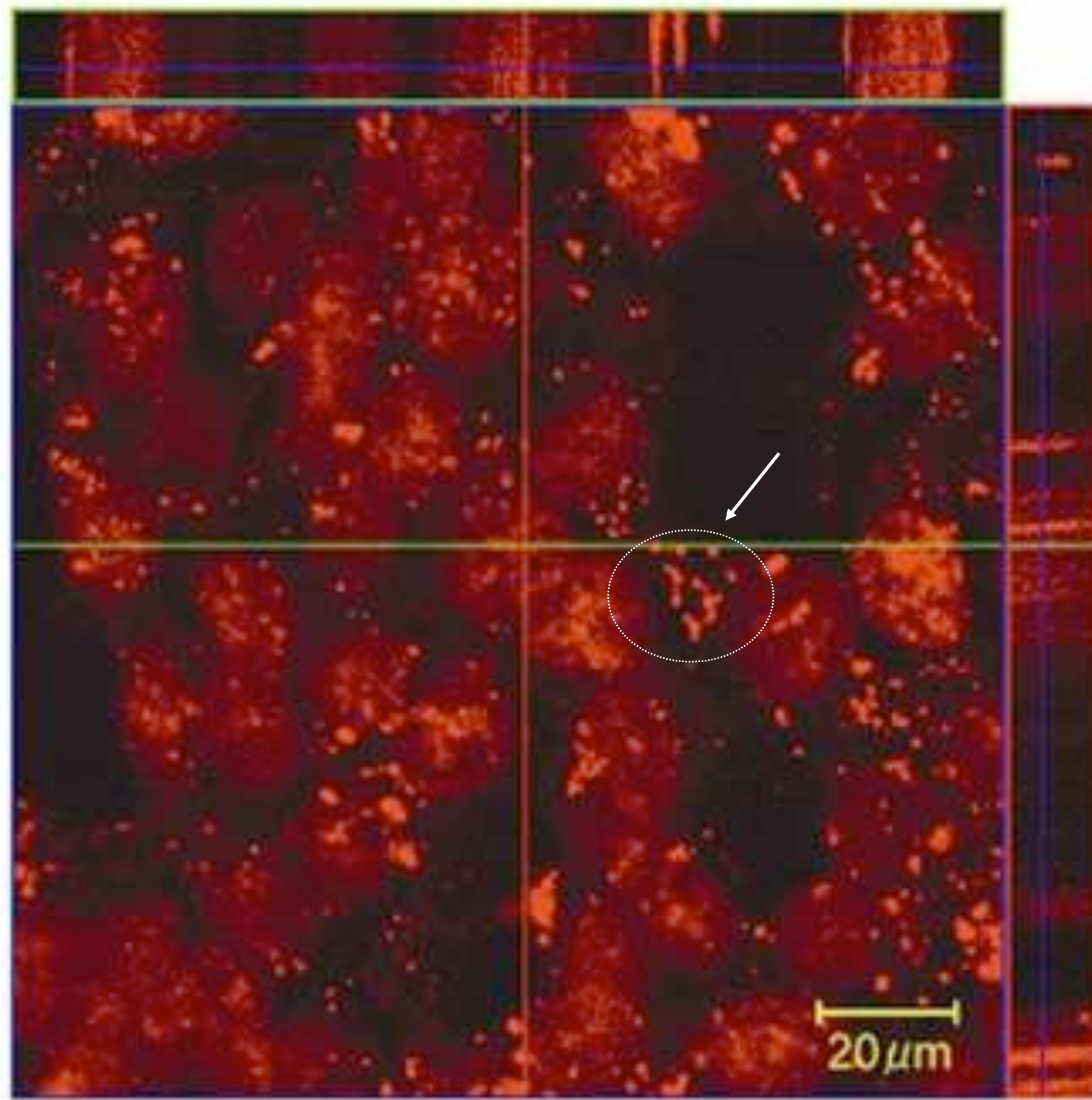


FL becomes detectable with drug release

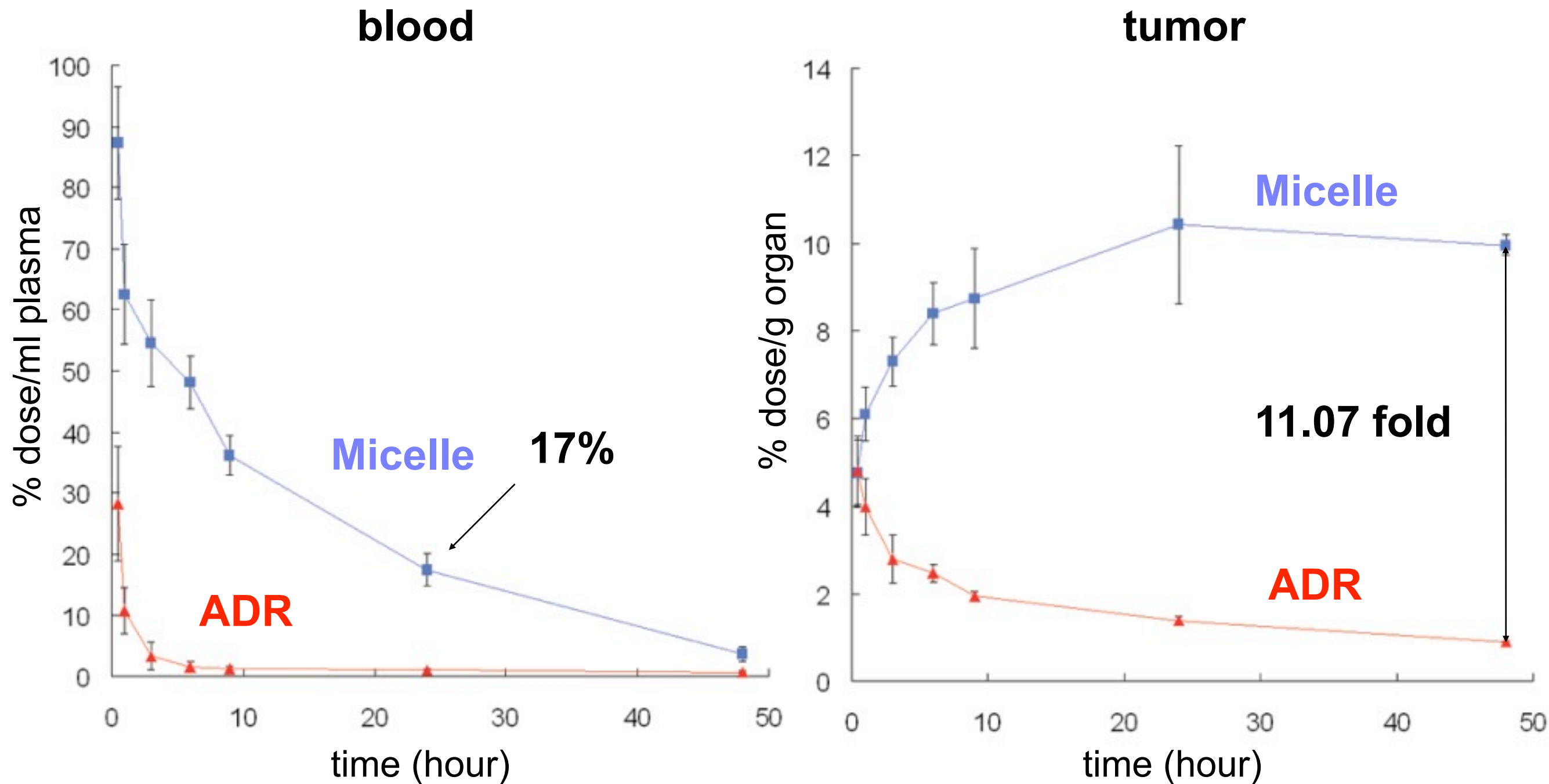
Intracellular distribution of ADR



Intracellular distribution of ADR



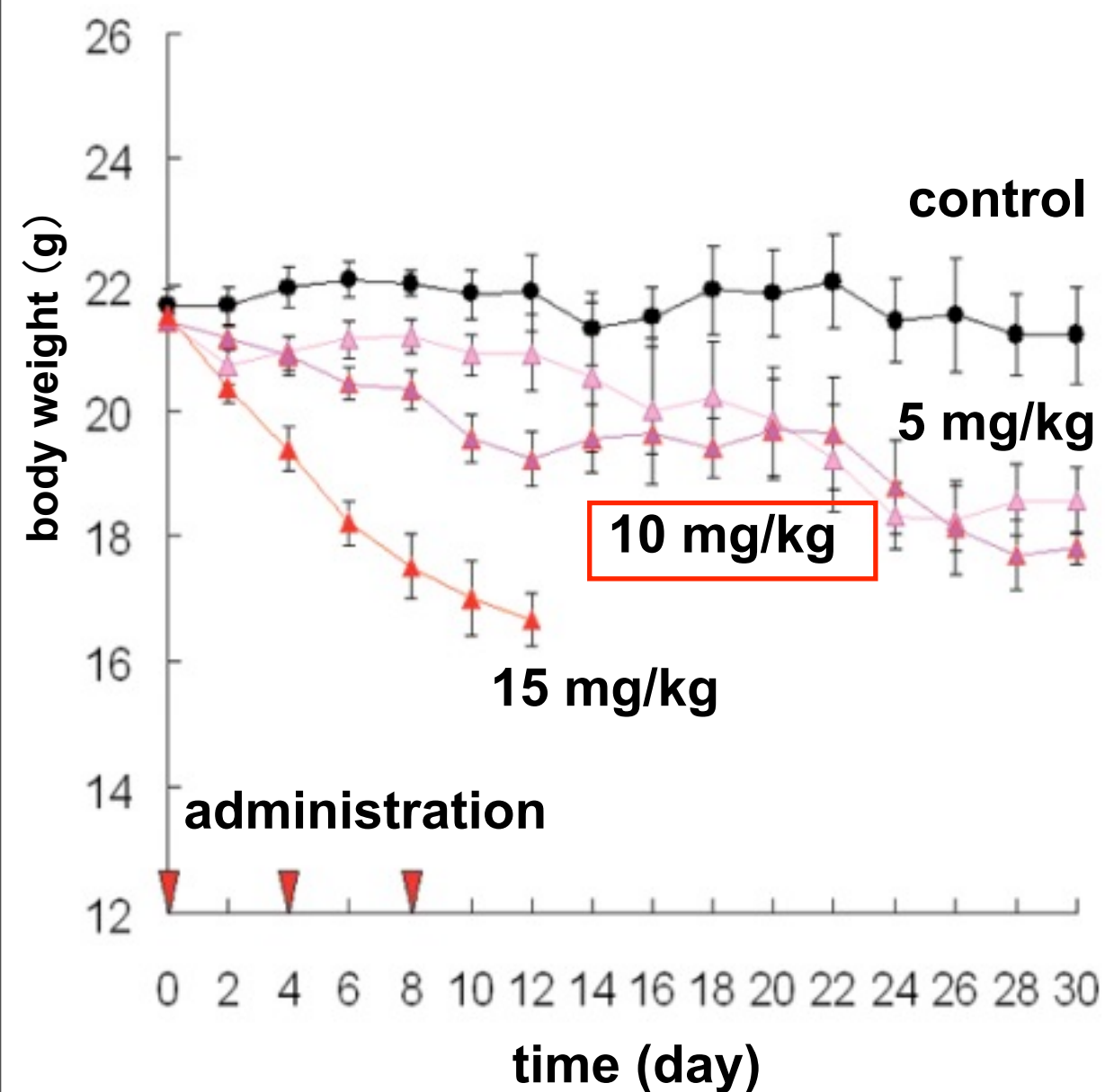
Biodistribution of free and micellar ADR



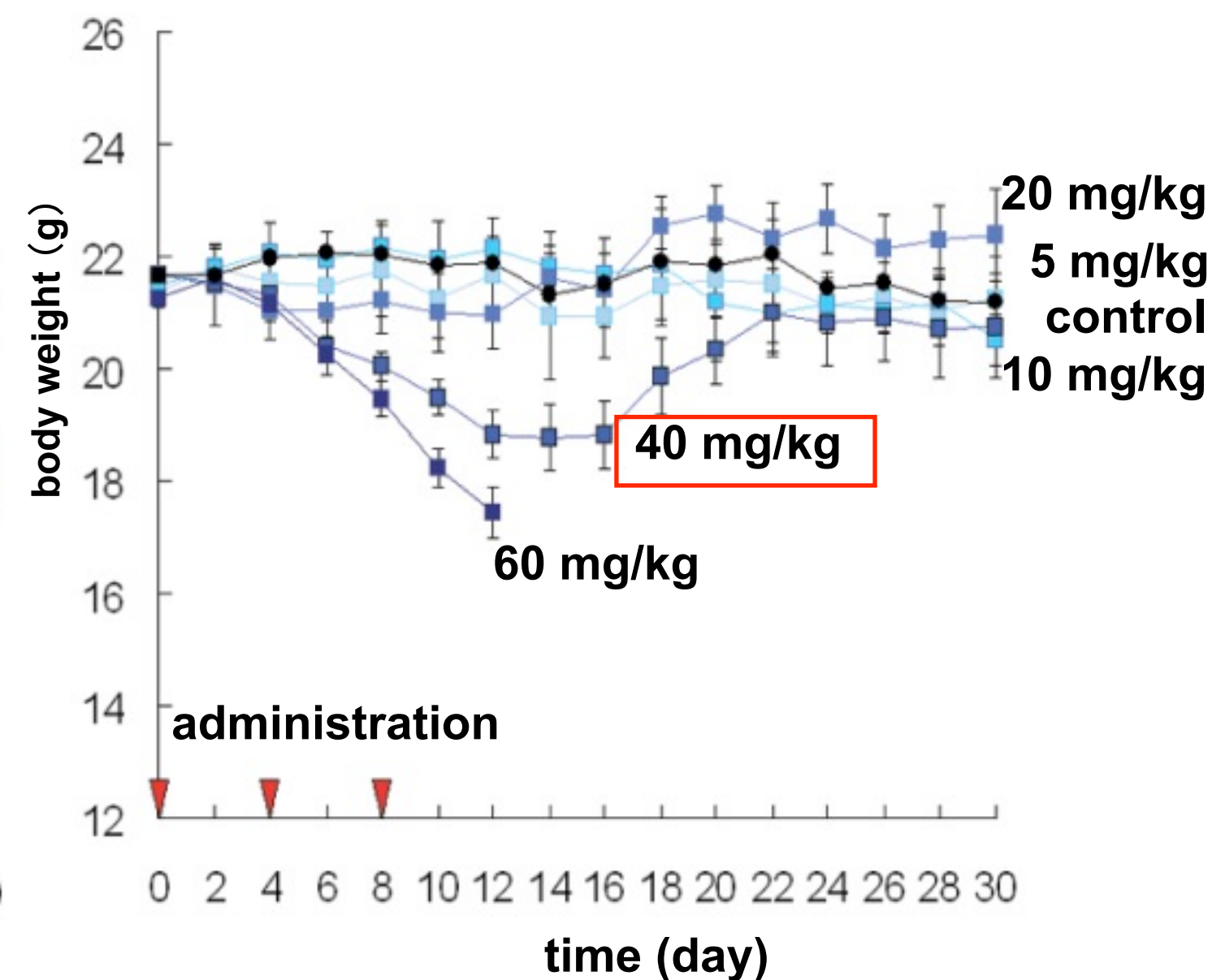
Prolonged circulation and tumor specific accumulation of micellar ADR

In vivo toxicity (body weight change) of free-ADR and micellar-ADR

Free-ADR



Micellar-ADR



Micellar-ADR exhibited more than 4 times higher MTD compared to free-ADR

In vivo antitumor activity

sample	dose (mg/kg) ^a	body weight change on day 30 (%) ^b	toxic death	duration days of tumor growth ^c	complete cure
control	0	-2.18±1.74	0/6	3.74	0/6
ADR	5	-13.35±0.59	0/6	4.21	0/6
	10	-16.84±1.26	0/6	14.59	1/6
	15	—	6/6	—	—
Micelles	5	-0.89±1.68	0/6	3.88	0/6
	10	-4.51±1.44	0/6	3.97	0/6
	20	3.13±1.60	0/6	22.05	2/6
	40	-4.07±0.92	0/6	27.83	3/6
	60	—	6/6	—	—

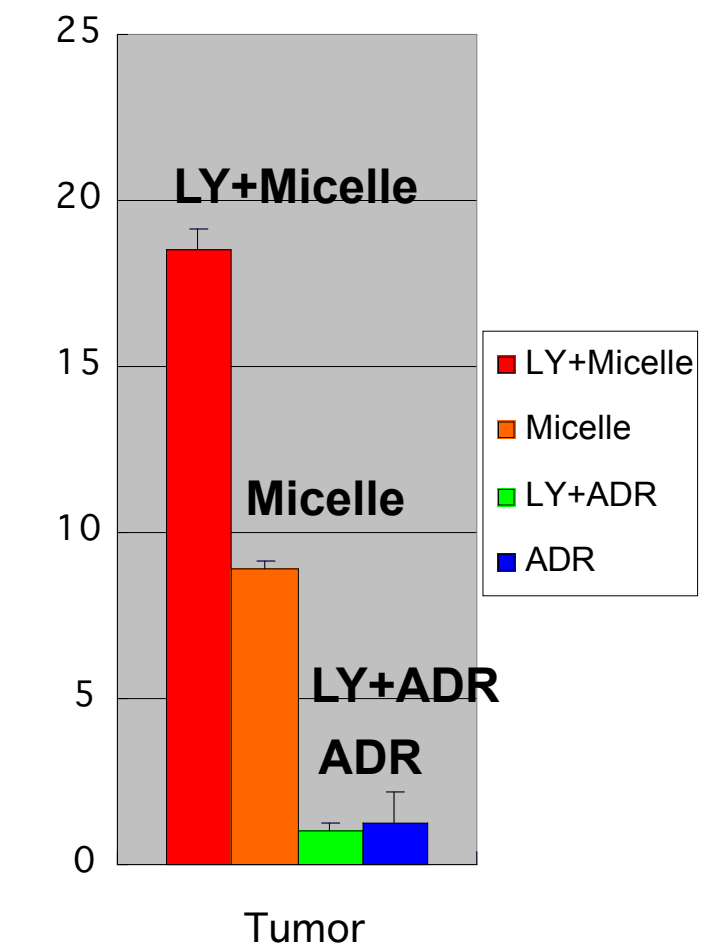
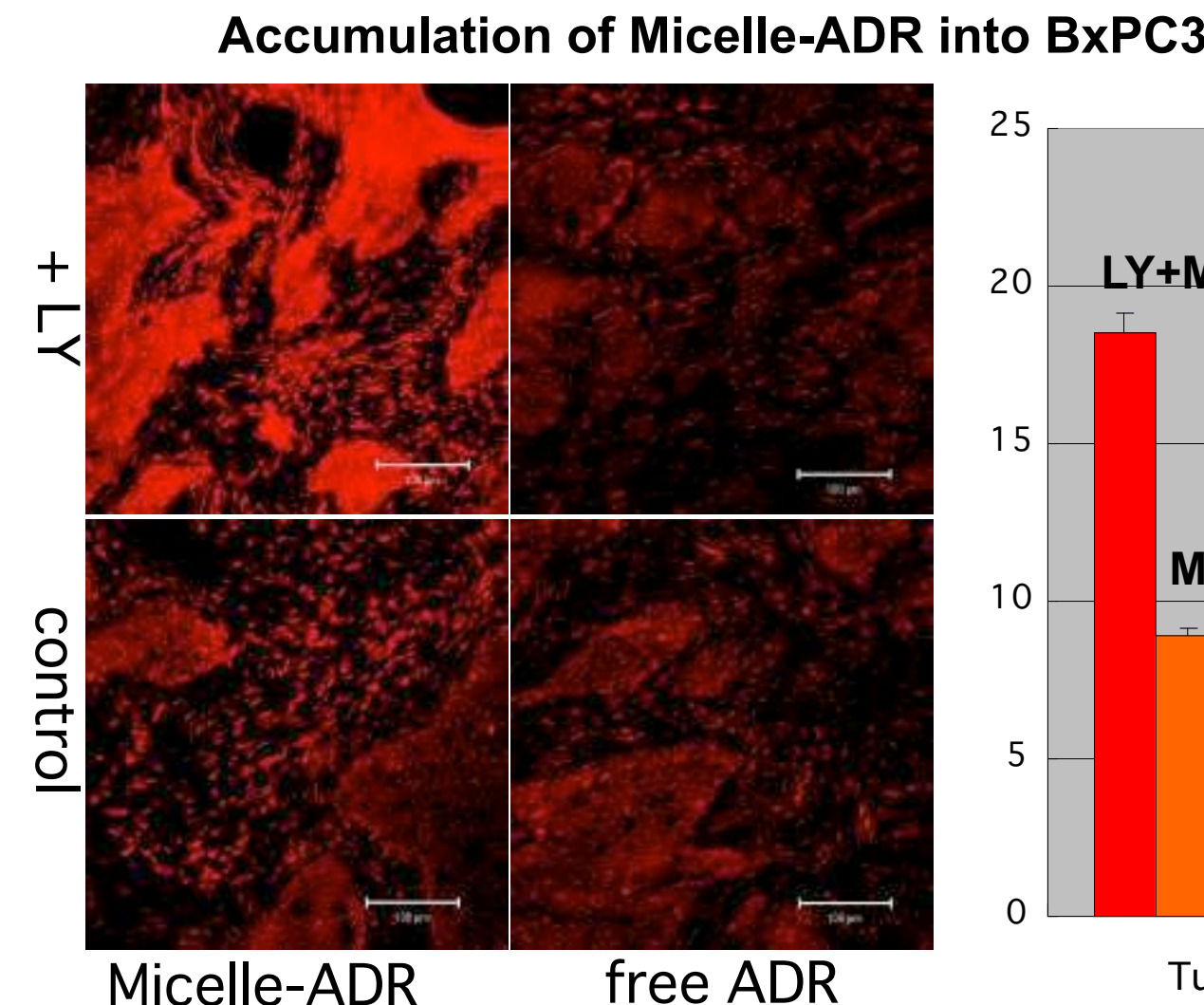
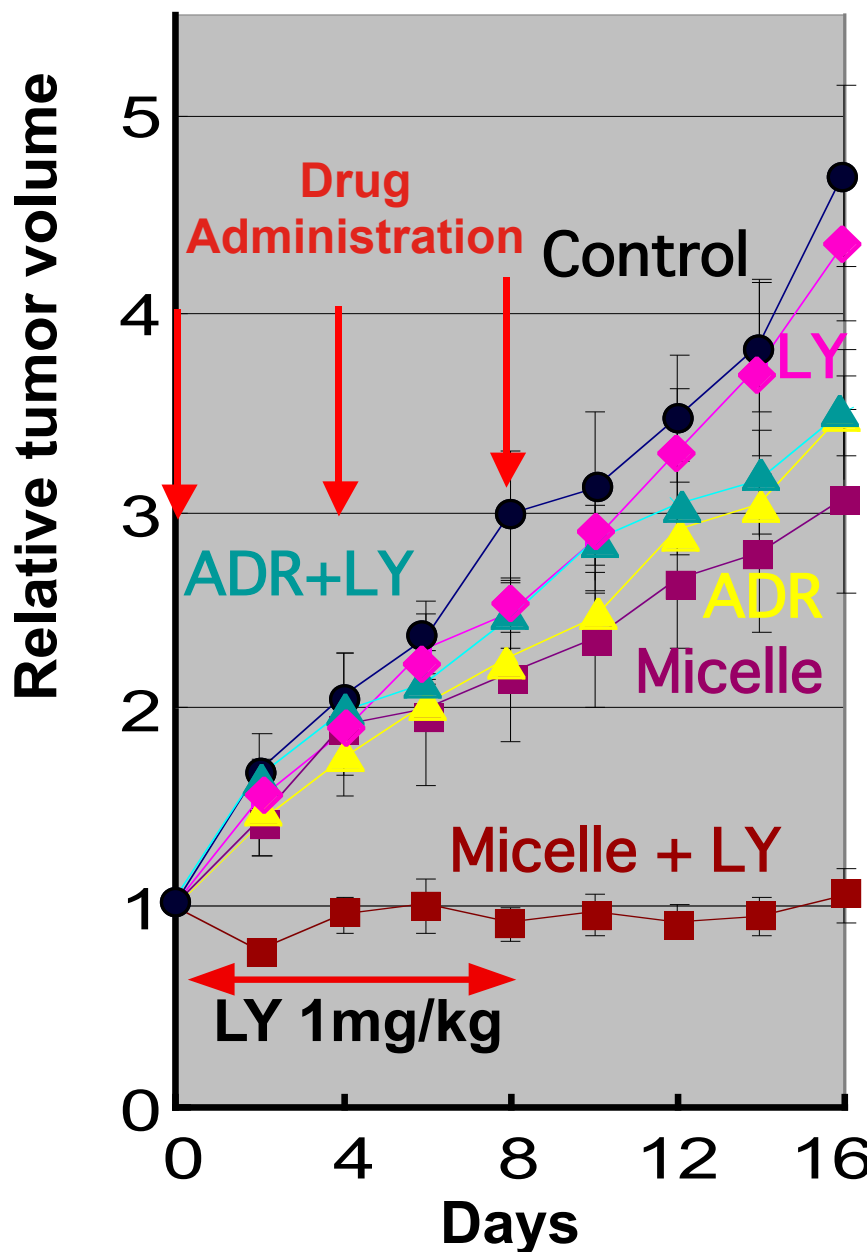
^aAdministrations were carried out three times with a 4-day interval, and doses were determined in free ADR equivalents.

^bBody weights were measured on day 30 after the first injection to compare long-term toxicity between ADR and the micelles. Values are expressed as mean±SEM.

^cDuration to reach 5-fold initial tumor volume.

Treatment of intractable pancreatic cancer by pH-sensitive polymeric micelles

Human pancreatic cancer(BxPC3)
(characterized by hypovascularity
and thick fibrosis)



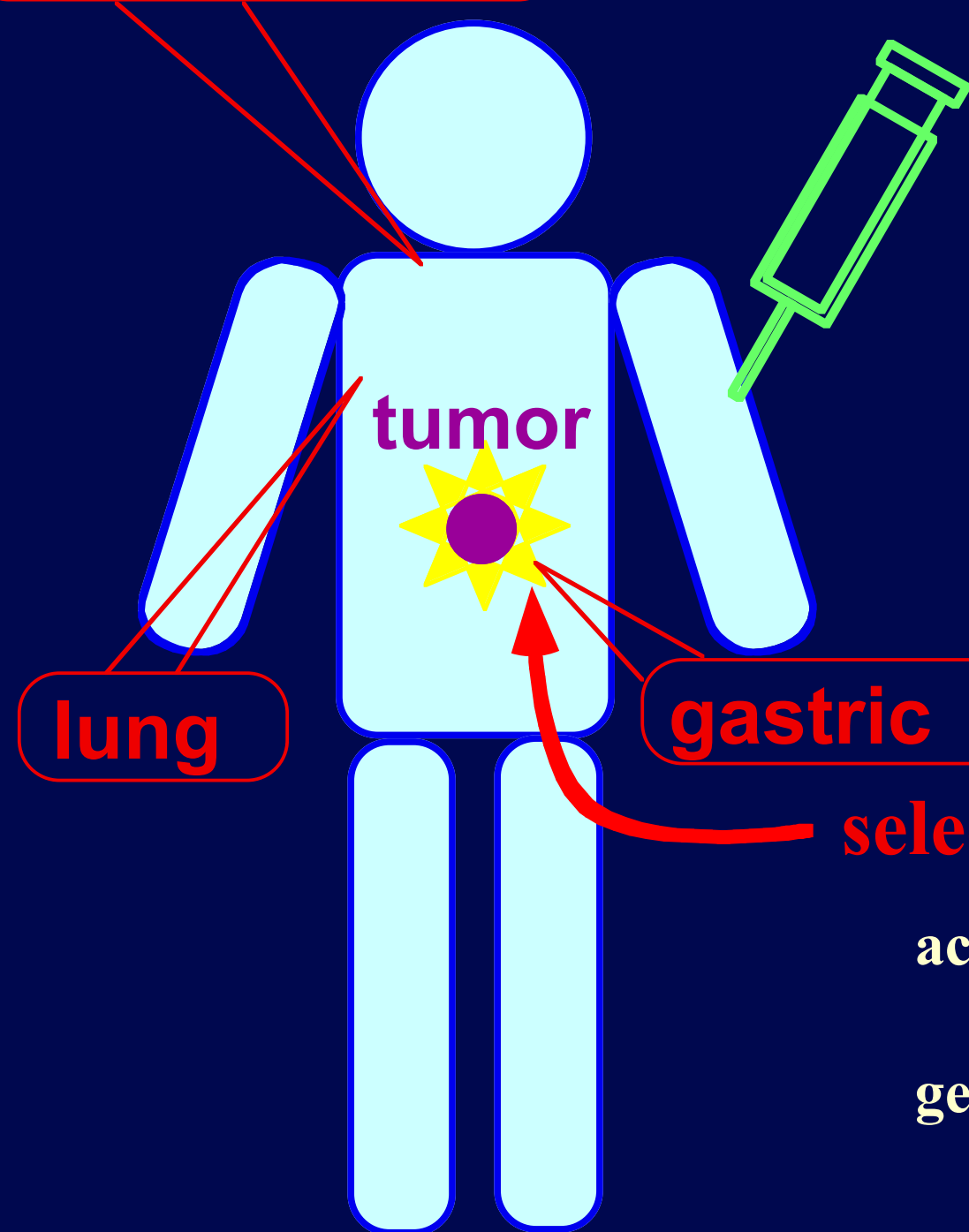
LY: TGF- β inhibitor

(Reagent to transiently increase
the permeability of tumor capillary)

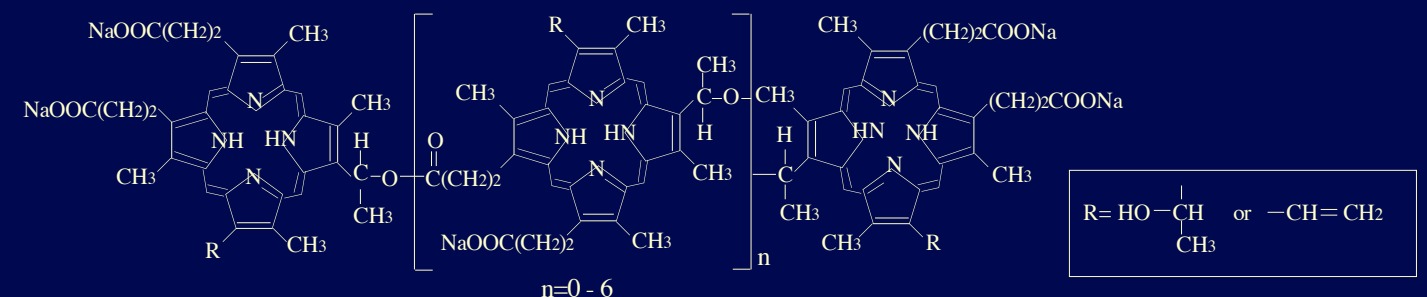
Photodynamic therapy (PDT)

esophageal

i.v. administration of photosensitizer



(A) Photofrin (PII)



(B) metallo-phthalocyanines (MePc)



selective irradiation of light

activation of photosensitizer

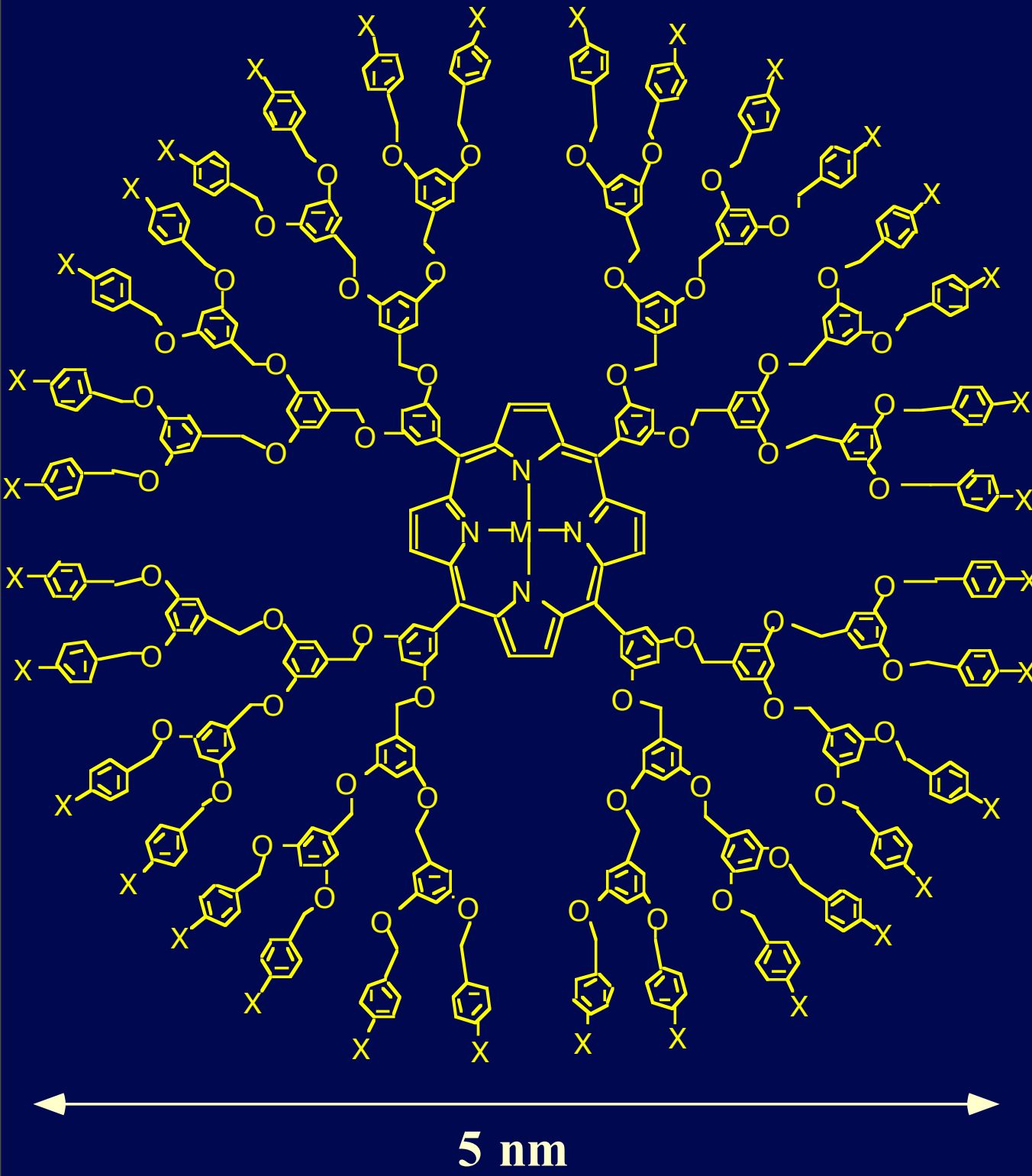


generation of highly reactive oxygen species



selective toxicity in tumor

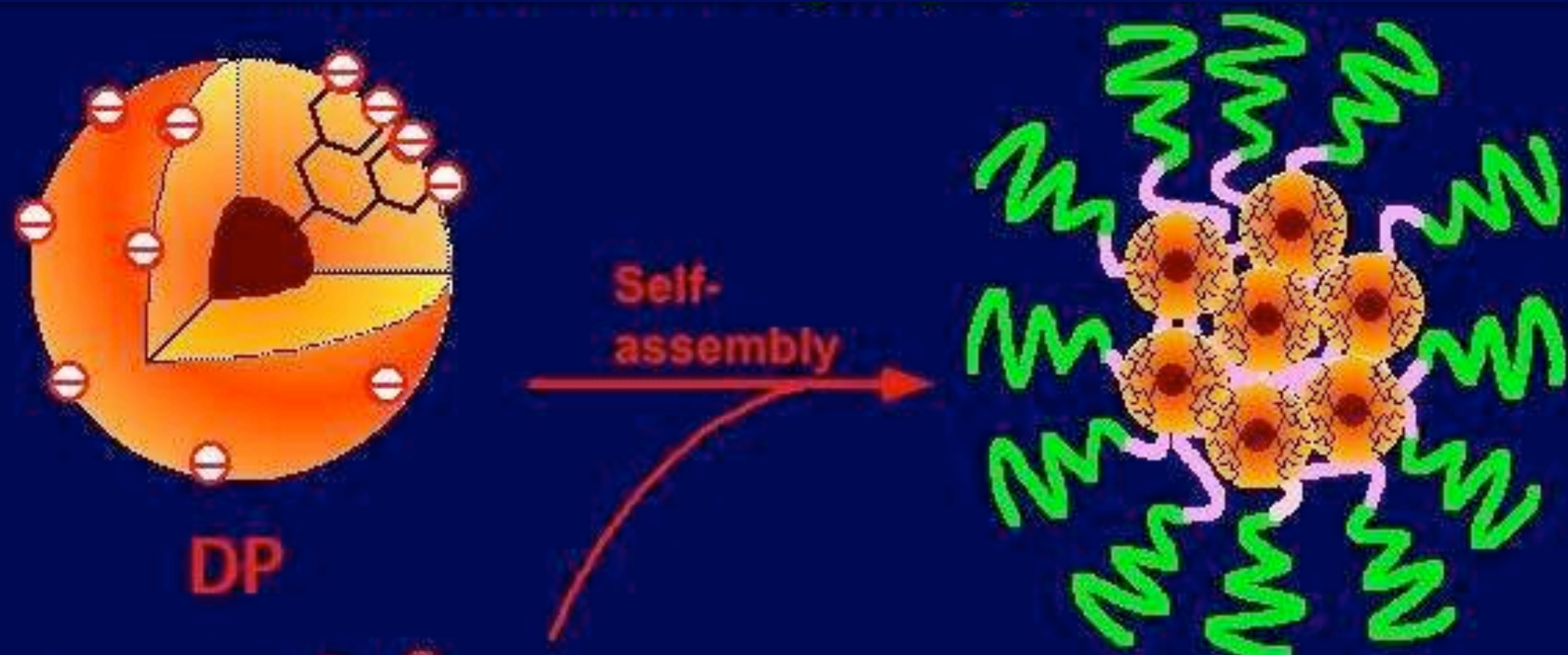
Ionic dendrimer porphyrins (DP) as a novel type of photosensitizer



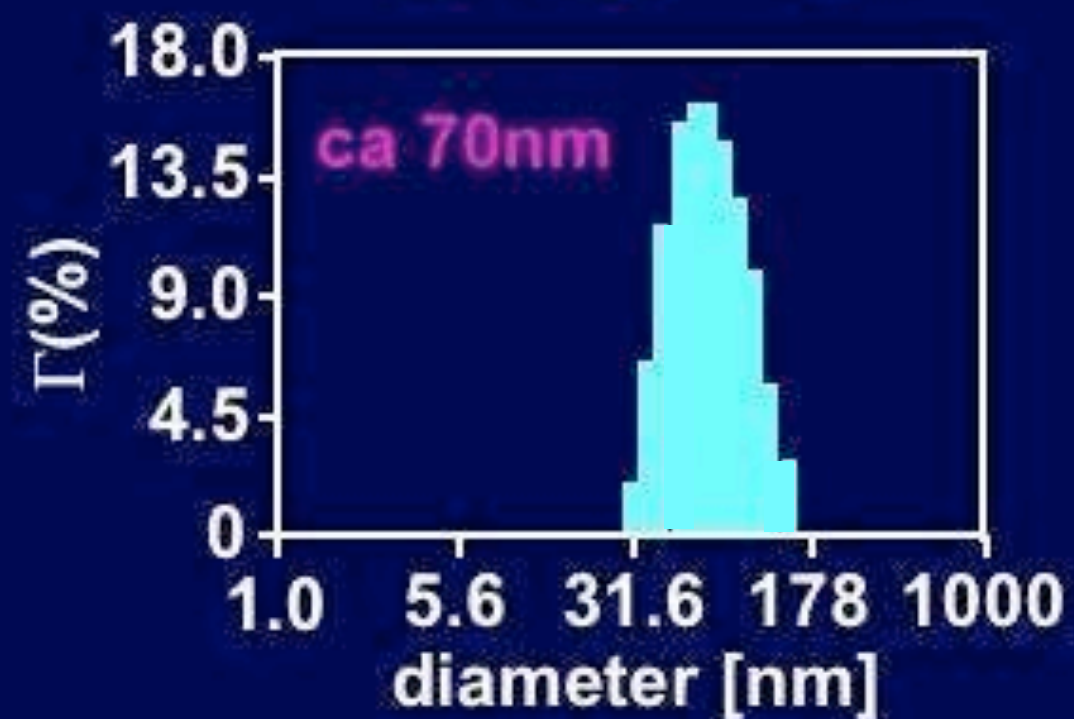
- **P32(+)DPZn:**
 $X=CONH(CH_2)_2NMe_3^+Cl^-$ 1)
or $CONH(CH_2)_2NH_3^+Cl^-$ 2)
 $M=Zn$
- **P32(-)DPZn:**
 $X=COO^-K^+$ 1)
 $M=Zn$

- 1) Sadamoto, R.; Tomioka, N.; Aida, T. *J. Am. Chem. Soc.* 1996, 118, 3978-3979
- 2) Zhang, G.; Kataoka, K.; et al, *Macromolecules*, 2003, 36, 1304-1309

Polyion complex (PIC) micelles incorporating ionic dendrimer porphyrin (DP)

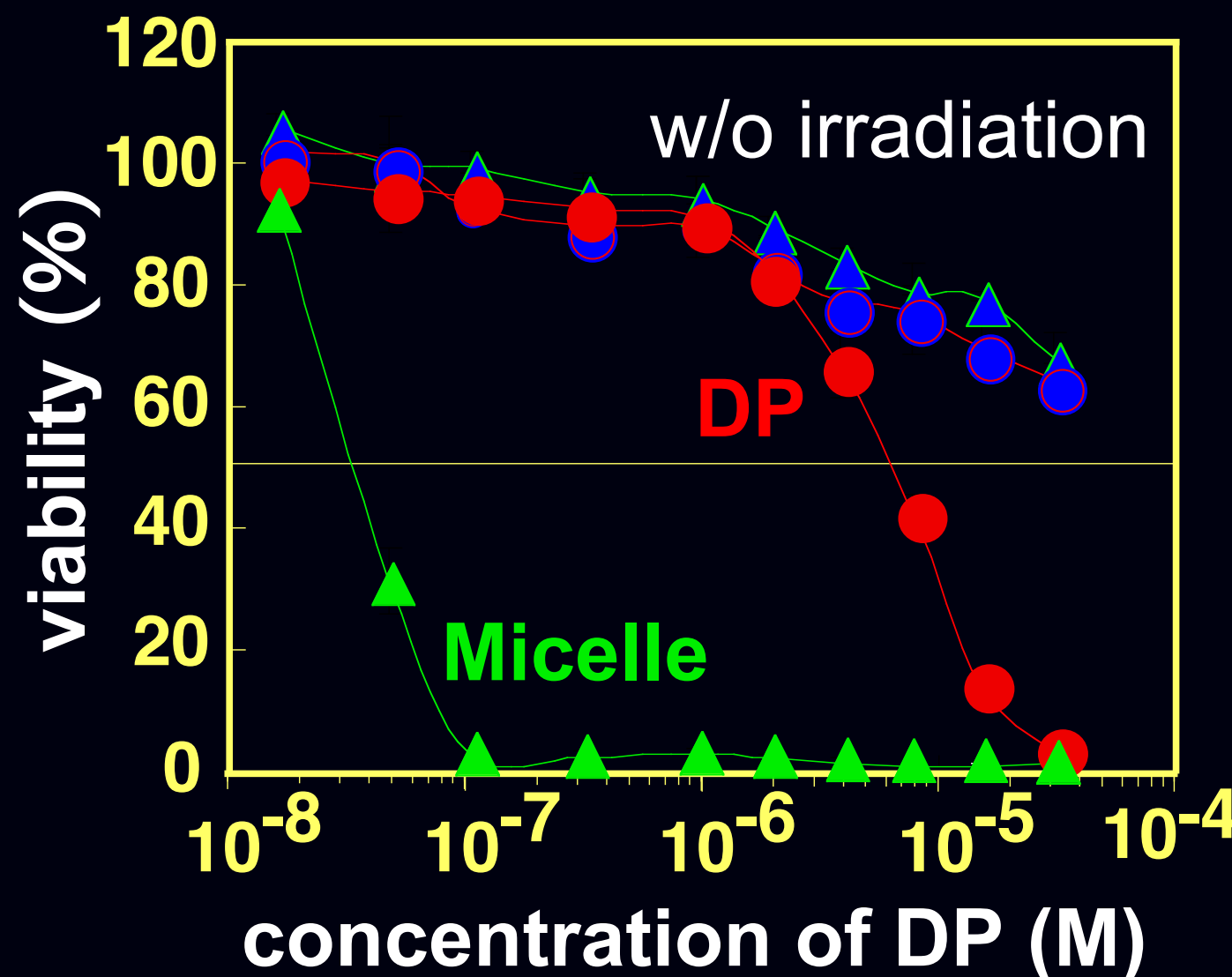


High stability against salt concentration ($>300\text{mM}$) and pH (6 - 8.5)



Photocytotoxicity of DP and DP-incorporated micelles

photocytotoxicity (LLC cells)



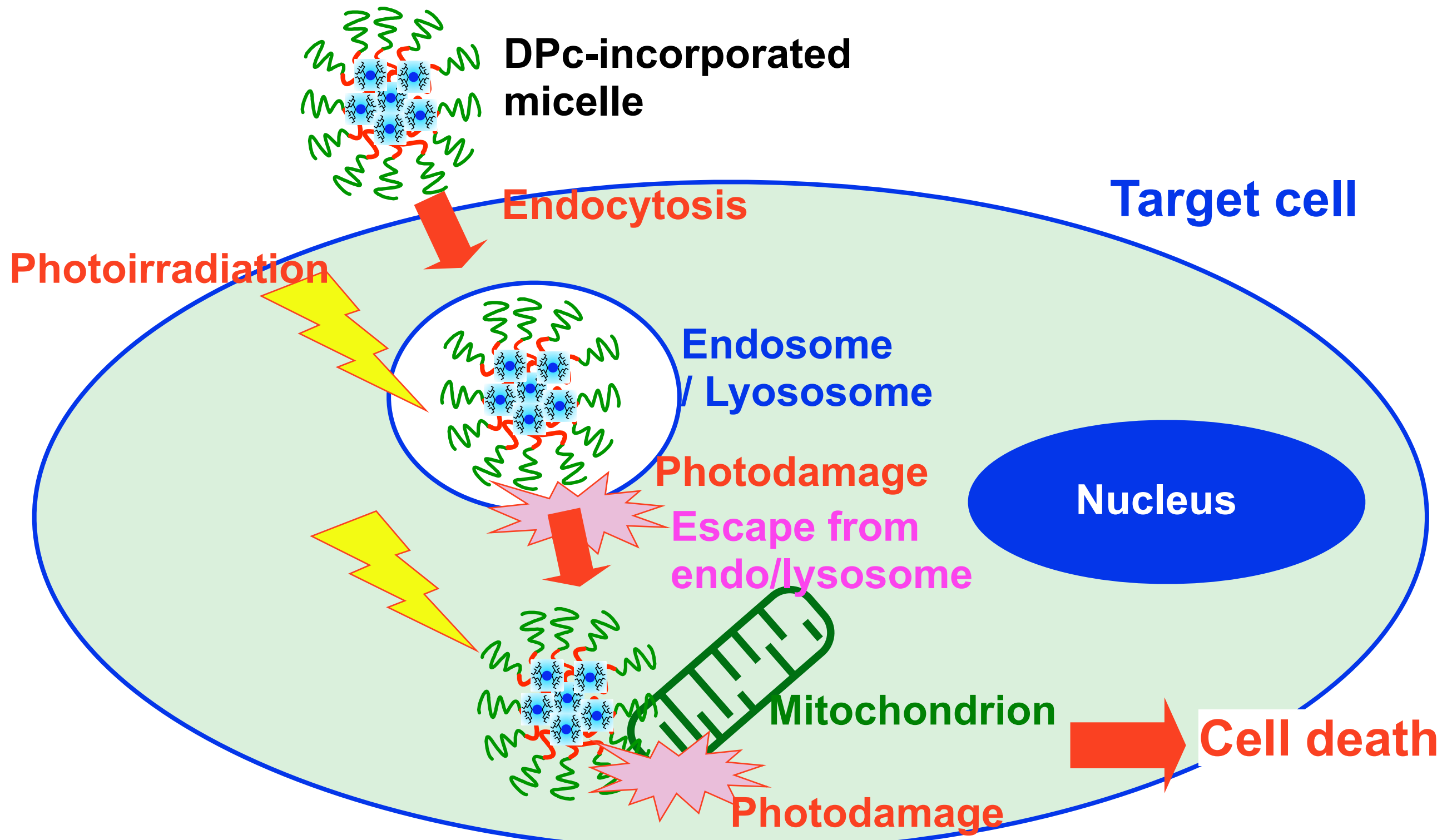
Incorporation of DP into the micelle achieved approximately 280-fold increase in photocytotoxicity.

This result ensures safety after PDT, because the micelle is assumed to dissociate finally.

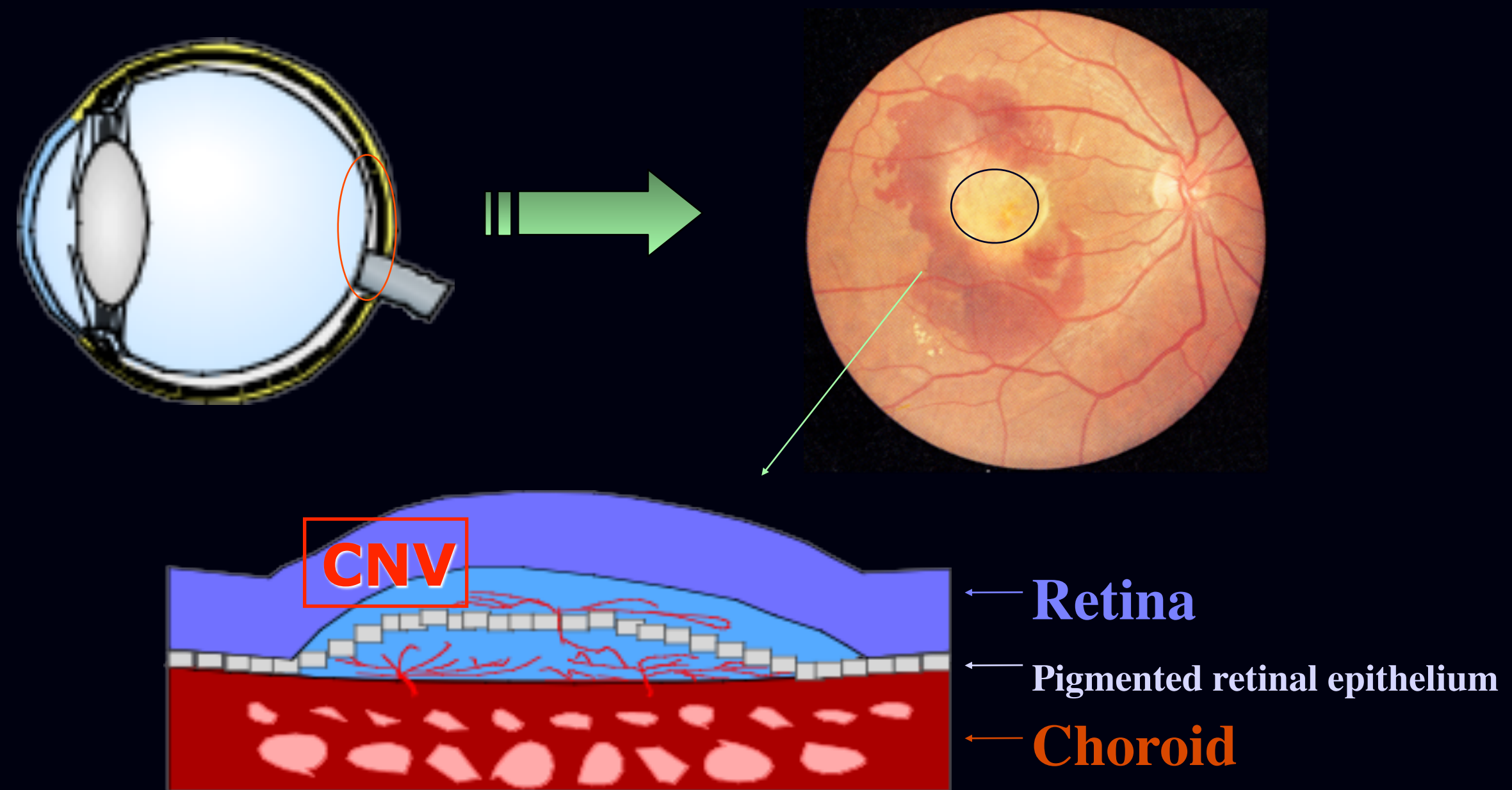
6hr incubation → wash with PBS
→ irradiation → 48hr incubation

Hypothetic Mechanism of Cell Death

endocytic uptake → photochemical disruption of endosomal membrane
→ endosomal escape → interactions with mitochondrial membranes and their photochemical disruption



Exudative age-related macular degeneration (wet AMD) is characterized by choroidal neovascularization (CNV), and is a major cause of visual loss in developed countries.



% of CNV Occlusion

Laser Intensity (J/cm ²)	CNV Occlusion [%]			
	1 day after PDT		7 days after PDT	
	PIC micelle	Visudyne*	PIC micelle	Visudyne*
5	63.6	--	81.8	--
10	75.0	31	81.3	6
25	88.8	83	83.3	33
50	73.3	54	80.0	36
100	90.9	42	81.8	44

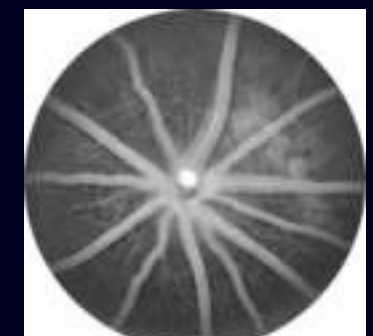
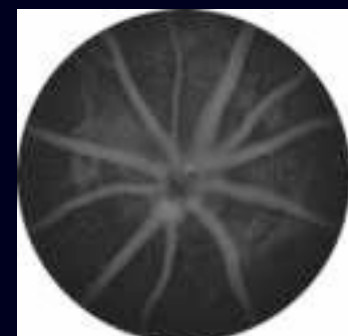
*Zacks et al. IOVS, 2002

Fluorescent imaging of eyeground

Before PDT



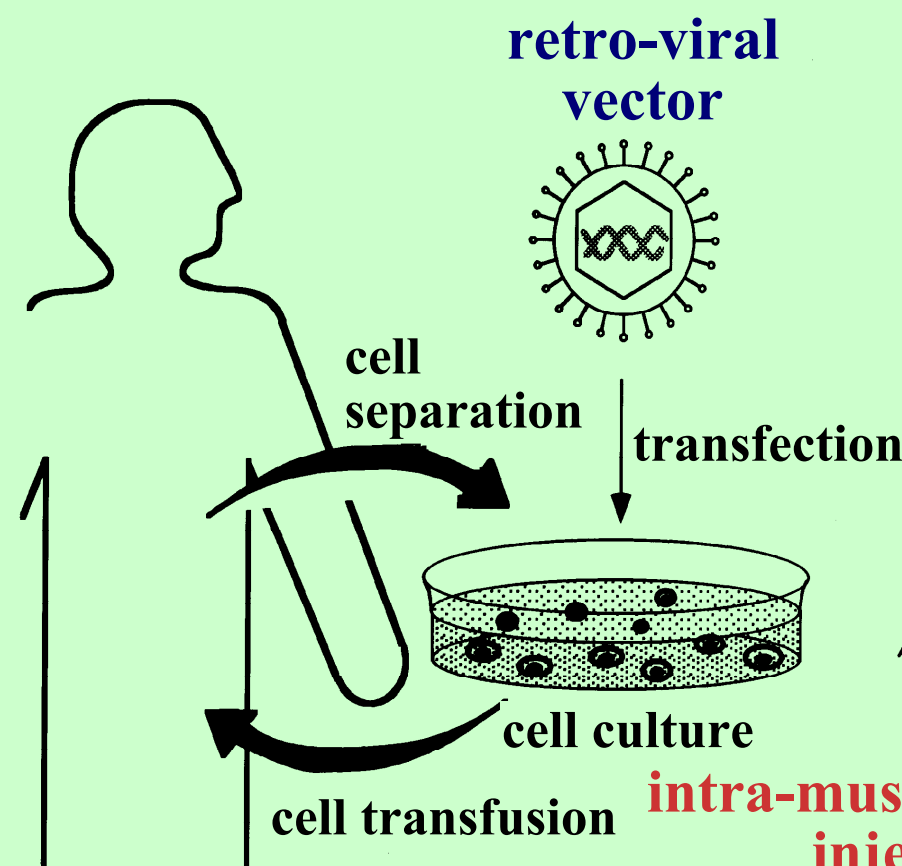
After PDT



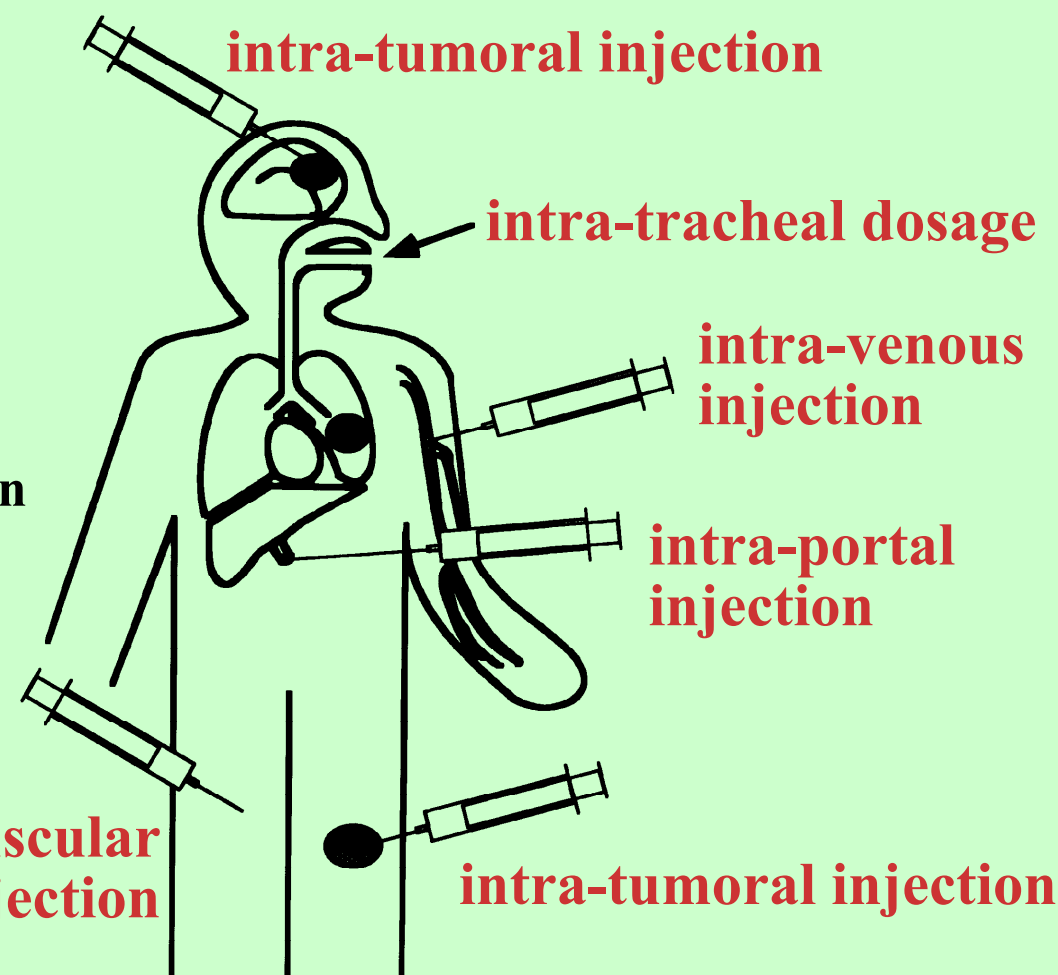
Target diseases for gene therapy

Cancer, Enzyme-deficiency, AIDS, Cardiovascular diseases, Diabetes, Tissue regeneration, etc.

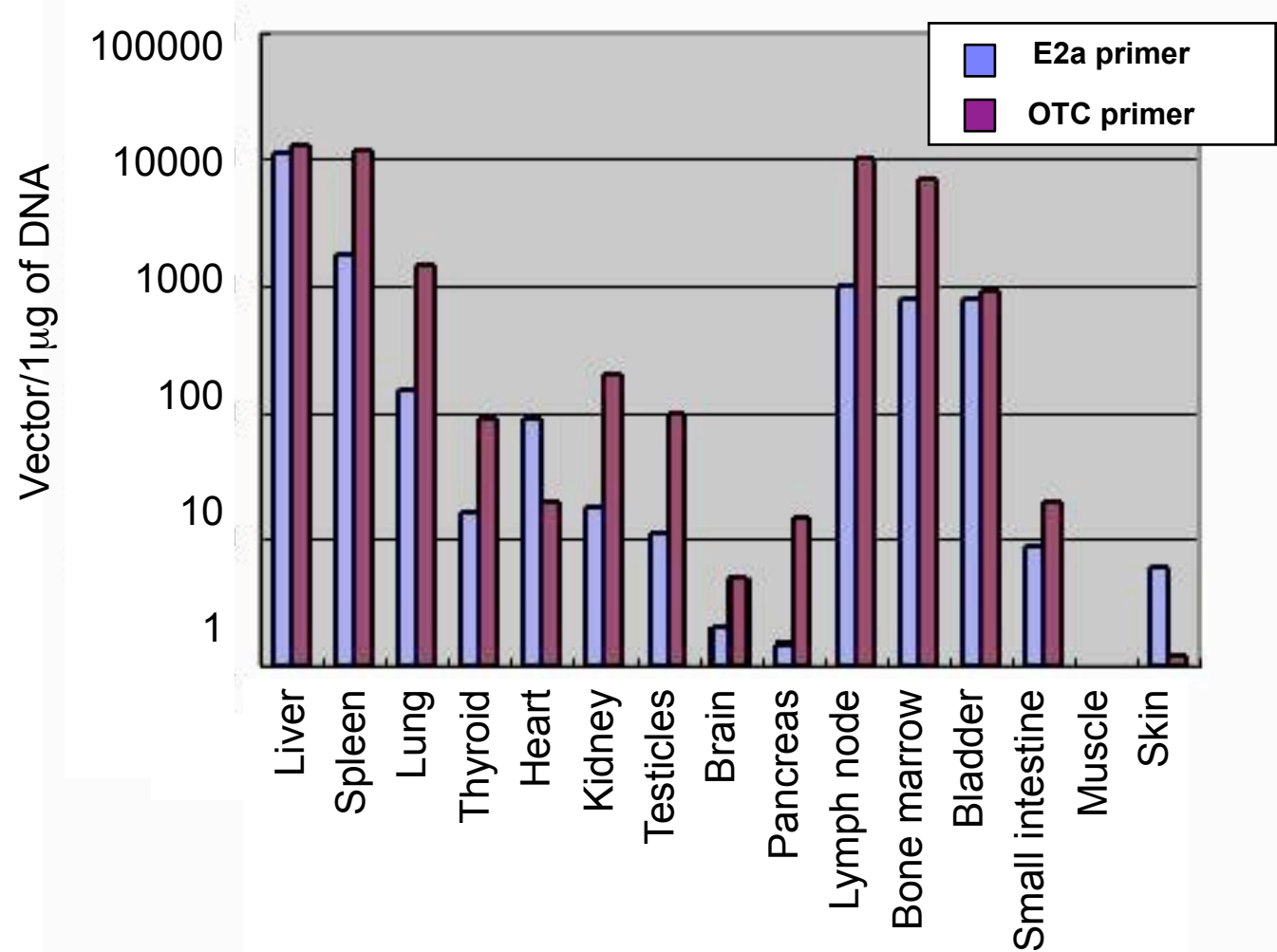
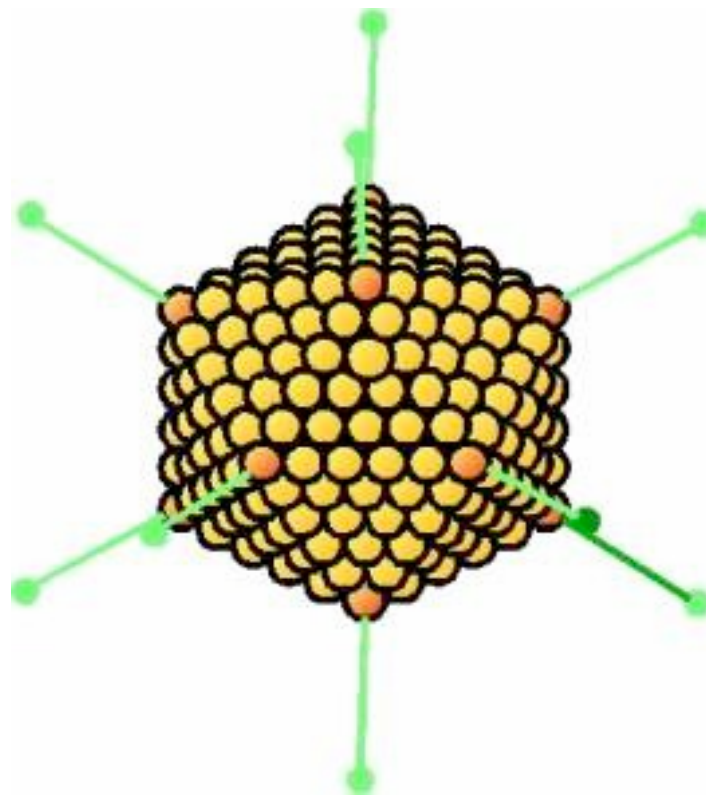
Ex vivo method



In vivo method

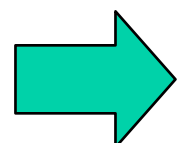


Gene Therapy Death Prompts Review of Adenovirus Vector



Traces of adenovirus DNA (E2a) and a curative gene (OTC).
Patient's target organ is the liver

- Inherent antigenicity
- Limited size in encapsulated gene
- Difficulties in large-size production

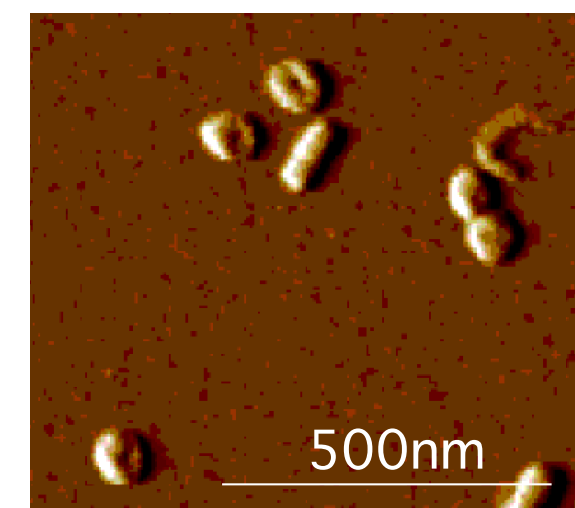
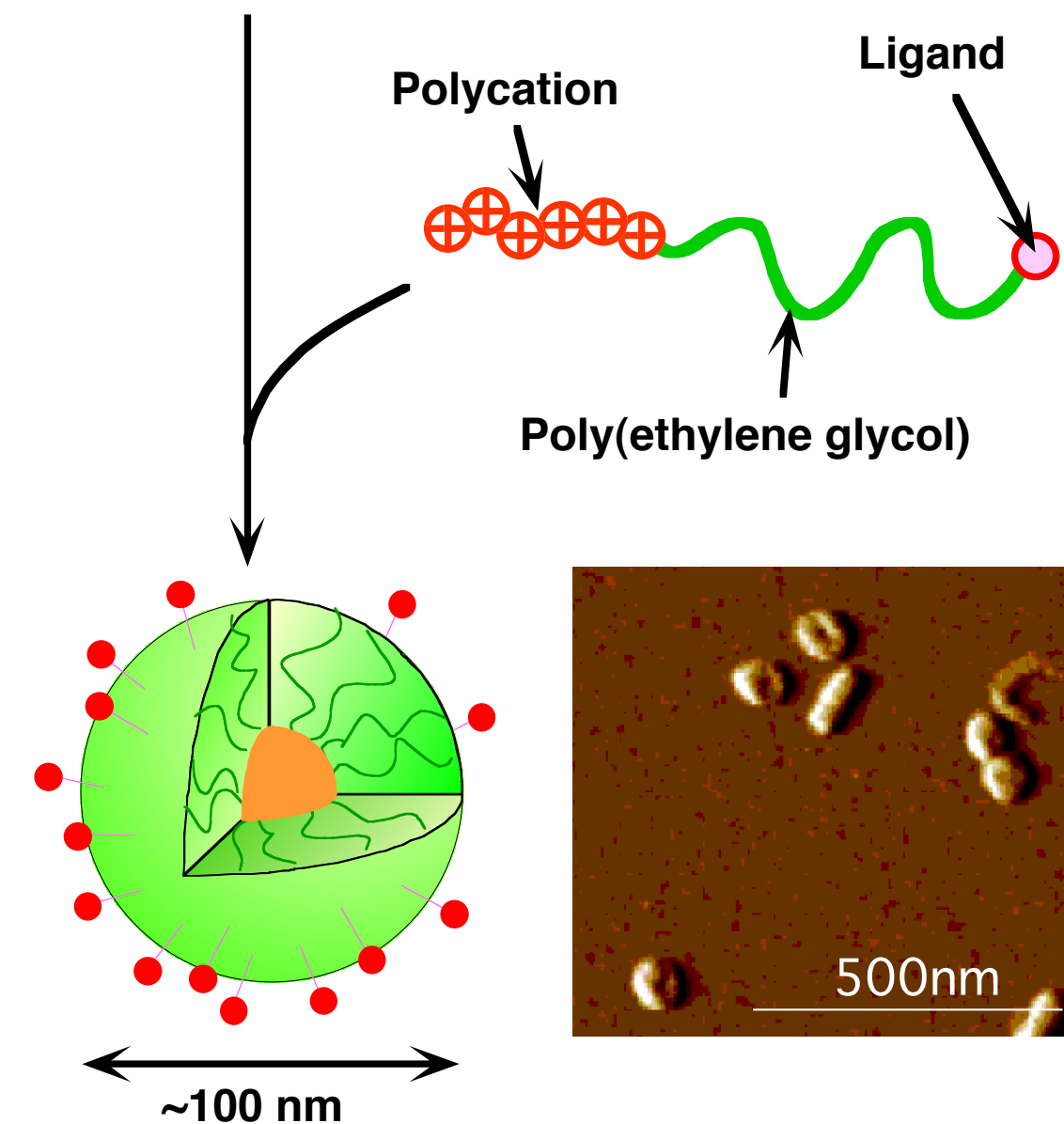
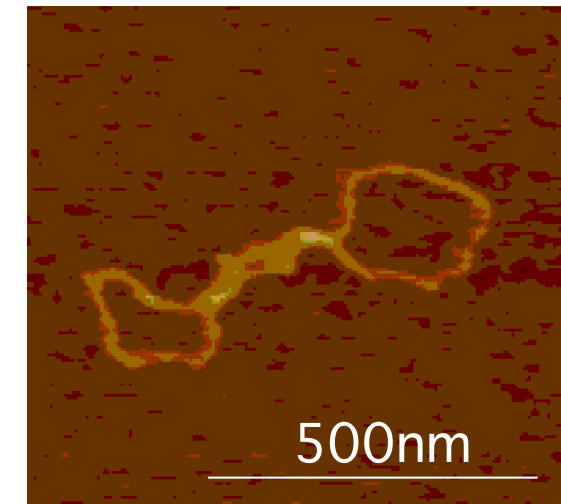
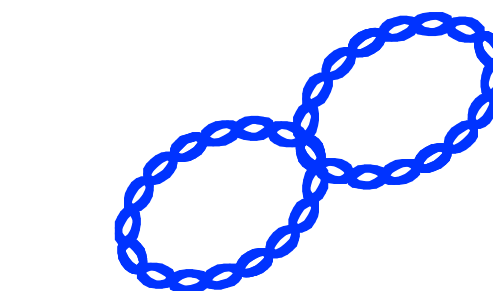
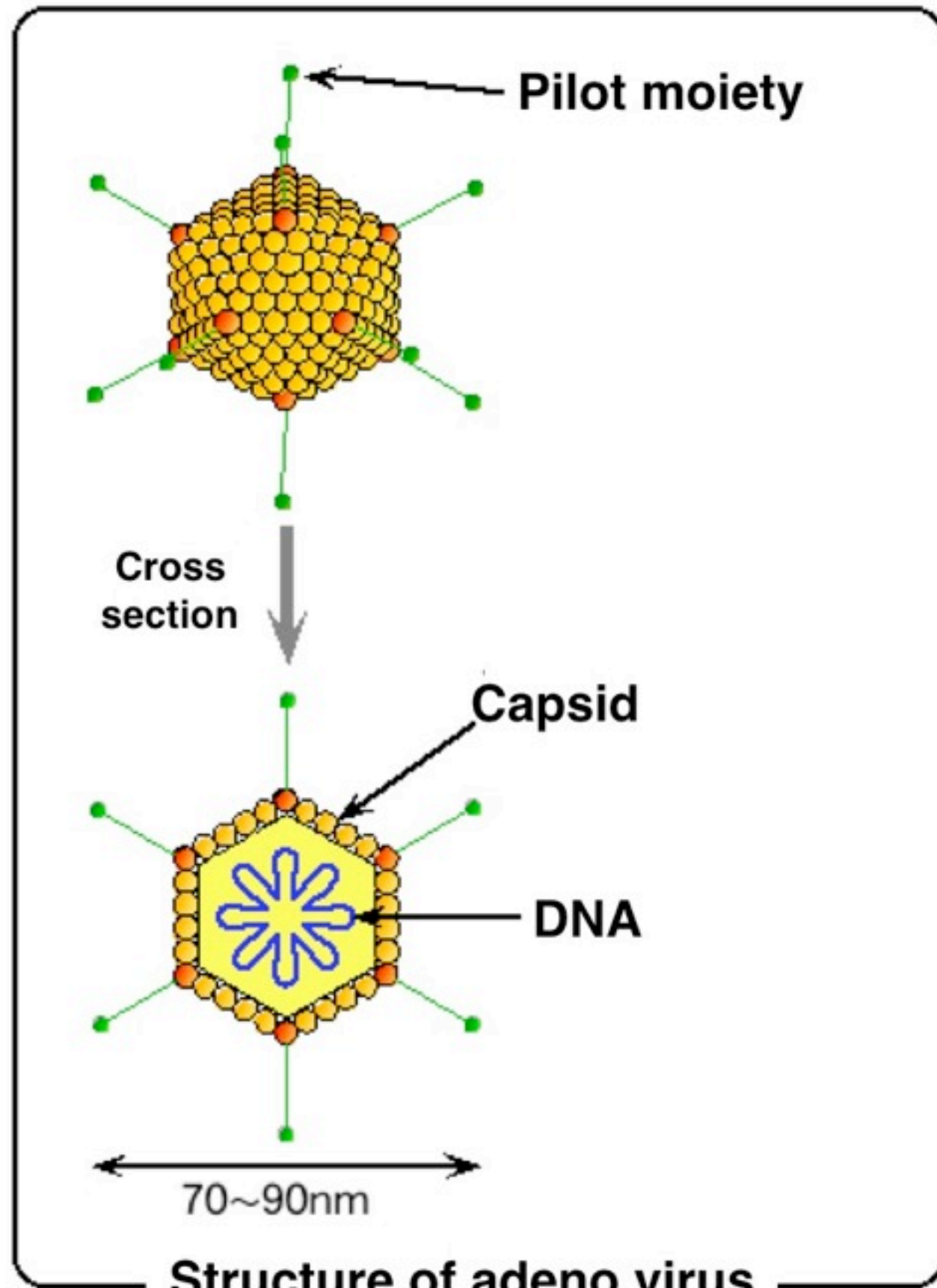


Gene therapy death of patients at University of Pennsylvania on September, 1999

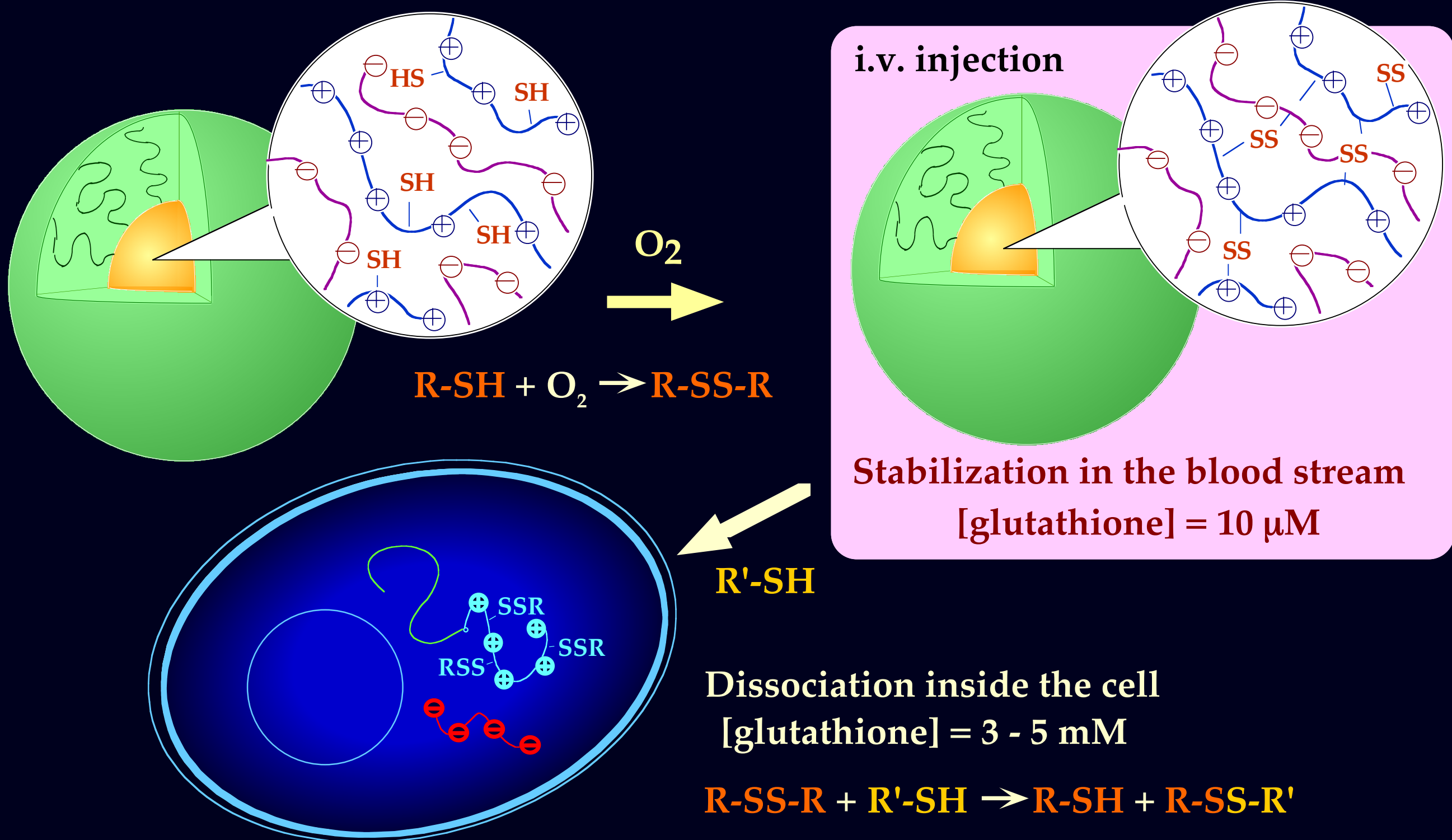
→ 38 trillion virus particles were dosed through i.v. route, yet only 1% of the transferred genes reached the target cells

→ Restricted clinical use of adenovirus vector

pDNA entrapped polymeric micelle for gene delivery

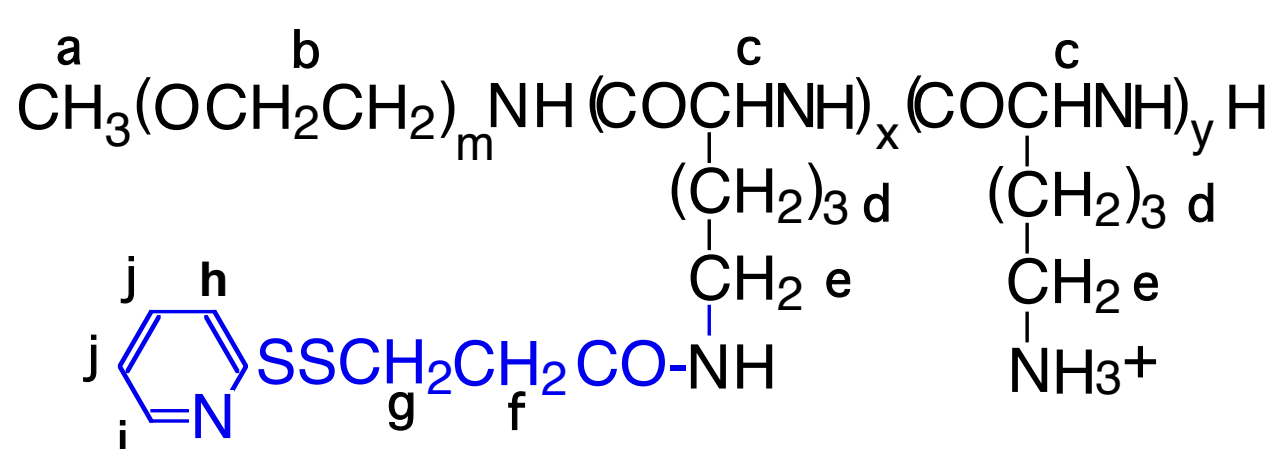
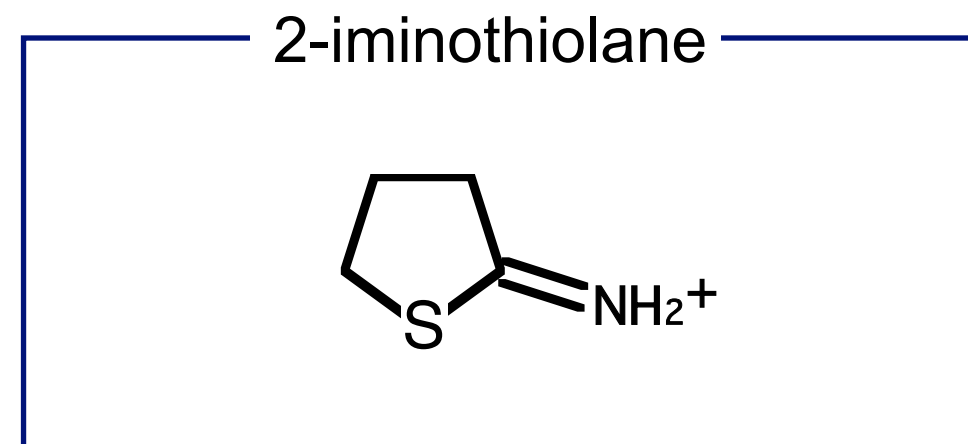
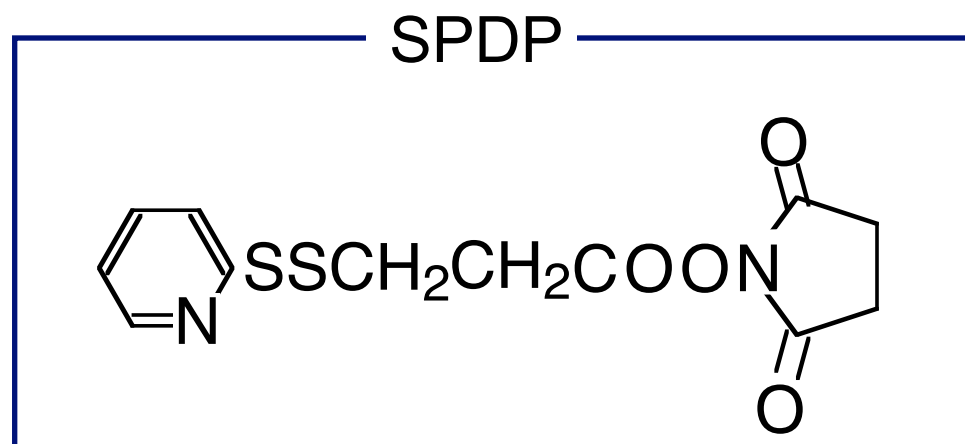


Environment-sensitive stabilization of core-shell structured PIC micelle by reversible cross-linking of the core through disulfide bond

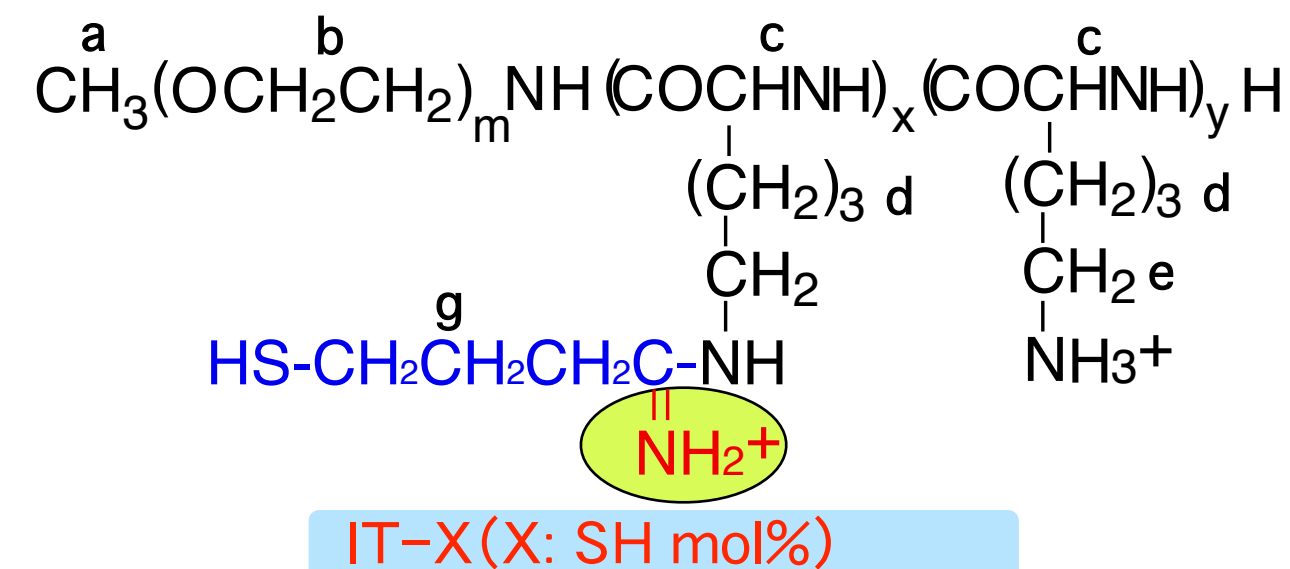
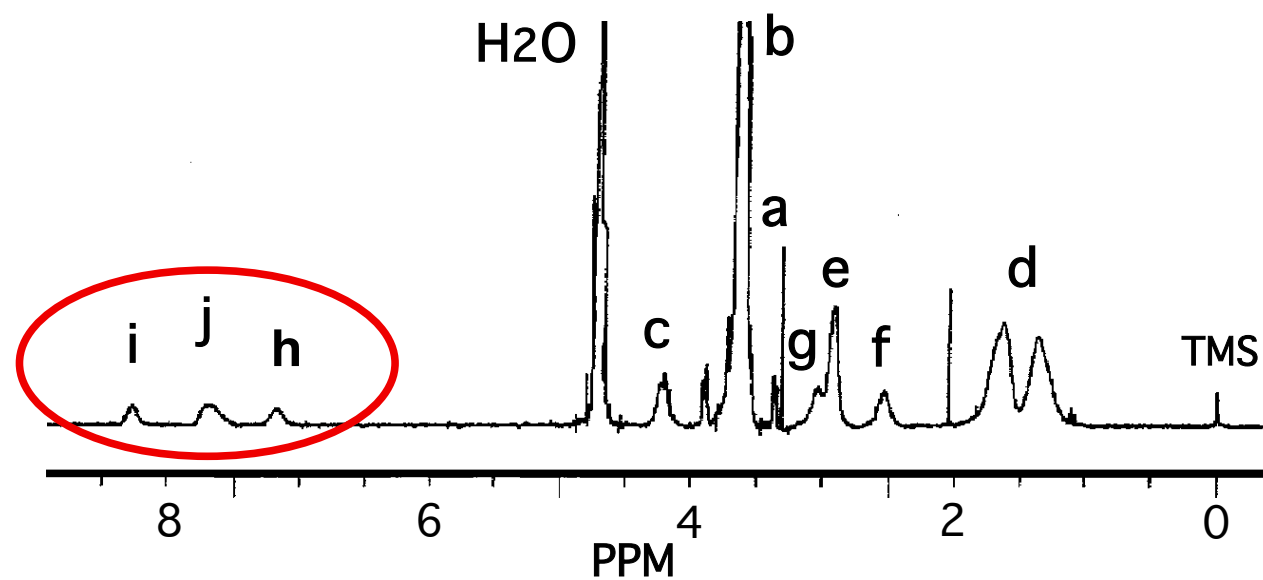


Y. Kakizawa, et al, JACS, 121, 11247 (1999); K. Miyata, et al, JACS, 126, 2355 (2004);
K. Miyata, et al, J. Contrl. Rel., 109, 15 (2005)

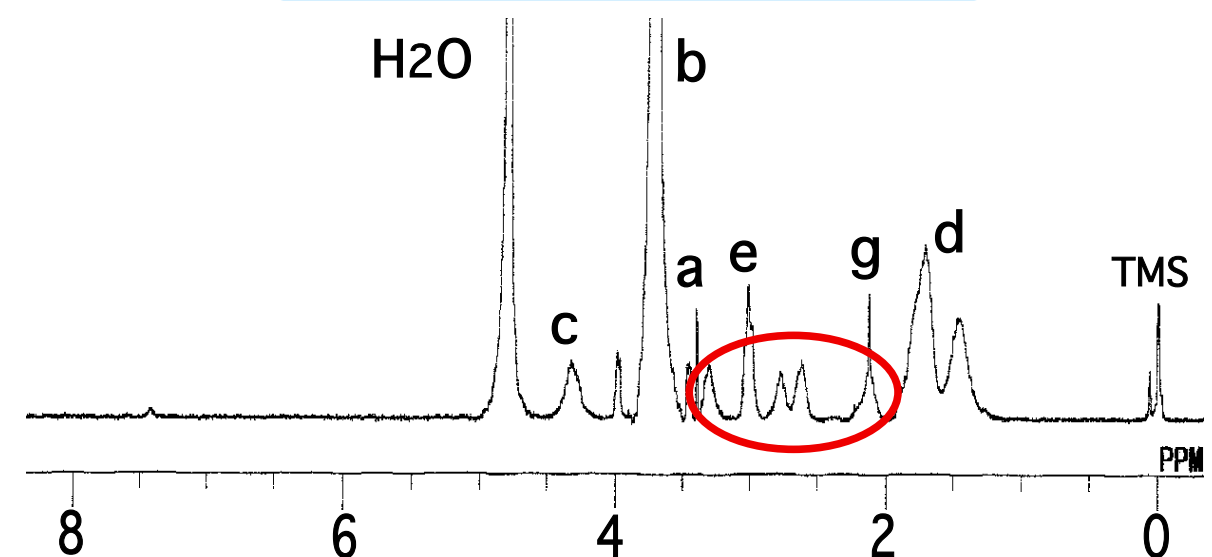
Preparation of thiolated PEG-PLL with controlled charge density



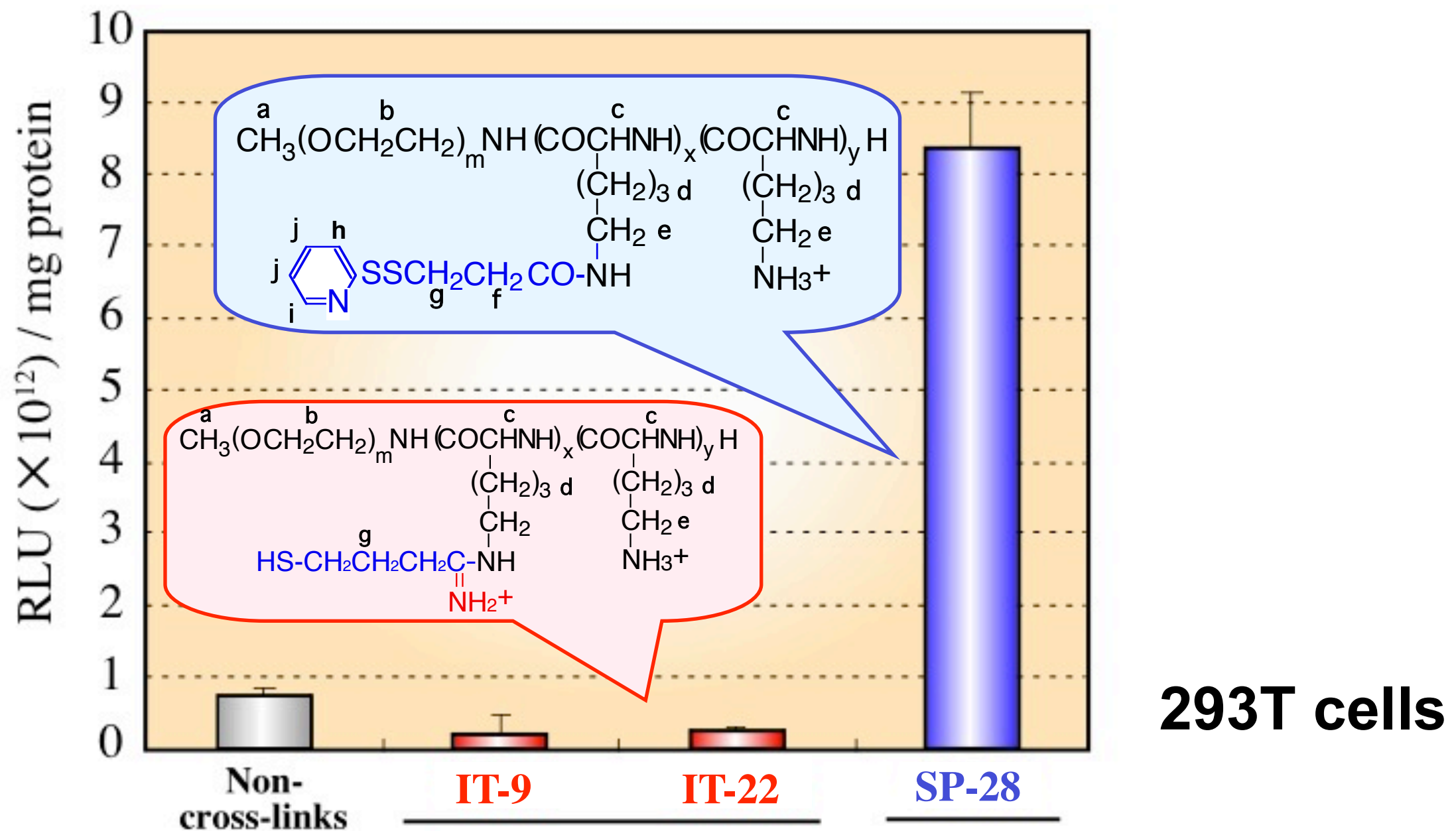
SP-X (X: SS mol%)



IT-X (X: SH mol%)



Improved Gene Transfection by SS Crosslinked Micelles



Improved stimuli sensitivity through charge compensated introduction of SS crosslinking

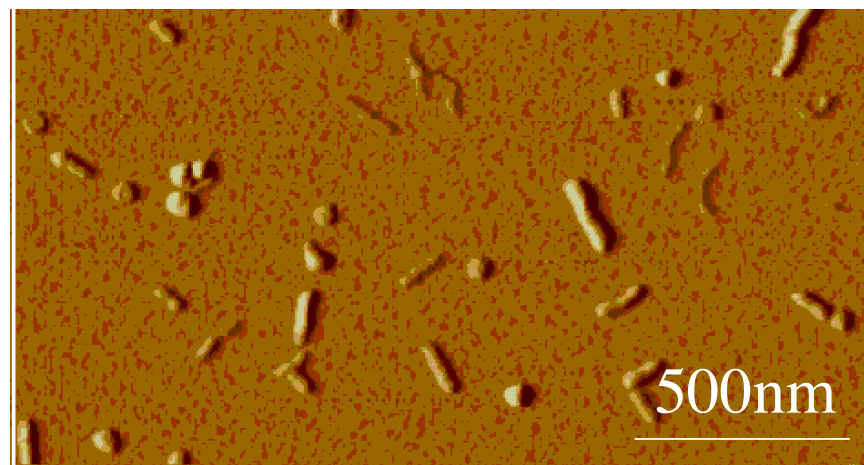


Remarkable increase in transfection efficiency

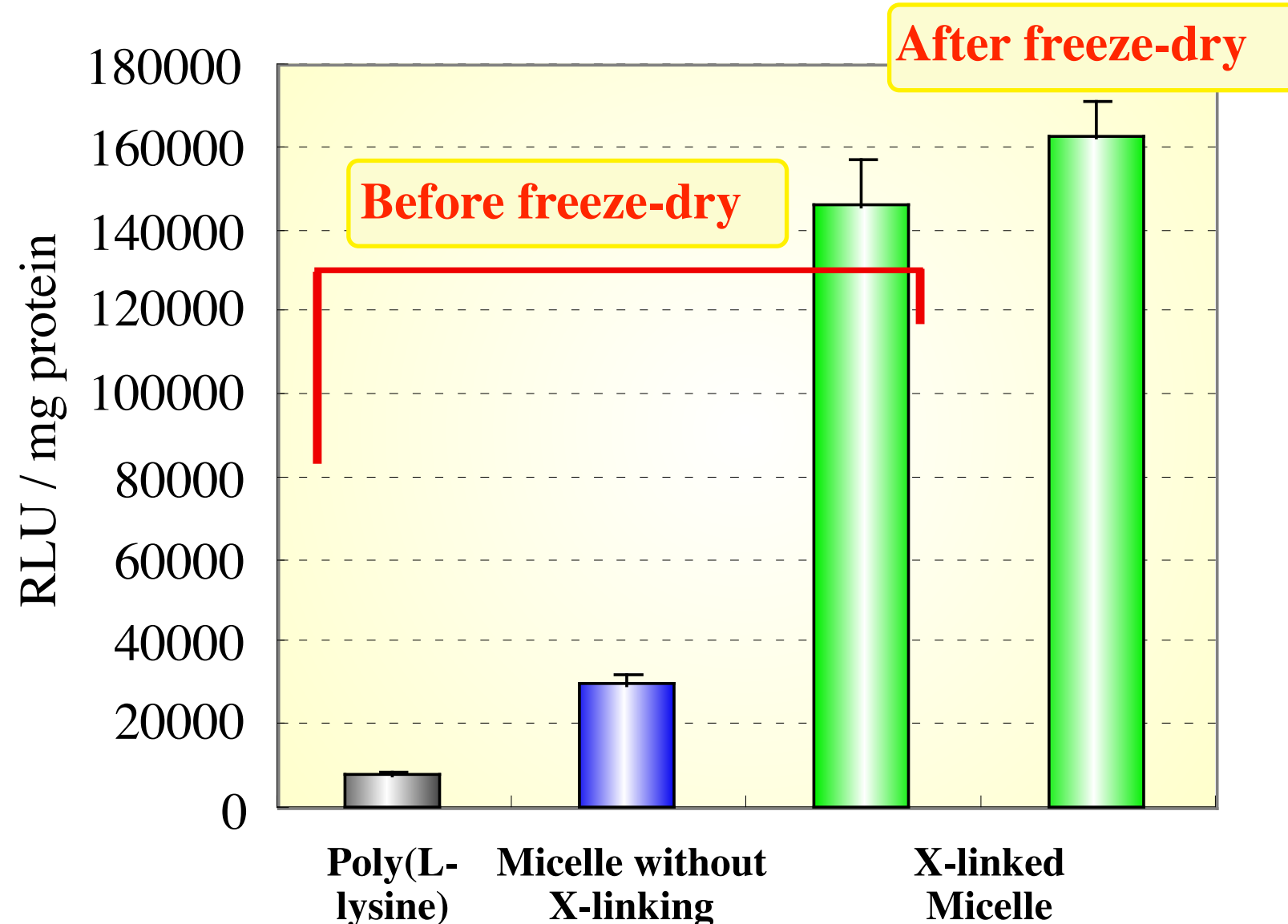
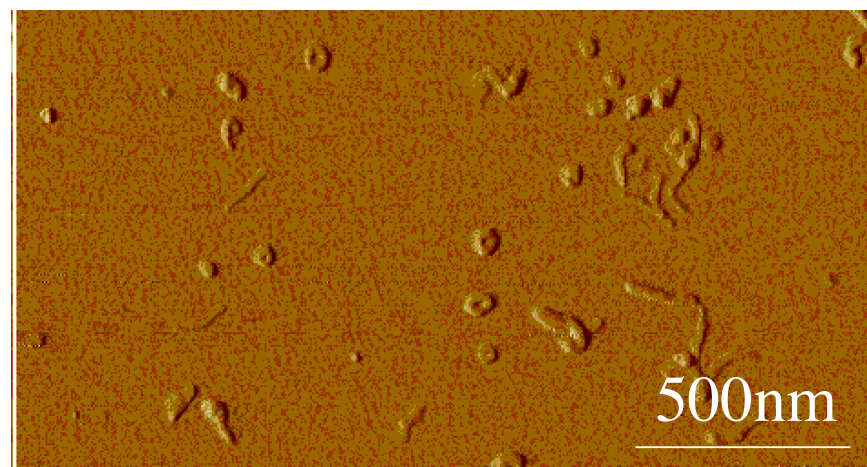
Enhanced gene transfection by freeze-dryable cross-linked micelle vector

	Poly(L-lysine)	Micelle without X-linking	X-linked Micelle
Size before freeze-dry (nm)	105.9	98.1	114.3
Size after freeze-dry (nm)	(1744.8)	(2176.5)	127.2

AFM of X-linked micelle

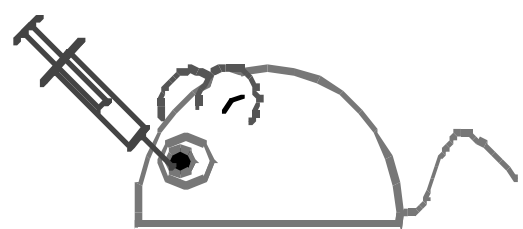


↓ After freeze dry



Liver transfection by systemic injection of cross-linked micellar vector

i.v. injection via
orbital vein

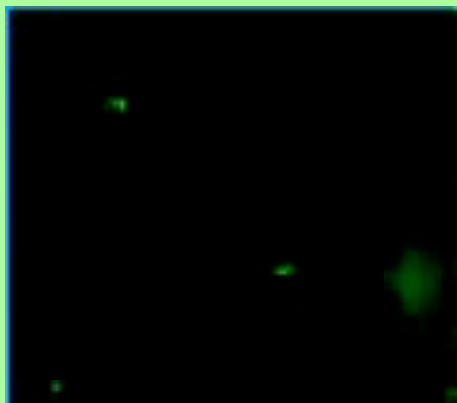


Liver was excised
at a defined day

The excised liver was treated with OCT
compound, and sliced with cryostat.

YFP gene expression in liver

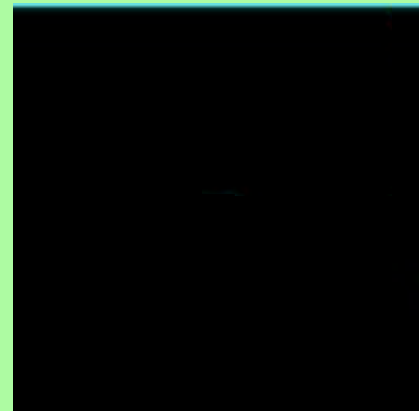
Day 0



Day 1



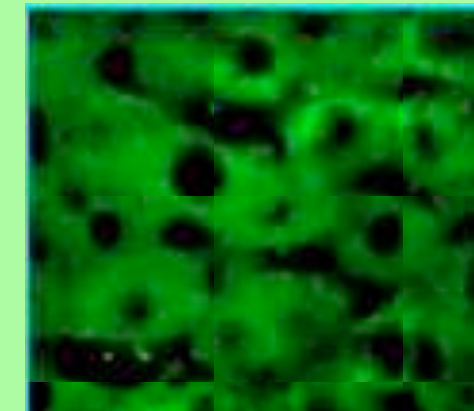
Day 2



Day 3

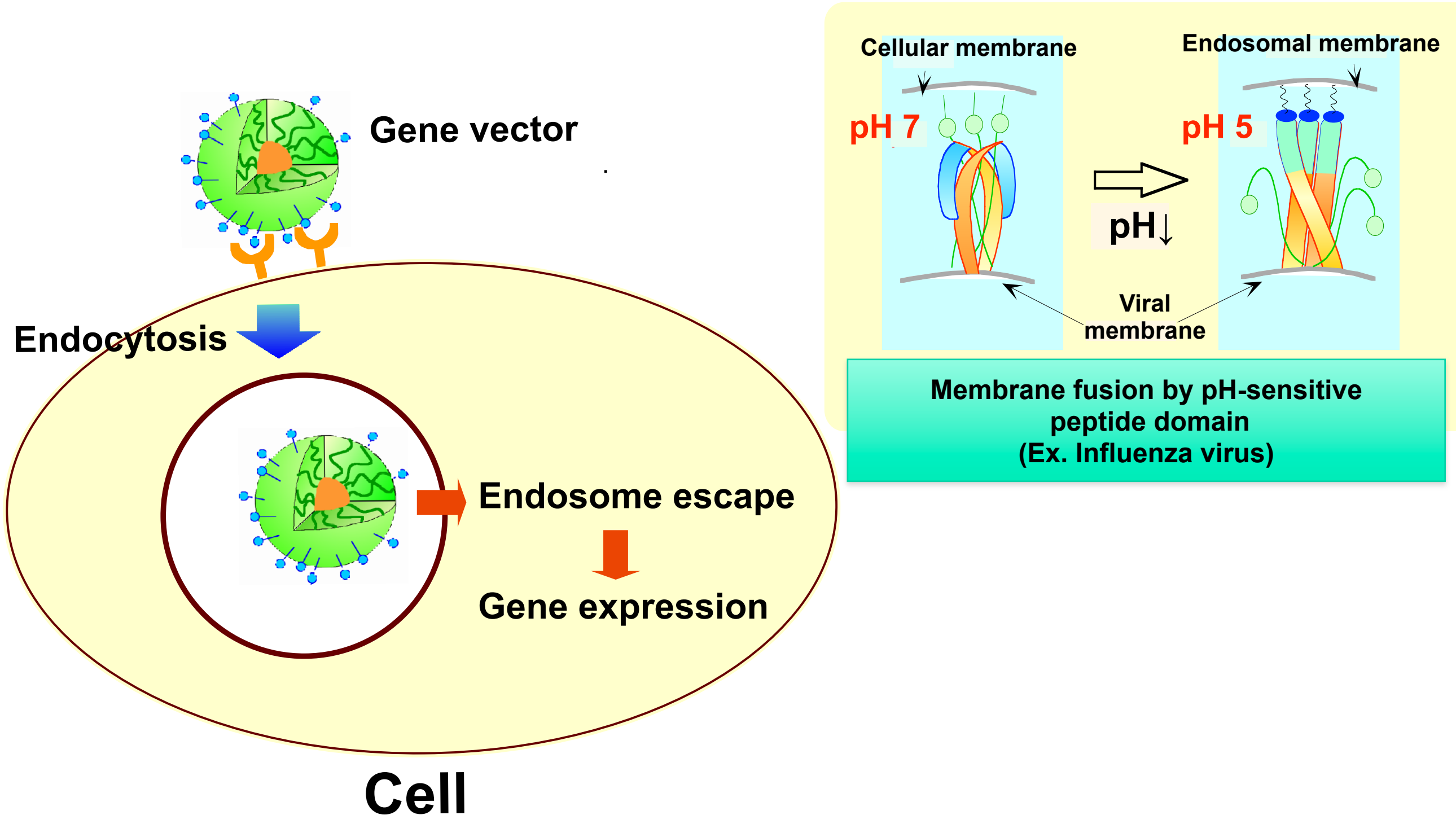


Day 5



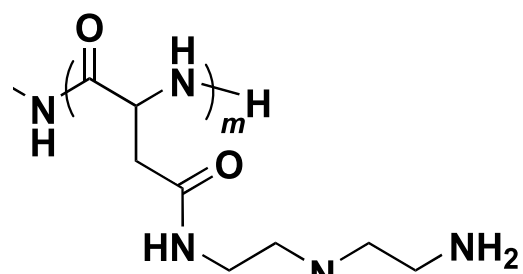
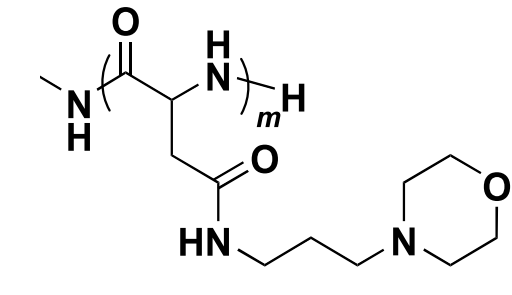
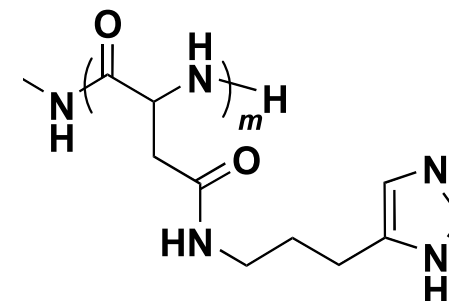
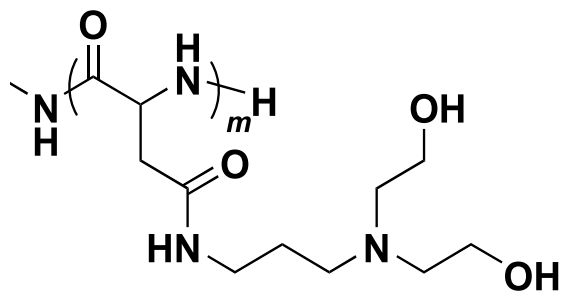
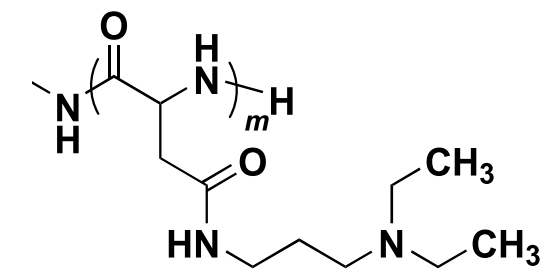
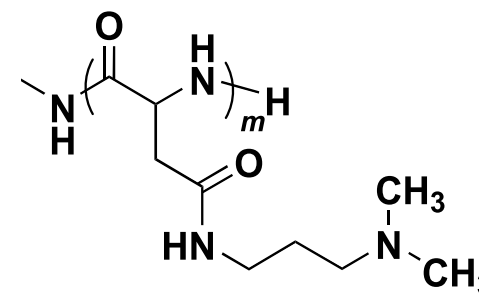
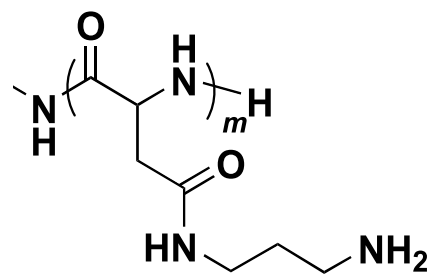
Homogeneous YFP gene expression was observed in liver parenchymal cells
5 days after i.v. injection of cross-linked polyplex micelles.

Endosomal escape: A key issue in intracellular gene and nucleic acid delivery

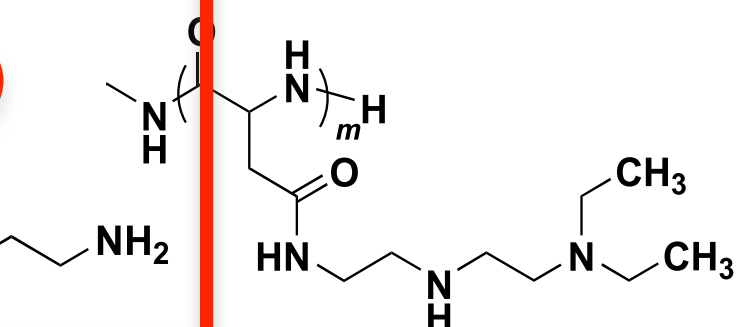
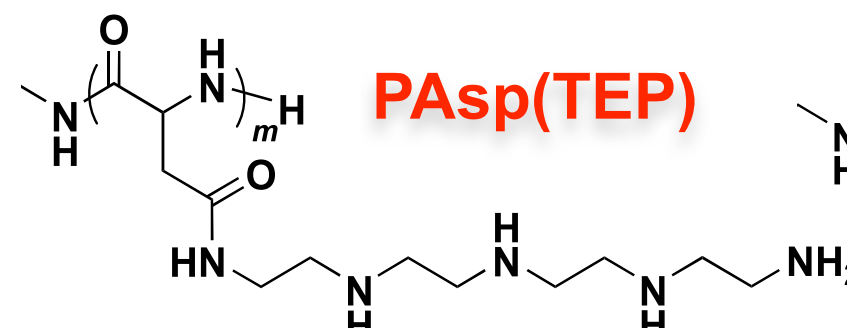
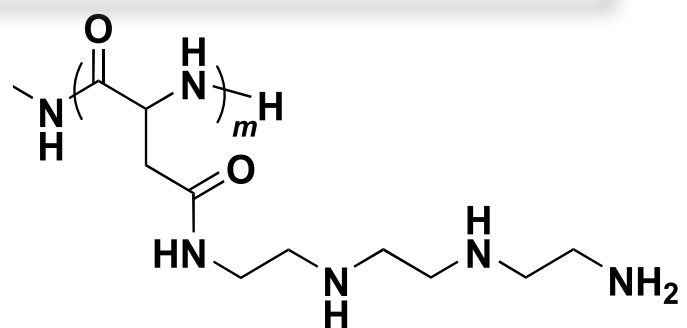
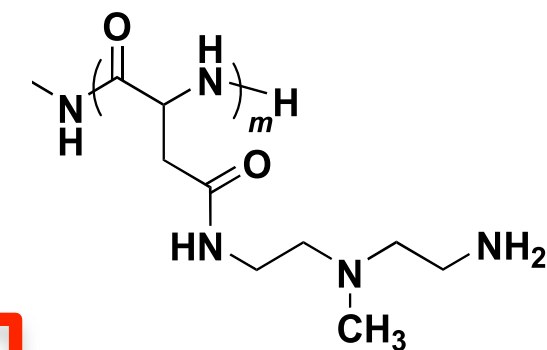
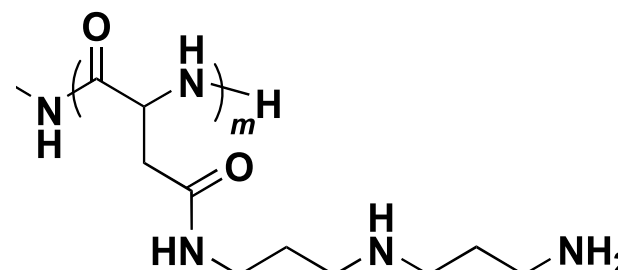


Challenge: Integrating endosome escaping units with minimum cytotoxicity into polyplex nanocarrier

Preparation of a Series of Cationic Polyaspartamides through Aminolysis Reaction of Poly(beta-benzyl aspartate)



PAsp(DET)



Preparation of a Series of Cationic Polyaspartamides through Aminolysis Reaction of Poly(beta-benzyl aspartate)

Observation of endosomal escape

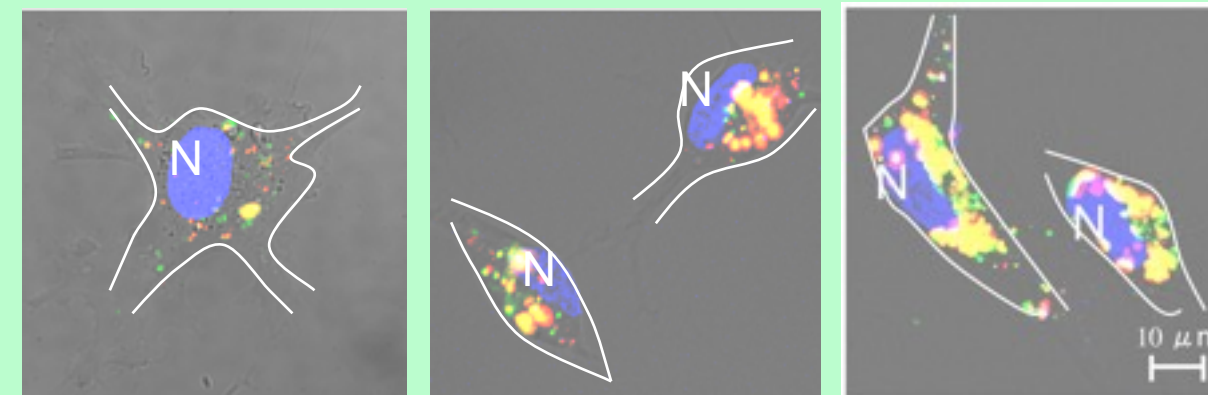
Incubation Time

3hr

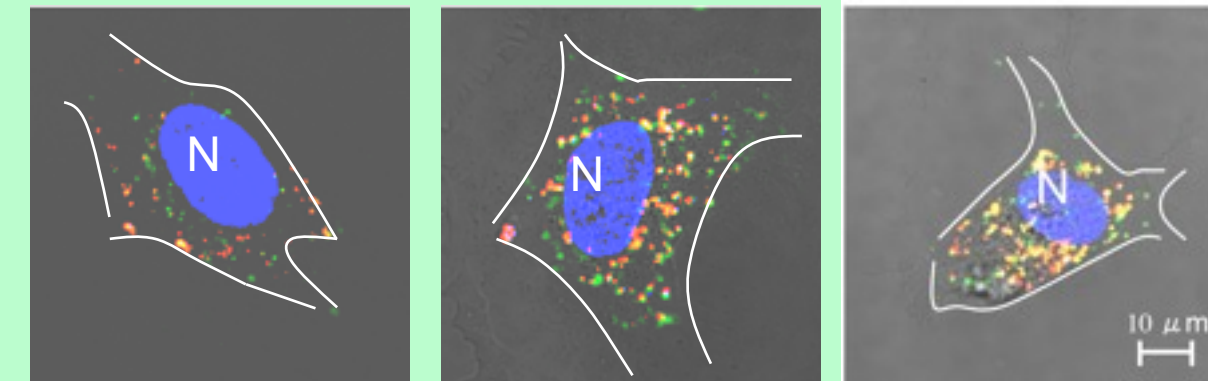
12hr

24hr

PAsp(DET)



P(Lys)

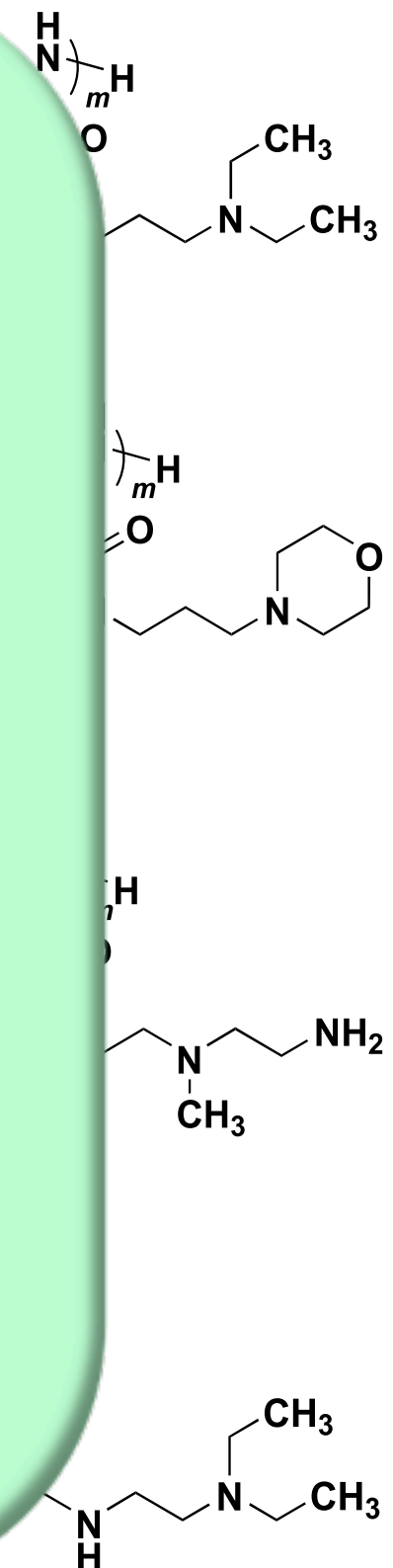


Green: Alexa-labeled dextran (endosome marker)

Red: Cy5-labeled pDNA

Blue: Hoechst 33258-stained nucleus

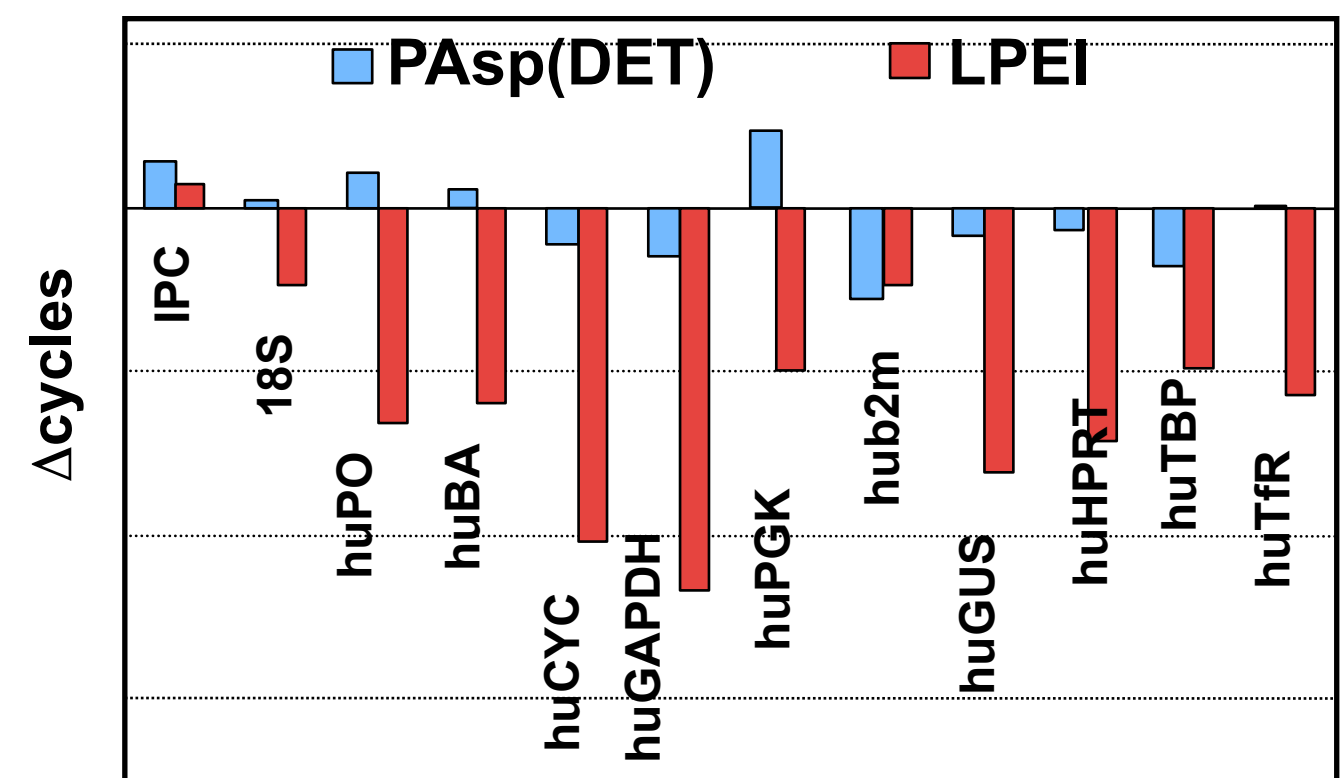
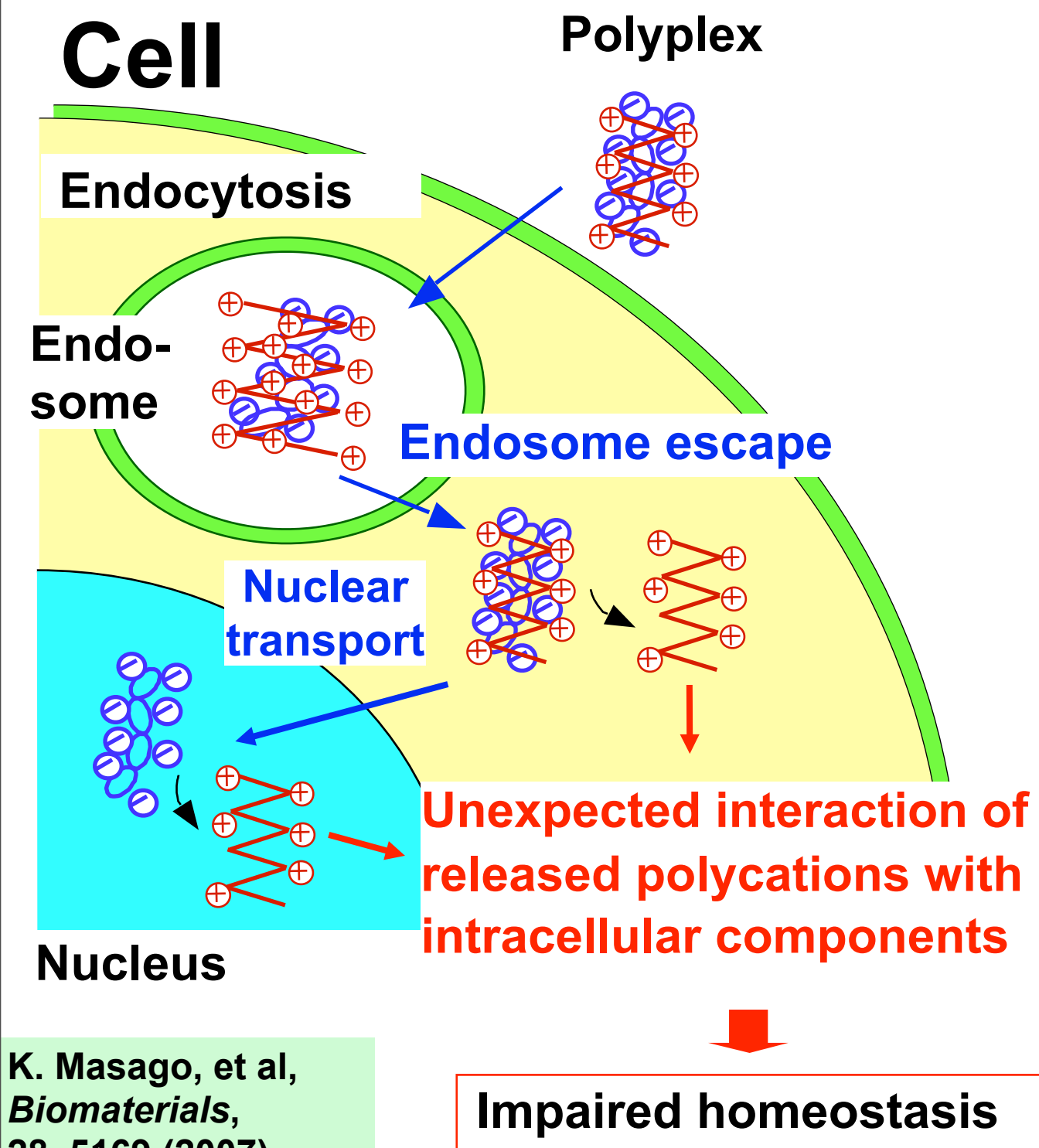
K. Miyata, et al, *J. Amer. Chem. Soc.*, 130, 16287-16294 (2008)



Biocompatibility assay of polycations by materials genomics

Adverse effect of polycations in polyplex due to the non-specific interaction with intra-cellular components

Change in the expression of house-keeping genes with polyplex transfection
(Evaluation by real-time PCR)



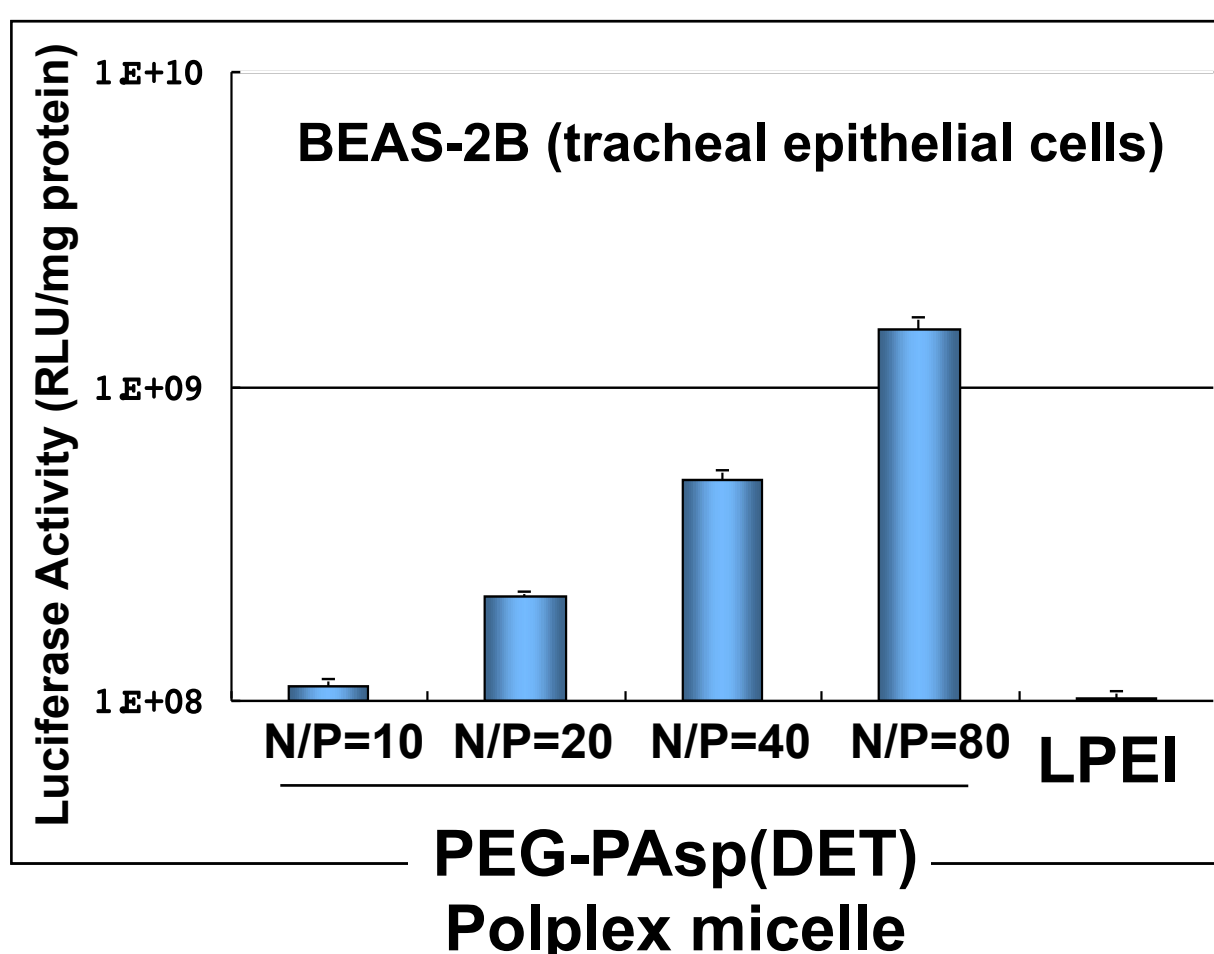
Significant decrease in the house-keeping gene expression for LPEI, yet no significant change for PAsp(DET)



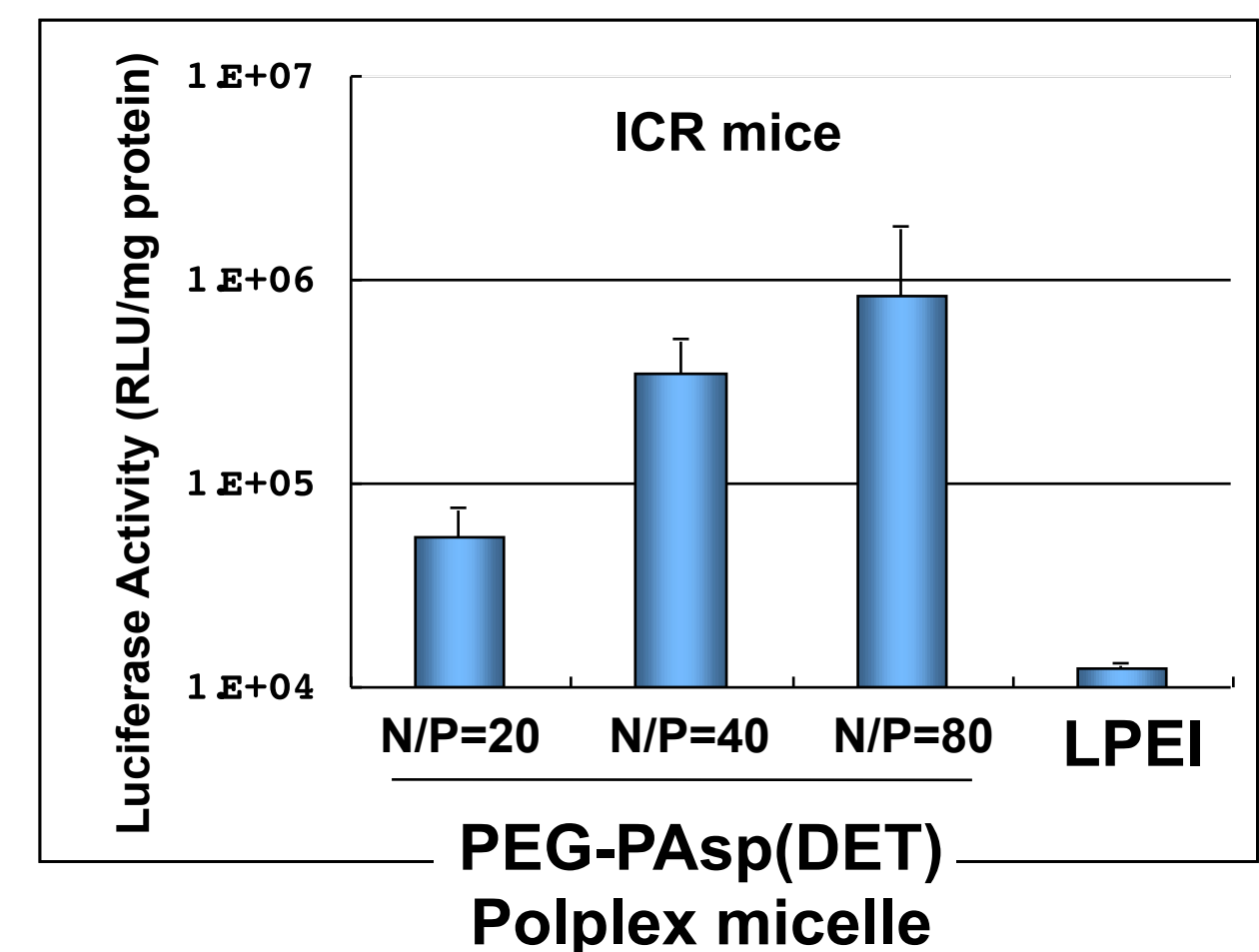
PAsp(DET) as biocompatible gene carrier from the standpoint of materials genomics

Gene Transfer to Lung by PEG-PAsp(DET) Polyplex Micells

Luciferase gene transfection to tracheal epithelial cells (in vitro)

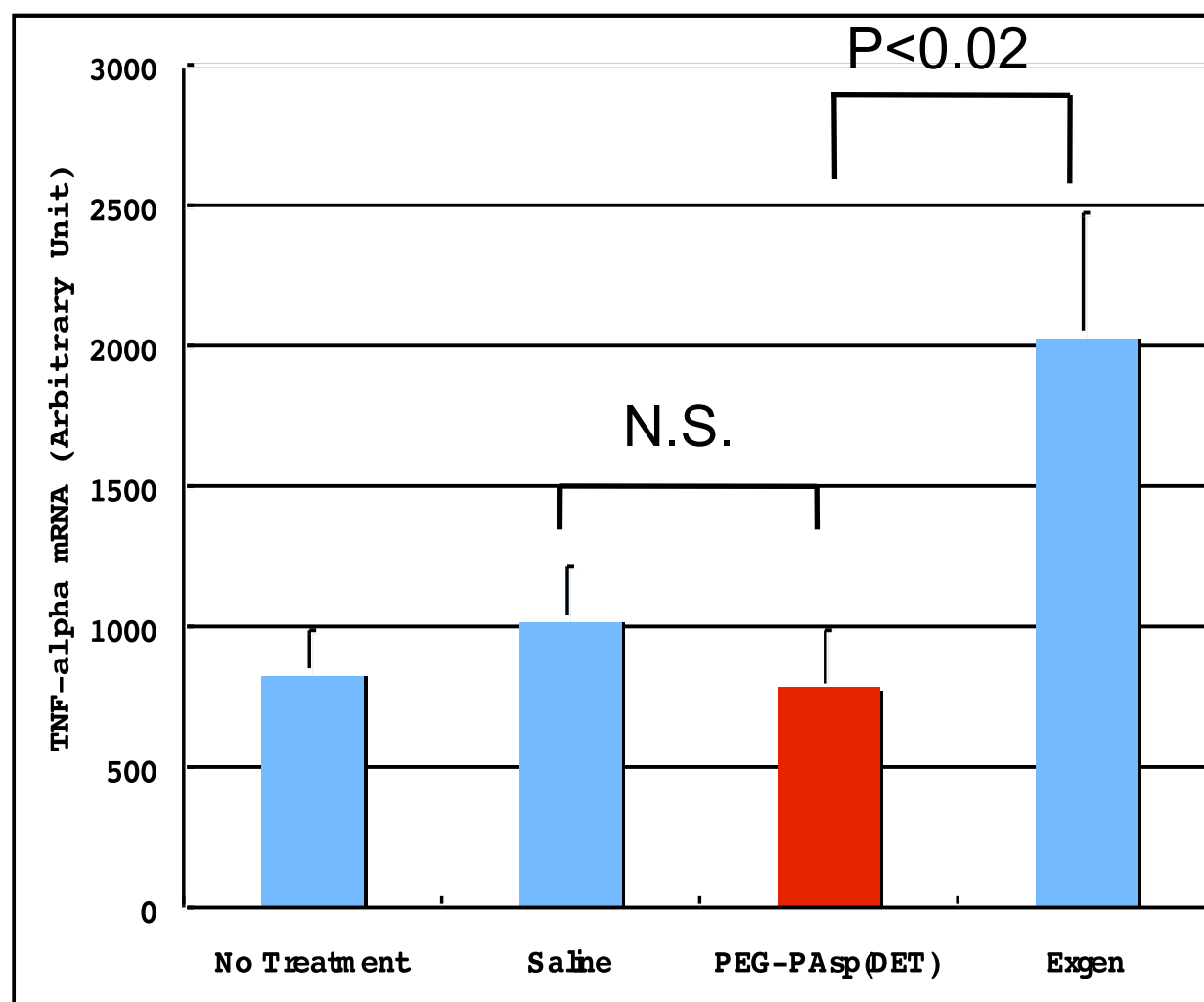


Luciferase gene transfection to lung via intratracheal administration (in vivo)

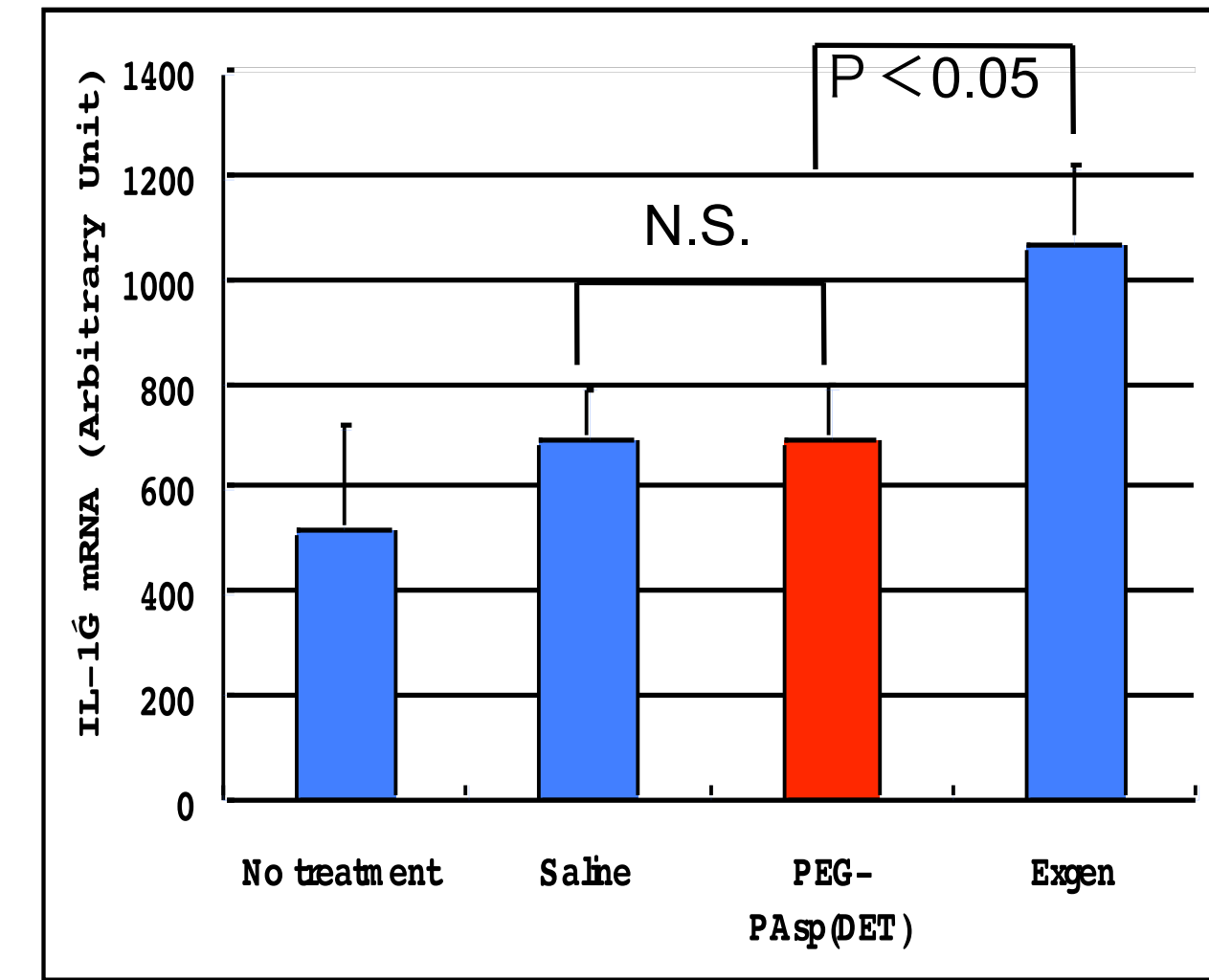


mRNA expression of inflammatory cytokines (TNF- α and IL-1 β) in the lung 1 week after the administration of polyplexes

TNF- α



IL-1 β

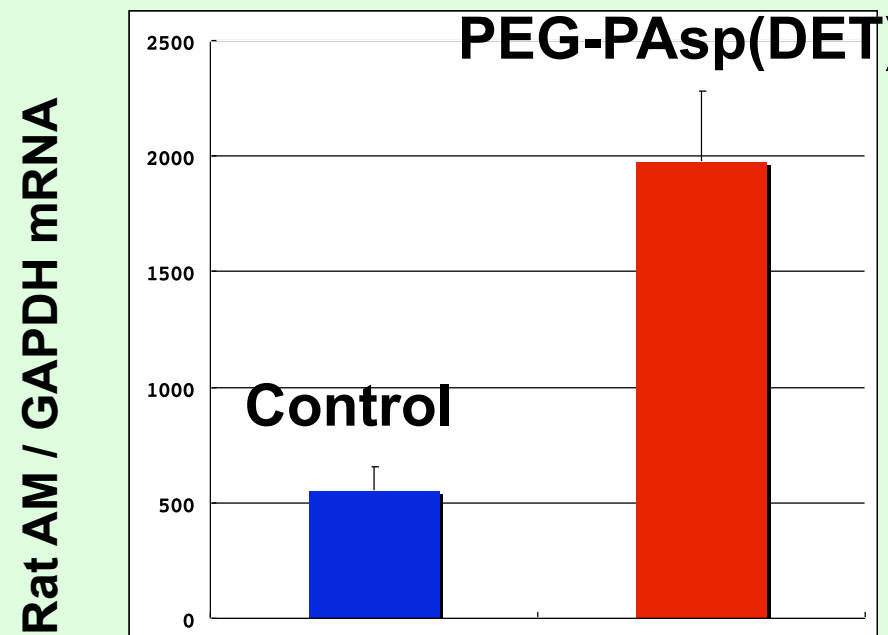


Adrenomedullin Gene Transfer by Intratracheal Administration of PEG-PAsp(DET) for the Treatment of PAH

Model Animals for Pulmonary Hypertension

- Day 0**
 - Subcutaneous injection of monocrotaline
- Day 25**
 - Measurement of right ventricular pressure by catheter
 - Gene transfer of AM gene by intratracheal administration
- Day 28**
 - Measurement of right ventricular pressure by catheter again and remove of the lung to measure RNA

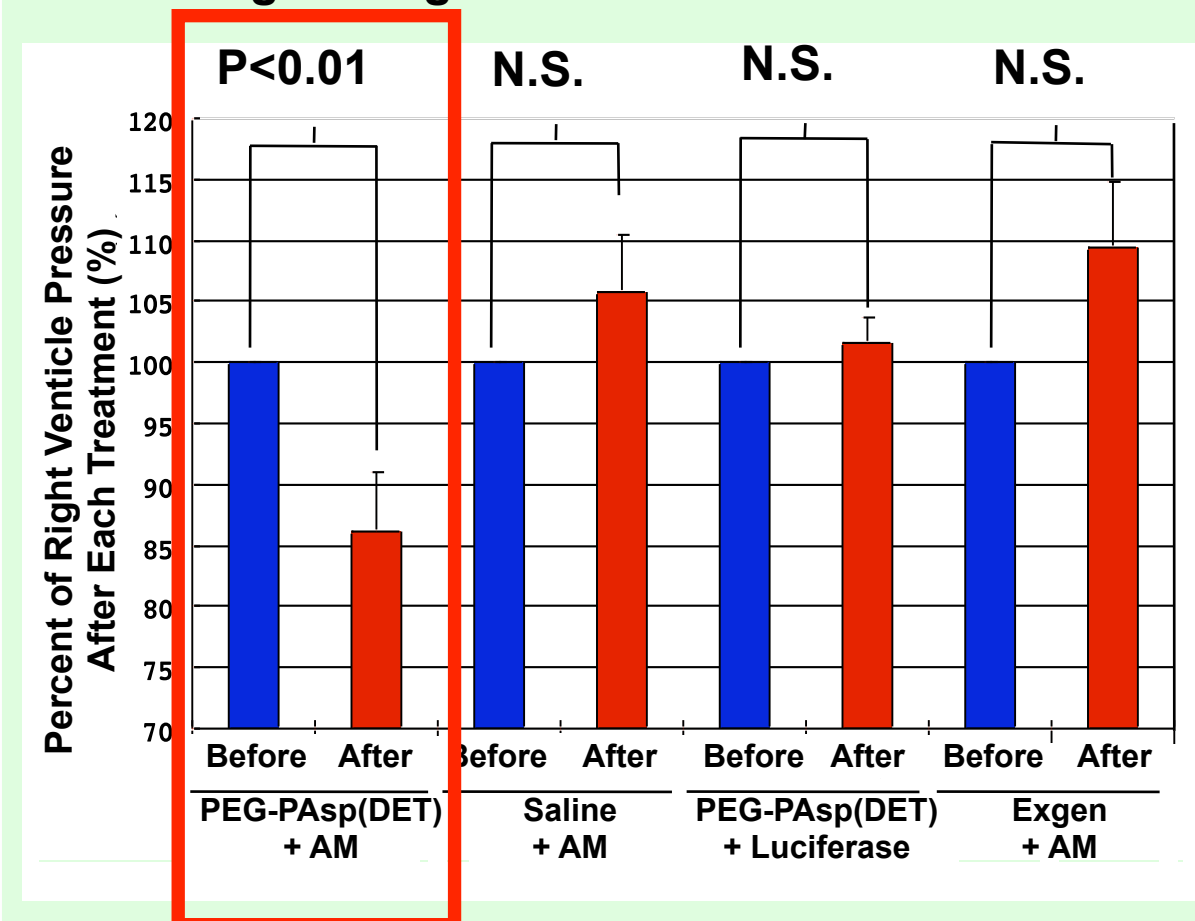
Measurement of adrenomedullin mRNA by Real Time RT-PCR



Pulmonary Arterial Hypertension

- Life-threatening disease characterized by progressive pulmonary arterial hypertension
- Death after 2 to 10 years of diagnosis.

Change in Right Ventricular Pressure



Trinity in Regenerative Medicine

Cell

- ES cell
- MSC cell
- iPS cell

Differentiation Control

- Drug
- Gene, siRNA
- Bioactive substance

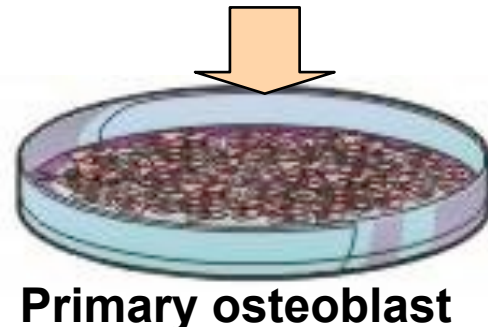
Scaffold

- PLLA, PLGA
- Calcium Phosphate
- Collagen

Need for drug and gene delivery systems

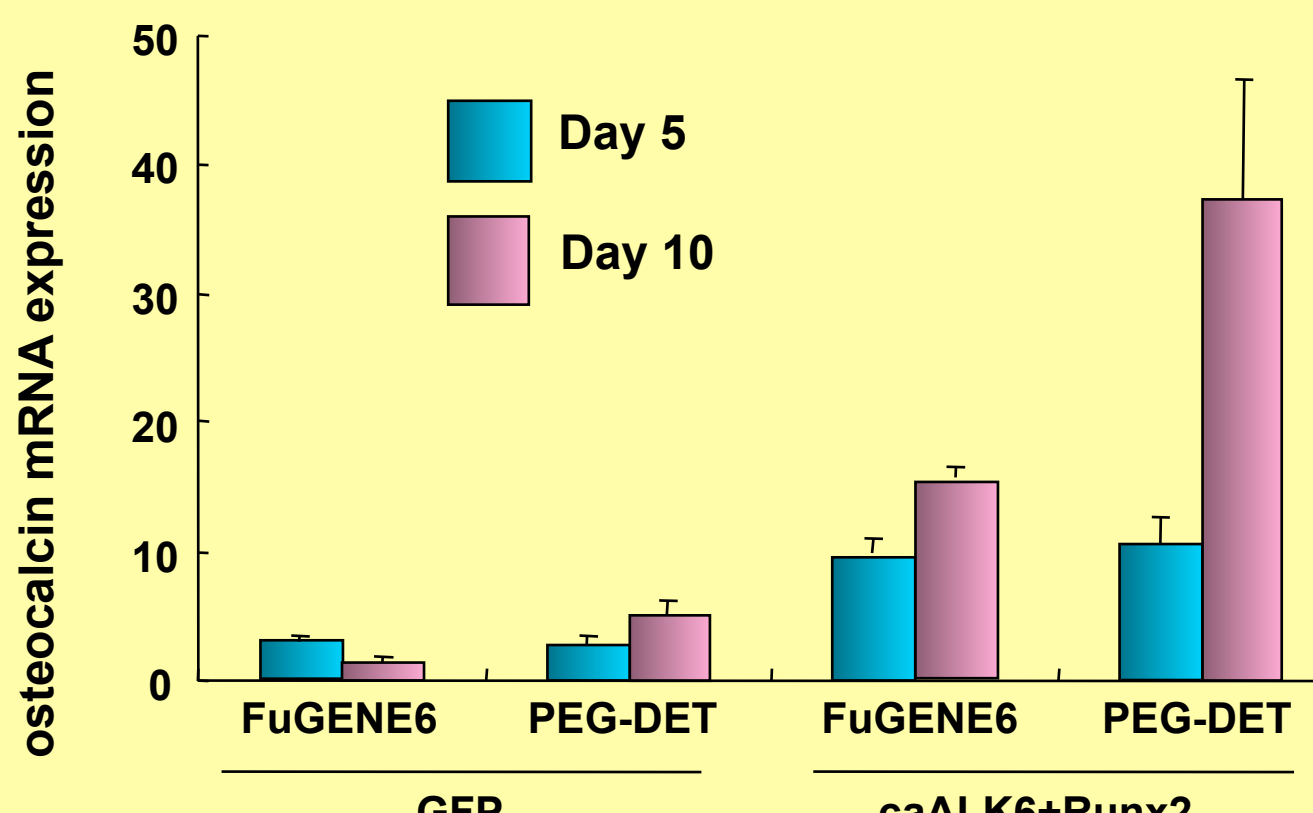
Induction of cell differentiation by delivering genes encoding osteogenic factor with polyplex micelles

pDNA encoding osteogenic factor
(caALK6+Runx2)



5, 10days

Estimation of osteocalcin (osteoblast differentiation marker) mRNA expression by real-time RT-PCR

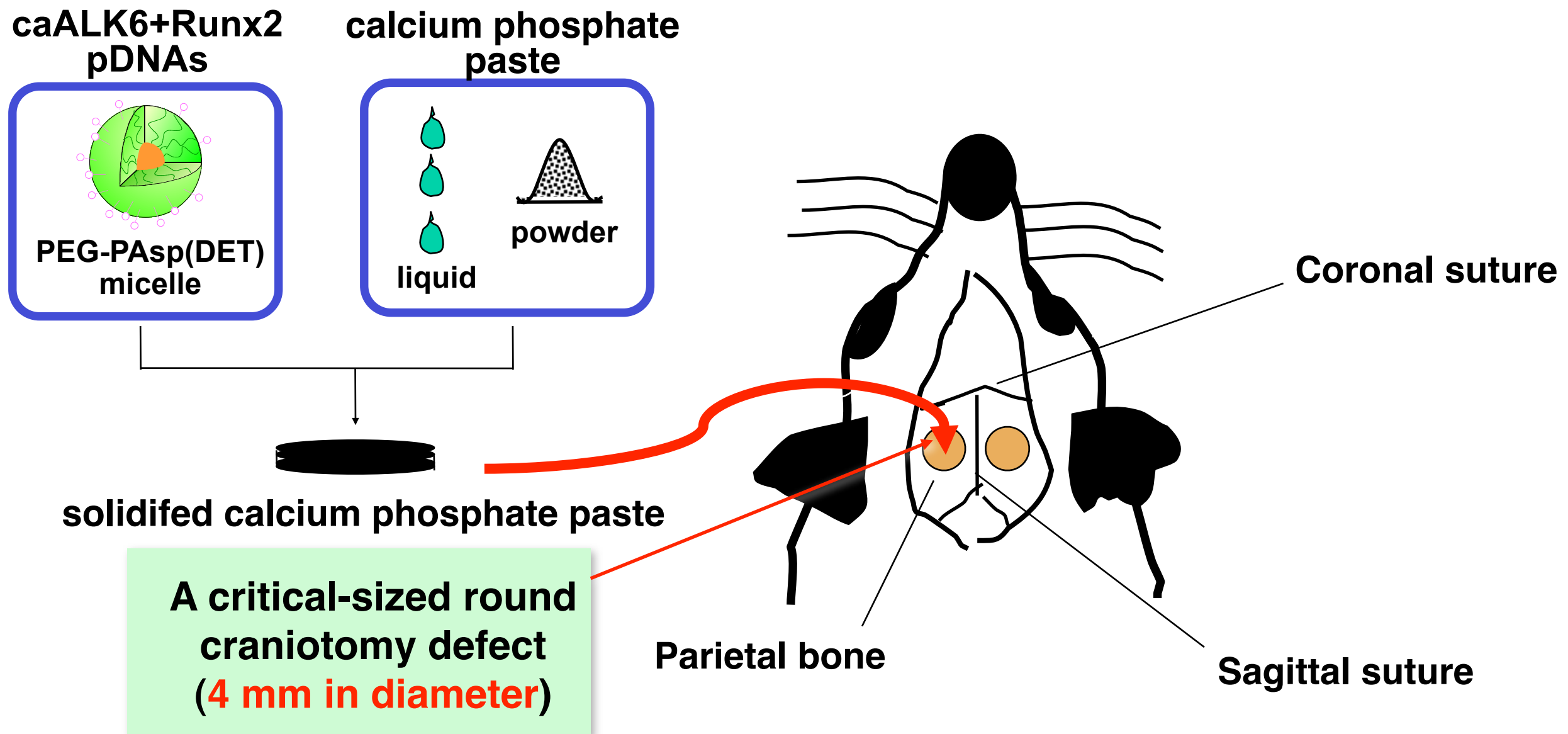


Only polyplex micelles successfully induce the cell differentiation.

K. Itaka, et al,

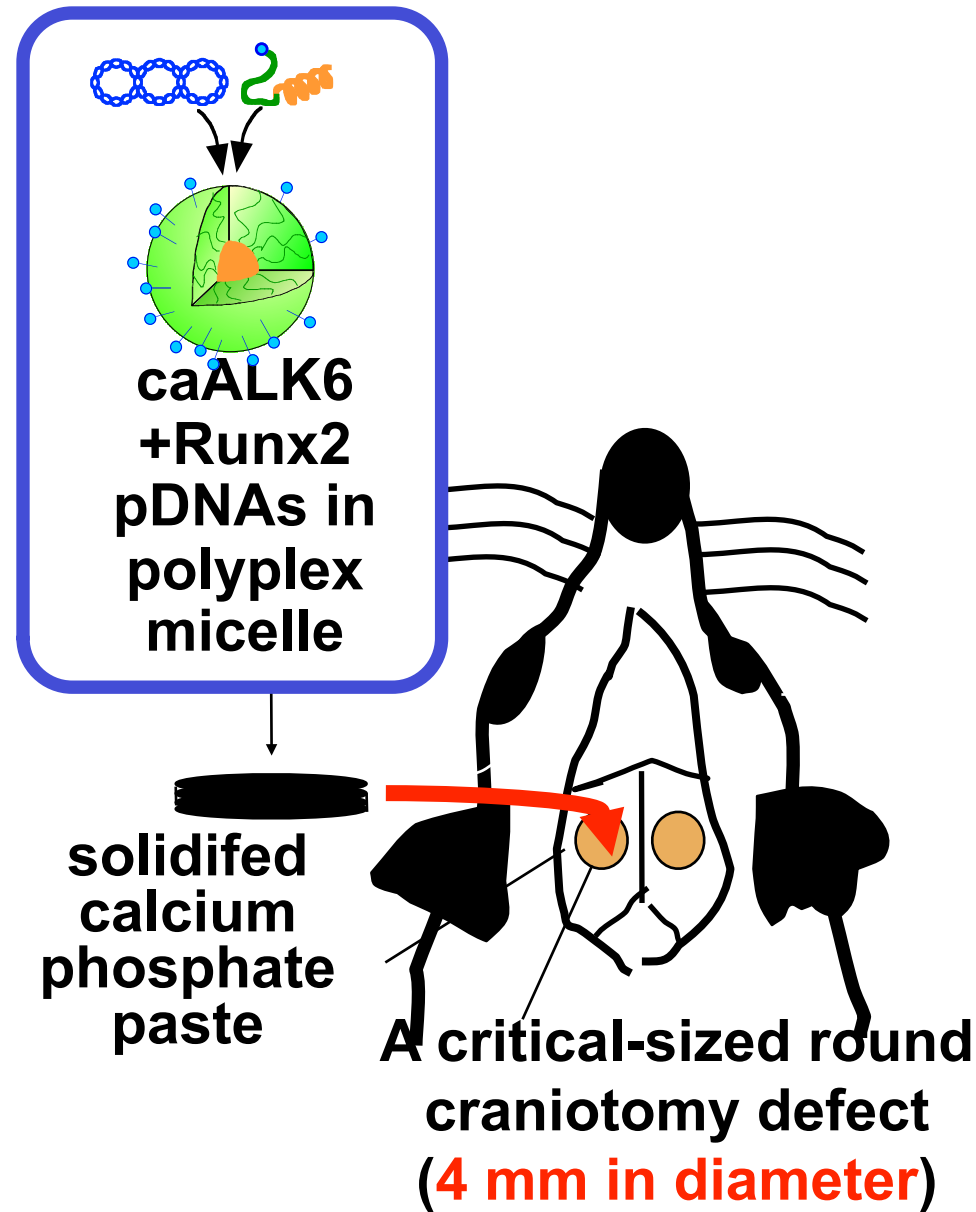
Molecular Therapy, 15, 1655-1662 (2007)

Bone regeneration based on *in vivo* transduction without cell source

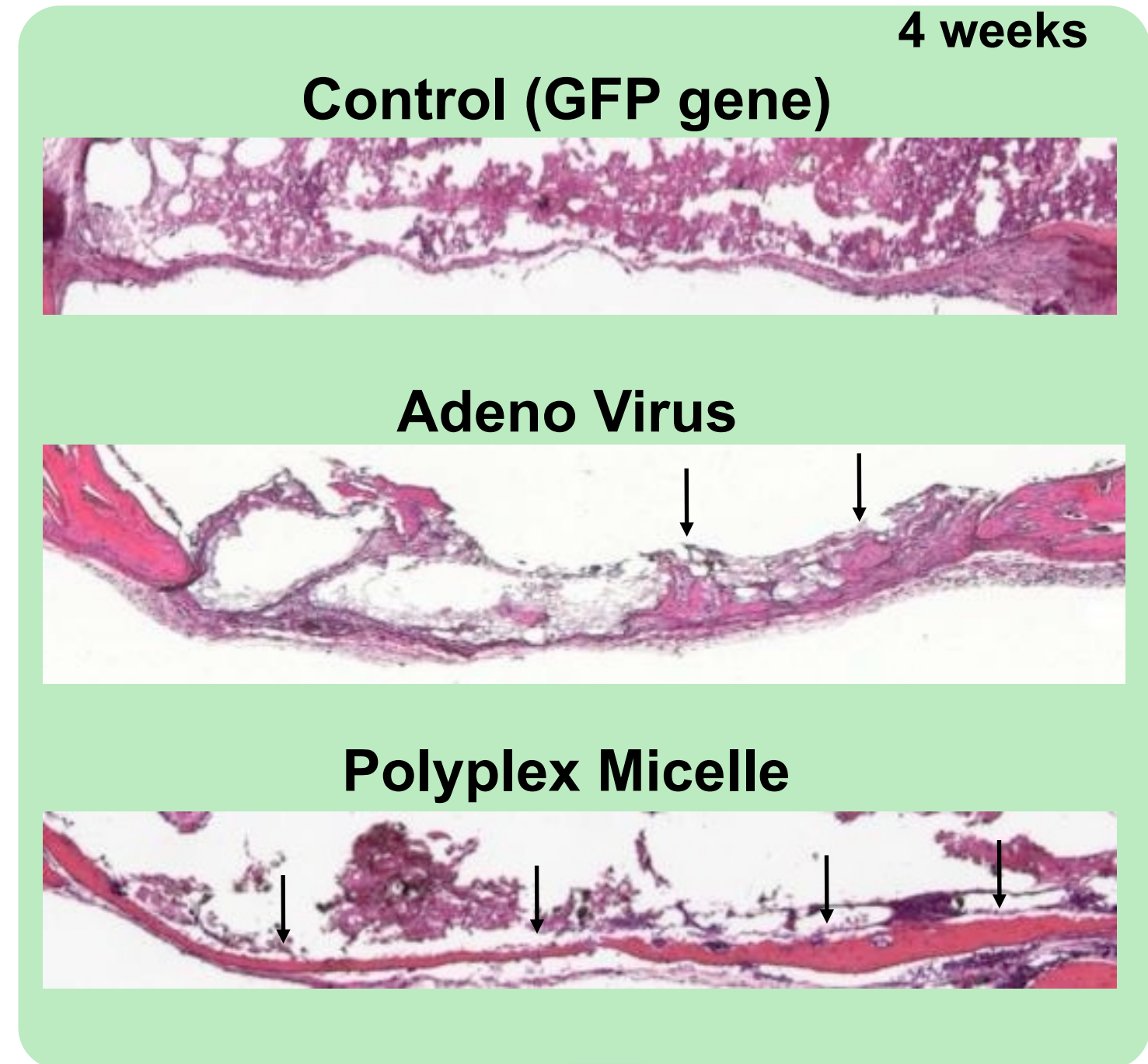
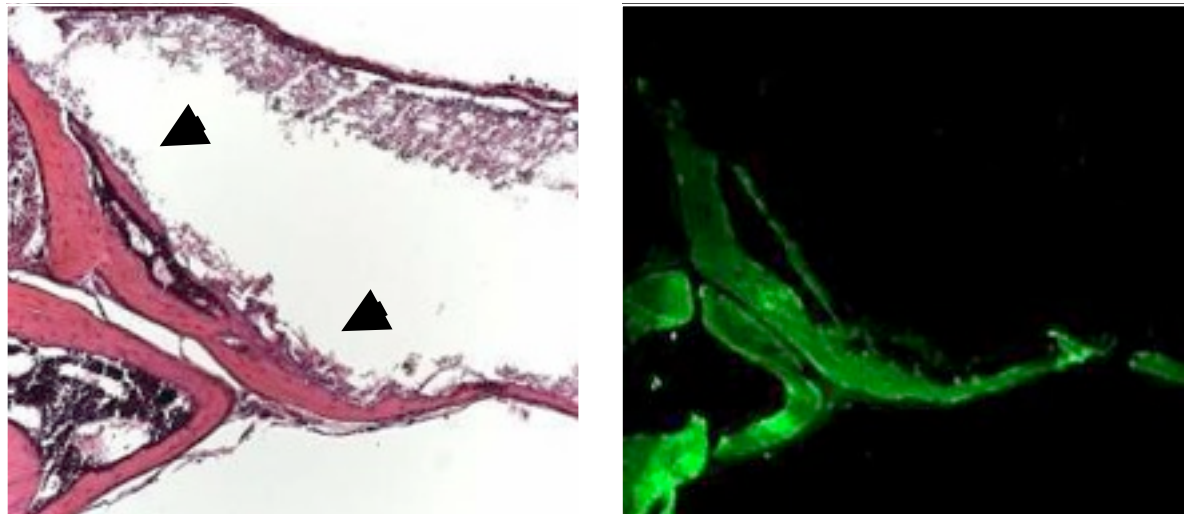


- Solidified calcium phosphate paste containing Runx2 and caALK6-expressing pDNAs (1.3 µg/mouse) were placed to cover the defects.
- The mice were sacrificed at 2, 4, 6 weeks after the operation for histological analyses.

Bone regeneration based on *in vivo* transduction without cell source



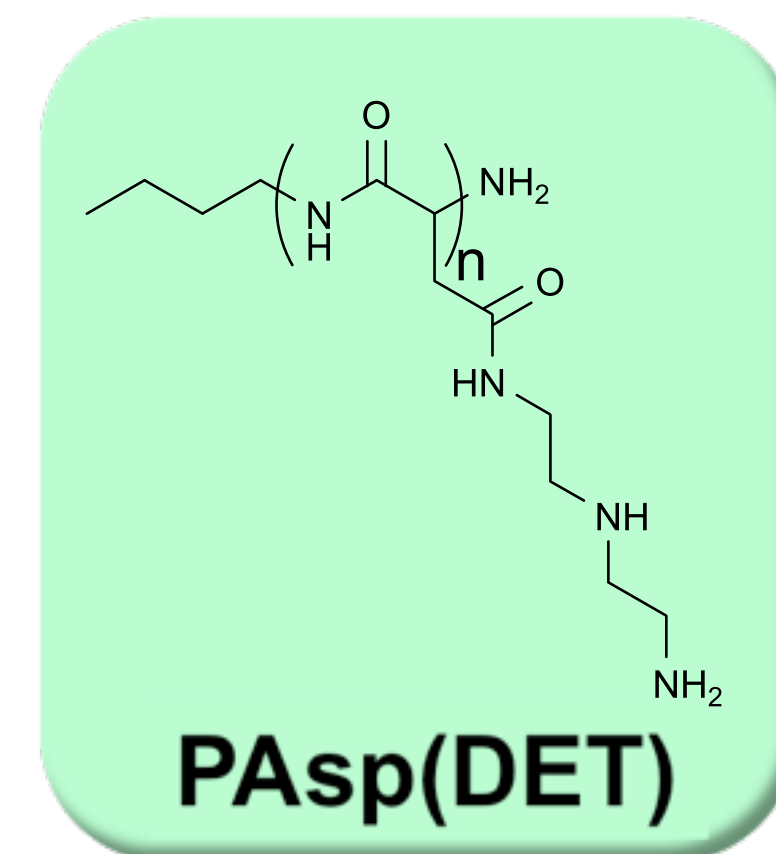
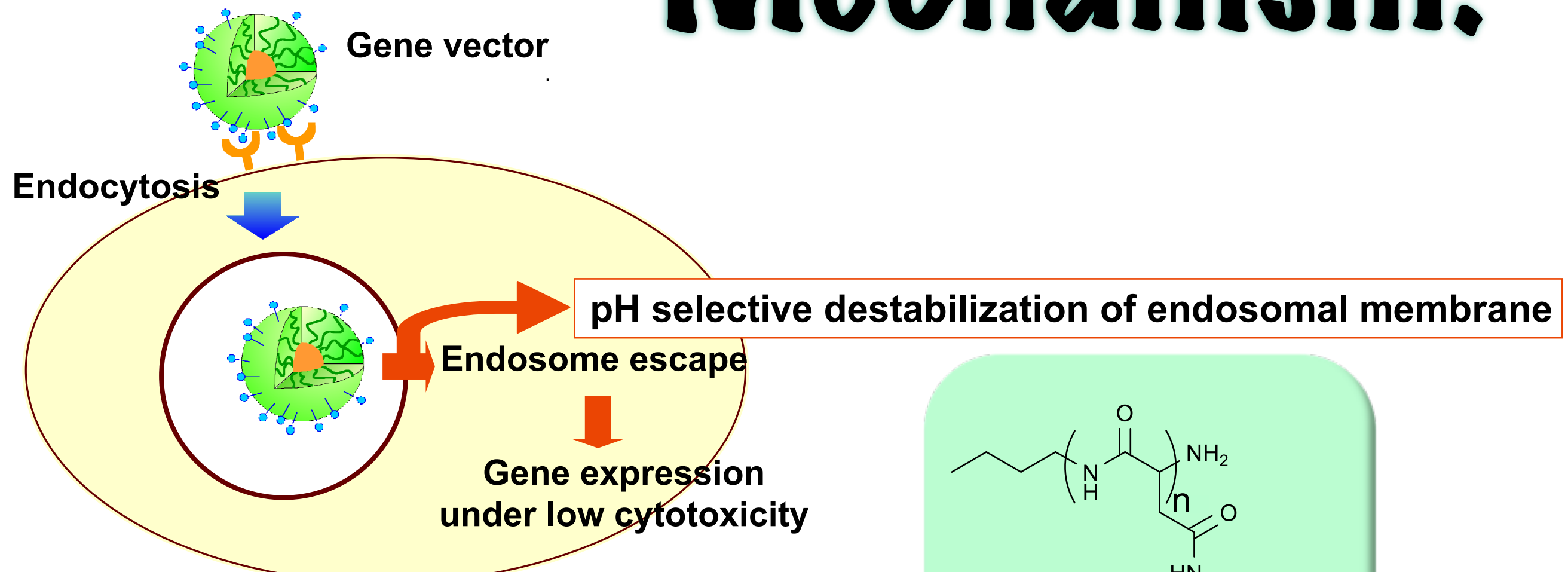
Immuno-staining of Type I collagen



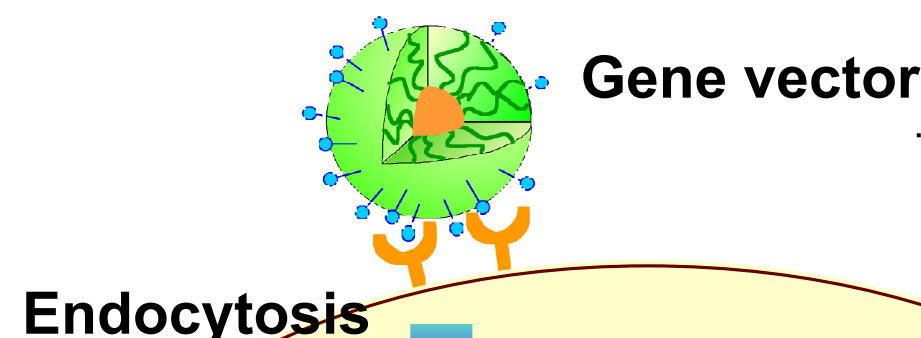
Polyplex micelles exceeded adeno virus to reveal substantial bone formation without inflammation

Mechanism of Endosomal Escape

Mechanism?

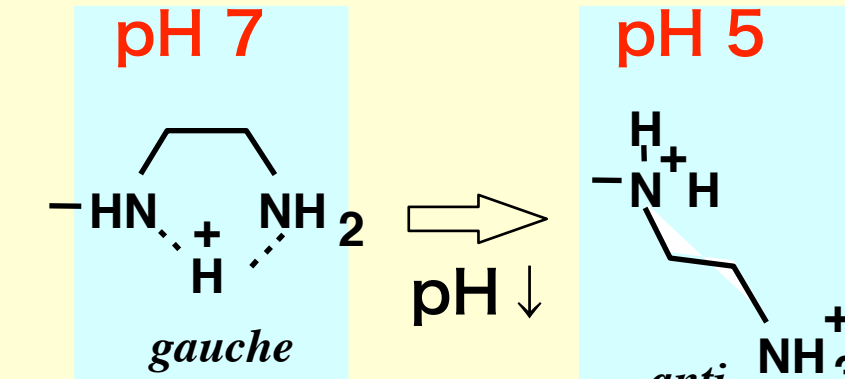


Mechanism of Endosomal Escape



Endocytosis

Me



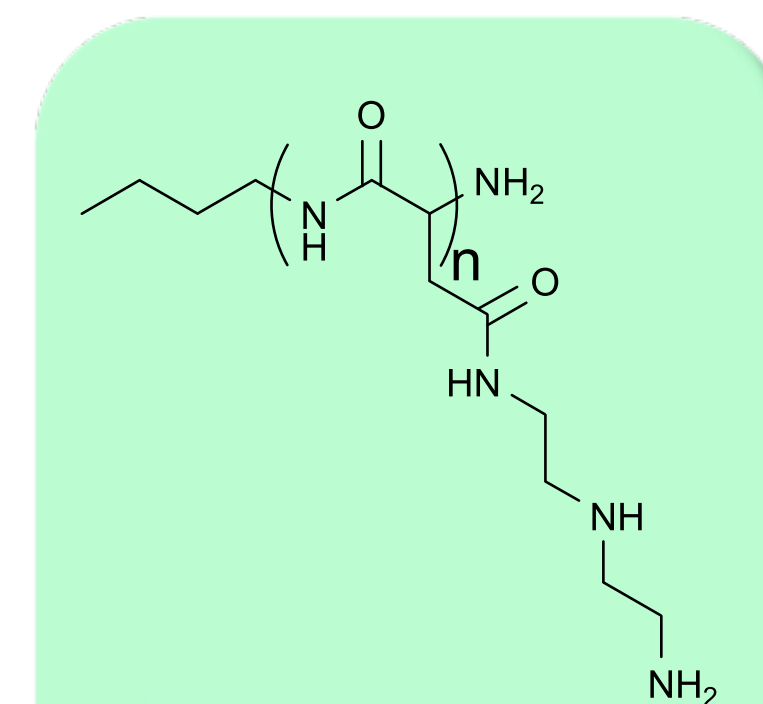
Membrane disruption induced by the protonation of diaminoethane units

pH selective destabilization of endosomal membrane

Endosome escape

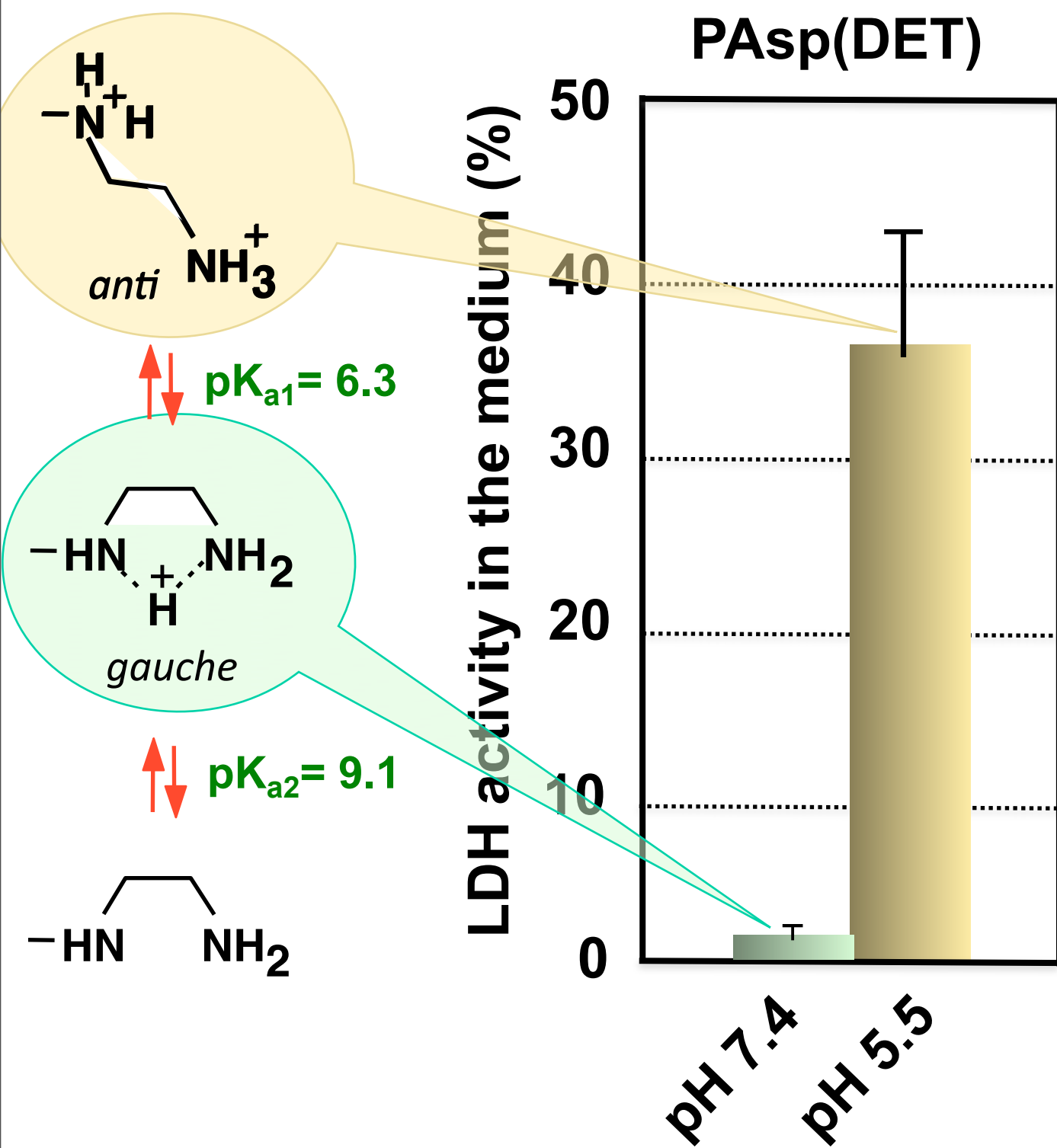
Gene expression
under low cytotoxicity

Cell



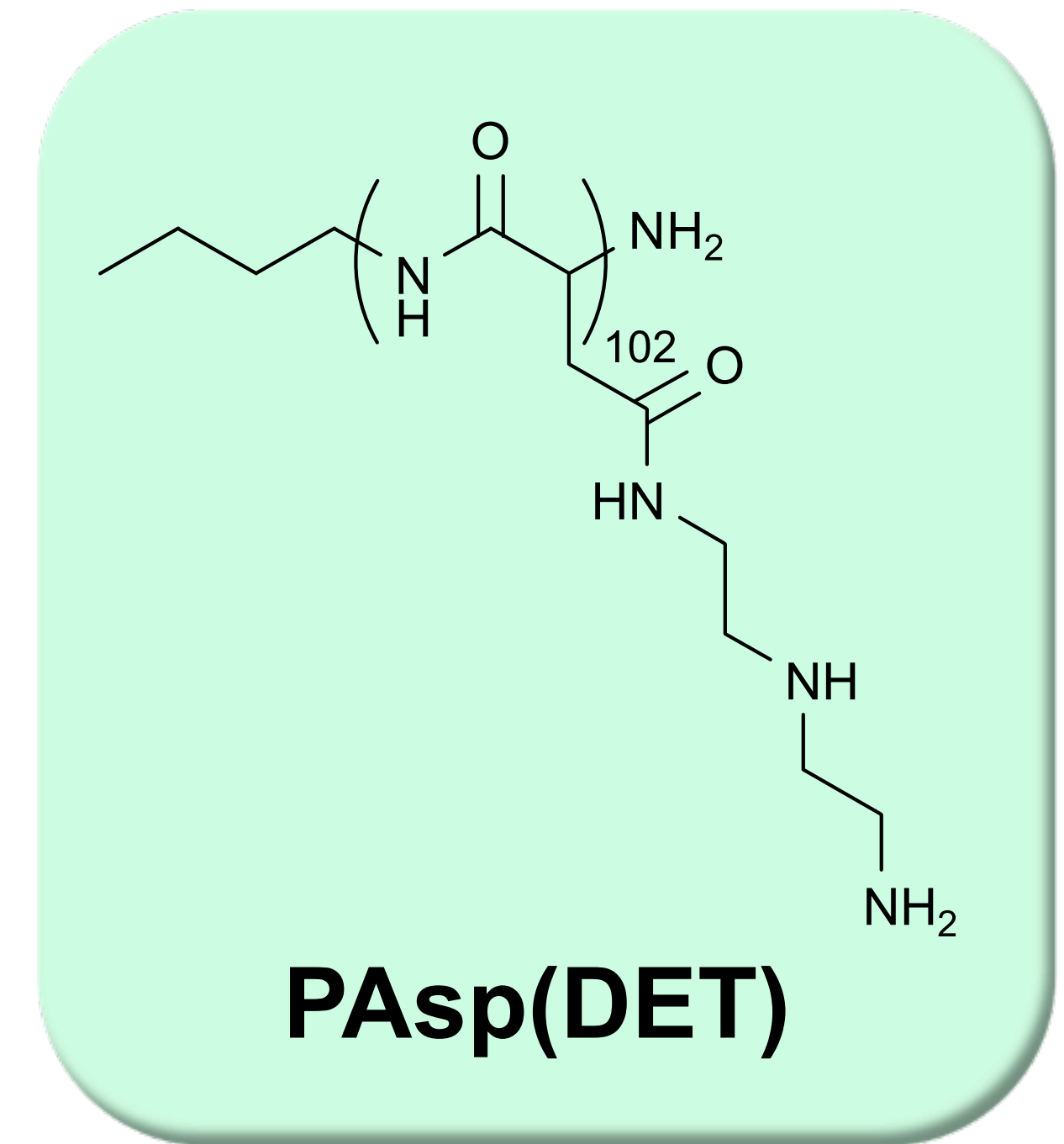
PAasp(DET)

Destabilization of endosomal membrane: Assay by the leakage of cytoplasmic enzyme (LDH)

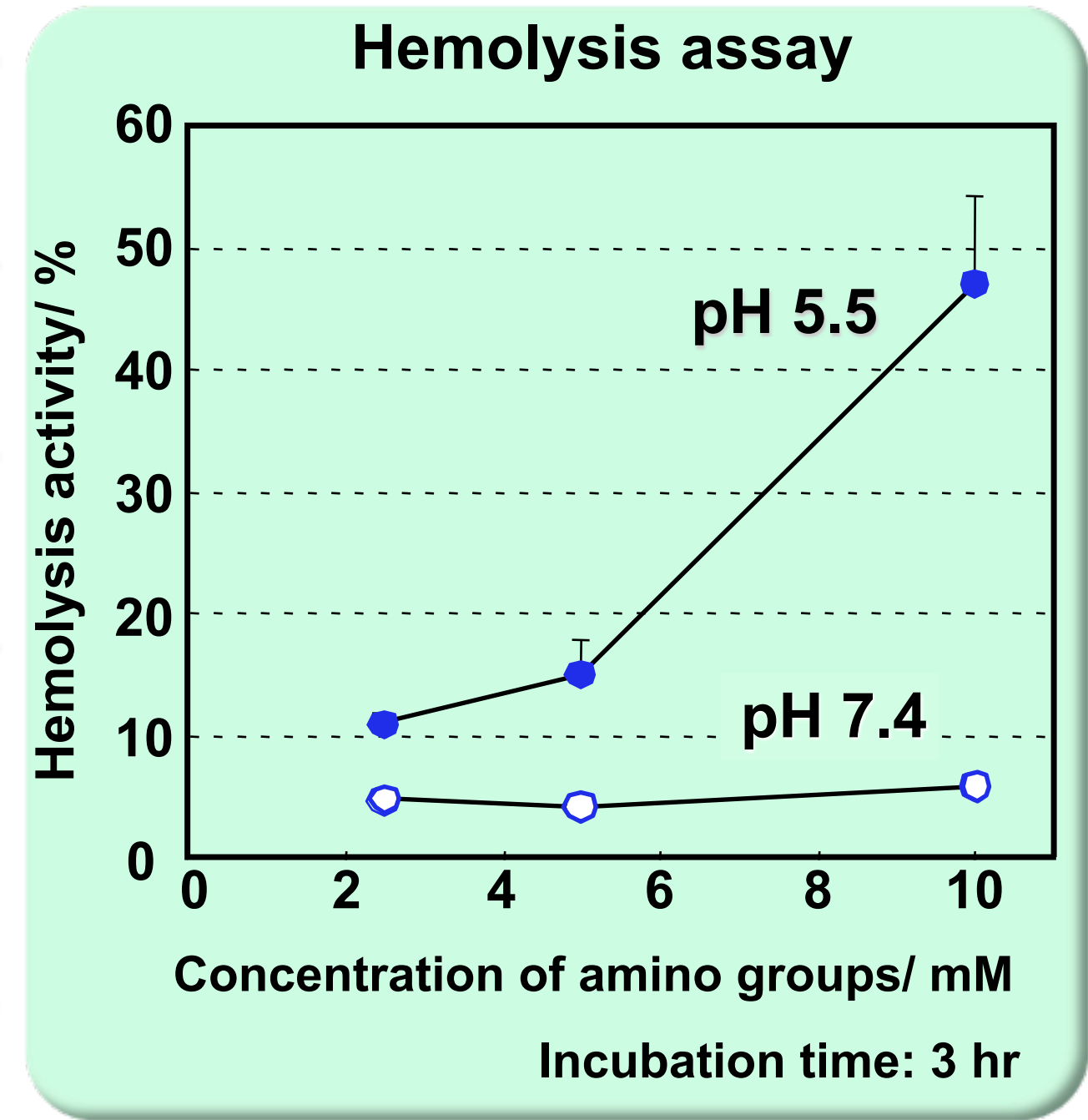
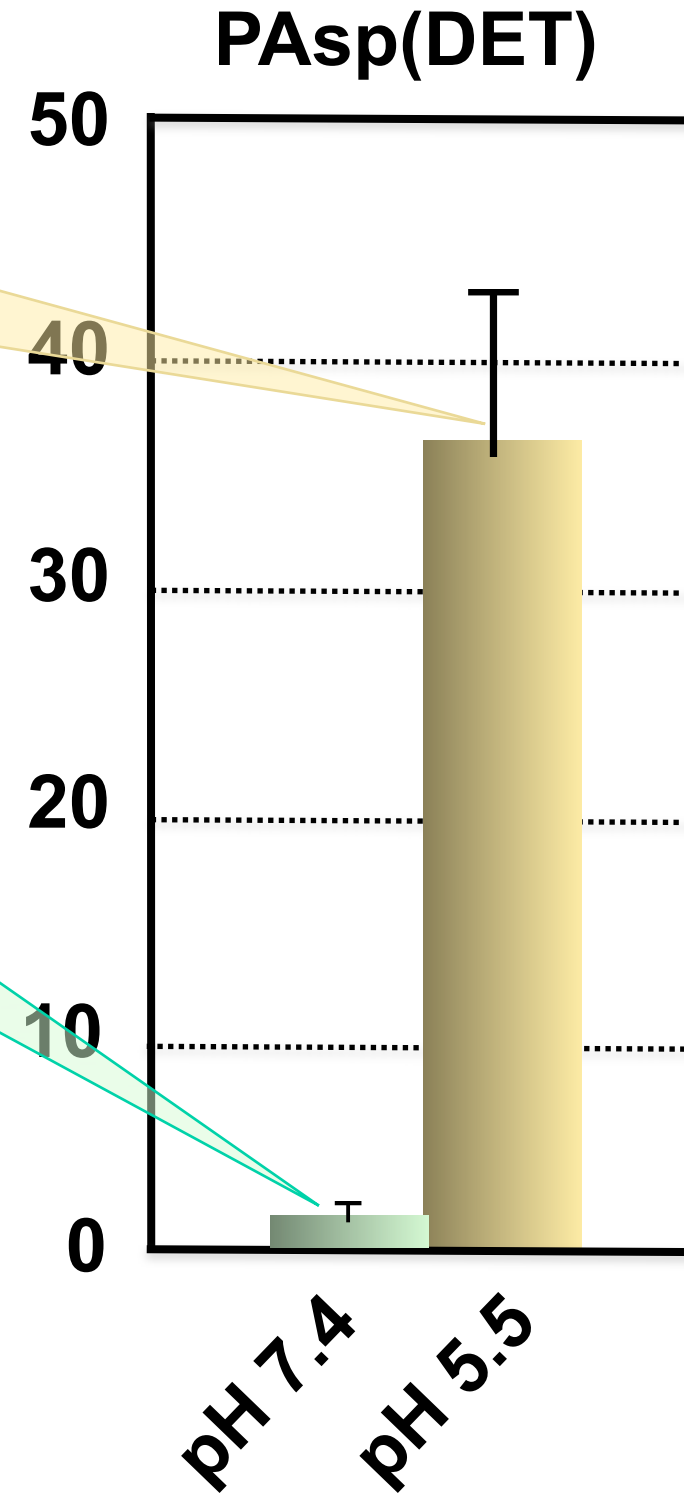
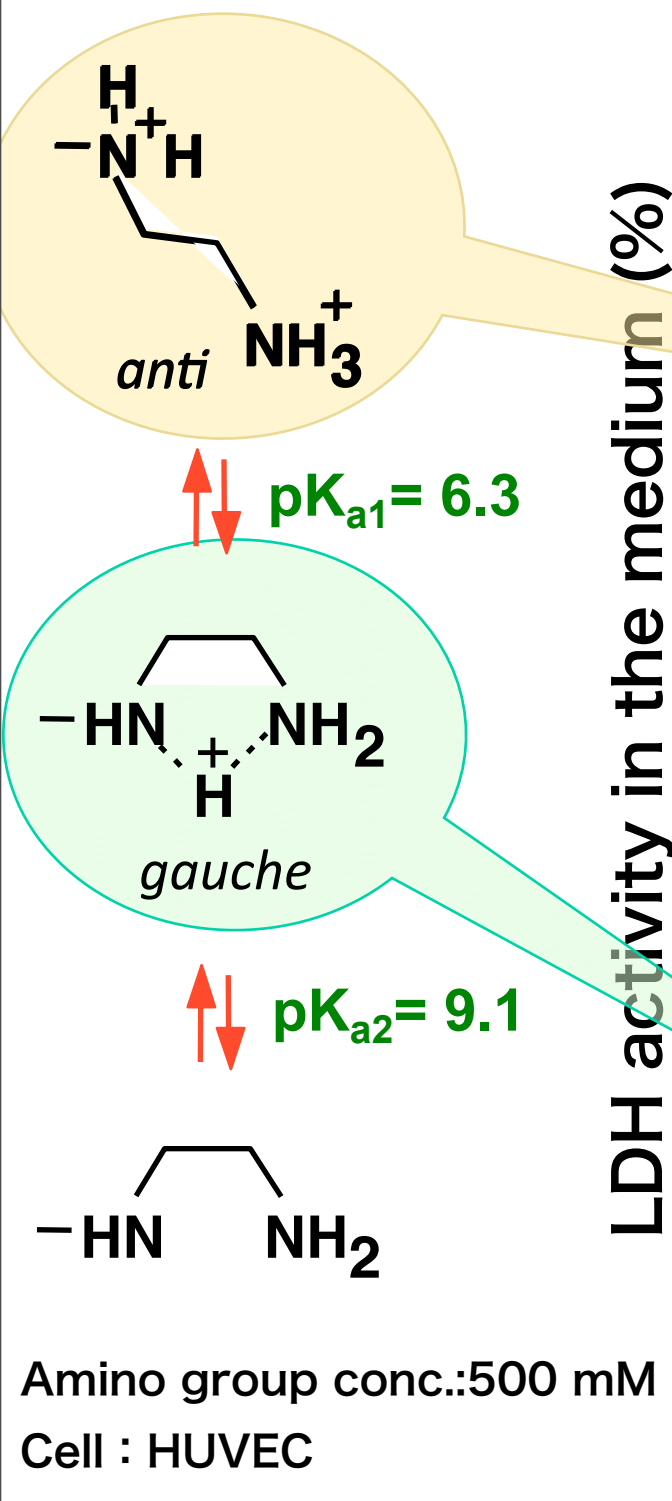


Amino group conc.: 500 mM

Cell : HUVEC

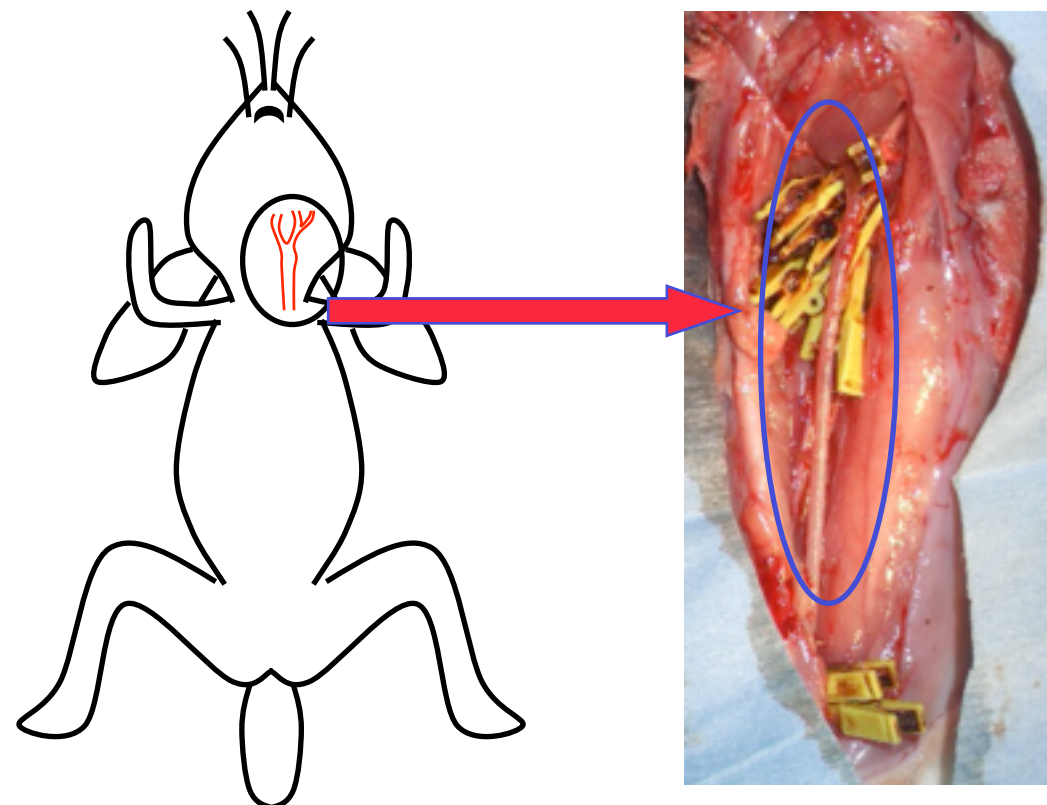


Destabilization of endosomal membrane: Hemolysis Assay

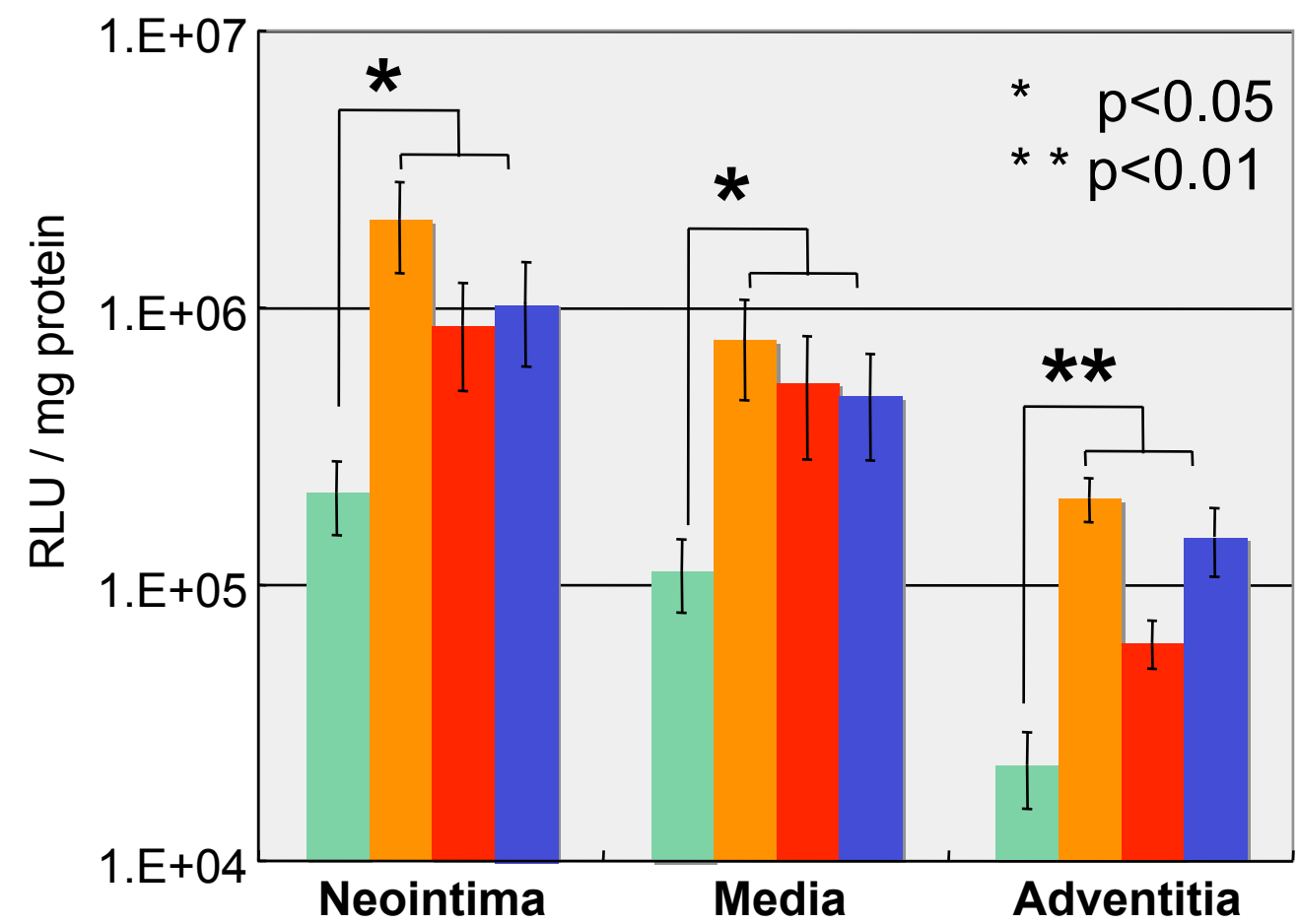
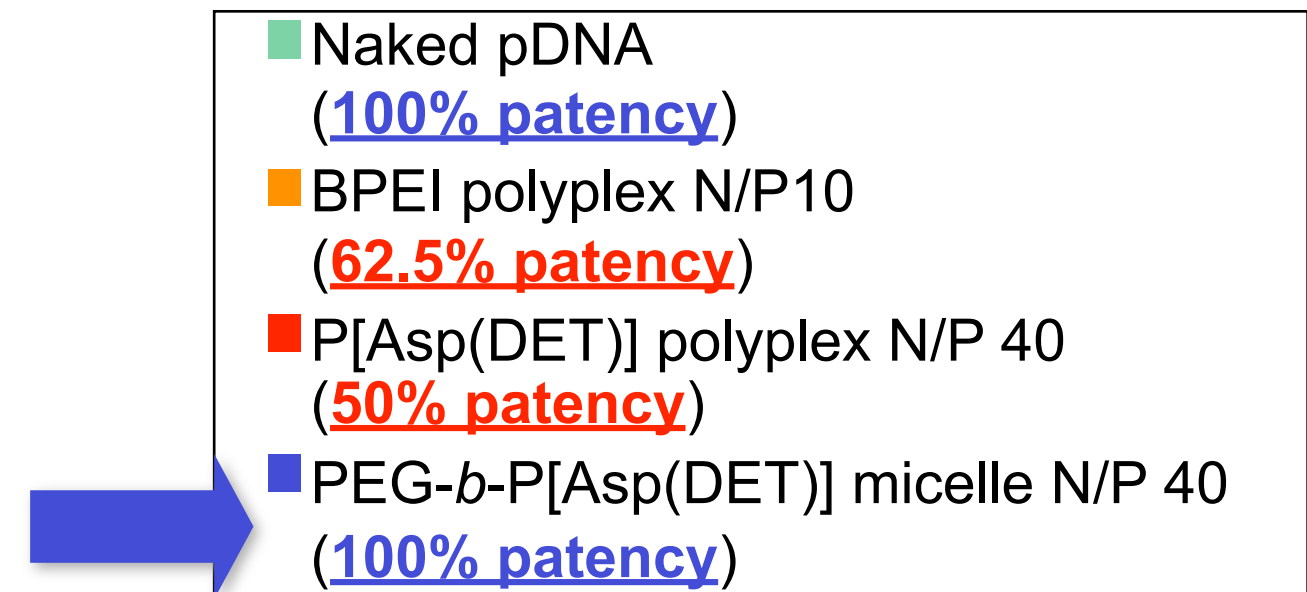
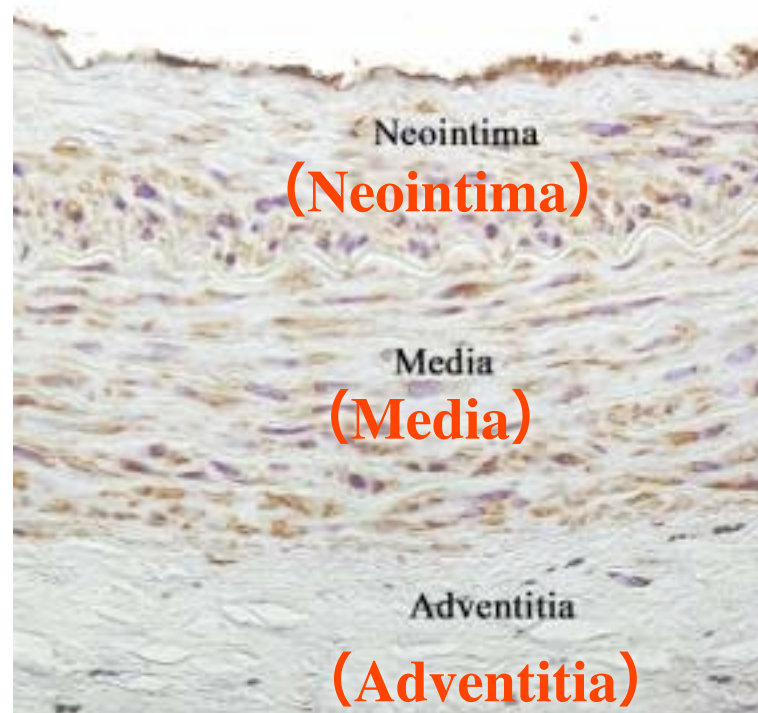


PAsp(DET) exerts membrane destabilization selectively at pH 5.5 to facilitate endosomal escape of polyplex micelles

Gene expression to rabbit carotid artery by micellar nano-vector



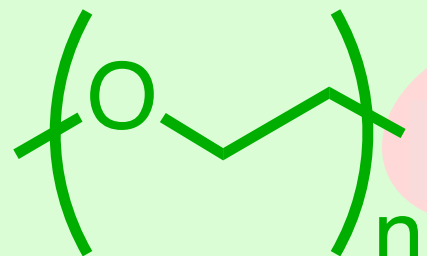
FLAG tag gene expression



Micellar nanovector achieved efficient gene transfer to carotid artery with neointimal hyperplasia without any vascular occlusion by intravascular method

Polymer Design for PEG-Detachable micelle

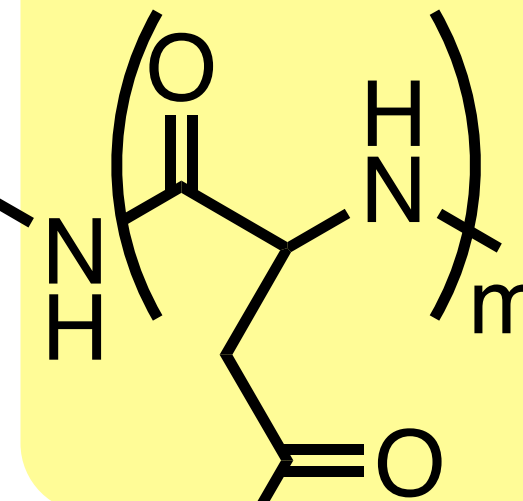
PEG



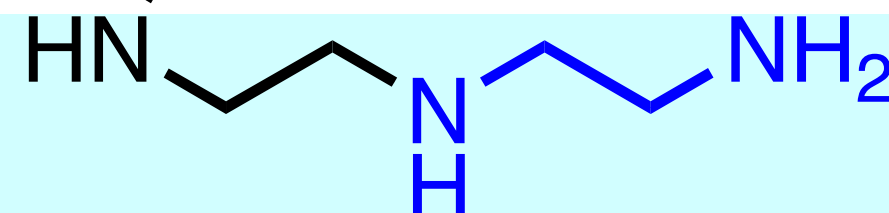
PEG shell layer contributes to biocompatibility and colloidal stability of polyplex micelles

BUT

Often reducing transfection efficacy due to steric effect

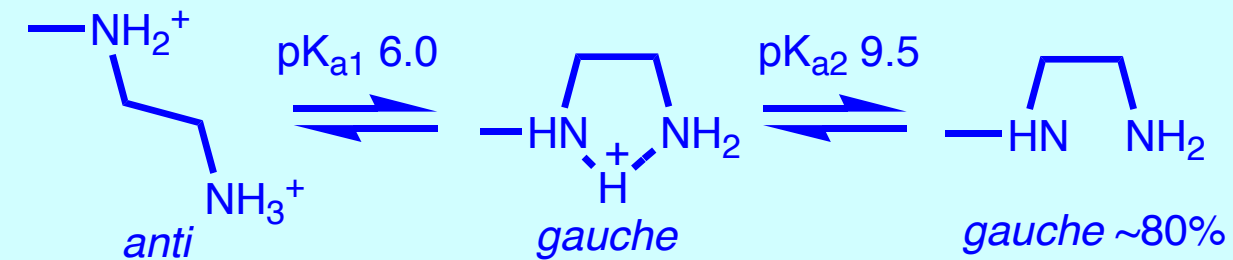


Polyaspartamide



<Ethylenediamine unit>

The two step protonation permits DNA condensation at pH 7.4 (mono-protonated) and high membrane disruptive ability in endosomal pH (di-protonated) to induce endosomal escape.

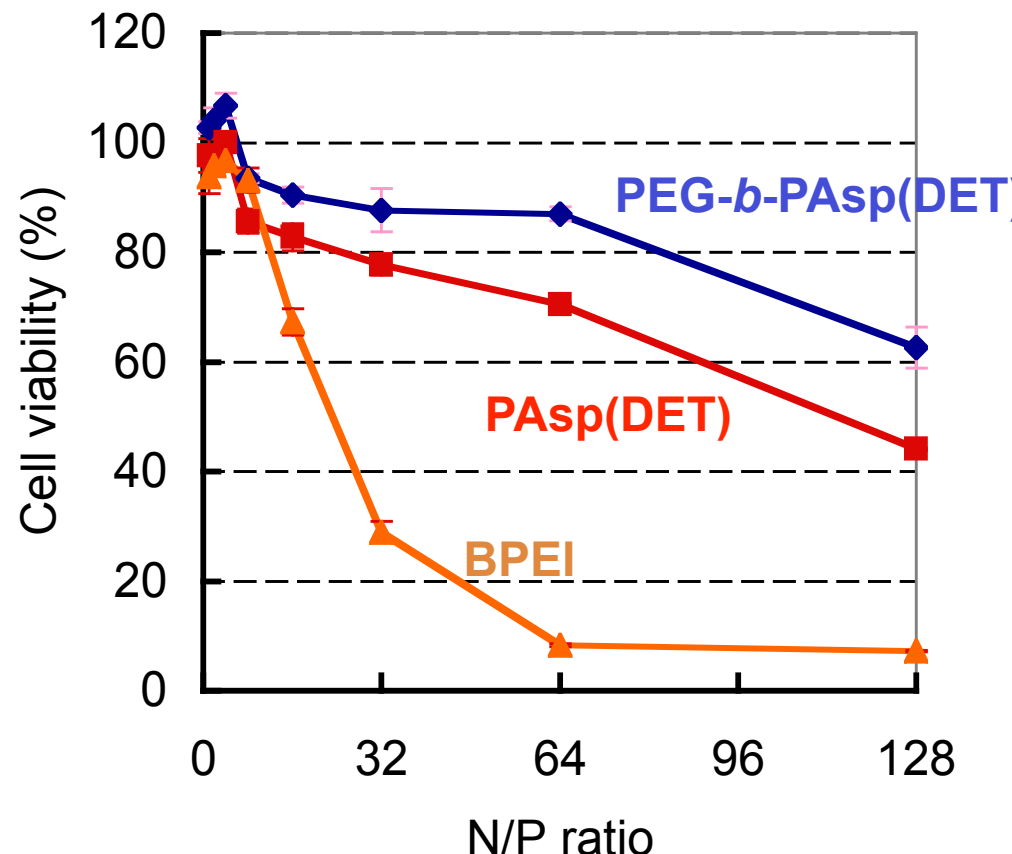


Transfection efficiency and cytotoxicity against vascular smooth muscle cells (SMC)

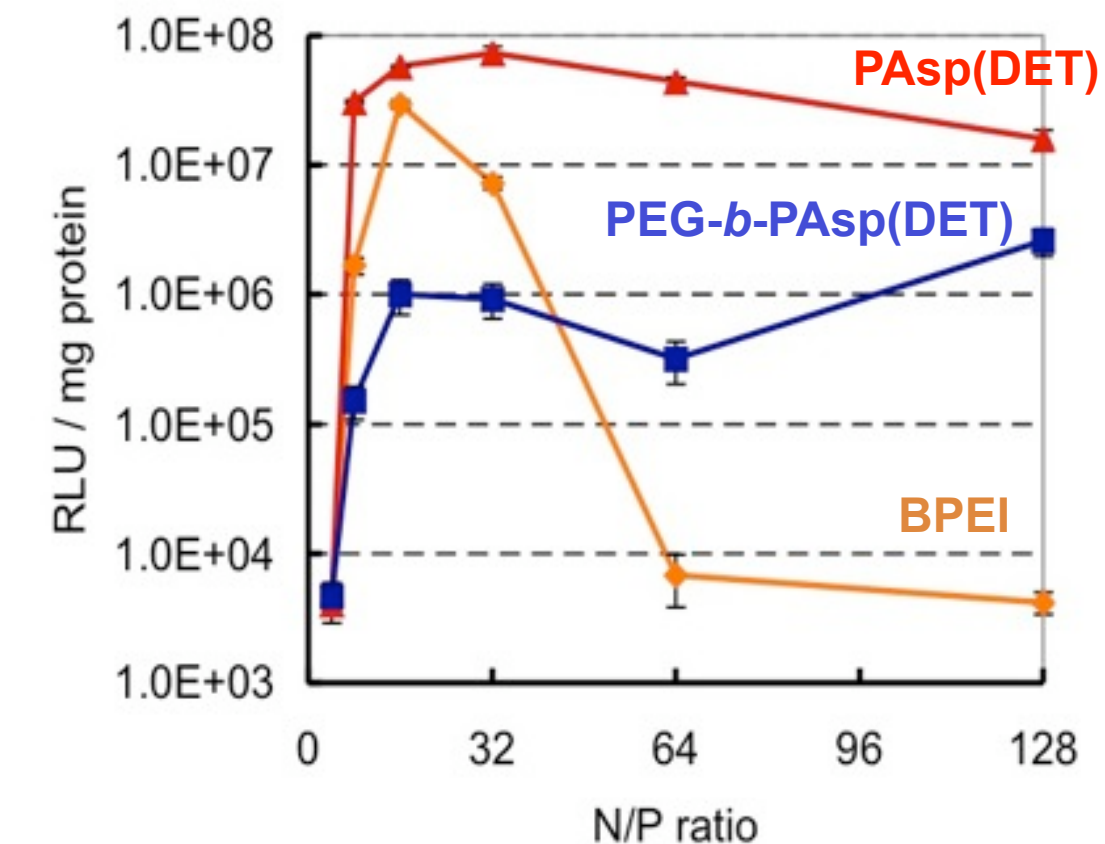
PAsp(DET)(98mer): polycation without PEG block and forming polyplex with plasmid DNA

BPEI: branched polyethyleneimine ($M_w=25\text{KDa}$)

Cytotoxicity assessment (MTT assay)



Transfection efficinency (luciferase assay)

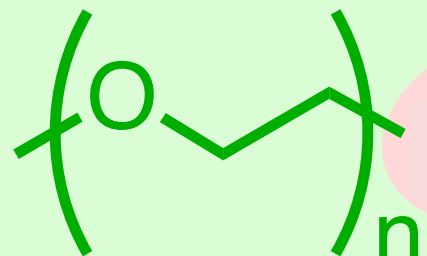


Lower cytotoxicity of PEG-*b*-PAsp(DET) and PAsp(DET) than BPEI.

Higher transfection efficiency of PAsp (DET) and BPEI polyplexes than PEG-*b*-PAsp(DET) micelles.

Polymer Design for PEG-Detachable micelle

PEG

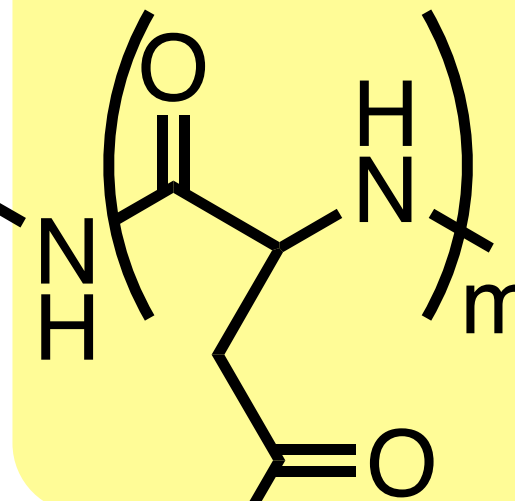


Disulfide linkage
(SS linkage)

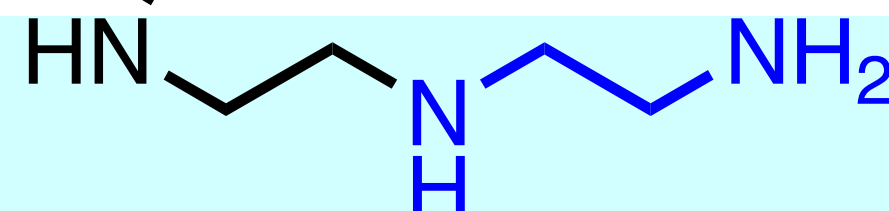
↓
Cleavable under intracellular
reduced environment

PEG-SS-P[Asp(DET)]

S. Takae, et al, JACS, 130(18)
6001-6009 (2008)

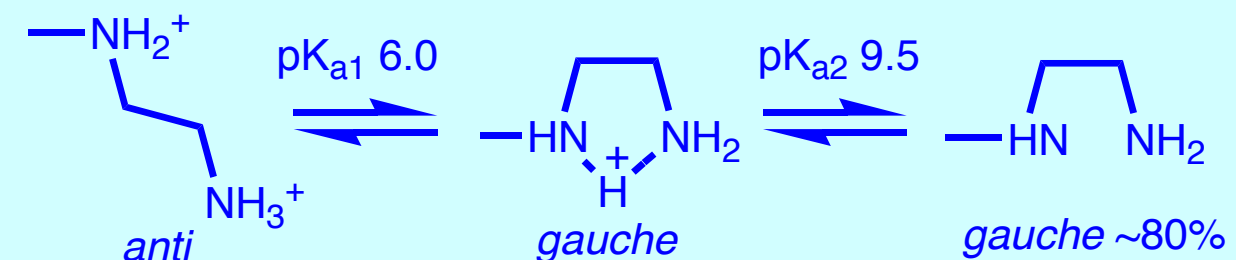


Polyaspartamide



<Ethylenediamine unit>

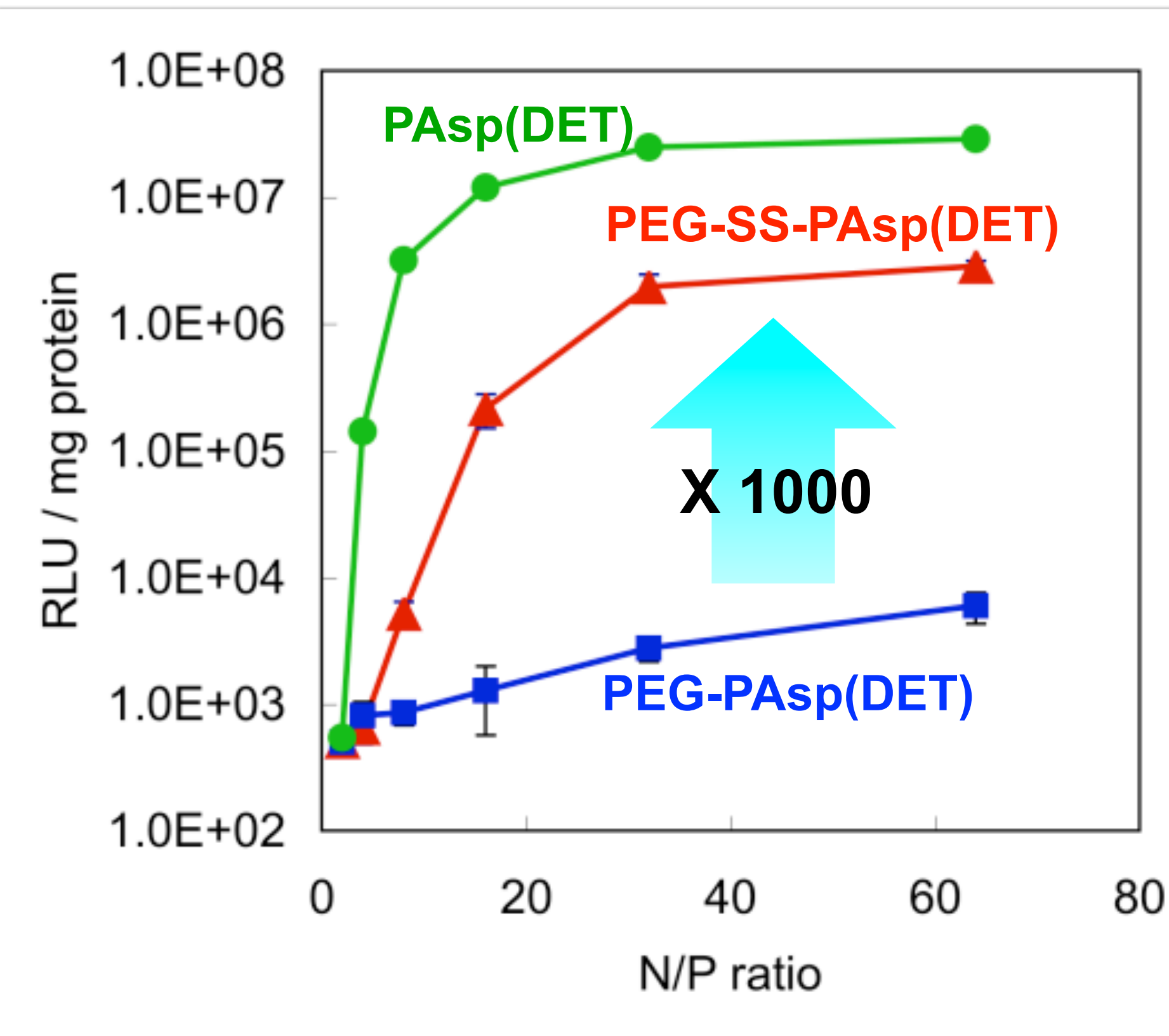
The two step protonation permits DNA condensation at pH 7.4 (mono-protonated) and high membrane disruptive ability in endosomal pH (di-protonated) to induce endosomal escape.



Kanayama, et al ChemMedChem, 2006, 1, 439-434

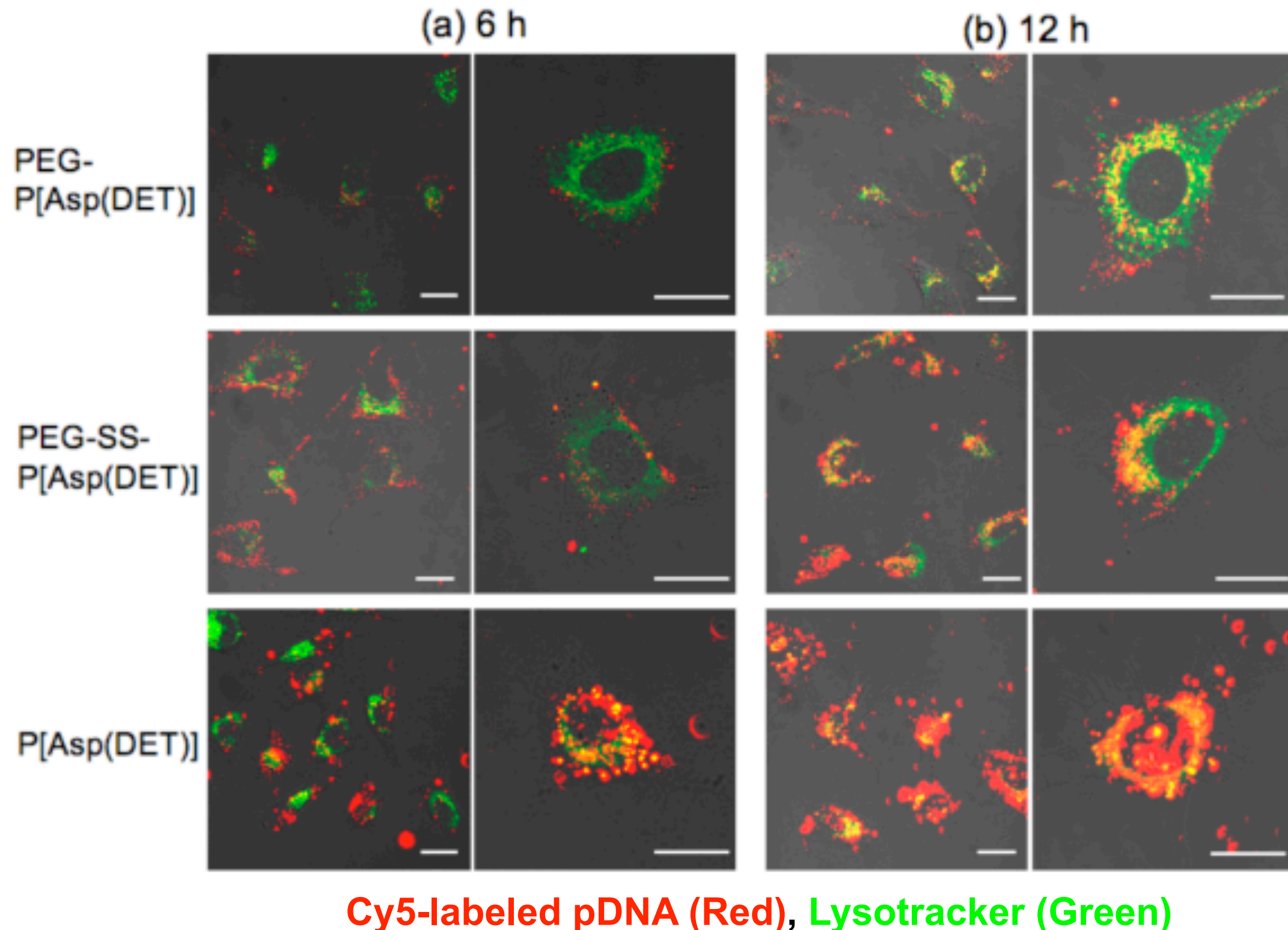
Transfection by PEG-detachable polyplex micelles

Luciferase assay (HeLa cells)

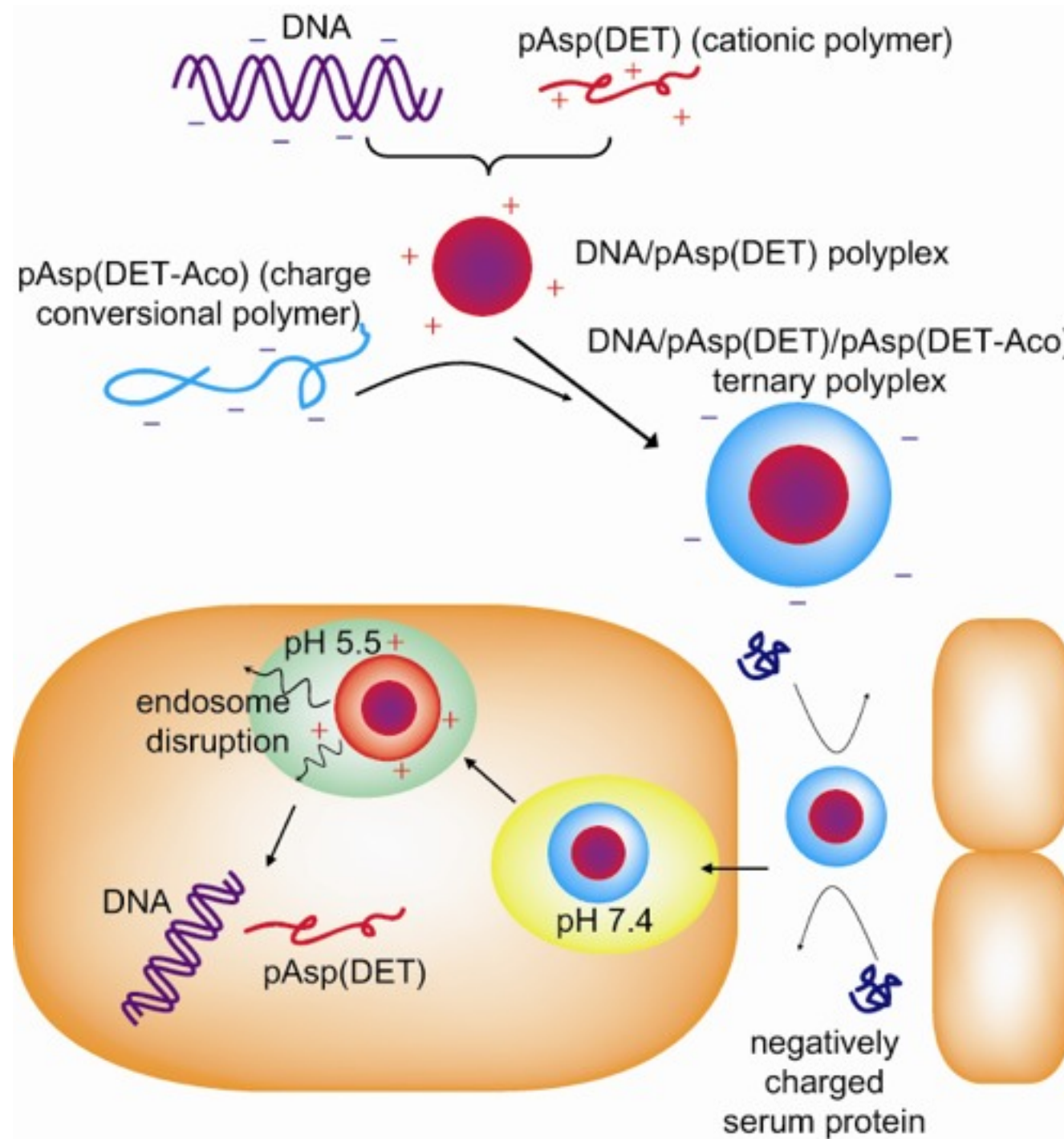


Transfection by PEG-detachable polyplex micelles

Time dependent change in intracellular distribution of pDNA



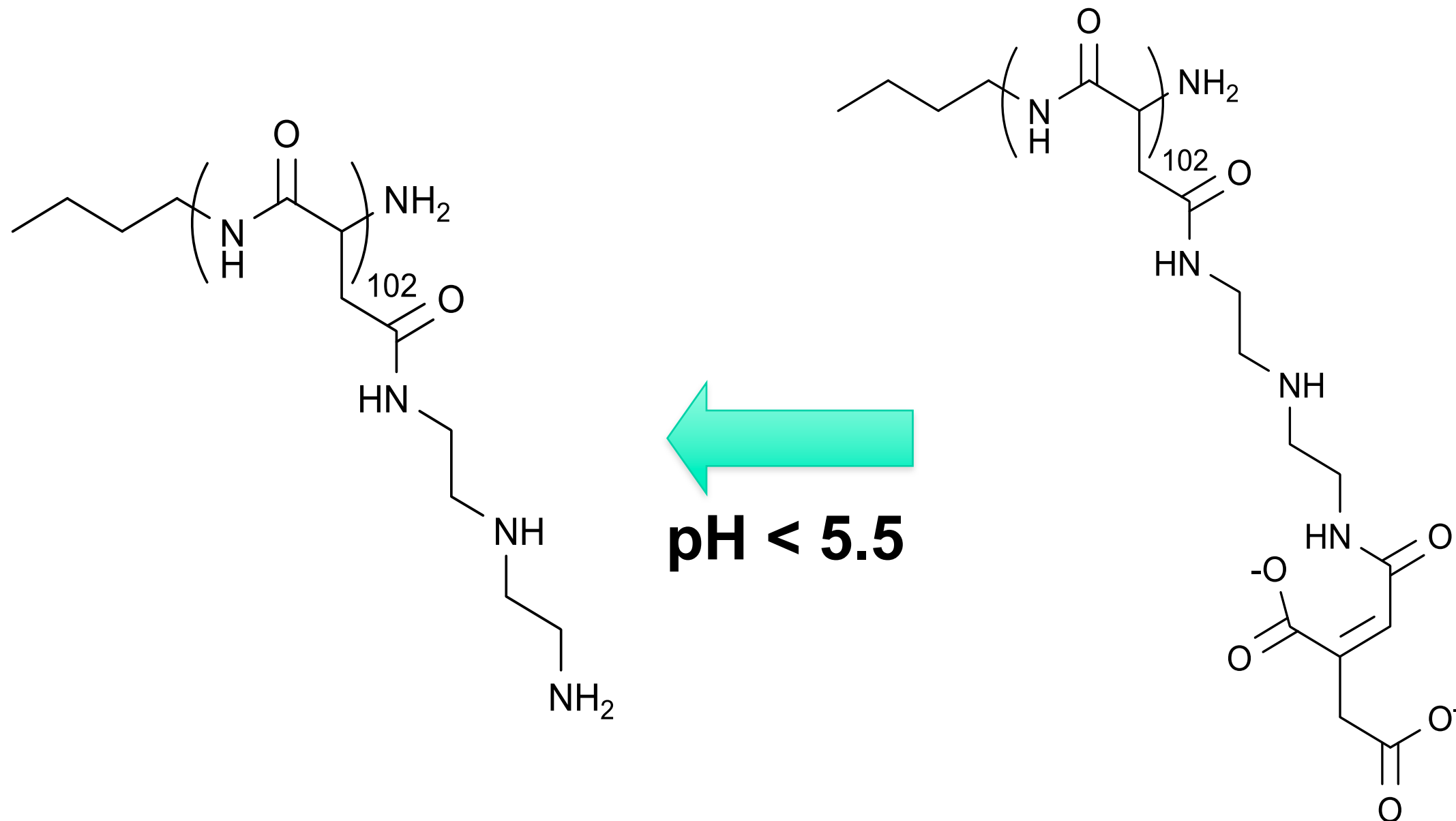
Charge-conversional polyplex system



If the polyplex had negatively charged in the cell exterior, it could reduce the toxicity.

If the charge of the polyplex turned to positive after internalization into the cell, it could disrupt endosome effectively.

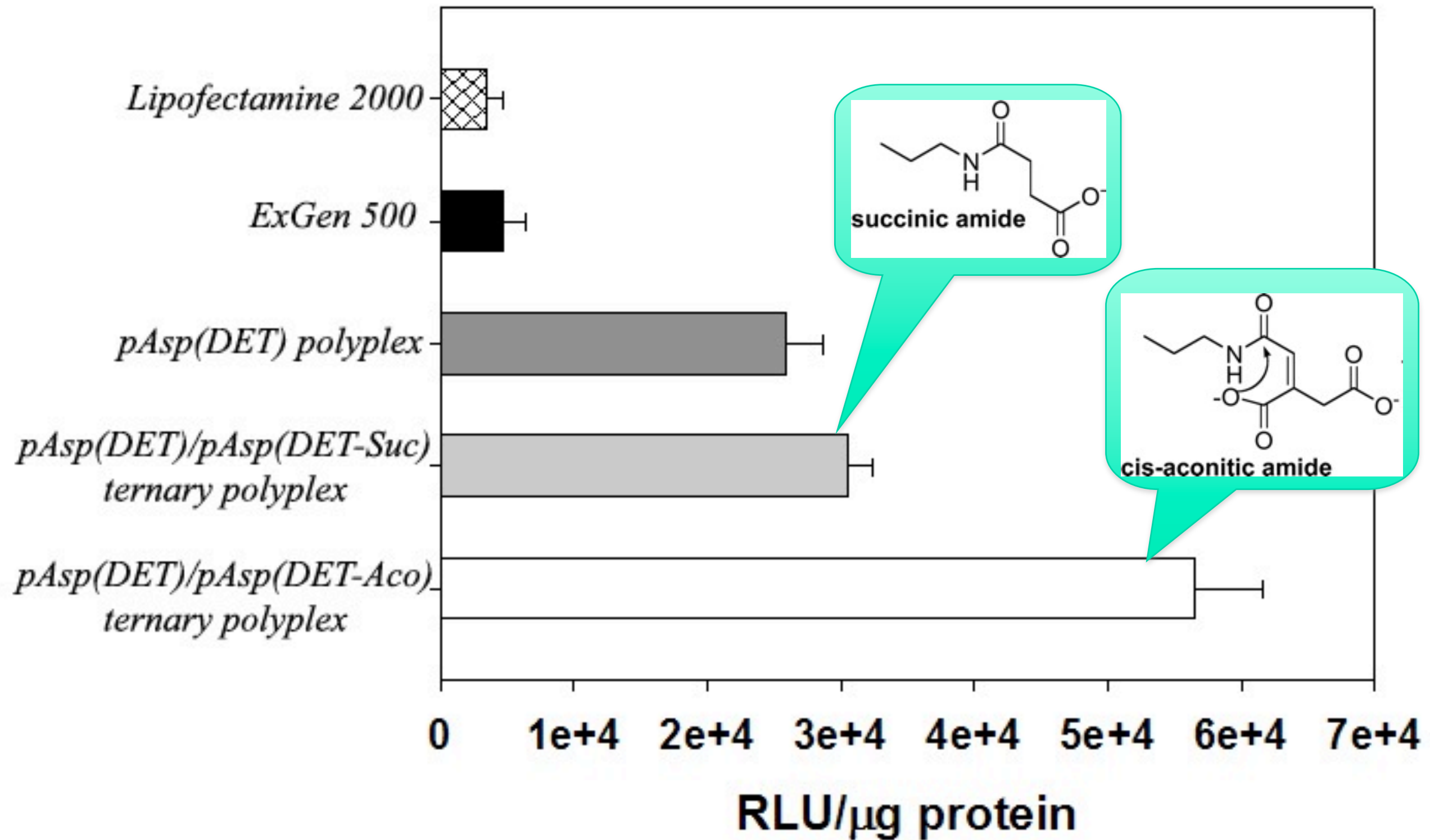
pAsp(DET)/pAsp(DET-Aco)



pAsp(DET) :
cationic polymer
with endosome
disruption moiety

pAsp(DET-Aco) :
charge-
conversional
polymer

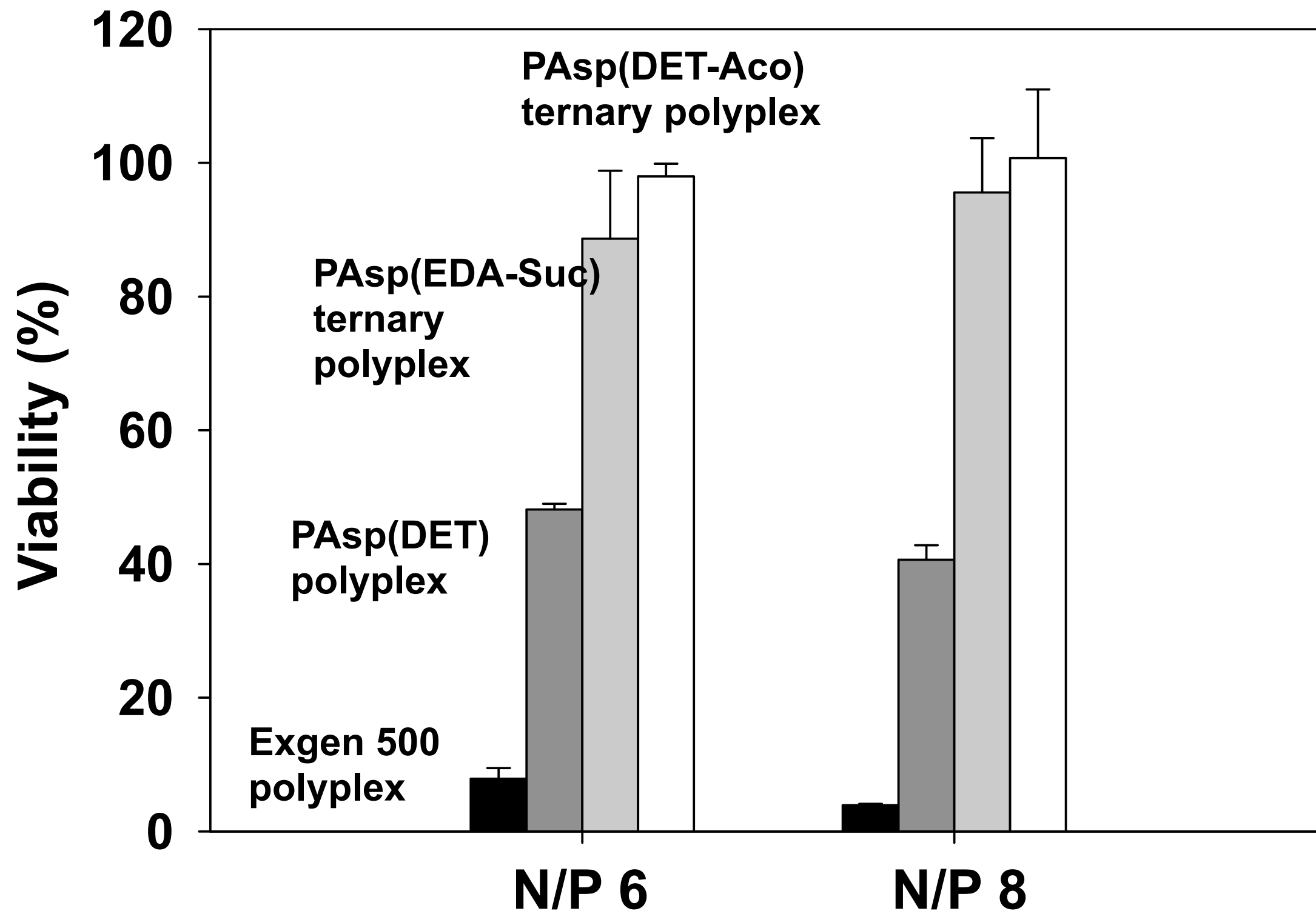
Transfection efficiency of ternary polyplex on HUVEC



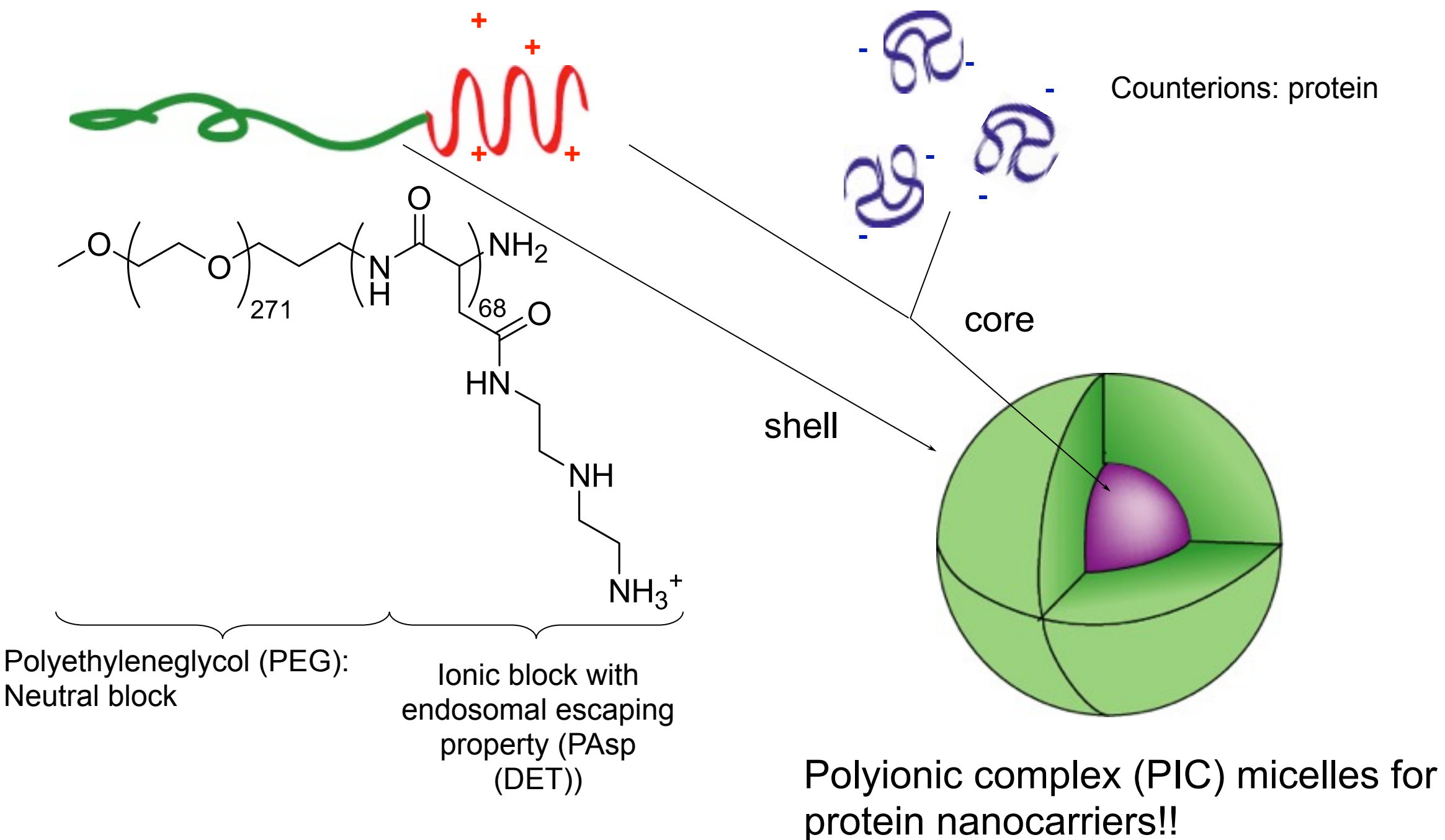
***HUVEC** (Human umbilical vein endothelial cells) are difficult to be transfected and sensitive to toxicity.

*The charge-conversional ternary polyplex (white) showed high transfection efficiency in this primary cells.

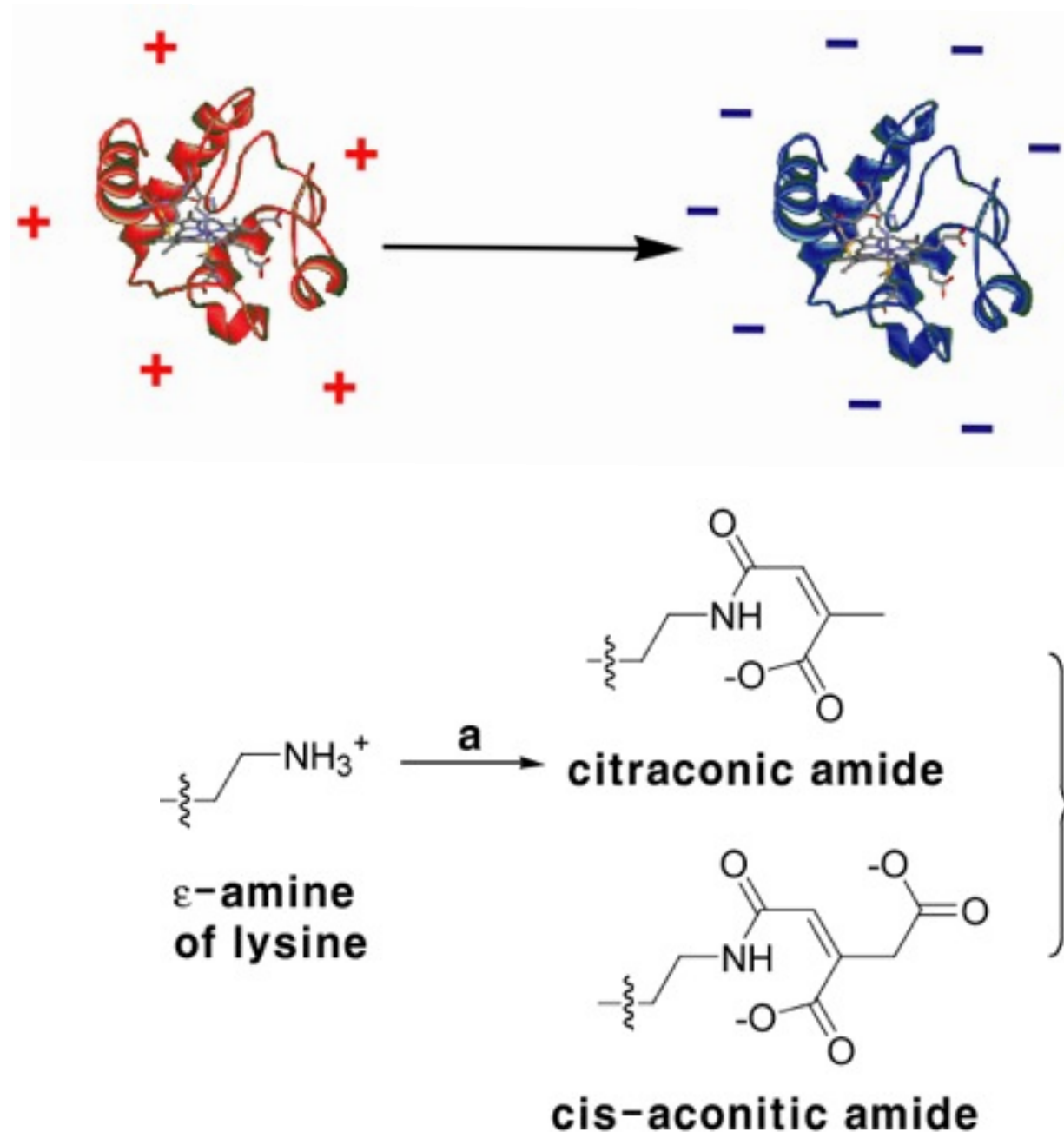
Cytotoxicity of ternary polyplex against HUVEC



PIC micelles: an efficient protein delivery system into cytoplasm



Charge-conversional modification of protein (Cytochrome C)

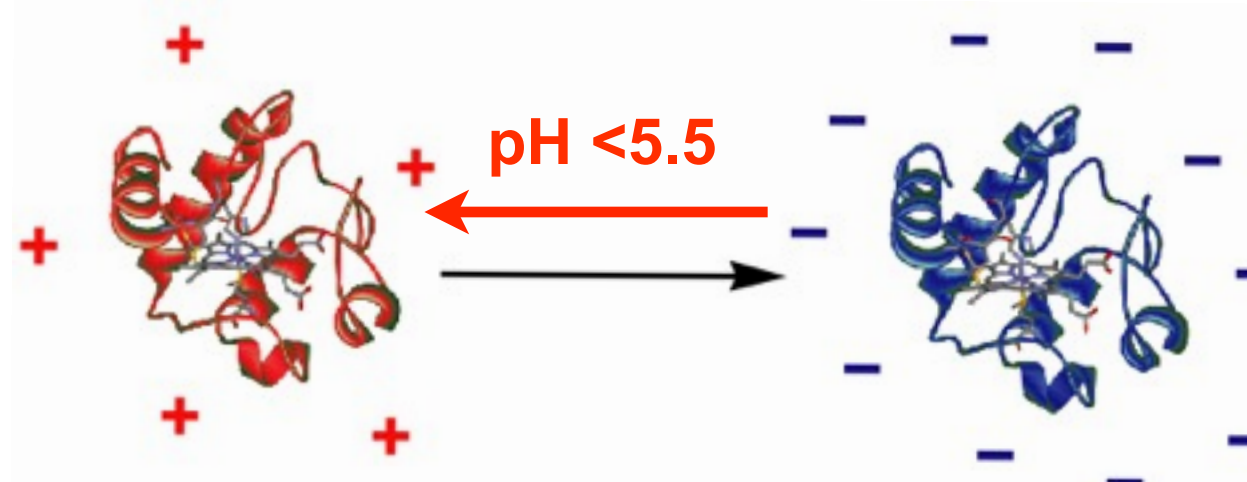


Protein	Charge density (Da/charge)
CytC	+1391
Cyt-Cit	-501
Cyt-Aco	-320

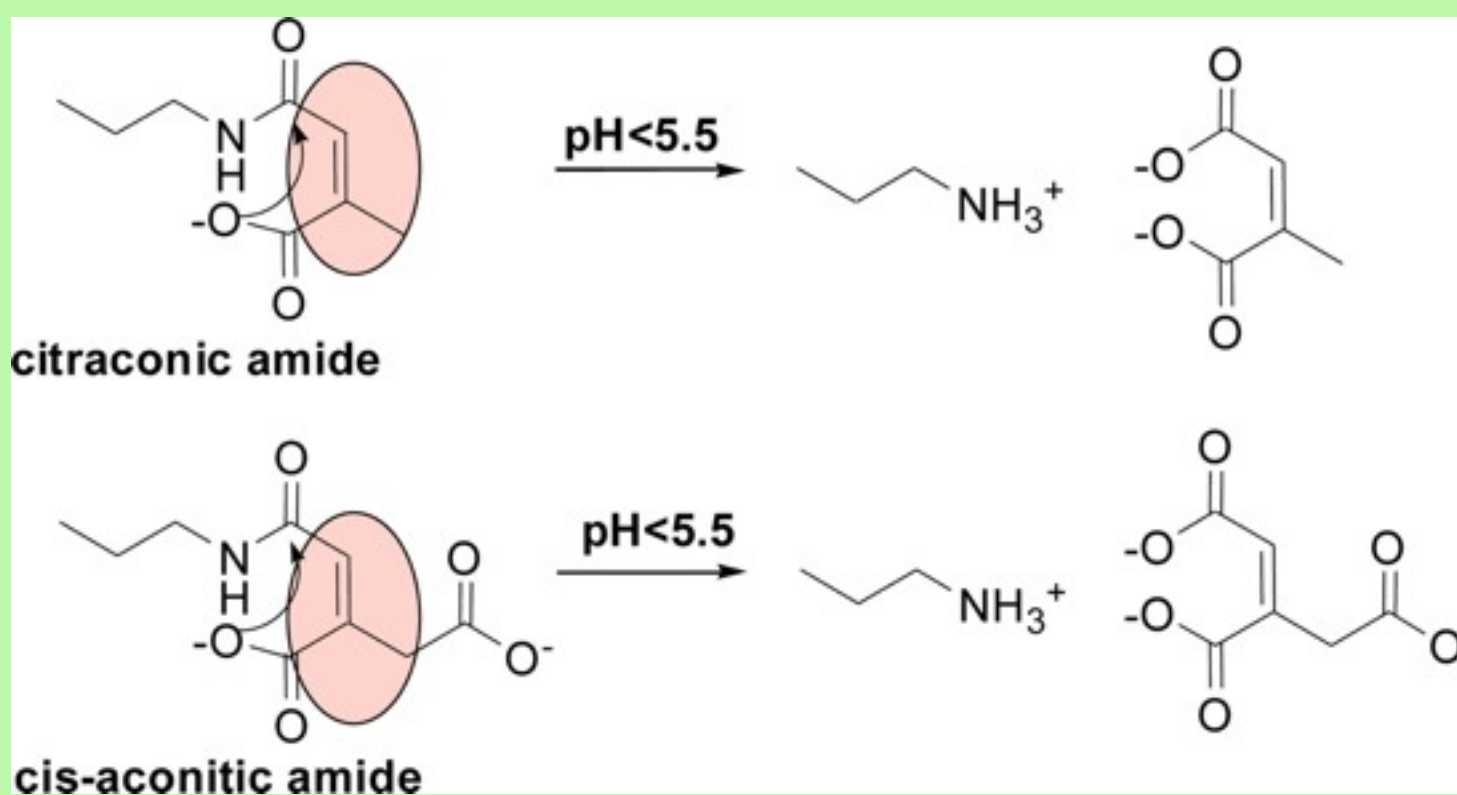
Charge-density can be increased by the charge-conversion!

a: citraconic anhydride or cis-aconitic anhydride

Charge-conversional modification of protein (Cytochrome C)



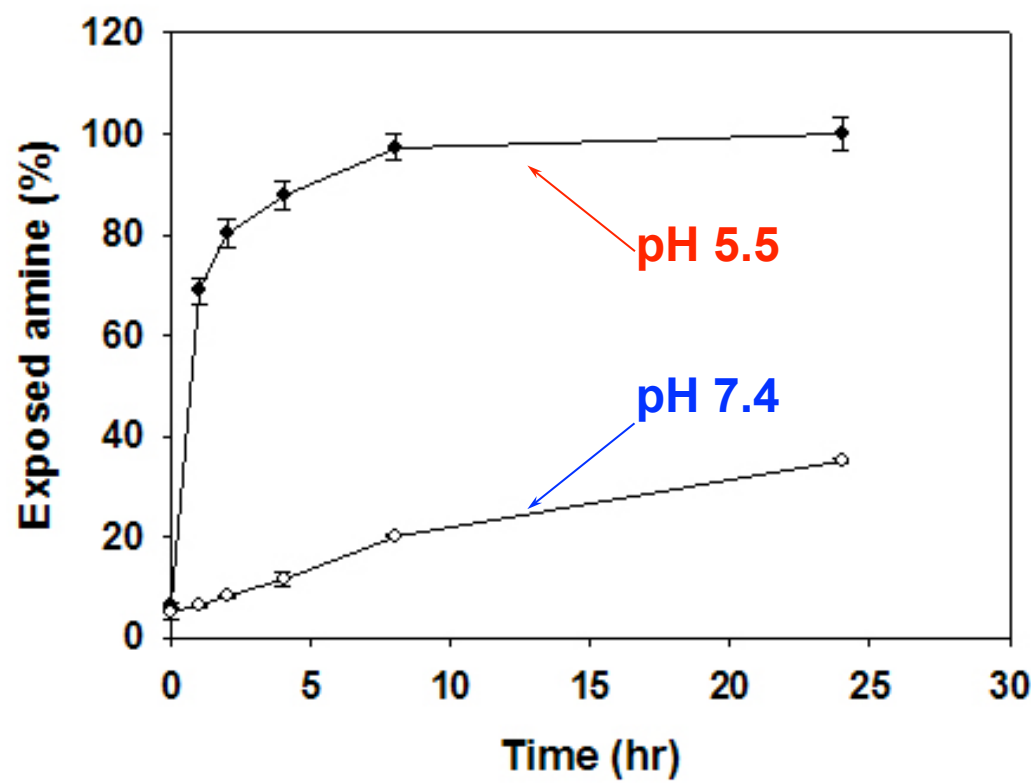
Protein	Charge density (Da/charge)
CytC	+1391
Cyt-Cit	-501
Cyt-Aco	-320



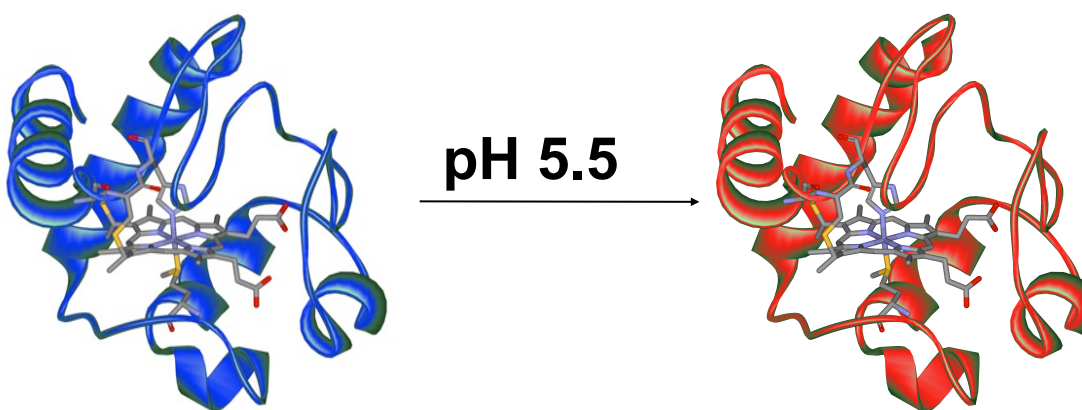
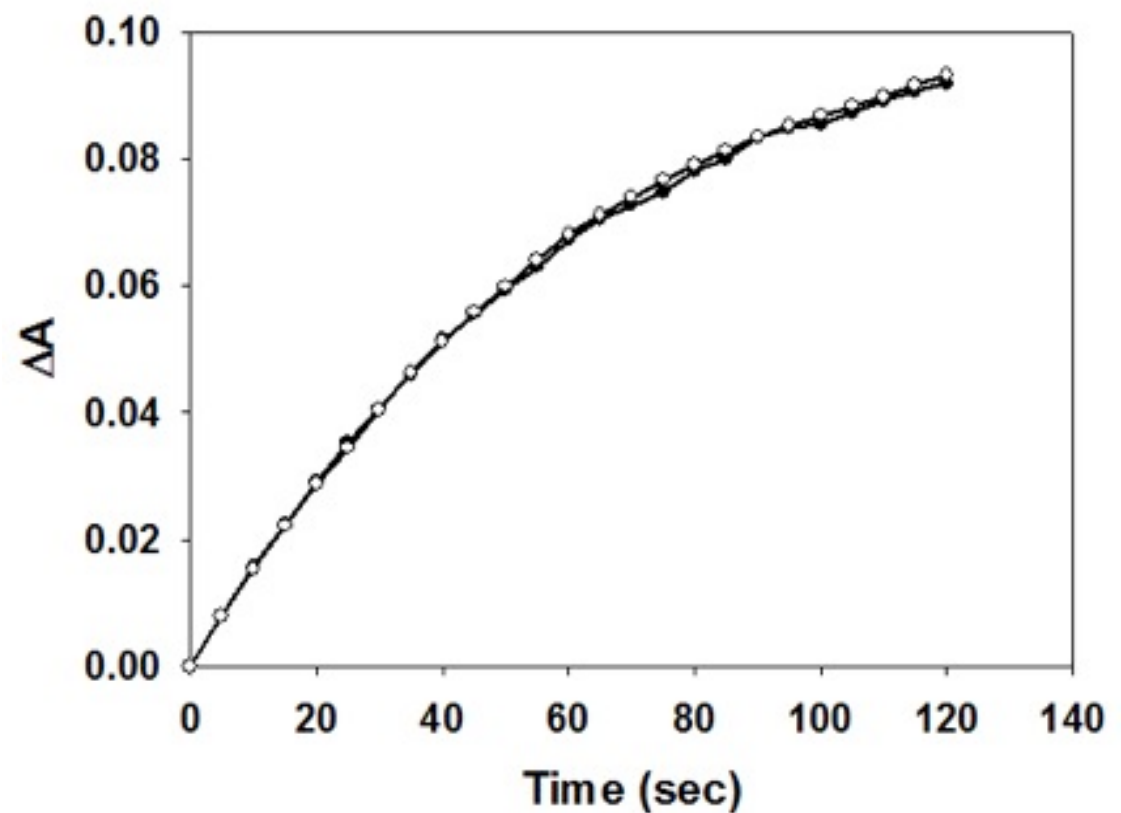
Charge-density can be increased by the charge-conversion!

Reversibility of the charge-conversion

pH-sensitive reversal



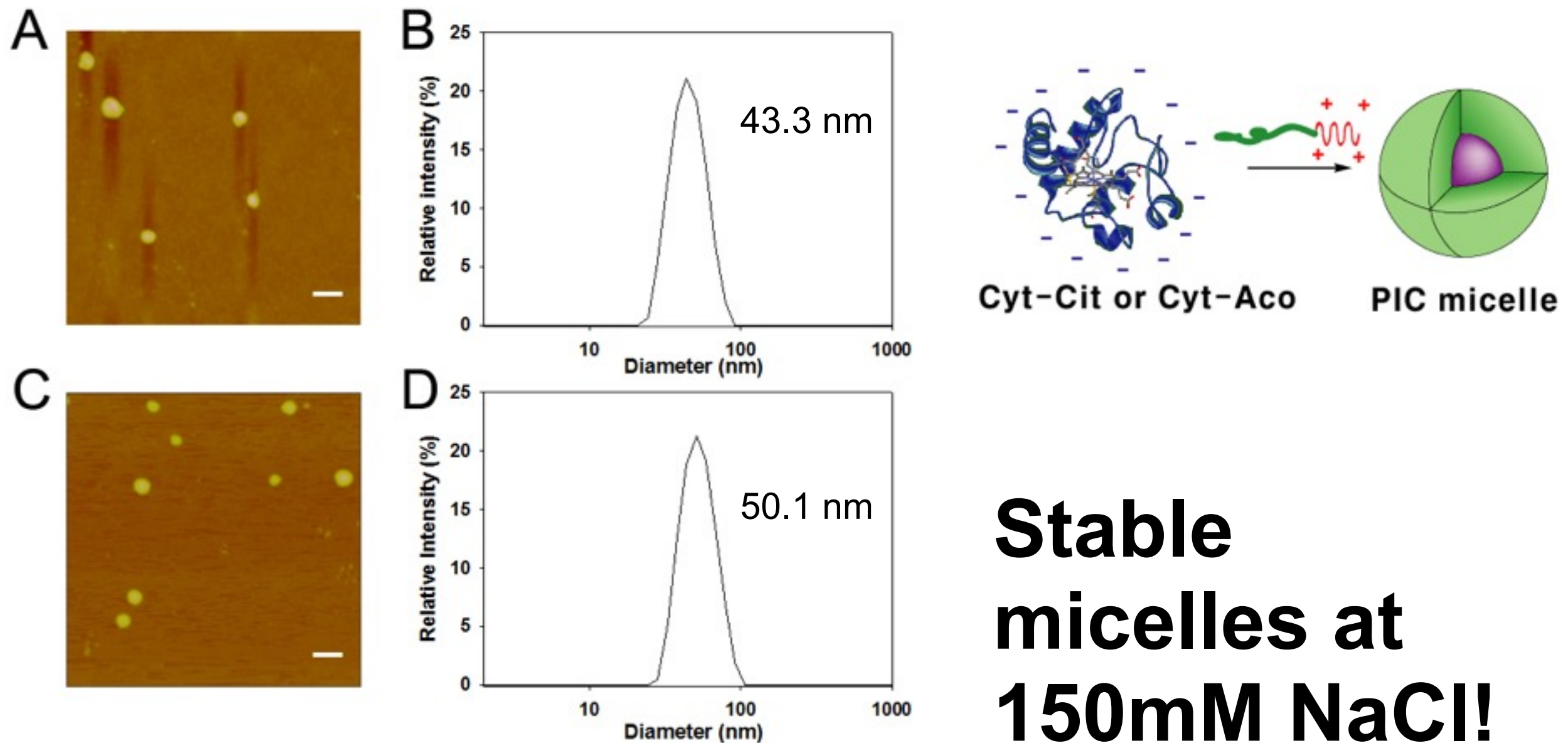
protein activity



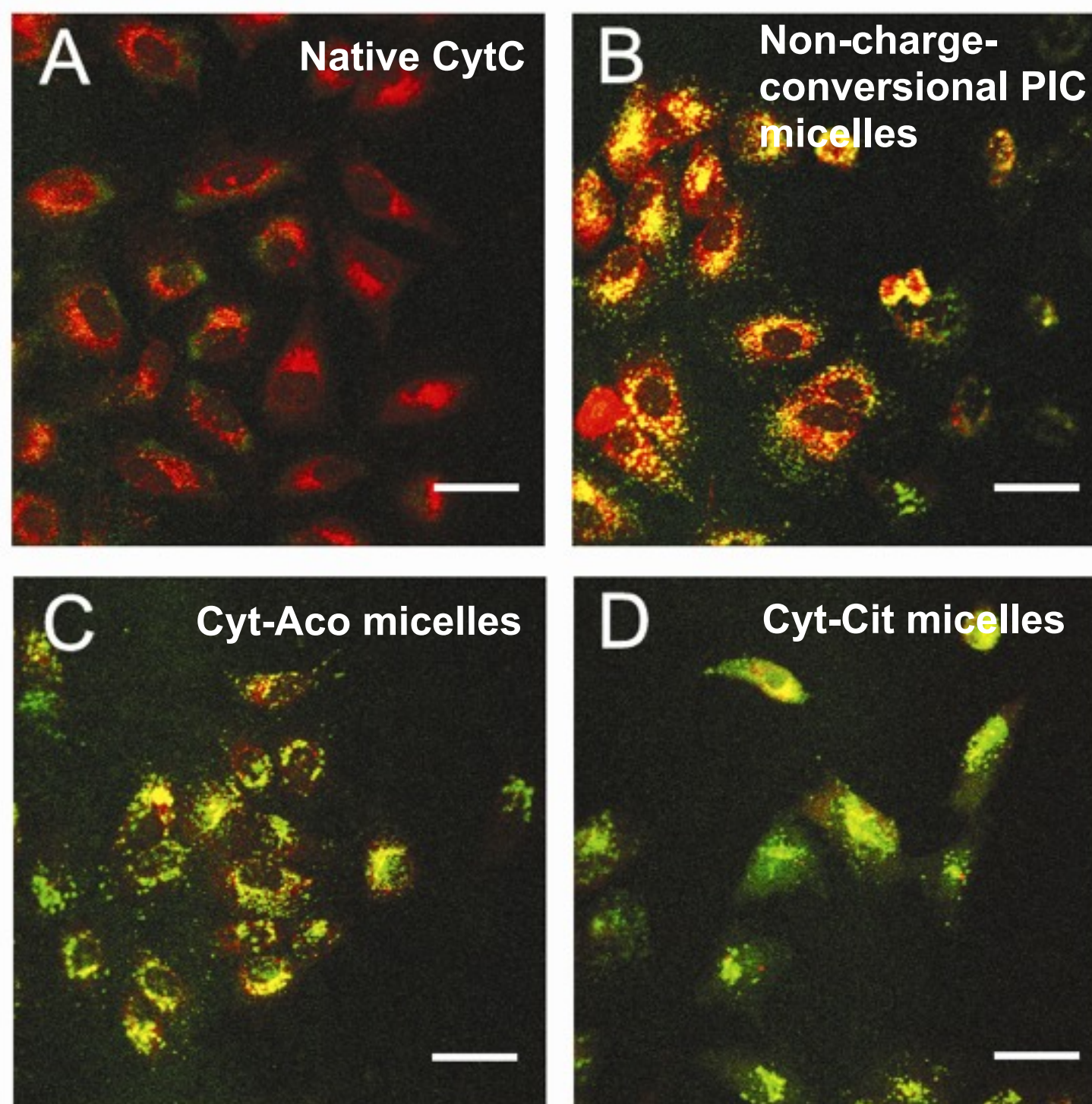
The charge-conversion can be reversed rapidly at endosomal pH 5.5.

The modification-reversion process does not affect on the protein activity.

Formation of the PIC micelles at physiological salt condition



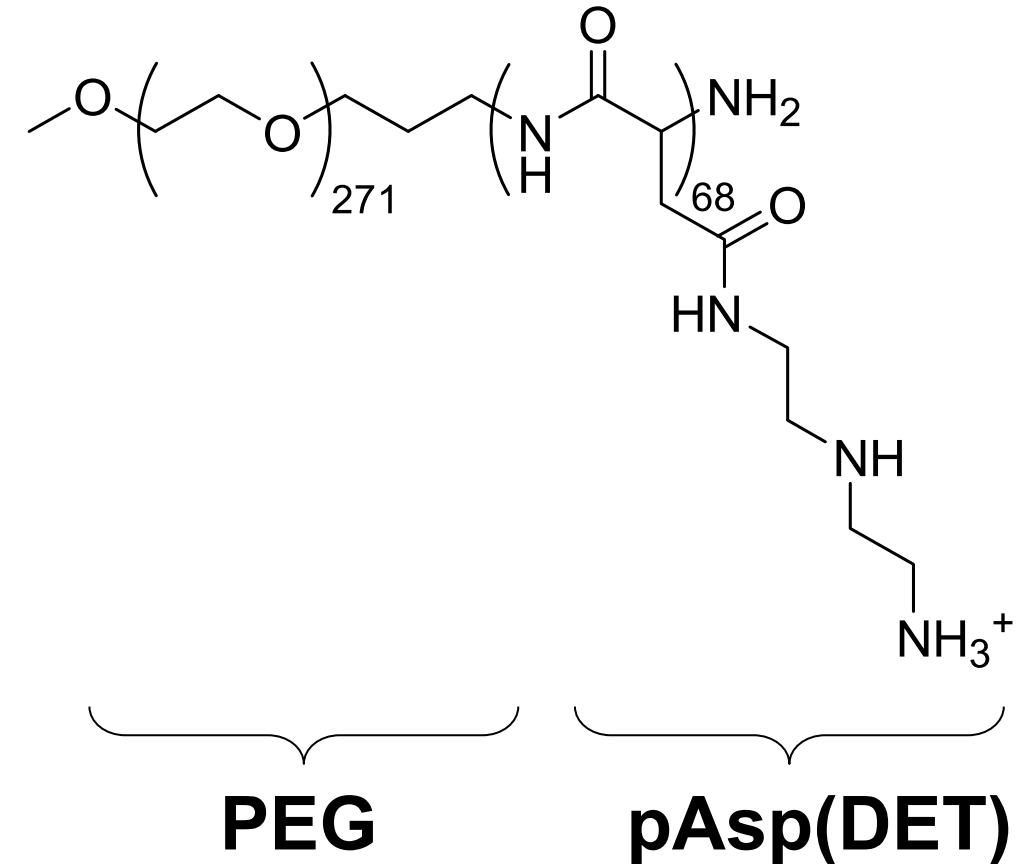
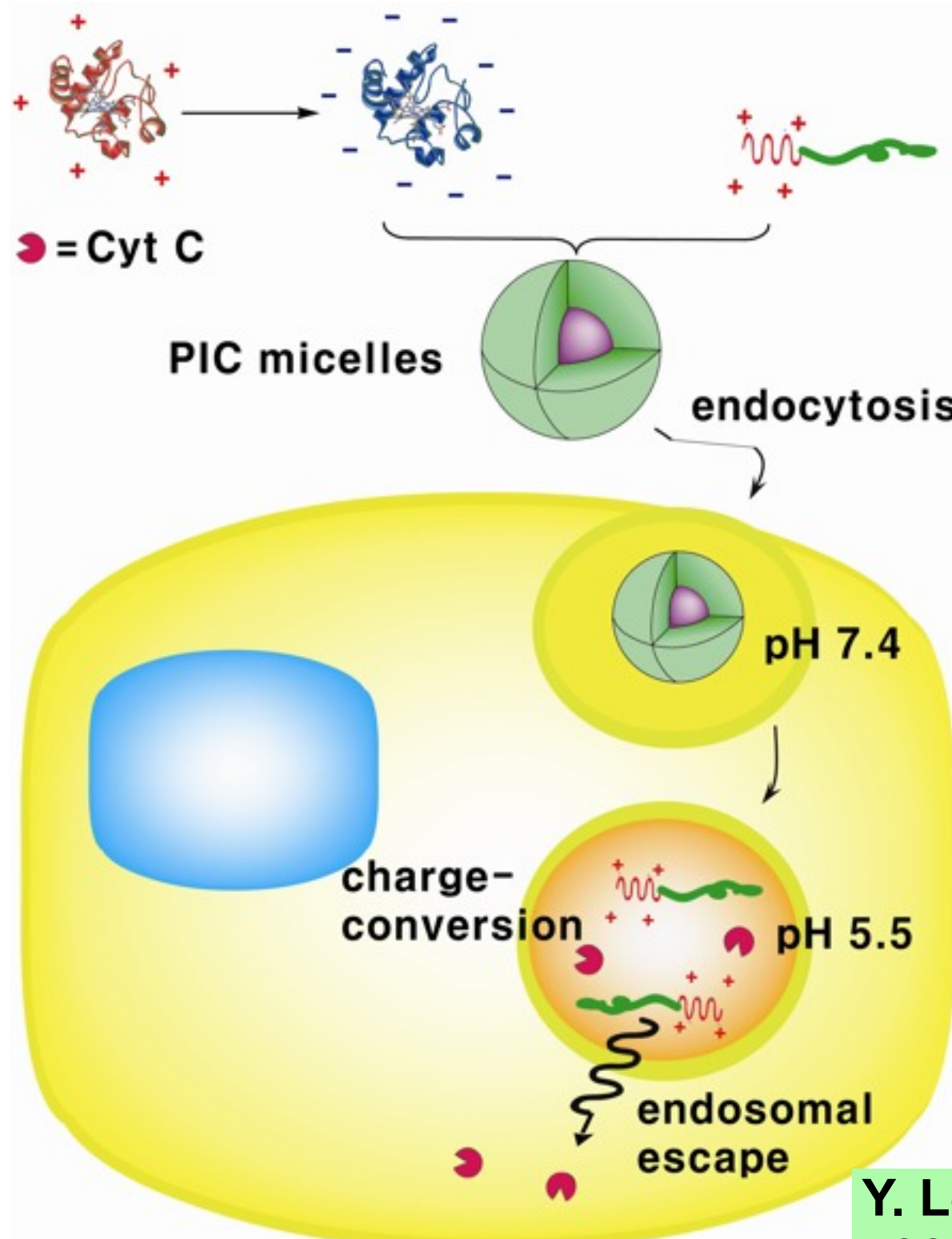
Intracellular protein delivery by charge-conversional PIC micelles



- Cyt-Alexa 488
(protein escaped from endosome)
- Endosome-Lysotracker Red
(endosome)
- Co-localization of green and red
(Cyt in endosome)

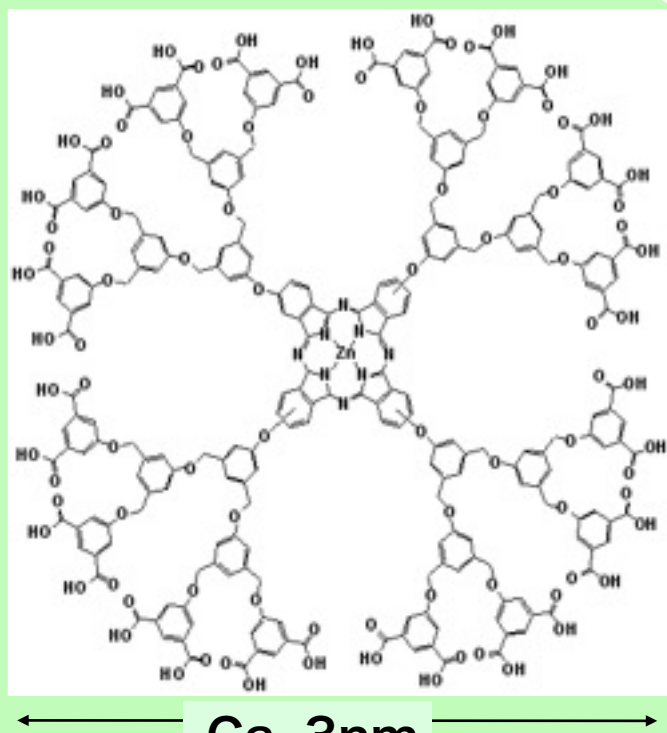
Cyt C: no internalization
Non-charge-conversional PIC micelles: efficient internalization (yellow) but no escape
Charge-conversional PIC micelles: efficient internalization and efficient escape (green)

Endosomal escape accelerated by PEG-pAsp(DET) polymer

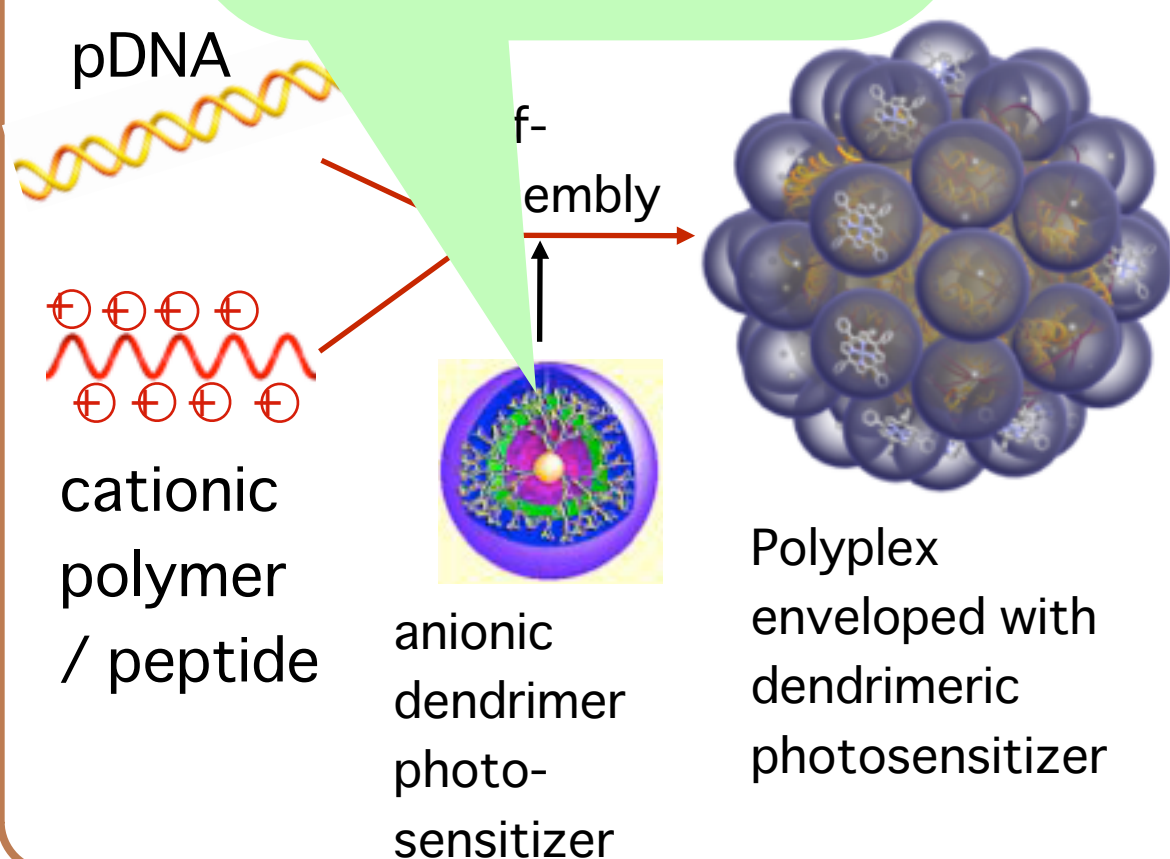


The released PEG-pAsp(DET) helps the endosomal escape.

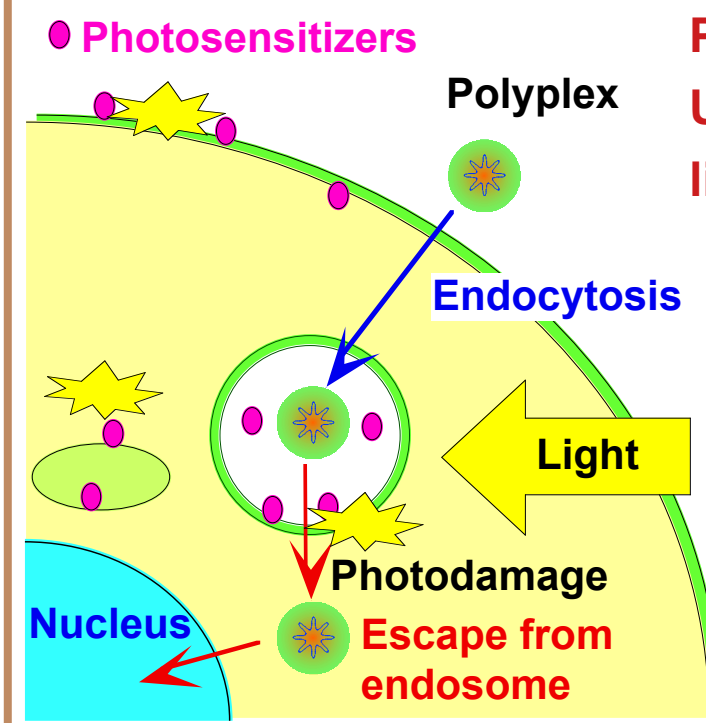
Endosomal escape: A key issue in intracellular gene delivery



Dendritic Photosensitizer



Challenge: Design of photosensitive polyplex with low cytotoxicity and high photochemical efficiency for site-directed gene transfer *in vivo*



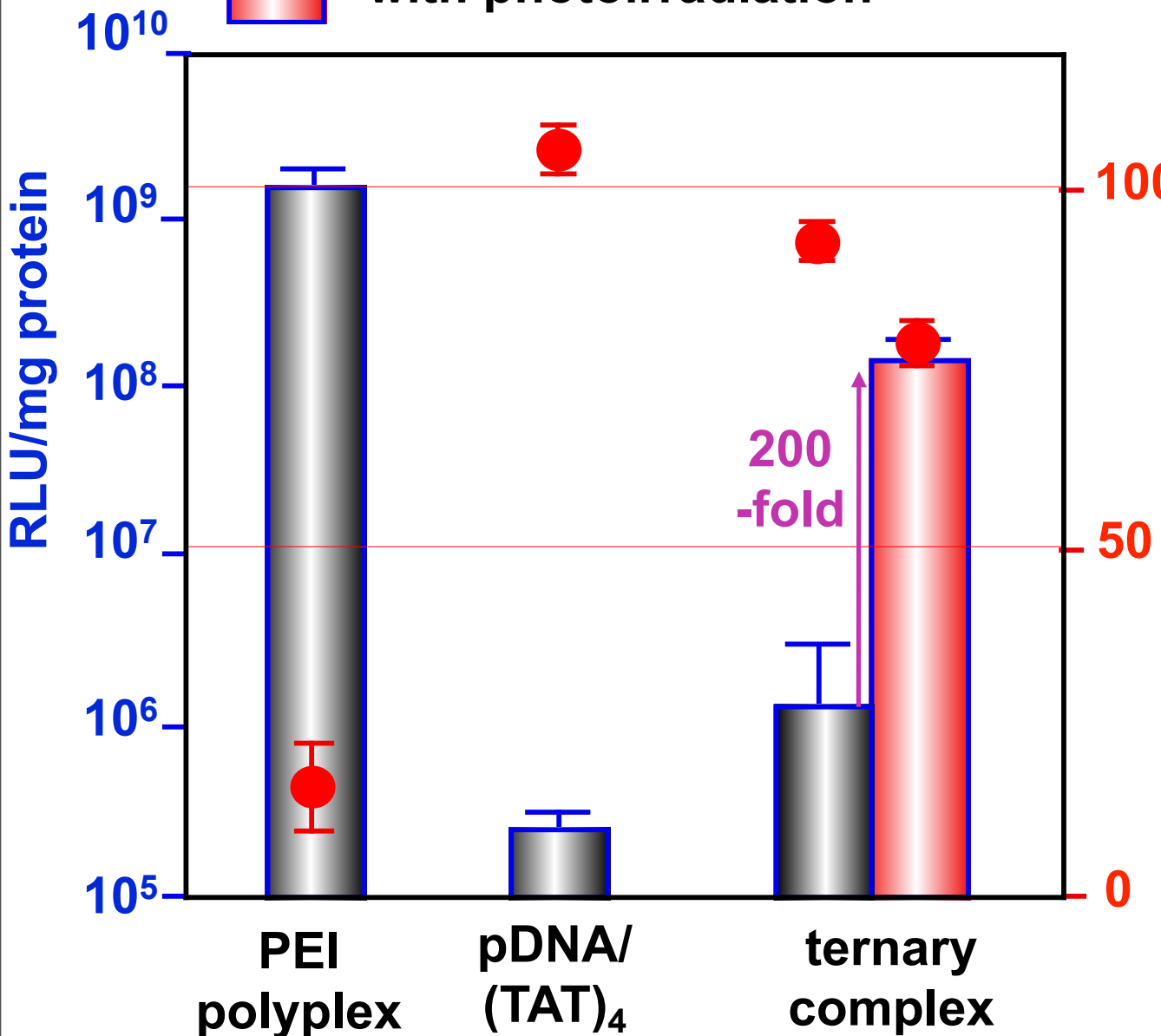
Photochemical transfection:
Use of photosensitizer and light illumination

A. Hogest et al,
Hum. Gene Ther.
11, 869-880 (2000)

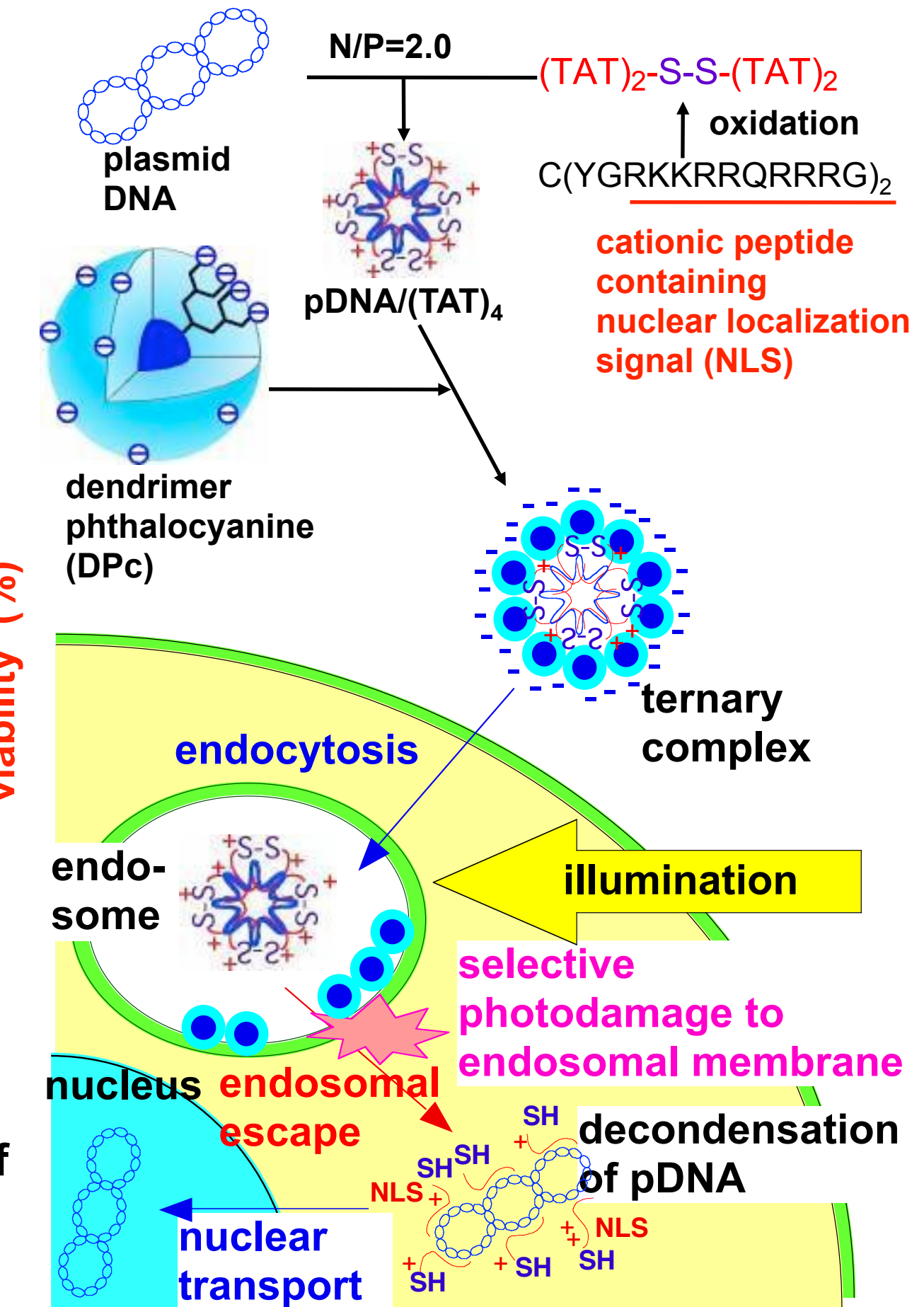
Temporal and spatial control of the transgene expression by light-responsive gene carriers

Transfection efficiency and photocytotoxicity of the ternary complex (incubation time: 48 h)

w/o photoirradiation
with photoirradiation



Remarkable photochemical enhancement of the gene expression was achieved with reduced photocytotoxicity



Intelligent gene carrier for temporal and spatial control of gene transfer in vivo

—Site-directed transfection using light-responsive gene carriers—

A part of conjunctiva in a rat eye was photoirradiated 2 h after subconjunctival injection of the ternary complex (150mL)



The fluorescent image of the YFP expression in a rat eye was observed by a stereoscopic microscope

Light-induced, site-directed transfection of the YFP gene
(Collaboration with Dept. Ophthalmology,
the University of Tokyo Hospital)



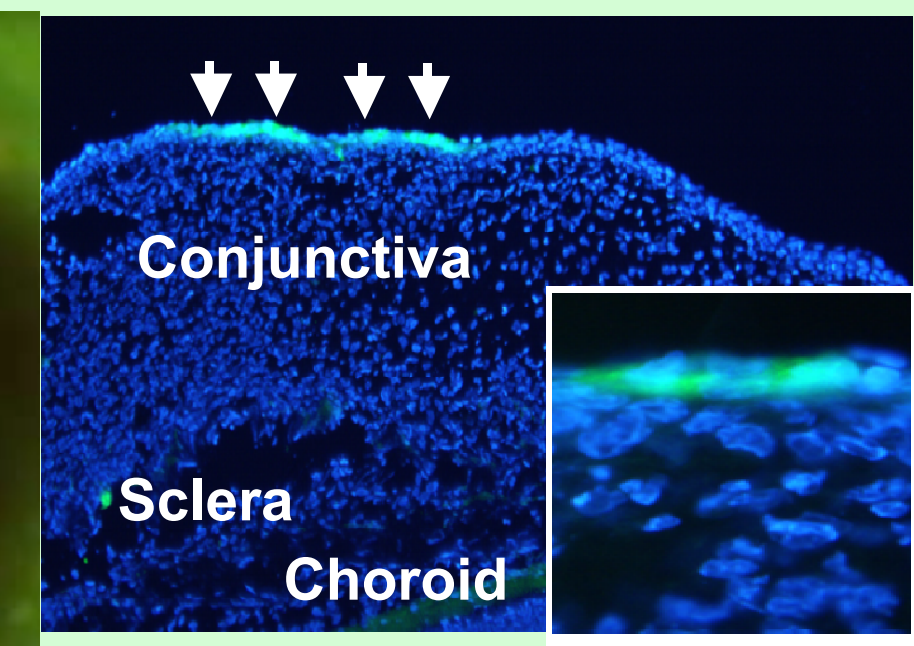
Applications for gene therapy of ophthalmic diseases such as AMD

YFP expression only at the laser-irradiated site

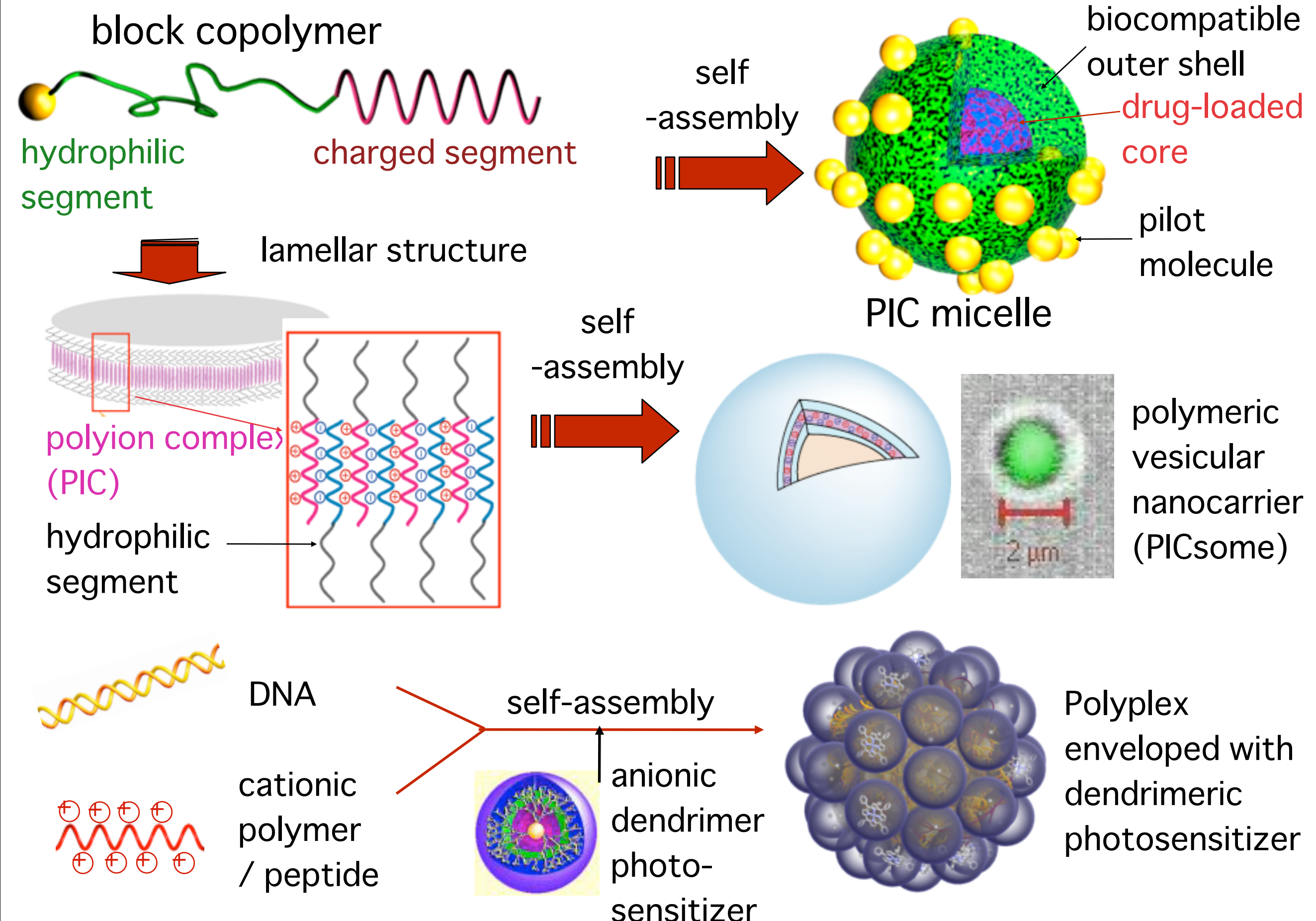
laser
irradiation



2 days after



Supramolecular nanocarriers based on polyion complex formation



Molecular Strategies for PICsome Formation

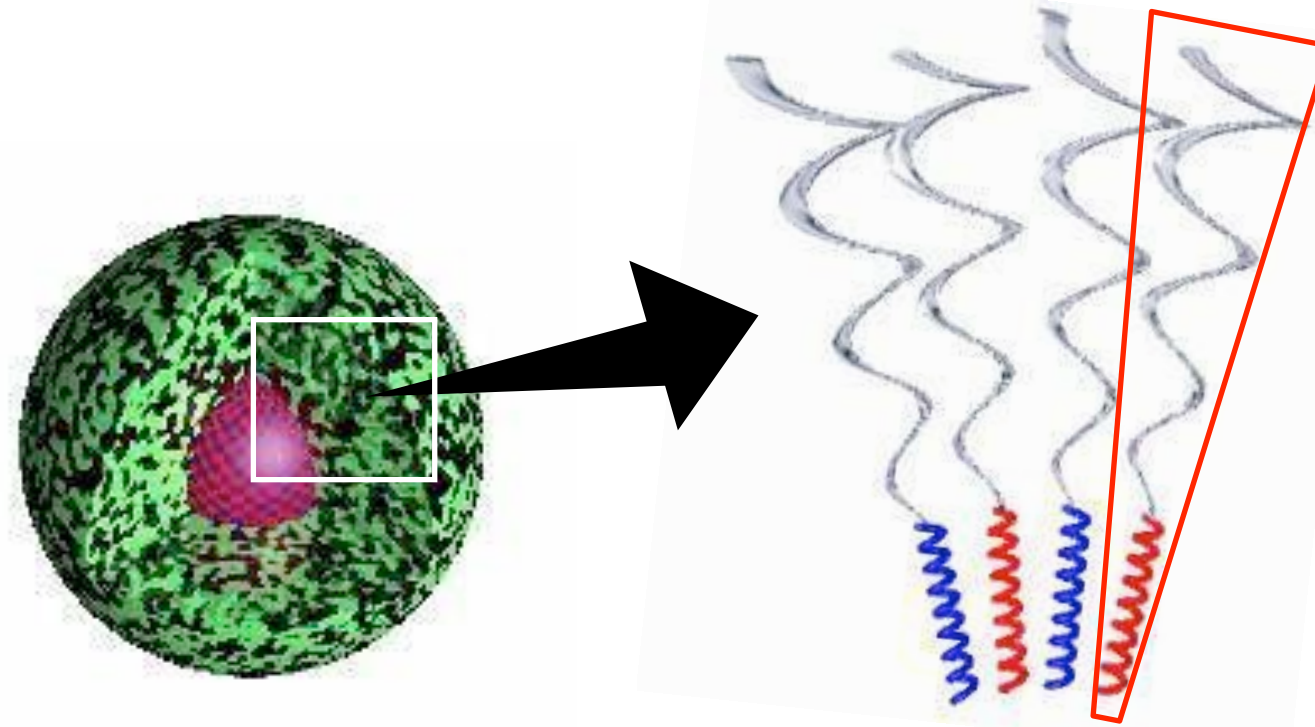
* Stabilize lamella phase to prevent micelle formation

DP of PEG (DP_{PEG}) = 270

DP of Polyion Segments (DP_{PI}) = 70



Formation of Micelles



PIC Micelle

Curved Interface
between
PEG and PIC Layer

Lowered ratio of
 DP_{PEG} to DP_{PI}



More
Planar?

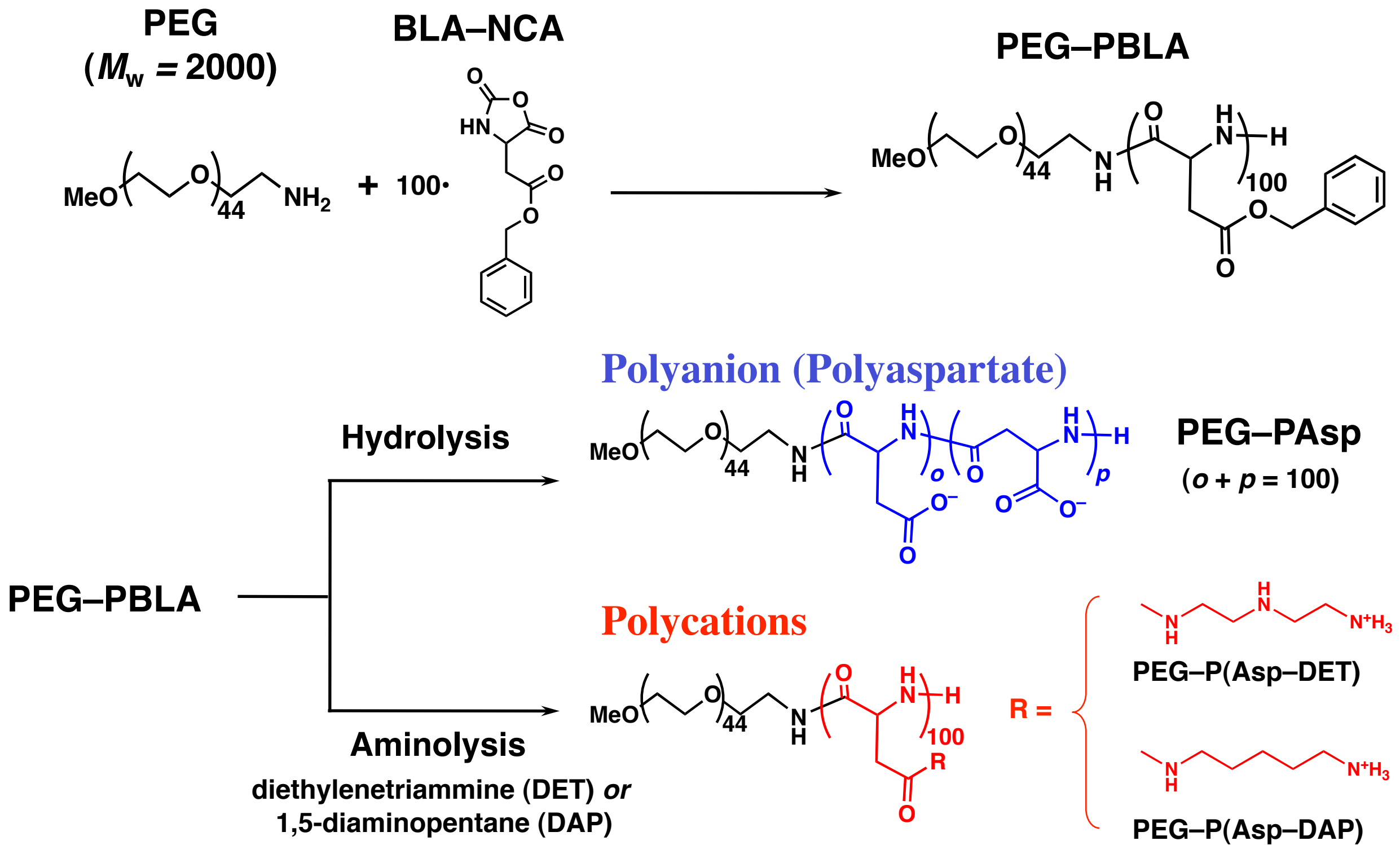
This Work

$DP_{PEG} = 45$

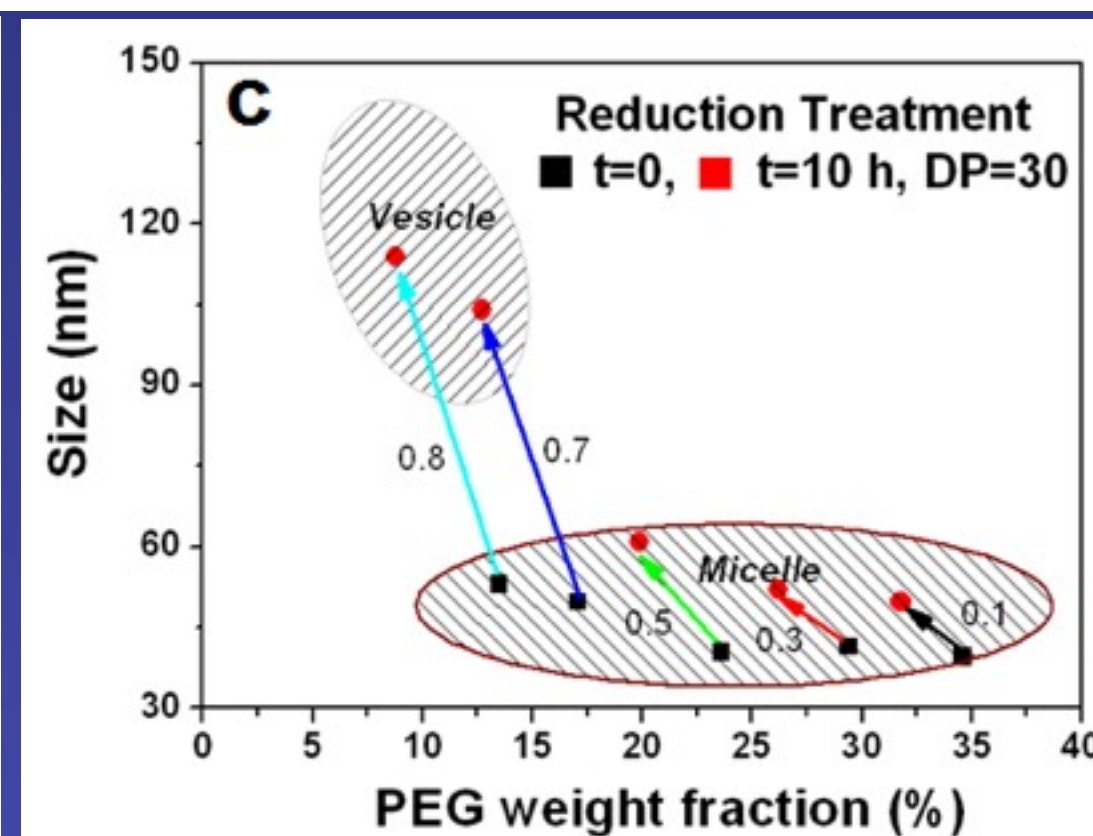
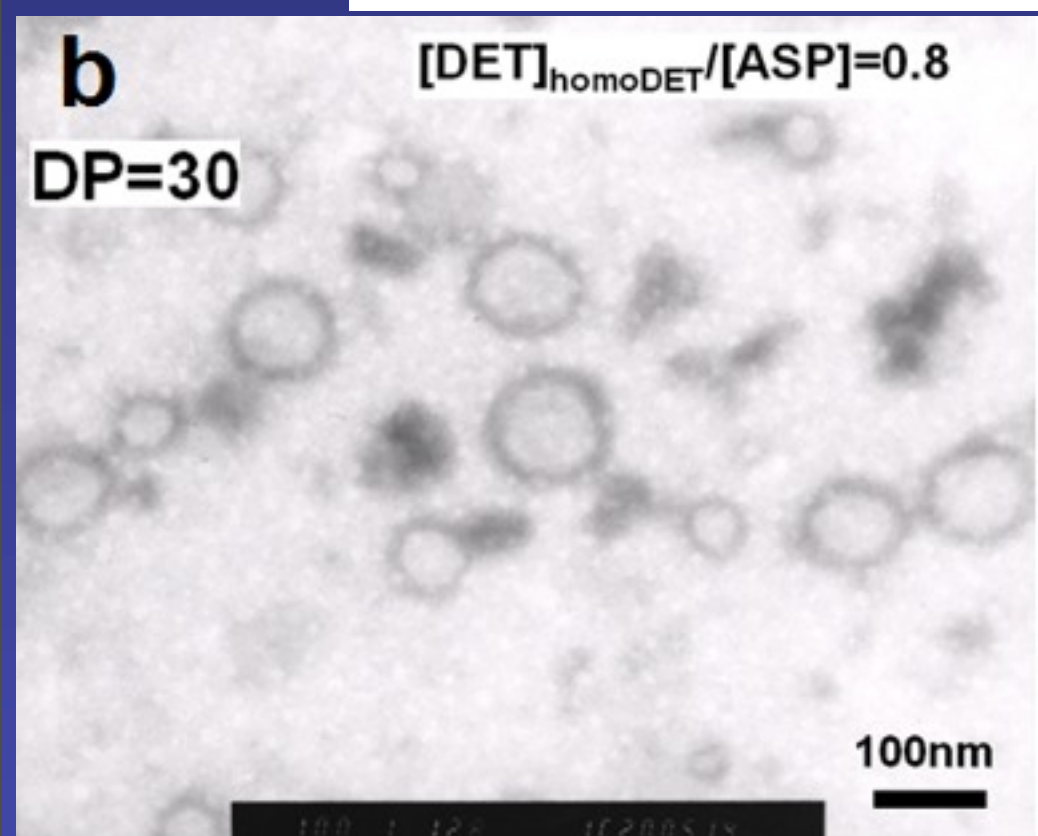
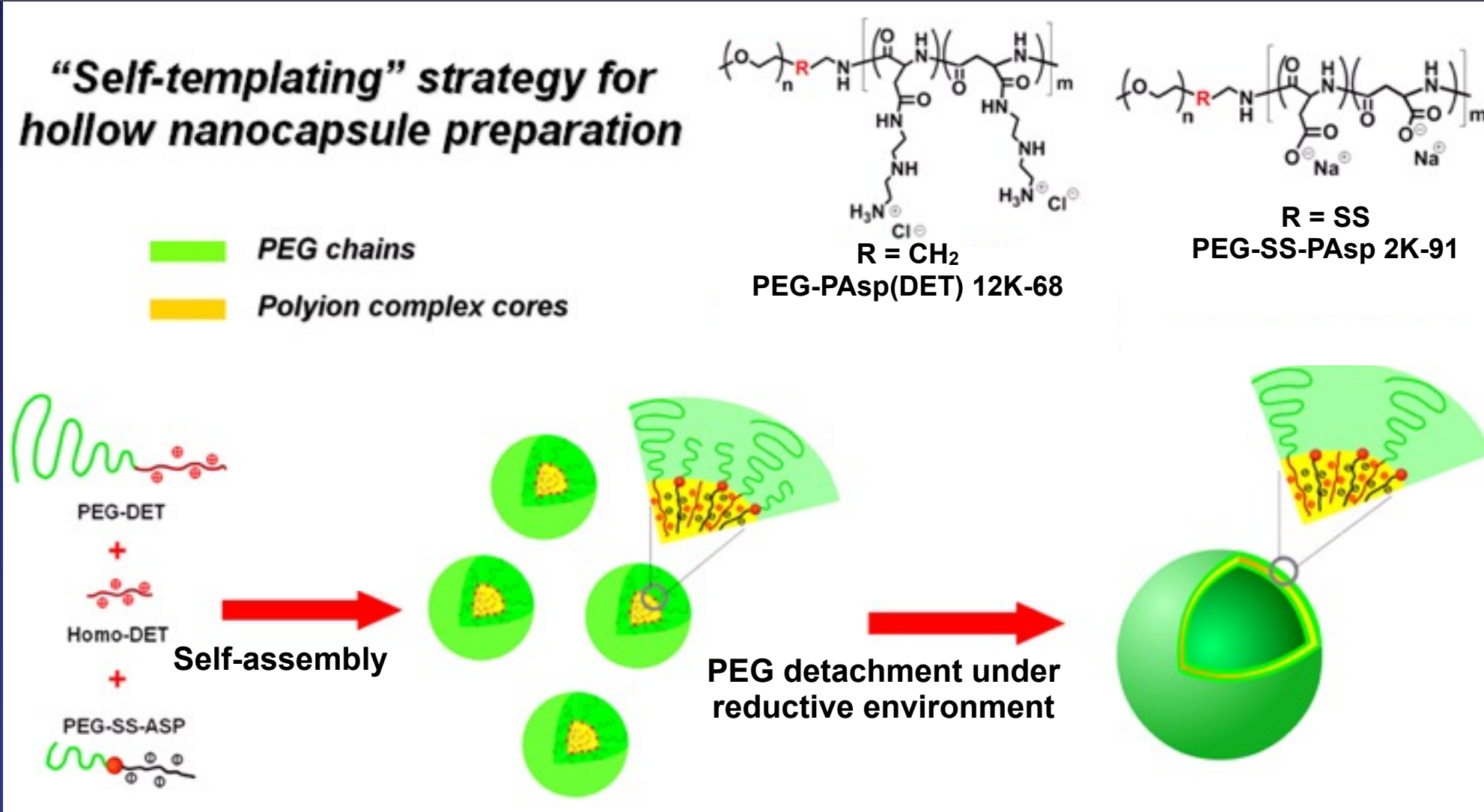
$DP_{PI} = 100$

Synthetic Scheme of Block Copolymers

- Chain length matching of a pair of oppositely charged segments

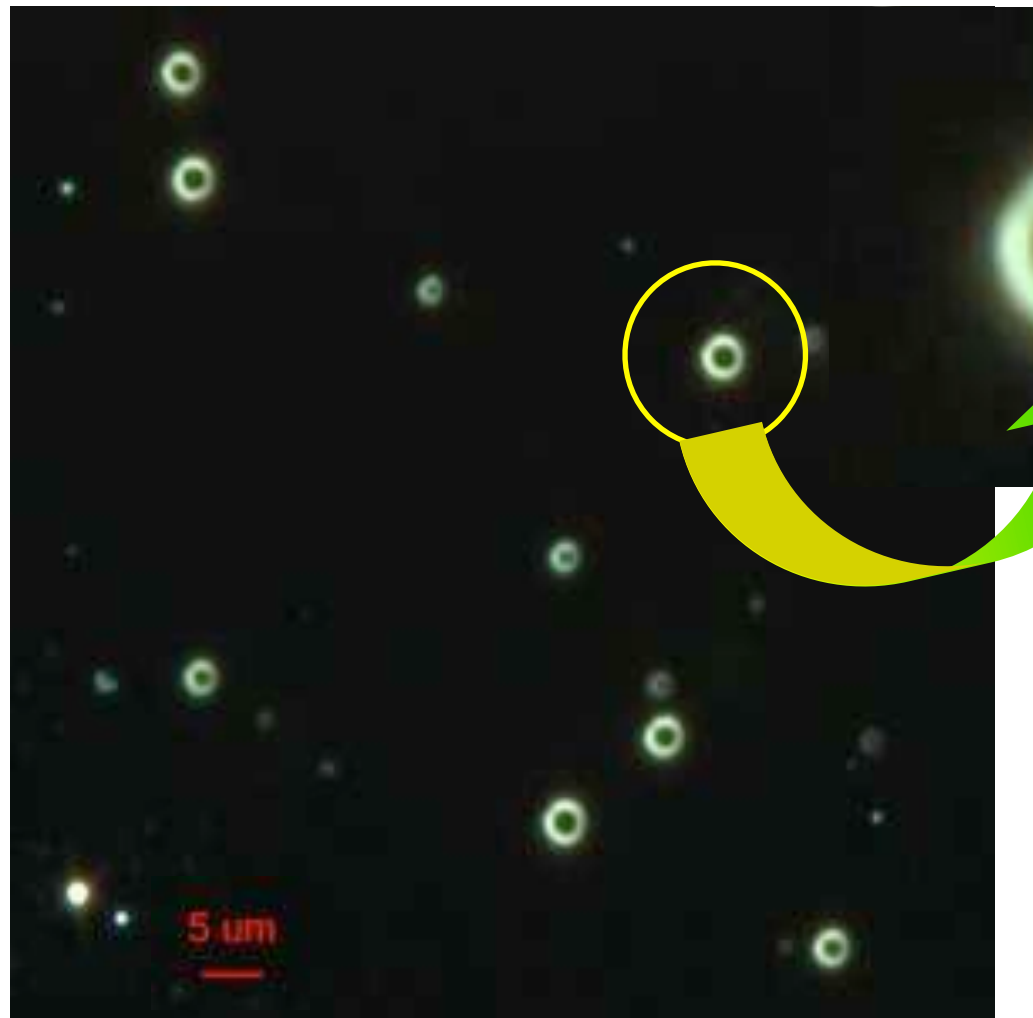


“Self-templating” strategy for hollow nanocapsule preparation

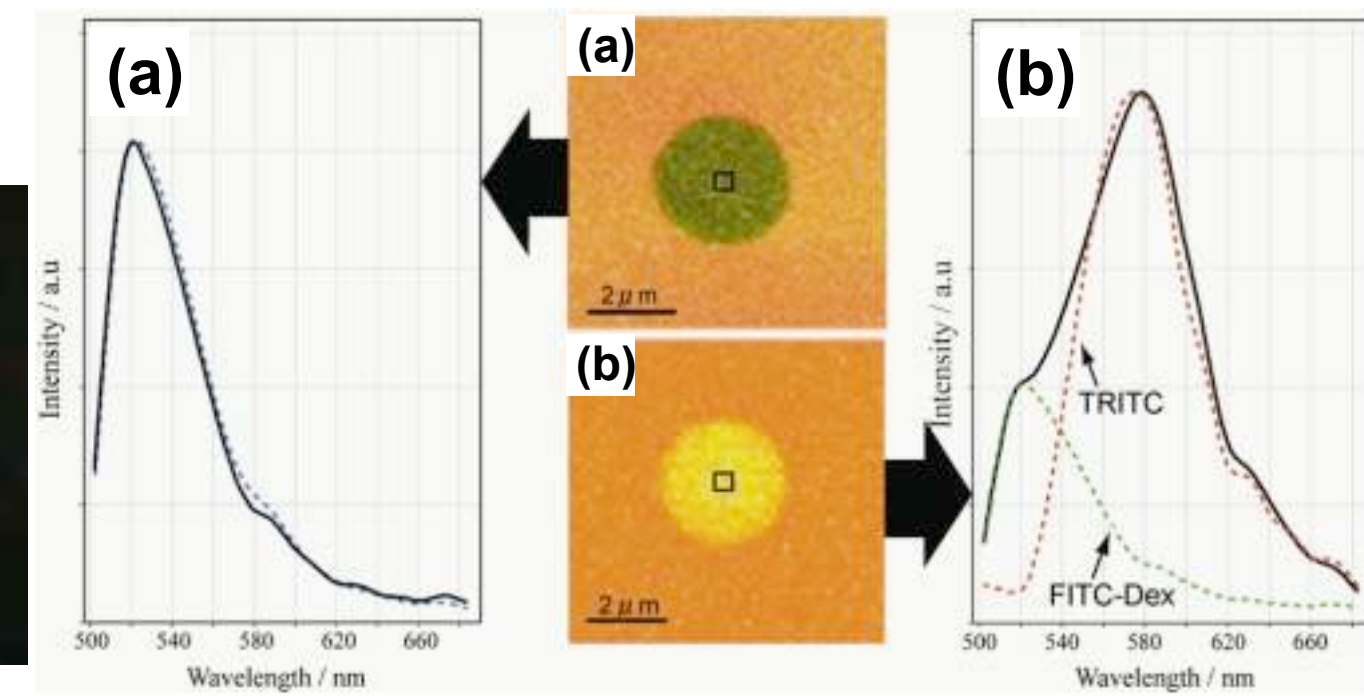


PEG weight fraction is a crucial factor for micelle-to-vesicle transition

Observation of Hollow Structure of PICsome



**Dark-field microscopic image
of PICsome**



**(a) FITC-encapsulated PICsome +
TRITC-dextran ($M_n=65,000\sim76,000$)**

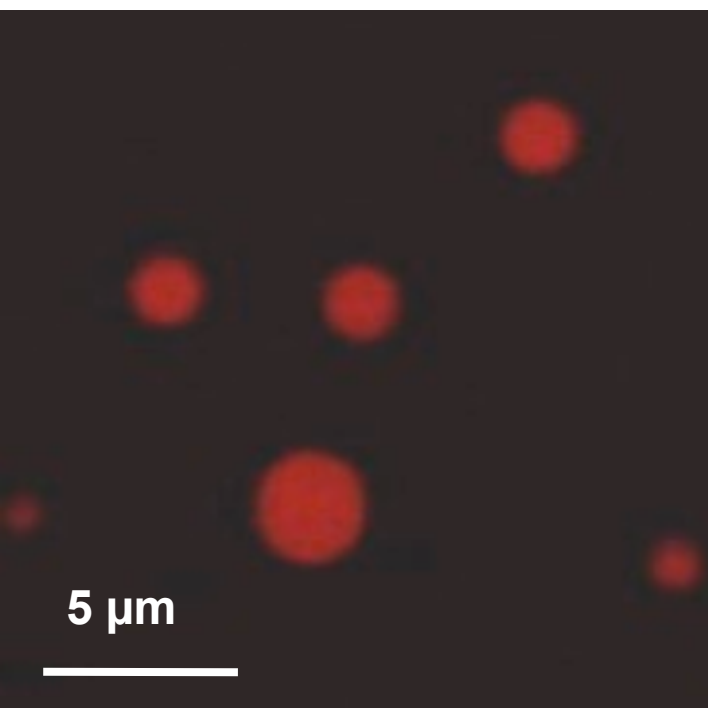
**(b) FITC-encapsulated PICsome +
TRITC ($M_w=443$)**

→ **Semi-permeable nature of
PIC membrane**

**Confocal laser scanning
microscopic image of PICsome
with entrapped FITC-dextran**

Myoglobin-encapsulated PICsome as Nanobio-reactor

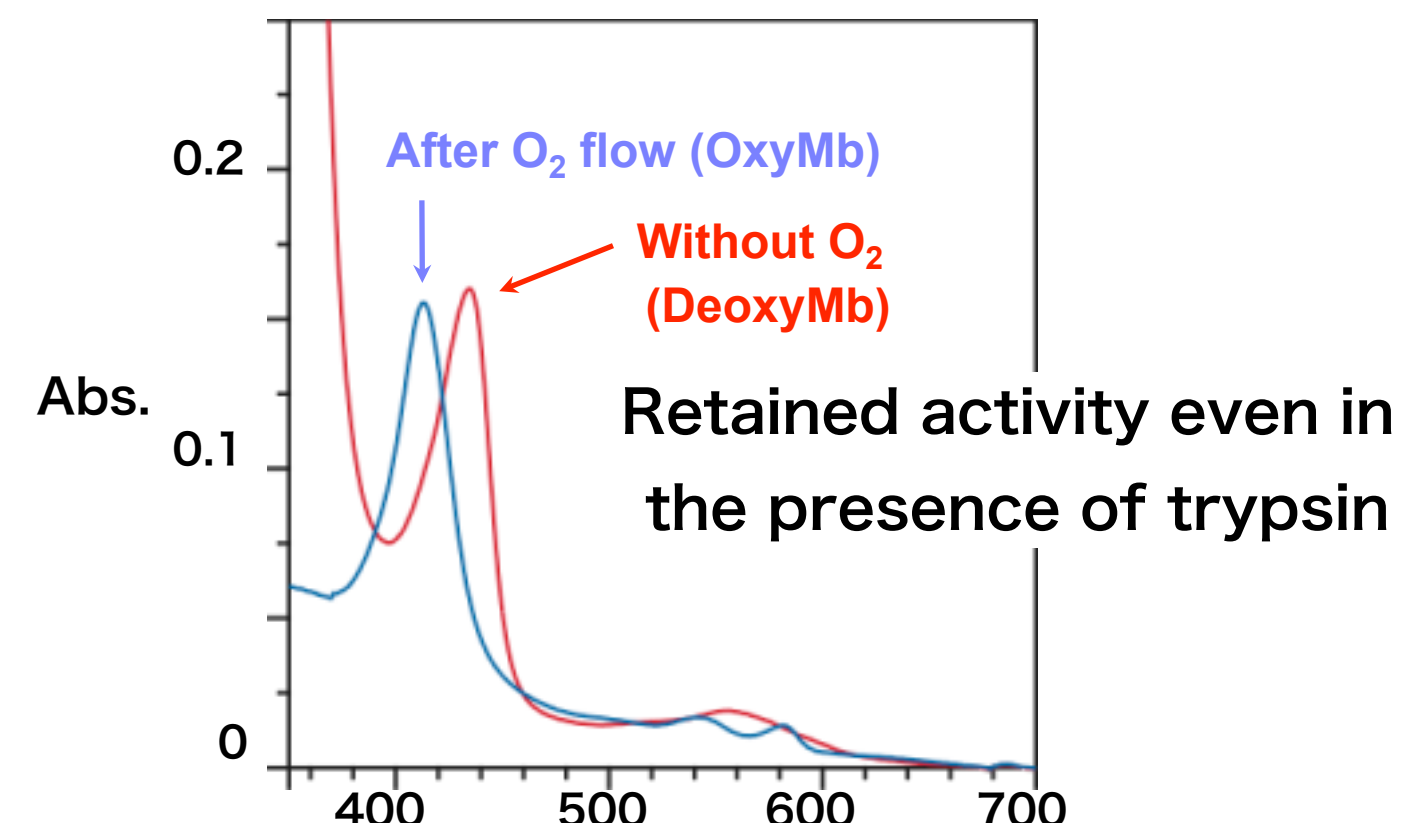
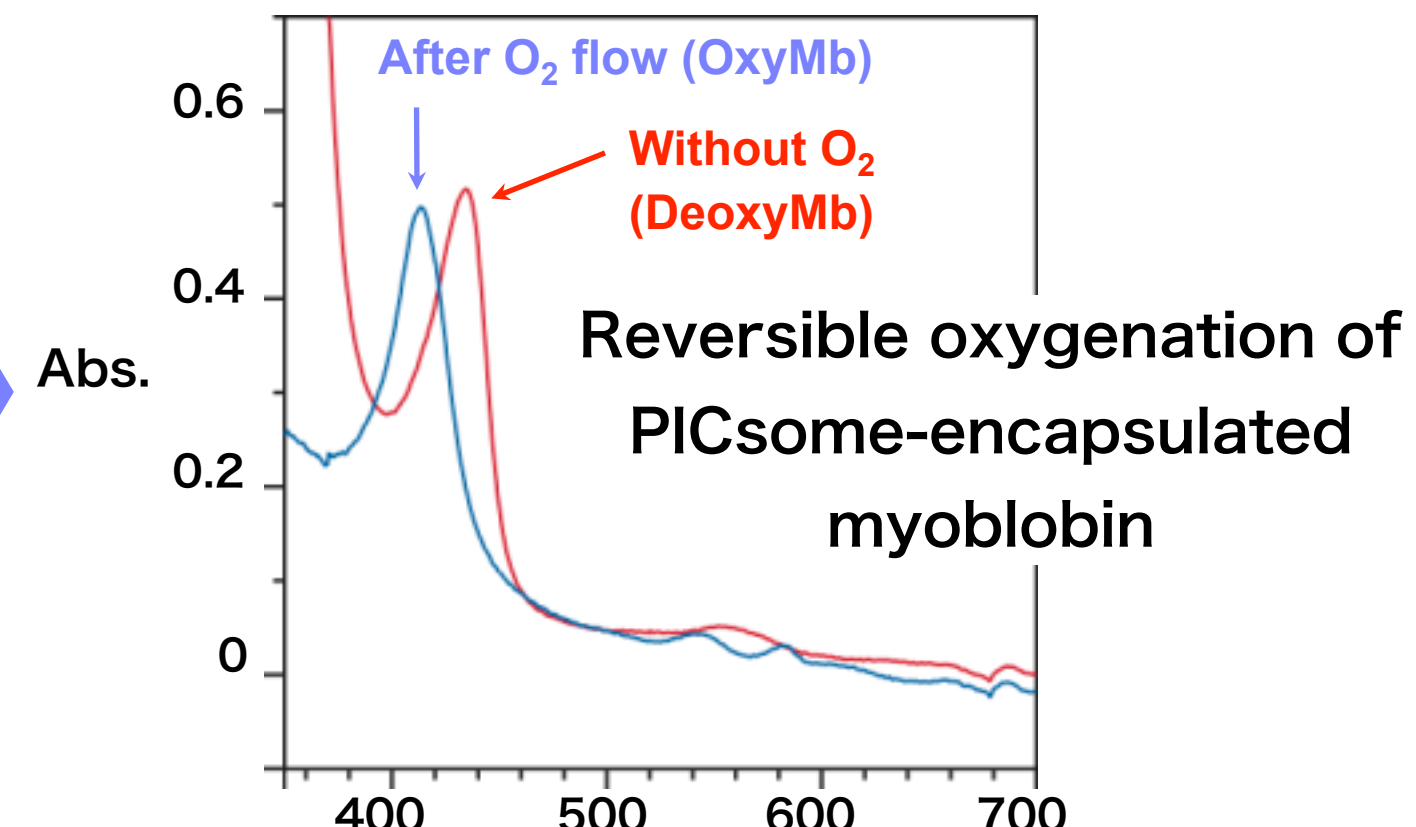
Encapsulation of oxygen carrier protein (myoglobin) ($M_w = 17,800$)



CLSM image of rhodamin-labeled myoglobin in PICsome

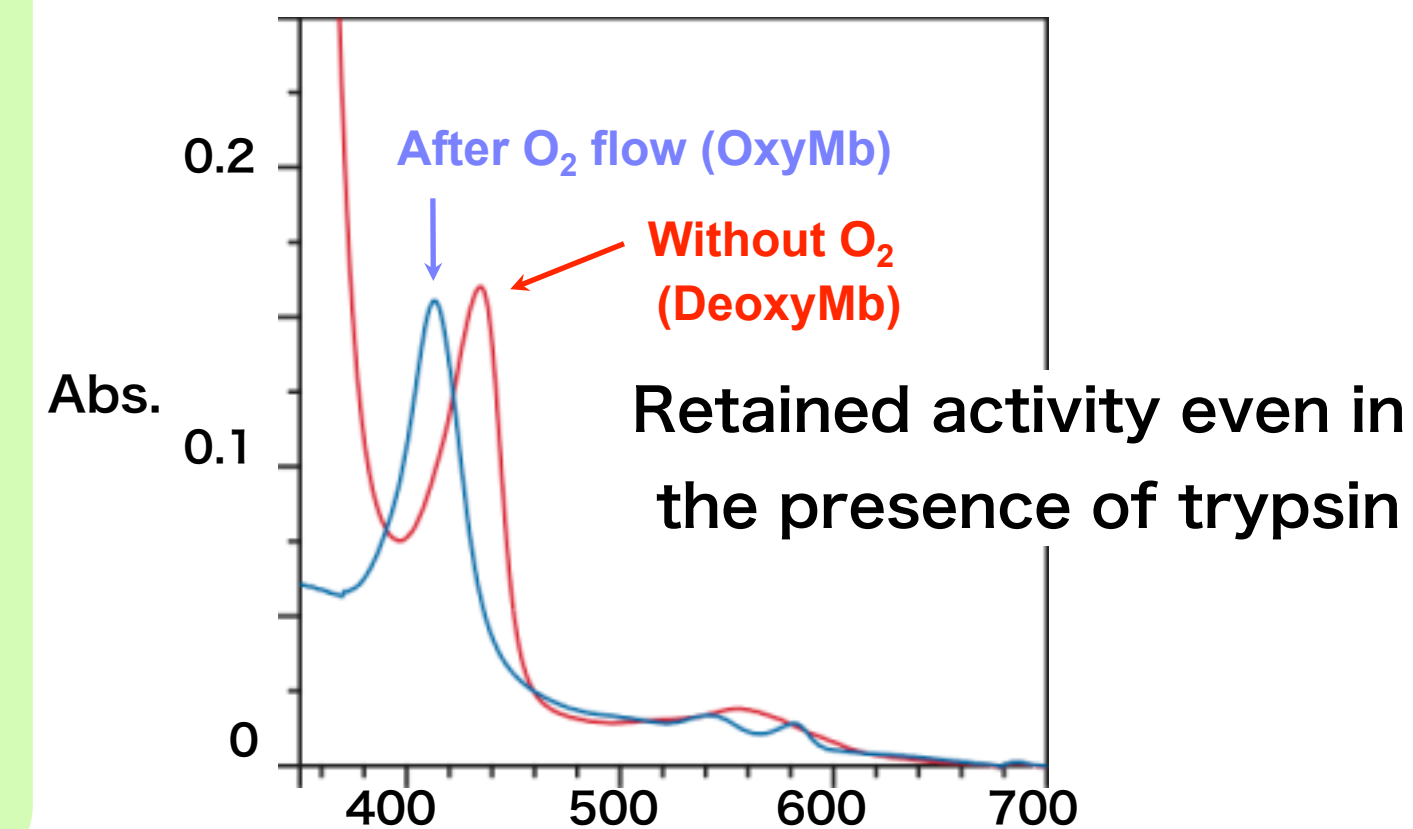
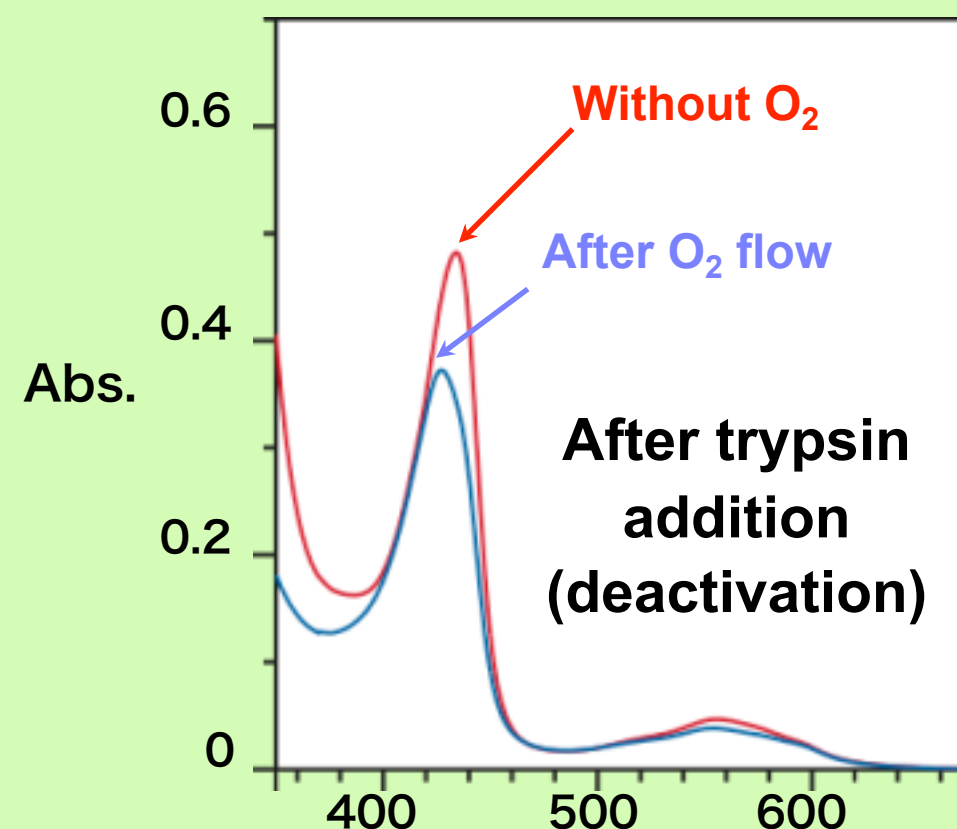
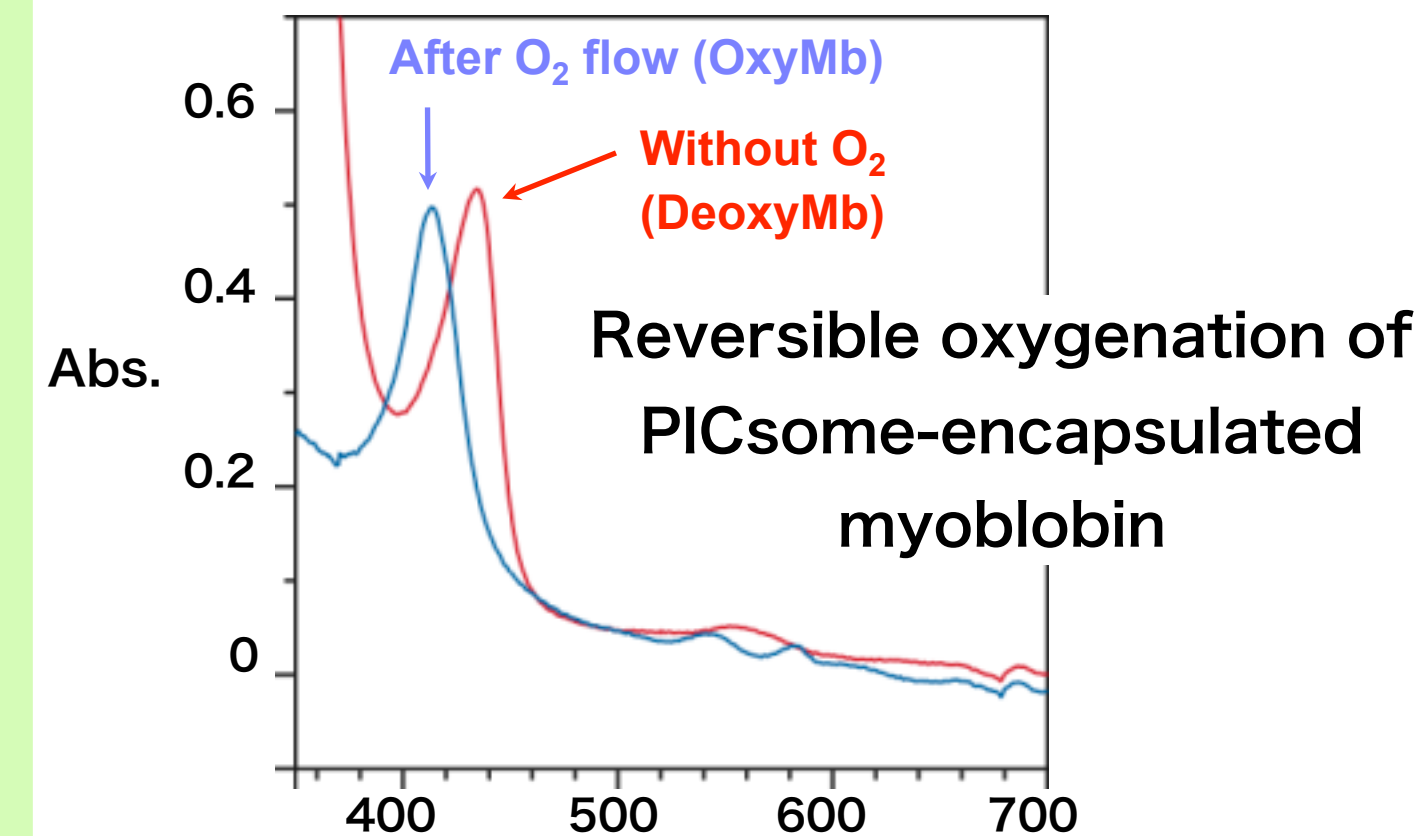
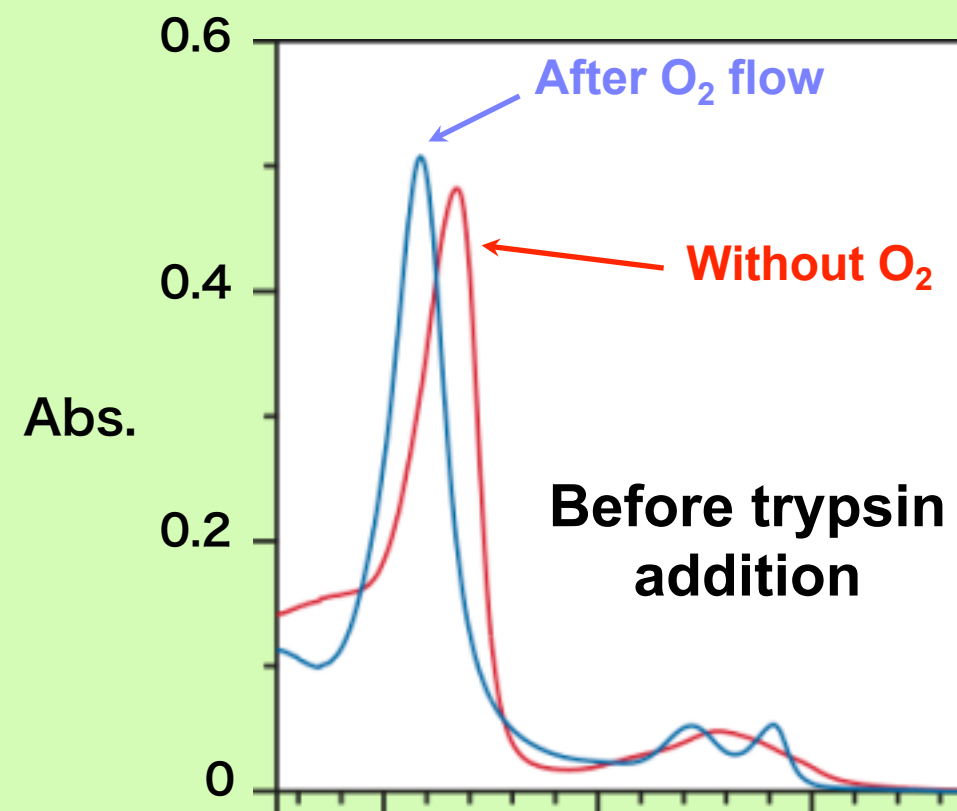
Activity evaluation

Trypsin addition

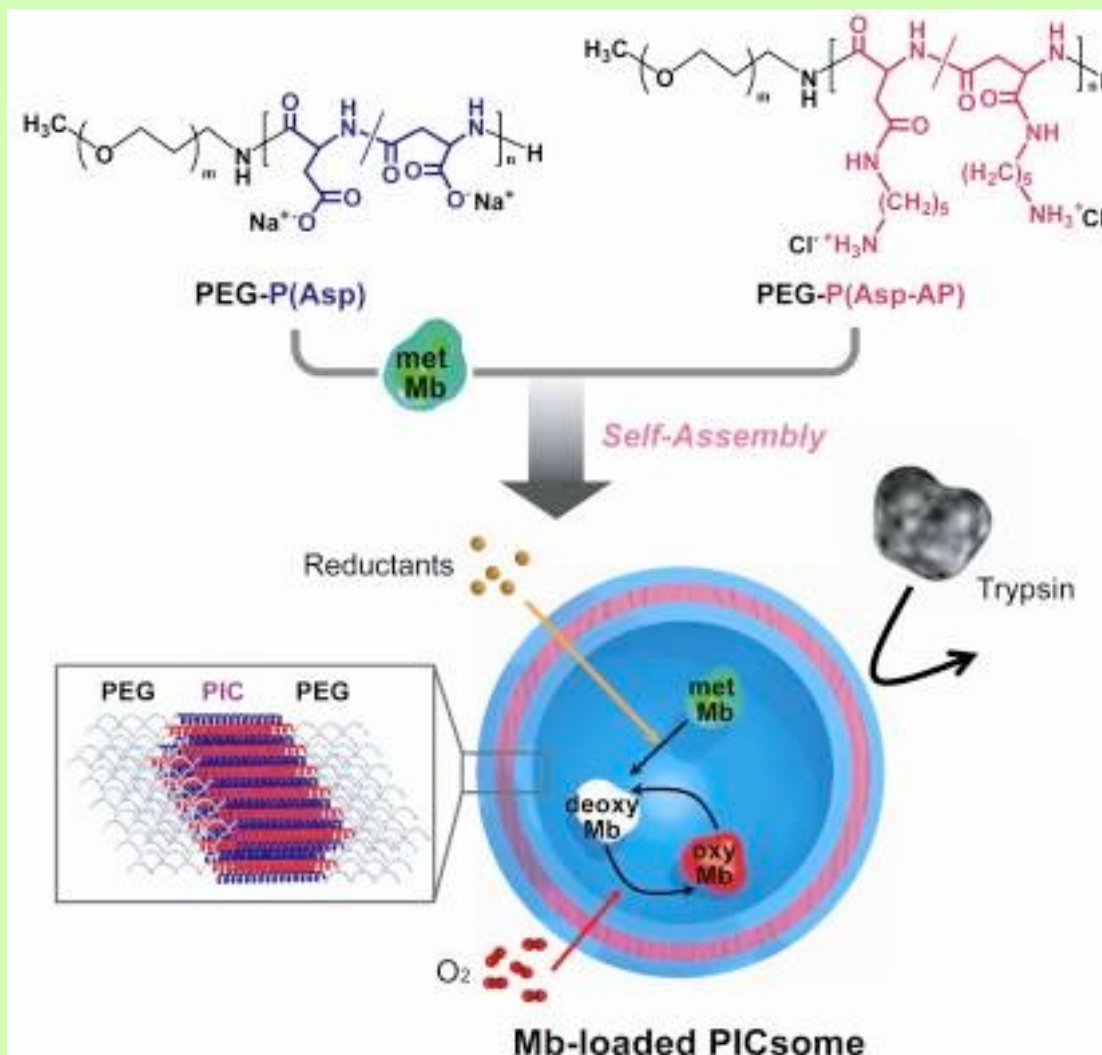


Myoglobin-encapsulated PICsome as Nanobio-reactor

Free myoglobin



Myoglobin-encapsulated PICsome as Nanobio-reactor

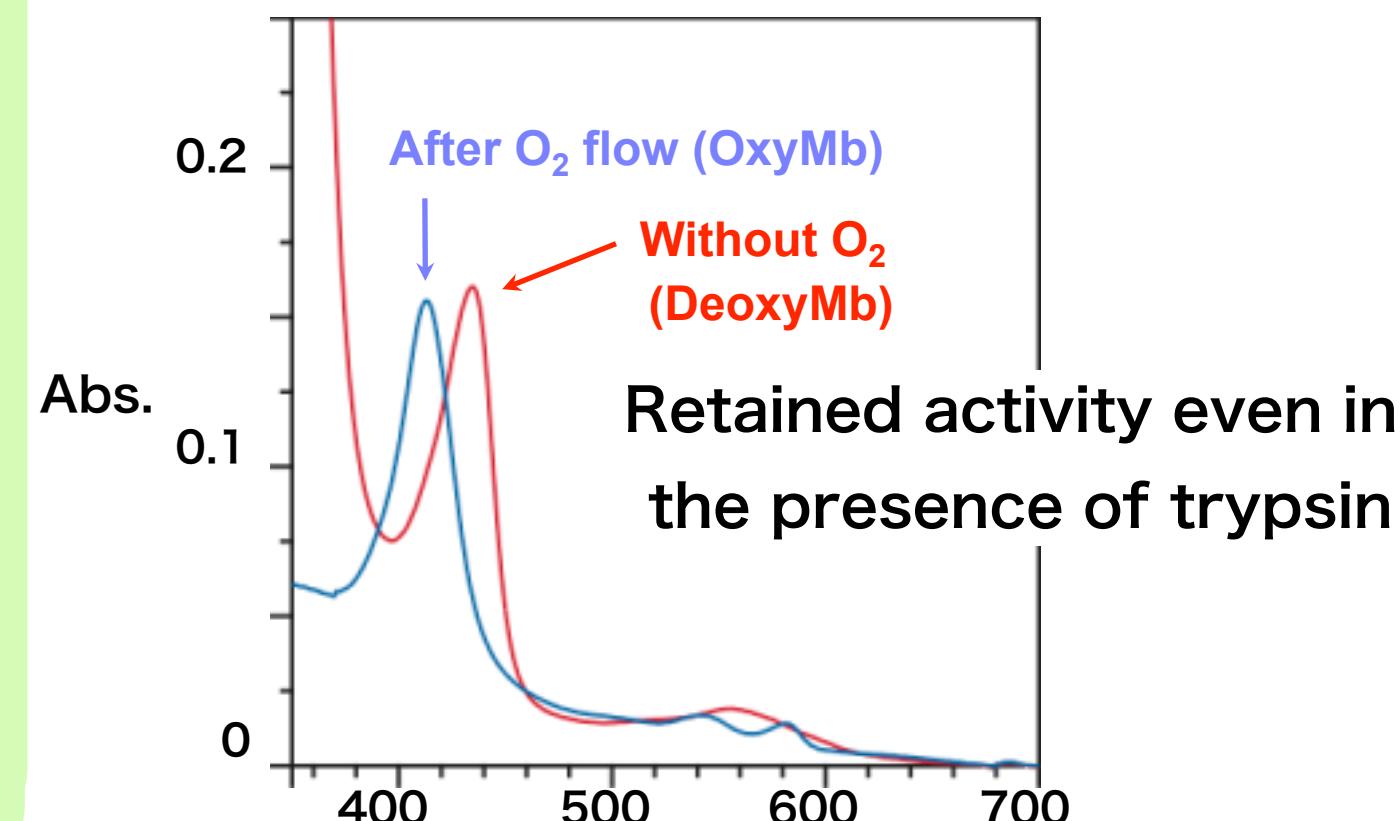
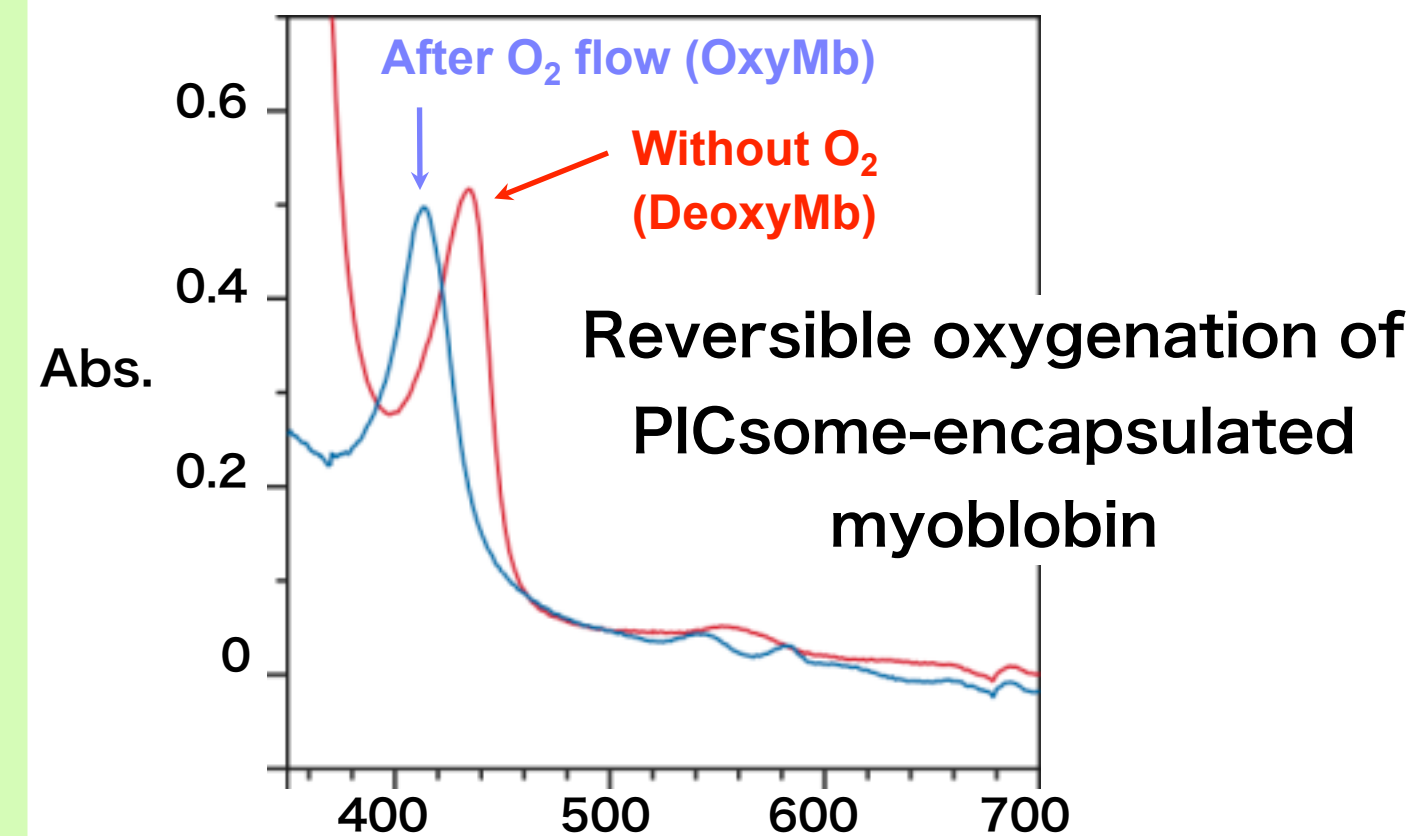


*Reversible O₂-binding

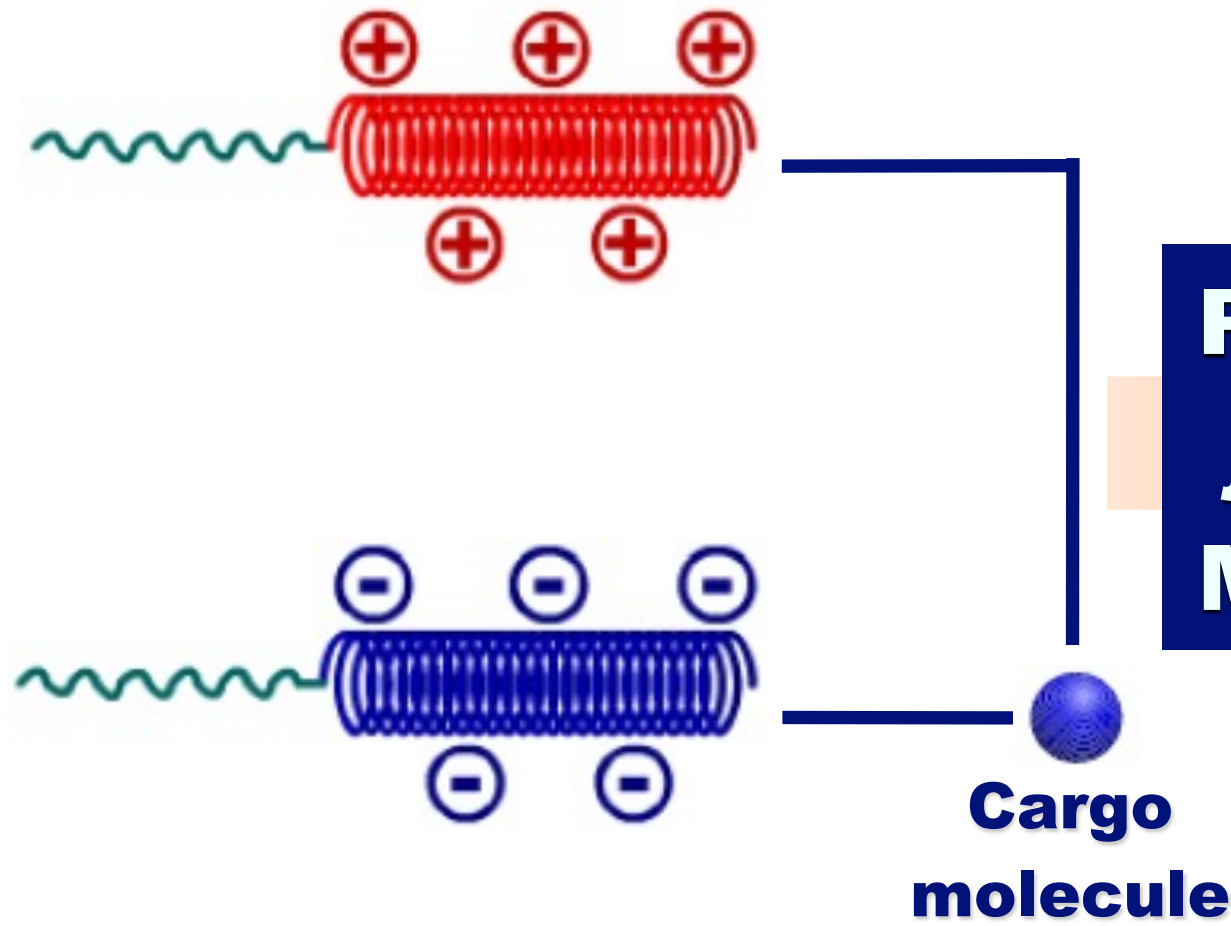
*High Proteinase Resistance

Promising Carrier for
Protein Delivery

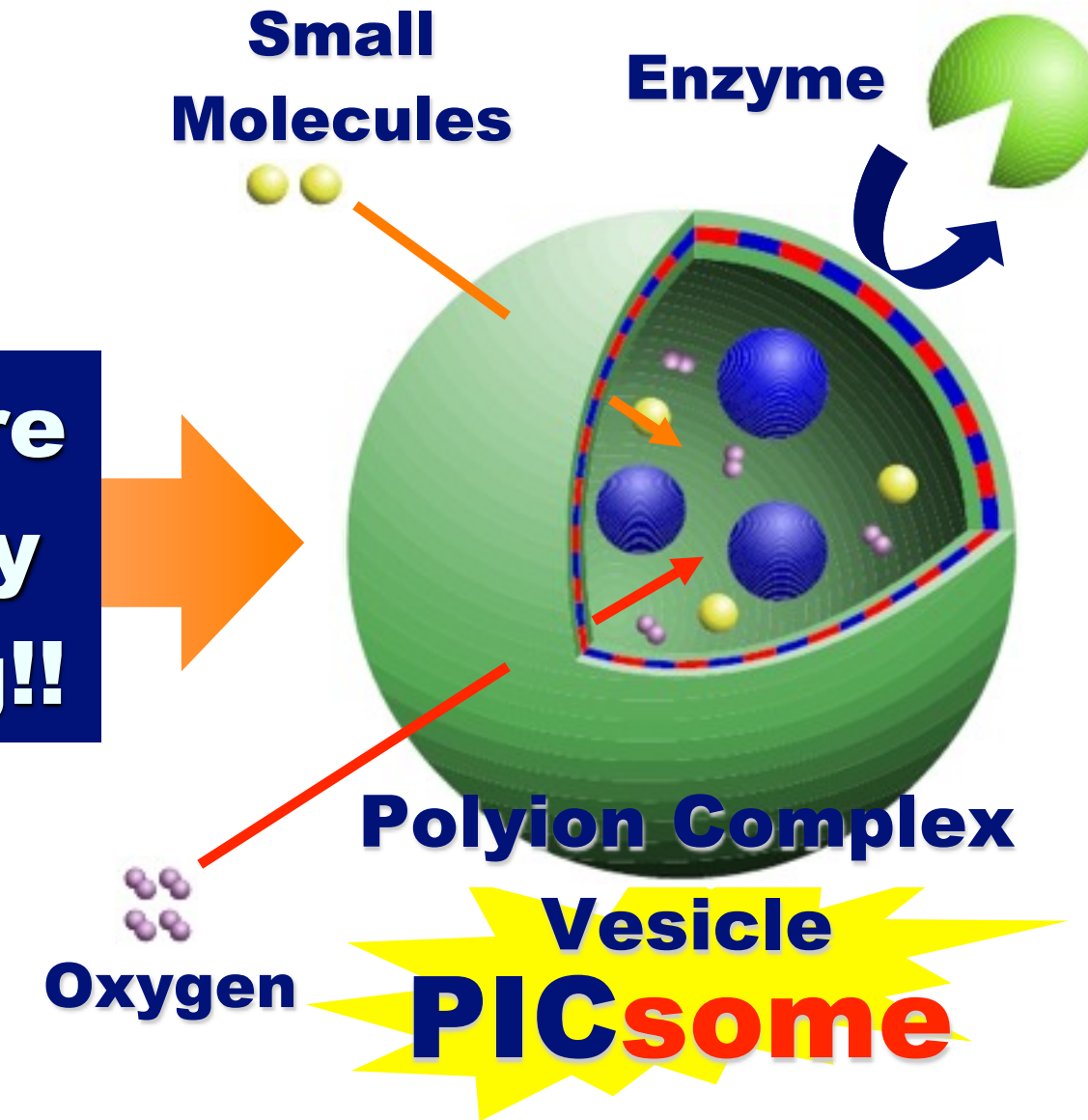
A. Kishimura, et al,
Angew. Chem. Int'l. Ed., 46, 6085-6088 (2007)



PICsome as Functional Nano-container



Prepare
just by
Mixing!!



Utilities

- Encapsulating Macromolecules
- Selective Permeability
- Proteinase Resistance
- pH Sensitivity

Applications

- ★ Bio-reacter
- ★ Artificial Organelle
- ★ Artificial Cell
- ★ Delivery Carrier